



Norwegian University of
Science and Technology

Lithological and structural analysis of the Rødberget-Rørvika-Varpneset transect, Mid Norwegian Caledonides

Testing tectonostratigraphic correlations and
structural models

Åse Hestnes

Geology

Submission date: June 2016

Supervisor: Allan George Krill, IGB

Co-supervisor: Deta Gasser, Norges geologiske undersøkelse (NGU)

Norwegian University of Science and Technology
Department of Geology and Mineral Resources Engineering

Acknowledgements

This master thesis has been carried out at the Department of Geology and Mineral Resources Engineering (IGB) at the Norwegian University of Science and Technology (NTNU), and is written in collaboration with the Geological Survey of Norway (NGU). Professor Allan Krill (NTNU) and Dr. Deta Gasser (NGU) have been the main supervisors for this project.

First and foremost, I would like to thank my supervisors, Deta and Allan, for their guidance and good help throughout this work. A special thanks to Deta for giving me this opportunity and for always helping with good advices.

I would also like to thank the Bedrock geology team at NGU for being helpful and welcoming. Especially Katia for company and guidance during fieldwork and always having an open door whenever I had questions, and Espen for being the go-to man I couldn't have made it without.

Thanks to my family and especially my parents, for the support they have given me through the years of study, and especially this last year. From you I get warm and encouraging words and you always find time and solutions whenever I need help.

Christine, Martin, Rasmus and Victoria, the years as a student would never have been the same without you. Looking forward for more "råls" together in the time to come.

Last but not least I want to thank Tom for all the help and support he has given me, and for reminding me that what is on top of the rocks is important too. The best outcrops wouldn't have been "the best" without you.

Abstract

Remnants of the Caledonian orogen are visible through tectonostratigraphic and structural fingerprints in Central Norway, and the detailed study of key localities is important for the understanding of the overall evolution of this orogeny. In this study, a lithological and structural analysis of the Rødberget-Rørvika-Varpneset transect on Fosen peninsula, South-Trøndelag, is conducted. In earlier studies, several tectonostratigraphic hypotheses were proposed for this area: 1) the central amphibolites belong to the Støren Nappe, whereas the surrounding mica schists belong to the Gula Nappe, 2) Seve Nappe Complex, Gula and Støren nappes are represented in the area, and 3) the entire area can be correlated to the Seve Nappe Complex. In addition, it was proposed that the central amphibolites represent a larger synformal structure. With the help of lithological mapping, geochemical analysis of aplites and amphibolites, and U-Pb zircon dating, these earlier proposed tectonostratigraphic correlations and structural models are tested in this study. The study area is divided into four units: the Rødberget, Trongen, Rørvika and Varpneset units. The Rødberget unit represents Baltoscandian basement, whereas the Trongen, Rørvika and Varpneset units are correlated with the Seve Nappe Complex based on the following lines of evidence: 1) lithological similarities to Seve Nappe Complex rocks in Central Norway and Sweden, 2) penetrative at least amphibolite-facies metamorphism, 3) U-Pb zircon dating of an intermediate layer within the central amphibolites yielding an age of 435.4 ± 3.3 Ma, interpreted to be the result of decompressional melting of amphibolites related to exhumation of the Seve Nappe Complex, and 4) the presence and geochemistry of aplites, which have intruded both mica schists and amphibolites, resembling similar intrusive rocks in the Seve Nappe Complex, which were emplaced at about 430 Ma. In addition, through a detailed structural analysis of foliations, lineations, fold axes and fold vergences it can be shown that the central Rørvika unit is not lying within a synform, but rather represents a wedge-shape structure where the vergence of the smaller folds reflects the movement of the lithologies in the area. Two large-scale models are proposed for the ductile structural evolution of the entire area: 1) an “obstacle and buckling” model, and 2) a “rotation” model. Both models are related to the evolution of antiformal basement windows and the Møre-Trøndelag Fault Complex (MTFC). Stress inversion of brittle structures shows that the study area has been affected by a NW-SE extensional event, reactivating the MTFC in Late Paleozoic to Late Mesozoic/Early Cenozoic. These results imply that the area of interest has experienced a different structural evolution than earlier proposed, with a different and more complex metamorphic and structural history. This has implications for tectonostratigraphic correlations across Trondheimsfjorden.

Sammendrag

Rester etter den Kaledonske orogenen kan i dag observeres gjennom tektonostratigrafiske og strukturelle spor i Midt-Norge, og studier av nøkkellokaliteter er viktig for forståelsen av utviklingen til denne fjellkjeden. Gjennom dette studiet er det gjennomført en litologisk og strukturell analyse av et transekt gjennom Rødberget-Rørvika-Varpneset på Fosen-halvøya i Sør-Trøndelag. Flere hypoteser til tektonostratigrafien i området er tidligere blitt presentert: 1) den sentrale amfibolitten tilhører Størensdekket, og de omkringliggende glimmerskifrene tilhører Guladdekket, 2) Sevedekkekomplekset, Gula- og Størensdekket er alle representert i området, og 3) hele området er korrelert til Sevedekkekomplekset. Det har også blitt foreslått at de sentrale amfibolittene representerer en større synform. Ved hjelp av litologisk kartlegging, geokjemiske analyser av aplitter og amfibol, og U-Pb datering av zircon, har de tidligere tektonostratigrafiske og strukturelle modellene blitt testet. Studieområdet er delt inn i fire enheter: Rødberget, Trongen, Rørvika og Varpneset. Rødberget representerer Baltoskandisk grunnfjell, mens Trongen, Rørvika og Varpneset er korrelert med Sevedekkekomplekset basert på følgende: 1) likheter til liknende litologier i sentrale Norge og Sverige, 2) minst amfibolittfacies metamorfose, 3) U-Pb datering av zircon fra amfibolitter som gir en alder på $435,4 \pm 3,3$ Ma. Denne alderen er tolket til å være et resultat av dekompresjonssmelting av amfibolitt relatert til ekshumasjon av litologier tilhørende Sevedekkekomplekset. 4) Geokjemiske analyser av aplitter som er intrudert i både glimmerskifer og amfibolitter, relatert til en hendelse av intrusjoner i Sevedekkekomplekset for omtrent 430 mill. år siden. Gjennom strukturell analyse av foliasjoner, lineasjoner, foldakser og folders vergens kan det vises at den sentrale Rørvika enhet ikke ligger i en synform, men representerer en vifte-formet struktur hvor vergensen til de mindre foldene reflekterer bevegelsesmønsteret til litologiene i området. To storskala modeller er foreslått for områdets utvikling: 1) en «hinder- og bulings» modell, og 2) en «rotasjons» modell. Begge er relatert til utviklingen av antiformer i grunnfjellsvinduer og Møre-Trøndelagforkastningssonen (MTFC). Invertering av spenningsfeltet til sprø forkastninger viser at studieområdet har vært påvirket av en NV-SØ ekstensjon, relatert til reaktivering av MTFC i sen paleozoikum til sen mesozoikum/tidlig kenozoikum. Disse resultatene antyder at studieområdet har vært gjennom en annen strukturell utvikling enn tidligere foreslått, med en annerledes og mer kompleks metamorf og strukturell utvikling. Dette har implikasjoner for tektonostratigrafiske korrelasjoner over Trondheimsfjorden.

Table of content

1	Introduction.....	1
2	Geological setting	5
2.1	Caledonian tectonostratigraphy	5
2.1.1	Southern segment.....	6
2.1.2	Northern segment.....	7
2.1.3	Central segment and related allochthons	7
2.2	The evolution of the Caledonian orogen	13
3	Methods.....	17
4	Field results	21
4.1	Geographic setting.....	21
4.2	Lithological description of mapped units	23
4.2.1	Rødberget unit.....	23
4.2.2	Trongen unit.....	25
4.2.3	Rørvika unit	33
4.2.4	Varpneset unit.....	37
4.3	Structural observations	41
4.3.1	Foliation.....	41
4.3.2	Mineral lineation.....	48
4.3.3	Fold systems	53
4.3.4	Brittle structures.....	67
5	Summary and structural model	83
6	Petrography, geochemistry and geochronology.....	87
6.1	Petrographic description of lithologies.....	87
6.1.1	Rødberget unit.....	87
6.1.2	Trongen unit.....	90
6.1.3	Rørvika unit	99
6.1.4	Varpneset unit.....	103
6.2	Geochemistry.....	108
6.2.1	Felsic aplites	108
6.2.2	Ams.....	109
6.3	Geochronology	113

7	Discussion.....	117
7.1	Protolith identification, metamorphic history and tectonostratigraphic correlation	117
7.1.1	The Rødberget unit – a piece of Baltoscandian basement.....	117
7.1.2	The Trongen unit – Gula or Seve nappe complex?	118
7.1.3	The Rørvika unit –Støren Nappe or Seve Nappe Complex?	119
7.1.4	Varpneset unit.....	124
7.1.5	The significance of aplites	126
7.2	Ductile structural evolution	128
7.2.1	Comments on foliation, lineation and fold axes	129
7.2.2	Large-scale structural models	133
7.3	Brittle structural evolution.....	140
8	Conclusions.....	145
9	References.....	147

List of figures

Figure 1.1: Clip of bedrock maps from Wolff 1976 and Wolff 1978.	2
Figure 1.2: Bedrock map of Robinson and Roberts (2008) and Gee et al (1985).....	3
Figure 1.3: Schematic sketch of interpreted synform.....	4
Figure 2.1: Map of the Scandinavian Caledonides.....	6
Figure 2.2: Map of the central segment.....	8
Figure 2.3: Profile from central Norway and Sweden.....	9
Figure 2.4: Conceptual sketch of the evolution of the Caledonian orogeny.	14
Figure 4.1: Geographic map showing location of the studied area.....	22
Figure 4.2: Map with units	23
Figure 4.3: Field observations of Ingdal granitic gneiss, Rødberget unit	24
Figure 4.4: Field observations of Ghms, Trongen unit.	27
Figure 4.5: Field observations of Hbs, Trongen unit	28
Figure 4.6: Profile Oksvika, Trongen unit	29
Figure 4.7: Field observations of Helle, Ams and metasediments, Trongen unit	30
Figure 4.8: Field observations of felsic material, Trongen unit.	31
Figure 4.9: Field observations of Ams, Rørvika unit.	32
Figure 4.10: Field observations of Amis, Rørvika unit.....	34
Figure 4.11: Field observations of Amfs, Rørvika unit.....	36
Figure 4.12: Field observations of felsic material, Rørvika unit.....	38
Figure 4.13: Field observations of Hcqs, Varpneset unit.....	40
Figure 4.14: Foliation pictures, Rødberget unit	41
Figure 4.15: Foliation measurements, Rødberget unit	42
Figure 4.16: Foliation pictures, Trongen unit.....	43
Figure 4.17: Foliation measurements, Trongen unit	44
Figure 4.18: Foliation pictures, Rørvika unit	45
Figure 4.19: Foliation measurements, Rørvika unit	45
Figure 4.20: Foliation pictures, Varpneset unit.....	46
Figure 4.21: Foliation measurements, Varpneset unit.....	47
Figure 4.22: Lineation pictures, Rødberget unit.....	48
Figure 4.23: Lineation measurements, Rødberget unit	48
Figure 4.24: Lineation pictures, Trongen unit.....	49

Figure 4.25: Lineation measurements, Trongen unit	50
Figure 4.26: Lineation pictures, Rørvika unit	51
Figure 4.27: Lineation measurements, Rørvika unit	51
Figure 4.28: Lineation pictures, Varpneset unit	52
Figure 4.29: Lineation measurements, Varpneset unit.....	52
Figure 4.30: Fold systems	54
Figure 4.31: Stereoplots of fold systems, all units	55
Figure 4.32: Folds pictures, Trongen unit	56
Figure 4.33: Profile over Oksvika, Trongen unit.	59
Figure 4.34: Oksvika pictures, Trongen unit.....	61
Figure 4.35: Fagerli outcrop, Trongen unit	62
Figure 4.36: Folds pictures, Rørvika unit.....	63
Figure 4.37: Folds pictures, Varpneset unit	64
Figure 4.38: Stereoplots brittle structures, all units.....	67
Figure 4.39: Brittle structures pictures, Rødberget unit	69
Figure 4.40: Brittle structure, detail, Trongen unit.....	69
Figure 4.41: Brittle structure, detail, Trongen unit.....	70
Figure 4.42: Brittle structures, Fagerli, Trongen unit.....	71
Figure 4.43: Brittle structures, Oksvika, Trongen unit	72
Figure 4.44: Brittle structures, detail, Rørvika unit.....	73
Figure 4.45: Profile Kleivneset, Rørvika unit	74
Figure 4.46: Pictures from Kleivneset, Rørvika unit.....	75
Figure 4.47: Brittle structures, detail, Rørvika unit.....	75
Figure 4.48: Panorama quarry, Rørvika unit	77
Figure 4.49: Stereoplots of brittle structures from quarry, Rørvika unit.....	78
Figure 4.50: Detailed pictures from quarry, Rørvika unit.....	80
Figure 4.51: Pictures of brittle structures, Varpneset unit.....	81
Figure 5.1: 3D sketch of the study area.....	85
Figure 6.1: Photomicrographs from the Rødberget unit.	88
Figure 6.2: Photomicrographs from the Rødberget unit, brittle sample	89
Figure 6.3: Photomicrographs from the Trongen unit, east Ghms.....	91
Figure 6.4: Photomicrographs from the Trongen unit, west Ghms.....	92
Figure 6.5: Photomicrographs from the Trongen unit, garnets	93

Figure 6.6: Photomicrographs from the Trongen unit, Helle	94
Figure 6.7: Photomicrographs from the Trongen unit, Ams	95
Figure 6.8: Photomicrographs from the Trongen unit, aplites	96
Figure 6.9: Photomicrographs from the Rørvika unit, Ams.....	97
Figure 6.10: Photomicrographs from the Rørvika unit. Amis.....	99
Figure 6.11: Photomicrographs from the Rørvika unit, Amfs	101
Figure 6.12: Photomicrographs from the Rørvika unit, Fams.....	102
Figure 6.13: Photomicrographs from the Rørvika unit, brittle sample	103
Figure 6.14: Photomicrographs from the Varpneset unit, Hcqs.....	105
Figure 6.15: Photomicrographs from the Varpneset unit, garnets	107
Figure 6.16: Location map of samples for geochemistry	108
Figure 6.17: Harker diagrams, aplites	110
Figure 6.18: Discrimination diagram for aplites	111
Figure 6.19: Discrimination diagram for Ams	112
Figure 6.20: Geochronology.....	115
Figure 7.1: Spider diagram of Ams and samples from the literature	121
Figure 7.2: Discrimination diagram of Ams and samples from the literature.....	122
Figure 7.3: Interpreted geological map over the Trondheim area.....	125
Figure 7.4: Spider diagram and discrimination diagram of aplites with literature....	127
Figure 7.5: Flow model	130
Figure 7.6: Rotation of lineations.....	132
Figure 7.7: Schematic sketch of a synformal fold with related parasitic folds	133
Figure 7.8: All axial planes from this study, stereoplot.....	133
Figure 7.9: Schematic sketch of wedge.....	135
Figure 7.10: Basement windows	136
Figure 7.11: Model 1: Obstacle and buckling.....	138
Figure 7.12: Model 2: Rotation	139
Figure 7.13: Stress inversion of brittle structures.....	141

Abbreviations

Act	Actinolite
Afs	Alkalifeldspar
Am	Amphibole
Amfs	Amphibolitic schist with layers and lenses of felsic material
Amis	Amphibolitic to intermediate garnet-bearing schist
Ams	Amphibolitic schist
BSD	Backscatter Electron Diffusion imaging
Bt	Biotite
Cal	Calcite
Chl	Chlorite
Czo	Clinozoisite
Ep	Epidote
Fams	Tonalitic gneiss
Fsp	Feldspar
GBM	Grain Boundary Migration
Ghms	Garnet-hornblende-muscovite schist
Grt	Garnet
Hbl	Hornblende
Hcqs	Hornblende-calcite-quartz schist
Helle	Quartz-garnet-biotite-muscovite-hornblende schist
Hqs	Hornblende-quartz schist
Ing	Ingdal Granitic Gneiss
Kfs	K-feldspar
LA-ICP-MS	Laser Ablation-Inductively Coupled Plasma-Mass Spectrometry
Ma	Million years
MORB	Mid-ocean ridge basalt
Ms	Muscovite
MTFC	Møre-Trøndelag Fault Complex
NGU	Geological Survey of Norway
NTNU	Norwegian University of Science and Technology
Op	Opaque mineral
Or	Orthoclase
Pl	Plagioclase
PPL	Plane polarized light
Qtz	Quartz
Rt	Rutile
SEM	Scanning Electron Microscope
SEM-CL	Scanning Electron Microscope cathodoluminescence
Ser	Sericite
SGB	Subgrain Boundary
Ttn	Titanite
XPL	Cross polarized light
XRF	X-Ray Fluorescence
Zr	Zirconium

Introduction

This thesis addresses the existing interpretation of the Caledonian rocks of a given area on Fosen Peninsula in Sør-Trøndelag, concerning the lithological and structural history. The aim was to collect new field data in the study area and to propose an alternative/new/more thorough interpretation. The main emphasize has been on the study of fold systems and related structures, as well as on the description of the lithologies. In addition, to get a better understanding of the processes that have affected the area, analysis of geochemistry and U-Pb dating of zircons has been done, and the brittle history has been studied.

The selected area for this study is situated on the Fosen Peninsula in Sør-Trøndelag County. From Wolff (1976, 1978), the area has been described as amphibolite/greenstone in a synform surrounded by mica schist (Fig. 1.1). The amphibolite/greenstone was interpreted to be part of the Støren group and the mica schist part of the Gula Group. Later, Robinson and Roberts (2008) came up with a new interpretation (Fig. 1.2a) where the central amphibolites/greenstones still correlated with the Støren group and the mica schist to the south with the Gula group, whereas the mica schist north of the central amphibolites/greenstones was interpreted to belong to the Seve Nappe Complex. A new interpreted profile was not proposed. On large scale maps from Gee *et al.* (1985) (Fig. 1.2b) and Corfu *et al.* (2014) (Fig. 2.2), the entire area of focus is interpreted to belong to the Seve Nappe Complex. The granitic gneiss west in the study area is interpreted as Precambrian basement gneiss by all previous authors.

Consequently, three hypotheses have been proposed for this small area in the Trondheim region:

1. The central amphibolites belong to the Støren Nappe, while the surrounding schist represents the Gula Nappe.
2. The lithologies of Seve, Gula and Støren Nappe are present in the area.
3. The entire area of study belongs to the Seve Nappe Complex.

As a basis for the structural understanding of this area, small folds verging towards the northeast were studied at the Rørvika ferry terminal. The existing theory was that these folds were part of a larger synform as parasitic folds (Fig.1.3). A northwest dipping synform had been interpreted by Wolff (1976, 1978) on the western side of the amphibolite/greenstone antiform (Fig.1.1), and consequently also on the eastern side of the antiform.

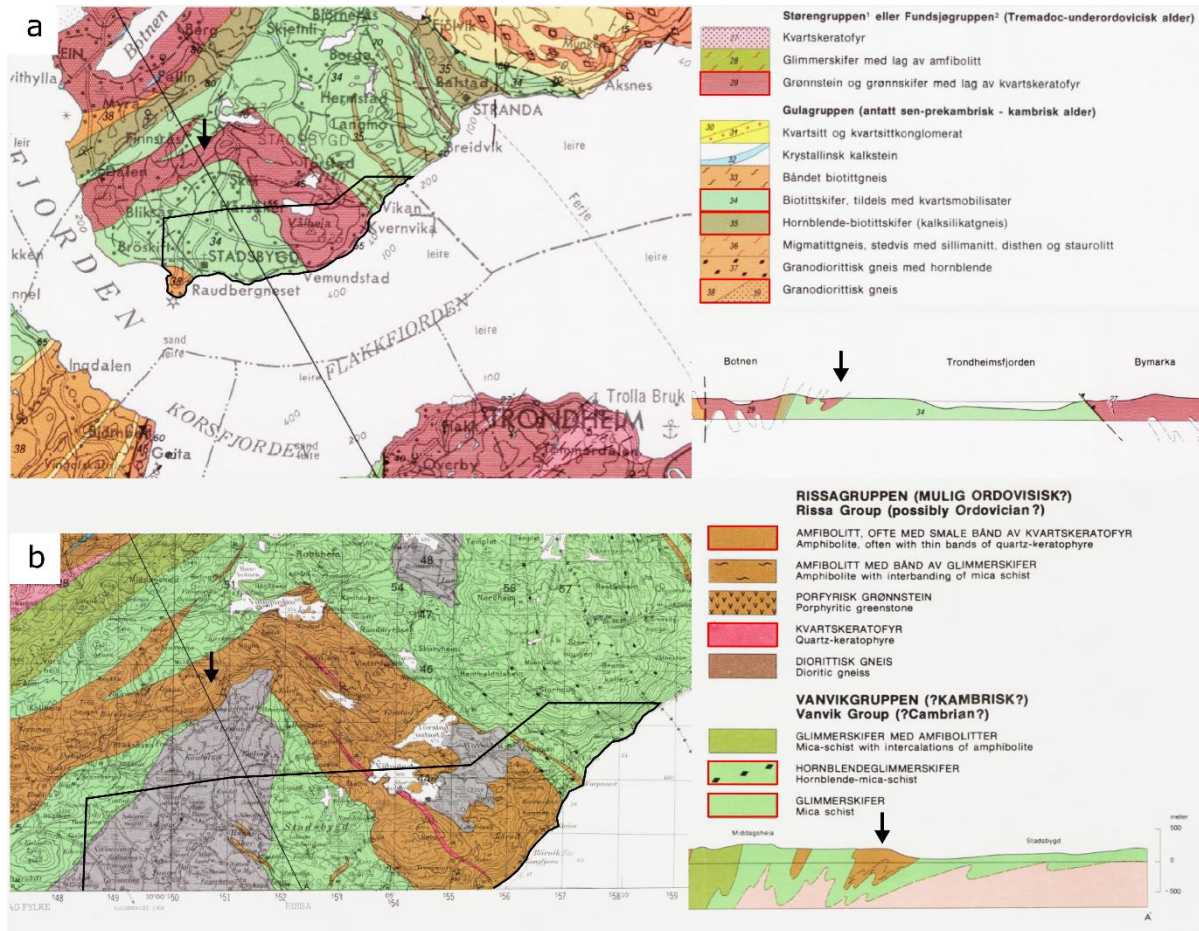


Figure 1.1: a) A clip of the bedrock map produced by Wolff (1976) with a scale of 1:250 000. b) A clip of the bedrock map by Wolff (1978). Note that for both a) and b) relevant lithologies are enhanced in the legend with a red box and that the interpreted synform is marked by an arrow both on the map and on the profile. The studied area for this thesis is marked by a solid black line. The amphibolites are correlated with the Støren Nappe, whereas the surrounding mica schists are correlated with the Gula Nappe. Notice that the colour of the central amphibolites/greenstones changes from a) to b).

From this, questions concerning the tectonostratigraphy and structural evolution of the study area arose. Are any of the hypotheses given above right? If not, how could the lithologies be related and where do they belong in the regional tectonostratigraphy? Does the central amphibolite area belong to the Støren Nappe south of the fjord? Are the mica schists to the east and to the west of the central amphibolite of the same unit? How would the units correlate to the southern side of the Trondheimsfjord? Is the central amphibolite located in the centre of a

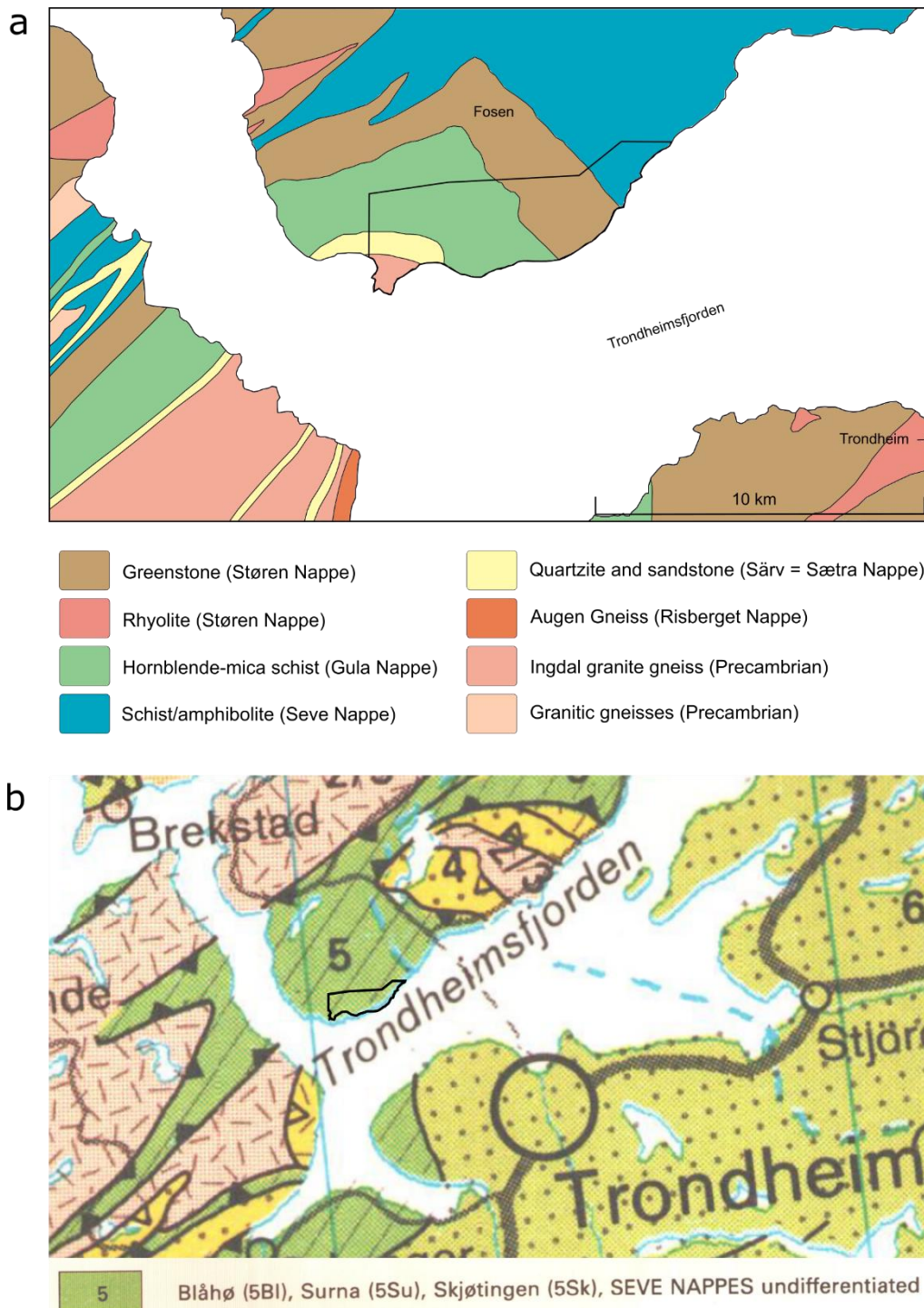


Figure 1.2: a) Modified map from Robinson and Roberts (2008). The study area for this thesis is marked with a black line. The area is interpreted to belong to the Gula, Støren and Seve nappes. b) Clip of the Trondheim region from the tectonostratigraphic map of Gee (1985). Study area enhanced with black line. In this model, the study area is entirely located within the Seve Nappe Complex.

synform? What is the pattern for the parasitic folds of the study area related to the folds observed at the Rørvika ferry terminal?

Through this study, old questions for an area central in the correlation of the northern and southern sides of the Trondheimsfjord were central. Together with new structural, geochronological and geochemical data, a new geological map is presented and interpreted. The remainder of this work is devoted to proposing a new interpretation for the given area on the Fosen Peninsula and discussing the implications this has compared to the regional geology of the Trøndelag region, Central Norway.

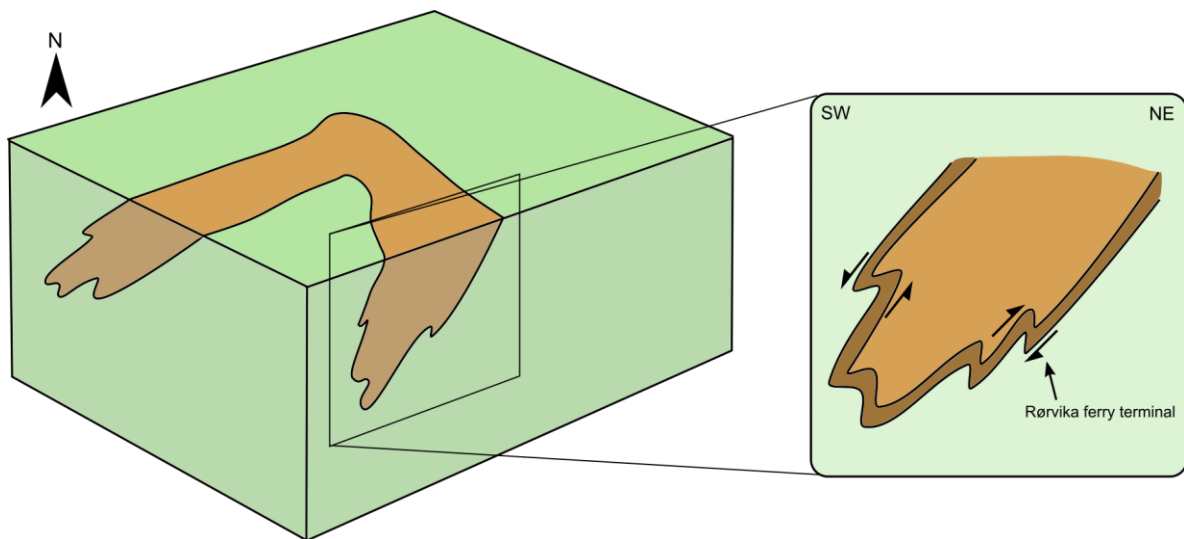


Figure 1.3: Schematic sketch of the structural interpretation of the synform according to Wolff (1976) and Wolff (1978) and showing how the NE-vergent folds observed at Rørvika ferry terminal could be related to it.

Geological setting

The geology of the study area is dominated by the effects of the continental collision between the two continents Laurentia and Baltica in Late Silurian to Early Devonian times in an event called the Scandian phase of the Caledonian orogeny. At the same time as the continental plate of Baltica was subducted beneath Laurentia as the ocean of Iapetus closed, slices of the Baltican basement, its cover and exotic terranes were thrust across the Baltoscandian craton towards the east-southeast (Stephens and Gee, 1985). Simultaneously, the western margin of the Baltican craton was subjected to shortening and high-grade metamorphism (Griffin *et al.*, 1985; Hurich *et al.*, 1989). Further, the study area is controlled by both ductile and brittle structures related to extension and transtension/strike-slip following the collapse of the Caledonian orogeny, mainly concentrated within a belt of semi-brittle to brittle faults called the Møre-Trøndelag Fault Complex (MTFC).

2.1 Caledonian tectonostratigraphy

Today, evidence of the Caledonian orogeny can be found all along the western margin of Scandinavia in Norway and Sweden (Fig. 2.1). The Caledonian rocks are divided into groups based on their characteristics and their interpreted origin. Stephens and Gee (1985) suggested to divide the units into four allochthons and this has since then been the most common way to subdivide the Caledonian rocks in Scandinavia. The rocks were grouped into the Lower, Middle, Upper and Uppermost Allochthons; the Lower and Middle Allochthons are interpreted as a derivation from Baltica and its outer margin, the Upper Allochthon derived from Iapetus, and the Uppermost Allochthon has its source from the Laurentian margin (Robinson and Roberts, 2008). Further research and more knowledge has shown that this model might be an oversimplification and a new way of looking at the Caledonides was proposed by Corfu *et al.* (2014); splitting the Caledonides into a southern, a central and a northern segment, and describing them due to their structures and composition. Below a short description of the

northern and southern segments of Norway follows, continued by a more thorough description of the central segment and the allochthons of Central Norway (Table 2.1).

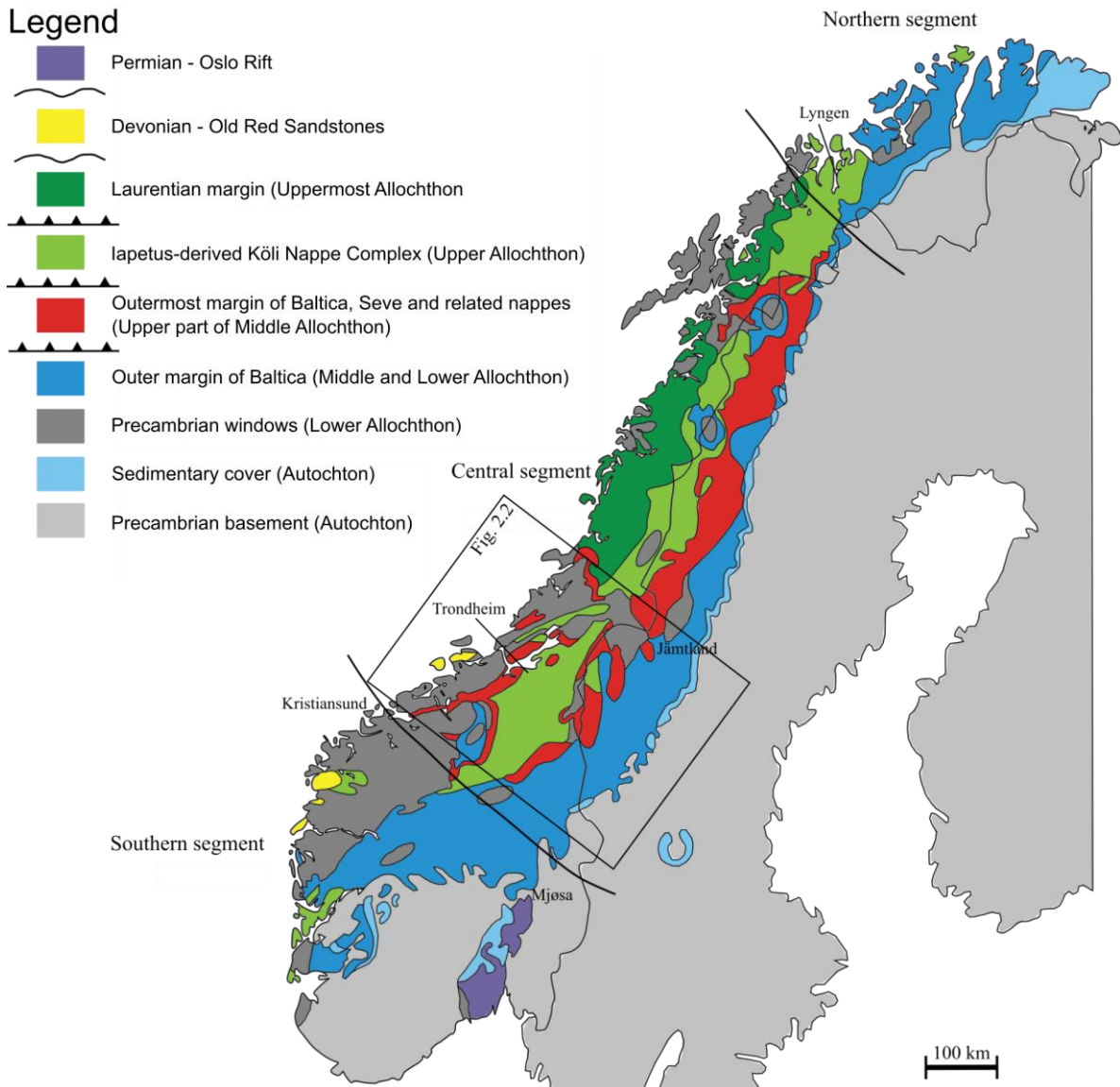


Figure 2.1: Map over the Scandinavian Caledonides in Norway and Sweden and the autochthon Precambrian basement. Modified from Gee *et al.* (2010). Shows the division on the southern, central and northern segment from Corfu *et al.* (2014).

2.1.1 Southern segment

The southern segment comprises the Caledonian rocks southwest of the axis between Mjøsa and Kristiansund (Fig. 2.1). The southern segment consists of autochthonous basement of Meso- to Neoproterozoic age in the east and southeast, overlain by parautochthonous to allochthonous Neoproterozoic and Cambrian rocks in a fold- and thrust belt. Moving to the northwest, allochthonous basement nappes of Meso- and Neoproterozoic age are situated below Paleozoic Nappes containing oceanic rocks. In the northwestern part of the area, the Western

Gneiss Complex (WGC) of Neo- and Mesoproterozoic age, experienced strong Caledonian deformation and up to ultra-high pressure metamorphism. Along the coast, several Devonian sedimentary basins occur (Corfu *et al.*, 2014).

2.1.2 Northern segment

The northern segment, including everything north and east of Lyngen, contains three main tectonic components above the basement (Fig. 2.1). The first is an autochthonous to parautochthonous sedimentary cover of Neoproterozoic to Paleozoic age lying on top of the basement. Second is the Kalak Nappe Complex, comprising allochthonous Mesoproterozoic to Early Paleozoic metasedimentary and igneous rocks. The uppermost unit consists of allochthonous meta-sedimentary and -plutonic rocks of Ordovician to Silurian age. The east to southeast-ward thrusting of the nappes structurally controls this segment, and no large-scale extensional shear zones have been described (Corfu *et al.*, 2014).

2.1.3 Central segment and related allochthons

The central segment, being the most relevant for this thesis, is described in more detail. As the name implies, the central segment is found in central Norway, between the southern and the northern segment (Fig. 2.1). Corfu *et al.* (2014) described four main components of this segment, from structurally below and towards the top being; 1) Late Neoproterozoic metasedimentary rocks in a basal fold-and-thrust belt with mafic dyke swarms and crystalline slivers in some areas. This is overlain by 2) the Seve Nappe Complex, comprising higher-grade metasedimentary, amphibolitic, and granitic and ultramafic rocks, again overlain by 3) Palaeozoic rocks in nappes with oceanic affinities. On top, there is 4) a complex nappe system comprising both Precambrian continental crust, Neoproterozoic to Early Palaeozoic platformal and flyschoid deposits, and Ordovician magmatic arc complexes (Fig. 2.1, Fig. 2.2).

The central segment shows mainly an upwards stepping of the thrustured nappes from east to west (Fig. 2.3). North-south undulations together with syn-compressional antiforms and late-orogenic extension result in basement to be exposed in windows. A major SW-trending, mainly post-Caledonian, strike-slip and normal fault zone has an important structural role in the area, MTFC (Fig. 2.2) (Seranne, 1992; Osmundsen *et al.* 2006).

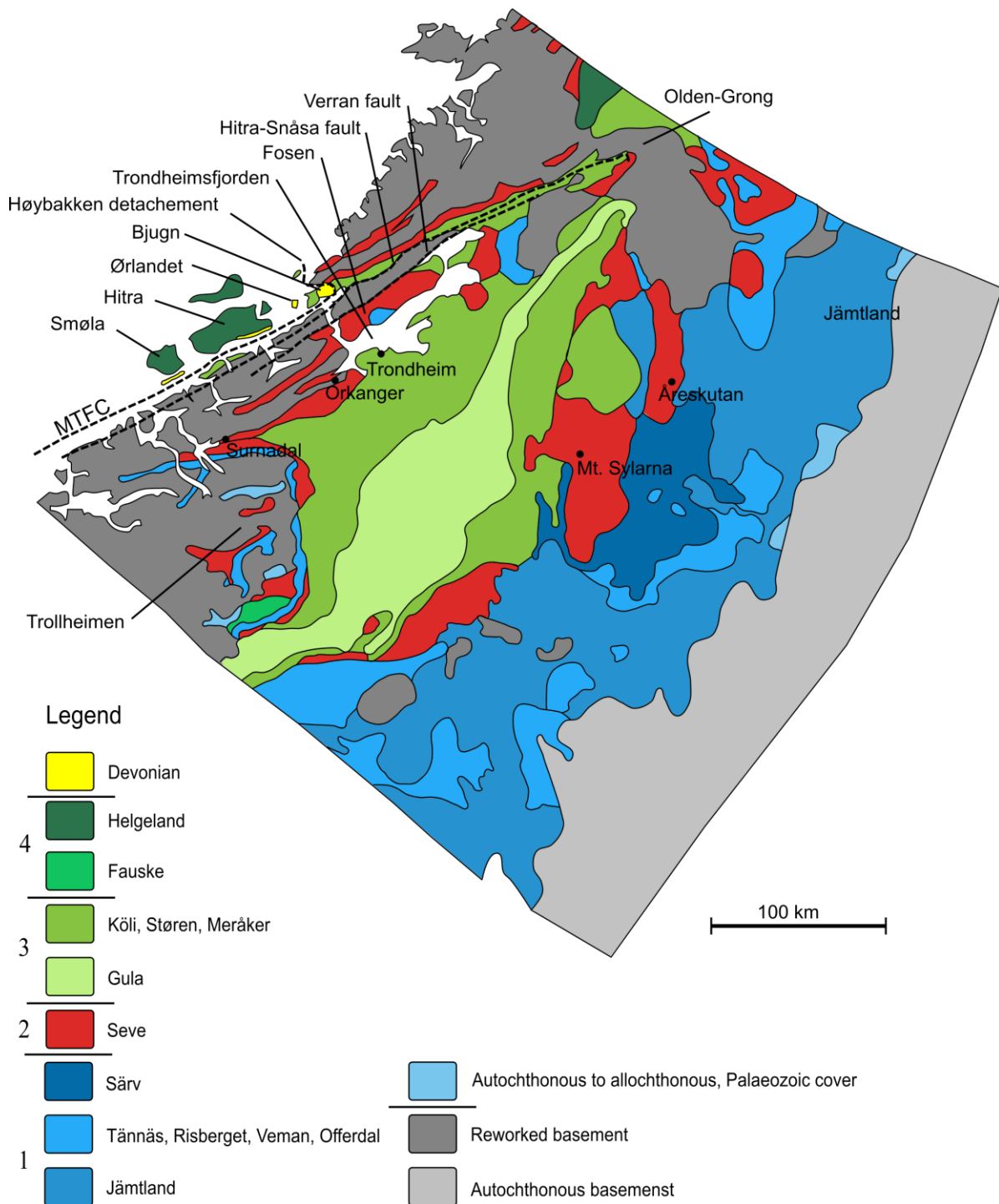


Figure 2.2: Map of the central segment. Colours coincide with those from Fig. 2.1. Modified from Corfu *et al.* (2014).

Baltican Basement

The Baltican crystalline basement is dated to ages ranging from 1650 to 1850 Ma in the foreland area in central Sweden (Gee *et al.*, 2014), while towards the southwest in the hinterlands of central Norway the autochthonous basement shows ages of about 1700-1650 Ma (Tucker *et al.*, 1990; Gee *et al.*, 2014) and 1150-900 Ma (Roffeis and Corfu, 2013;

Gee *et al.*, 2014). The basement consists of granitoid intrusive rocks from Late Paleoproterozoic later intruded by rapakivi granites at 1508 Ma and gabbros at 1657 +5-3 Ma and 1462±2 Ma (Tucker *et al.*, 1990).

It has been suggested that the basement exposed in the hinterland of the Caledonian orogen is not autochthonous compared to the Fennoscandian shield exposed in the foreland (Tucker *et al.*, 2004). This is shown by Nilsen and Wolff (1989) and Robinson (1997) when describing two levels of basement nappes exposed for example in Trollheimen and at Rekdalshesten. Both levels of basement have Neoproterozoic quartzite and pebble sized conglomerate on top, and the upper level is folded and thrust above the lower level. A second indication of the basement not being autochthonous came from deep seismic data taken from Trøndelag and into the basement in Sweden, known to be autochthonous. The seismic profile shows a shallow dipping major reflector interpreted to be the boundary between the allochthons and the autochthon. The basement windows lie above this boundary (Hurich *et al.*, 1988; Palm *et al.*, 1991; Juhojuntii *et al.*, 2001).

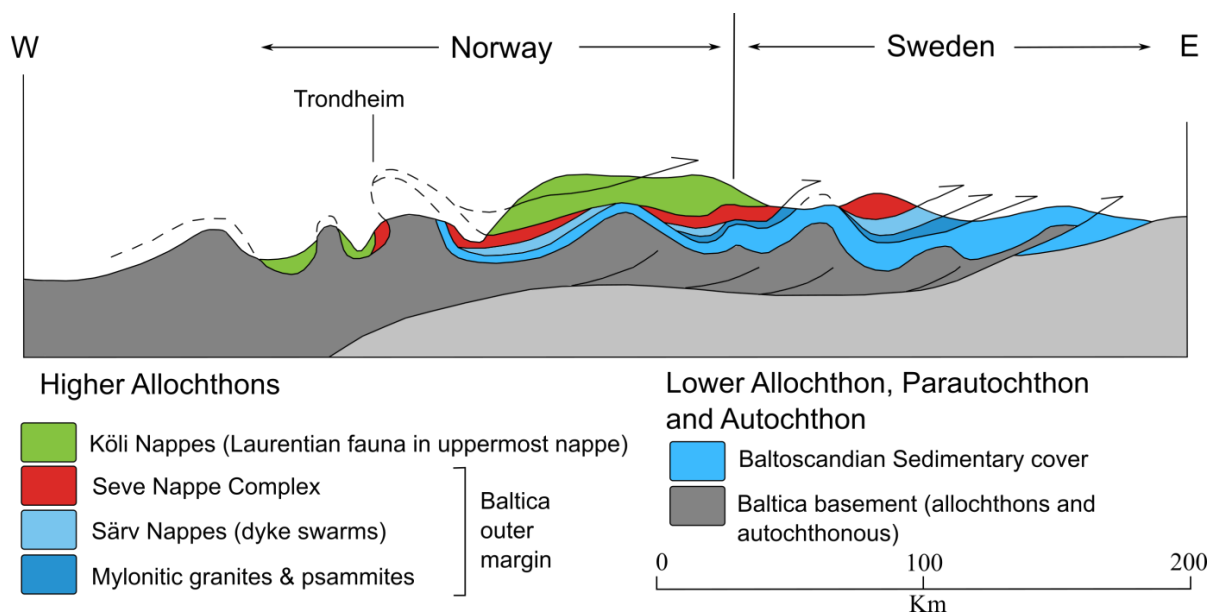


Figure 2.3: Profile from central Norway and Sweden, across the area around Trondheim. Modified from Gee *et al.* (2010).

Autochthon and fold-and-thrust belt

A thin cover of autochthonous to parautochthonous quartzites and conglomerate overlies the Paleoproterozoic to Mesoproterozoic basement in the foreland area of the central segment, being of Ediacaran to Cambrian age (Gee, 1980; Siedlecka *et al.*, 2004). This cover is again overlain by the Jämtlandian Nappe Complex in Central Sweden, a sedimentary sequence

estimated to be 2,5 km thick (Gee, 1975) where the facies indicates a lateral transition from a platformal margin to a foreland basin setting and at the same time shows Ordovician and Silurian episodes of subsidence and uplift (Corfu *et al.*, 2014). The Jämtlandian Nappe Complex comprises clastic sedimentary rocks and dolomite of Neoproterozoic age, tillite, quartzite, Cambrian shale, and greywacke, quartzite, as well as limestones and shale of Ordovician to Lower Silurian age (Gee, 1975; Nystuen *et al.*, 2008; Hedin *et al.*, 2014).

The Jämtlandian Nappe Complex is overlain by thrust sheets of the Veman/Tännäs Nappe, Offerdal Nappe, and Särsv Nappe, respectively containing megacrystic augen-gneiss, deformed metasandstones, and metamorphosed feldspathic sandstones and arkoses cut by mafic dykes. These nappes are found again west of the Trondheim synform, there with a higher grade of metamorphism and deformation (Krill, 1985; Roberts and Stephens, 2000; Hollocher *et al.*, 2007). In the Trondheim region, a nappe named Risberget correlates to the Tännäs Nappe in central Sweden. The Risberget Nappe contains rapakivi granites dated to two ages of 1659 Ma to 1642 Ma and 1190 Ma to 1180 Ma (Handke *et al.*, 1995).

Seve Nappe Complex

The Seve Nappe Complex overlies the fold-and-thrust-belt described above (Fig. 2.2). This nappe complex has a higher metamorphic grade than the nappes below and above, and it comprises psammitic and pelitic schists and gneisses, orthogneisses, amphibolites, eclogites and peridotites. The Seve Nappe Complex was by Zwart (1974) and van Roermund (1985) divided into three belts from east to west; lower, middle and upper Seve nappes. The lower Seve Nappe Complex is similar to the Särsv nappe below but it also contains retrogressed eclogites, the middle Seve Nappe Complex comprises migmatitic gneisses, amphibolites, eclogites and garnet peridotites, and the upper part of the Seve Nappe Complex consists of garnet micaschists. Detrital zircons from the Seve nappes show an Archaean component as well as many ages of 1800-1000 Ma (Gee *et al.*, 2014), and dolorite dykes and gabbros with an age of 605-610 Ma (Svenningsen, 2001; Paulsson and Andréasson, 2002; Root and Corfu, 2012). The metamorphic evolution has been studied in the Jämtland area where garnet show Sm-Nd ages of 460-450 Ma in the lower and central Seve Nappe Complex (Brueckner and van Roermund, 2007), and metamorphic zircons of the central nappe indicates an age of 446 Ma (Root and Corfu, 2012). In Åreskutan Nappe, southern Jämtland, Ladenberger *et al.* (2013) dated the peak-temperature metamorphism in garnets of central Seve Nappe Complex to 442±4 Ma, which is similar to the ages of leucogranites of 442 ± 3 Ma and 441 ± 4 Ma. From the same study, felsic segregations from within a migmatitic amphibolite showed a crystallization age of

436±2 Ma and pegmatites crosscutting the Caledonian foliation to an age of 428±4 Ma and 430±3 Ma.

Trondheim and Köli Nappe Complex

The Seve Nappe Complex is overlain by thrust sheets containing sedimentary and volcanic rocks of Palaeozoic age and mainly oceanic origin (Gee, 1975; Stephens and Gee, 1985; Roberts and Stephens, 2000). These rocks belong to the Trondheim Nappe Complex (south of the Grong culmination) and Köli Nappe Complex (north of the Grong culmination, Fig. 2.2). The Trondheim Nappe Complex is divided into the Meråker, Gula and Støren nappes, respectively from east to west (Fig. 2.2). Both Meråker and Støren Nappe contain ophiolites and island arc complexes of early Ordovician age, overlain by volcanic and sedimentary rocks of late Ordovician to early Silurian age (Gee, 1975; Grenne *et al.*, 1999; Slagstad, 2003). The relationship and the affinity of Meråker and Støren Nappe is discussed, with faunal evidence suggesting an affinity of the Støren Nappe to the Laurentian side of Iapetus (Pedersen *et al.*, 1992), and the affinity of the Meråker Nappe of Baltican origin due to Ordovician black shales comparable to black shales deposited on the Baltoscandian Platform in central and southern Sweden (Gee, 1981). Later, Hollocher *et al.* (2012) pointed out the similarity in map pattern (Fig. 2.2) and the discussion is still active. The affinity of the Gula Nappe is also under debate, the nappe containing continentally-derived rocks that might be related to a microcontinent with its origin suggested from Baltica but still largely unknown (Grenne *et al.*, 1999; Roberts *et al.*, 2002; Roberts, 2003).

Structurally above the Köli Nappe Complex and north of the Grong-Olden culmination, the Helgeland Nappe Complex is situated. It is a composite unit consisting of Precambrian to Ordovician margin platform rocks of Laurentian affinity, later intruded by granitoid batholiths with an age of 477 to 430 (Nordgulen *et al.*, 1993; Roberts *et al.*, 2007).

Devonian deposits

Several late- to post-orogenic sedimentary basins overly the Caledonian tectonostratigraphy as so-called 'Old Red Sandstone' basins (Steel *et al.*, 1985). These are found in the Trondheim region at Smøla, Ørlandet, Bjung and Hitra (Fig. 2.2). These basins are dominated by coarse conglomerates of continental origin mostly deposited as alluvial fans within the basins. At Hitra, the sediments are fine-grained sandstone, also of continental origin deposited in fluvial or alluvial plain environments. After deposition the sediments have been affected by deformation and by low-grade metamorphism (Seranne, 1992; Robinson and

Roberts, 2008). Based on palynological studies done north of Ørlandet an age of 403-394 Ma was given for the deposition of the sediments (Tucker *et al.*, 1998) and Ar-Ar studies of detrital K-feldspar suggested deposition at 387-382 Ma (Tucker *et al.*, 2004).

The sedimentary rocks in the Devonian basins in the Trondheim region lie on the upper plate of a major extensional detachment fault called the Høybakken detachment zone (Fig. 2.2) that carried both the Devonian sediments and the immediately underlying substrata for tens of kilometres to the southwest from their original site of deposition (Seranne, 1992; Osmundsen *et al.*, 2006). Seranne (1992) described the Høybakken detachment as a sharp tectonic contact with a low angle striking mainly north-south. The age of activity is interpreted to be 389 and 386 Ma, based on dating of synkinematic muscovite in shear zones and is also related to the formation of the Middle Devonian sedimentary basins (Piasecki and Cliff, 1988).

Table 2.1: Tectonic units used to describe the Caledonian succession of central Norway in this chapter, modified from Gee (1985), Robinson and Roberts (2008) and Corfu *et al.* (2014).

Classification based on allochthons	Tectonic units used during the description of the central segment (Corfu <i>et al.</i> , 2014)	Tectonic unit (Gee, 1985; Robinson and Roberts, 2008)
Late orogenic sedimentary rocks	Devonian	Devonian
Uppermost Allochthon	Helgeland, Rödningsfjället, Heggmo	-
Upper Allochthon	Köli, Støren, Meråker, Leka, Reisa, Gula	Trondheim Nappe Complex - Meråker Nappe - Gula Nappe - Støren Nappe Köli Nappes (Central Sweden) Seve (Blåhø) Nappe
Middle Allochthon	Kvitvola, Rondane, Tännäs, Veman, Offerdal, Akkajaure, Seve	Särv (Sætra) Nappe
		Risberget Nappe
Lower Allochthon	Osen-Røa, Jämtland	Absent in Trondheim region Jämtland Nappes (Central Sweden)
Autochthon, Parautochthon, Lower Allochthon	Autochthonous to allochthonous cover	-
Parautochthon, Lower Allochthon	Reworked basement	-
Autochthon	Autochthon	Precambrian crystalline basement

The Høybakken detachment terminates to the MTFC, which is an extensive structure that can be related to fault complexes in east Greenland, north Scotland and the Maritime Provinces of Canada (Ziegler, 1987), and can be directly related to the Caledonian mountain

chain and its break-up. Related to the major lineament of the MTFC, a high angle fault called Hitra-Snåsa Fault (Fig. 2.2) is observed (Grønlie and Roberst, 1989), which again splays into the Verran Fault (Fig. 2.2) (Seranne, 1992).

The MTFC has been active and reactivated several times, with brittle-ductile dextral transpression in Silurian time (Seranne, 1992), brittle-ductile to brittle and dextral transtension in Devonian time (Seranne, 1992; Braathen *et al.*, 2002; Osmundsen *et al.*, 2006), and brittle sinistral strike-slip motion in Carboniferous time (Torsvik *et al.*, 1989; Seranne, 1992).

2.2 The evolution of the Caledonian orogen

Break-up of Rodinia and independent drift of Laurentia and Baltica

Orogens generally show the remnants of a classical Wilson cycle, where continents rift and drift apart and then later close again and collide to build a new orogen. In Mesoproterozoic time, at about 1050 Ma, a supercontinent called Rodinia existed, where most continents were assembled together (Powell *et al.*, 1993; Hoffman, 1999). When this supercontinent started to break up at 725-750 Ma (Powell *et al.*, 1993), the continents of Baltica and Laurentia, then at an equatorial position, together drifted towards the south. By 600-580 Ma, these two continents drifted apart from each other, forming the Iapetus Ocean between them. Somewhere around the boundary between Cambrian and Ordovician the plate movement reversed, and the two continents started to drift towards each other again (Ramberg *et al.*, 2008).

Torsvik *et al.* (1996) and Torsvik *et al.* (2012) have proposed a different plate tectonic reconstruction, unlike the most popular theory of Baltica and Laurentia breaking apart from Rodinia, and then later they moved together again. They propose that the Caledonian margin might have rotated and was facing other terranes and continents as Baltica moved further north in the Late Neoproterozoic. Avalonia-Baltica plate collided with Laurentia about 430 Ma at an equatorial position.

The closure of Iapetus: onset of subduction and arc-magmatism

From the Late Cambrian onwards, subduction and arc-processes started on both the Laurentian and Baltican Iapetus margins, slowly closing the Iapetus Ocean. As the ocean closed, in Late Cambrian time, subduction-zone ophiolites and oceanic and/or continental arcs formed, and from about 480-470 Ma, the ophiolites of the Köli Nappe got emplaced on top of the Baltoscandian margin, on the Gula microcontinent (Fig. 2.4a) (Grenne *et al.*, 1999; Roberts and Stephens, 2000; Slagstad, 2003; Slagstad *et al.*, 2014). This was followed by a

subduction of the Seve nappes beneath the Köli nappes at about 450-445 Ma, where the Seve nappes were exposed to ultra-high pressure, then later exhumed and thickened (Fig. 2.4b) (Brueckner and van Roermund, 2004; Hacker and Gans, 2005).

The period from 445 to 435 Ma (Fig. 2.4c) is characterized by a magmatic event where dykes intruded the Köli Nappe. These dykes show derivation from both melting of a mantle in a continental rift setting and melting of mafic crustal rocks (Dunning and Grenne, 2000; Hansen *et al.*, 2002; Nilsen *et al.*, 2007). During the same period, batholiths intruded the Laurentian margin in an arc setting on the other side of the Iapetus Ocean (Nordgulen *et al.*, 1993).

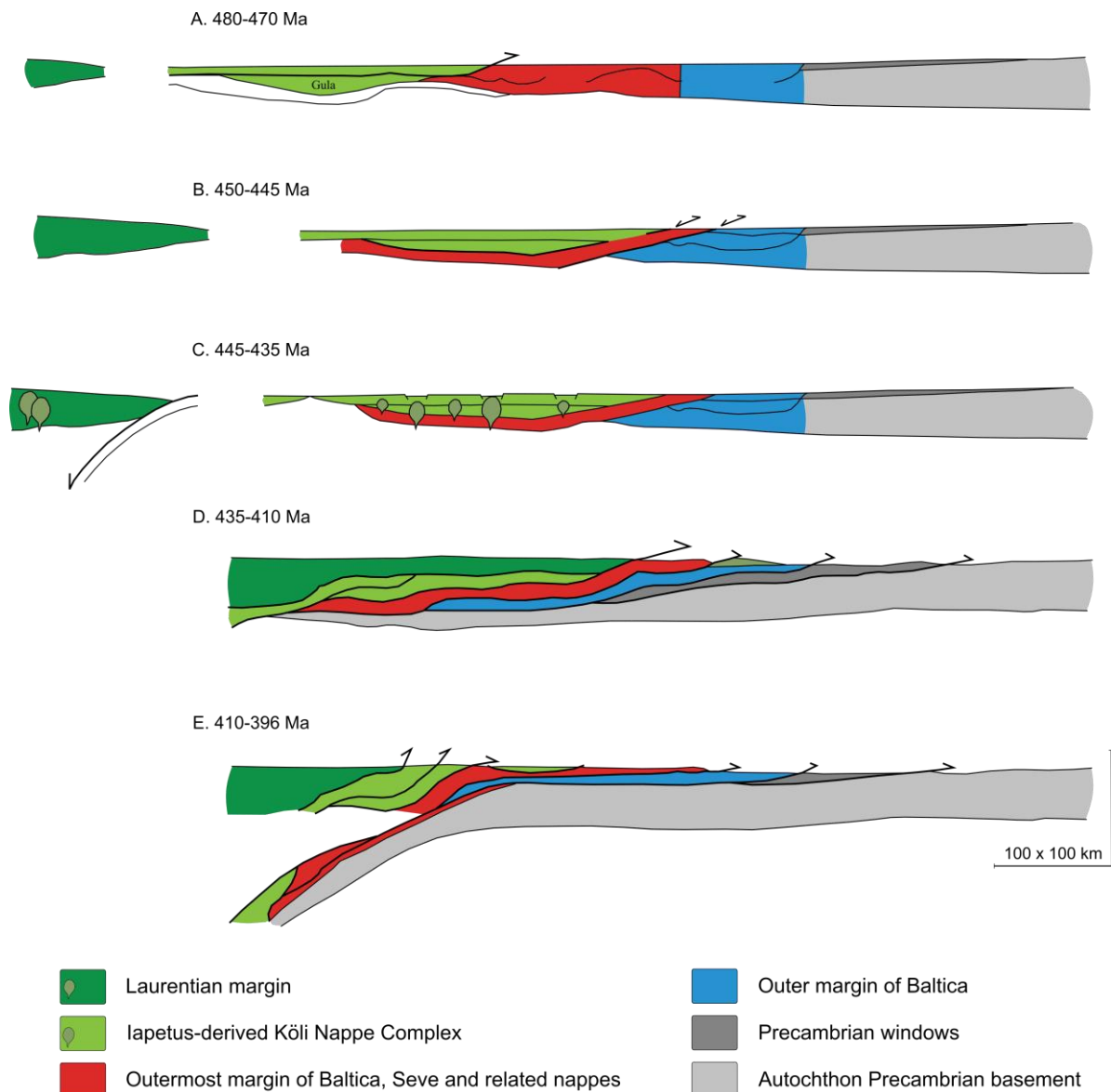


Figure 2.4: Conceptual sketch of the evolution of the Caledonian orogeny. Modified from Hacker and Gans (2005).

Continent-Continent collision: the Scandian phase

From about 430 Ma onwards, the continents of Laurentia and Baltica collided with the Baltican margin being subducted below the Laurentian, creating the Caledonian orogen in the main collisional Scandian phase (Torsvik *et al.*, 1996). The Scandian phase resulted in nappes being thrust on top of the Baltic shield, causing rocks to be moved great distances (Gee, 1985).

From 430 - 410 Ma (early-Scandian phase) there was a westward stacking of nappes where both the nappes of outer and outermost margin of Baltica, Iapetus-derived nappes and the nappes with Laurentian affinity got transported on top of the Precambrian basement (Fig. 2.4d) (Gee, 1985). In the early Middle Scandian phase (410 – 406 Ma) the imbrication and the deep level thickening continued. The gravitational potential created possibilities for a foreland and hinterland-directed extension, which further led to deposition in the Devonian basins at the surface (Roberts and Sturt, 1980; Tucker *et al.*, 2004).

From 406 – 396 Ma, in late Middle Scandian, the subduction and imbrication continued now including parts of the Baltican Proterozoic basement (Fig. 2.4e). This subduction led to high pressure to ultra-high pressure metamorphism, local partial melting and formation of pegmatites, metamorphic zircon growth at 401 ± 2 Ma and early top-to-southeast fabrics in the basement. Towards the end of this period, parts of the subducted slab broke off and were thrust above the cooler basement and Neoproterozoic cover above the basement (Tucker *et al.*, 2004; Robinson and Roberts, 2008).

Extensional collapse

By the early Middle Devonian, in early Late-Scandian time, 396 – 390 Ma, the basement slab continued to cool at the same time as the rocks underwent top-to-west ductile extension developing into a sinistral shear field. Early folds related to the thrusting were deformed into isoclinal to recumbent folds that became refolded in open and more upright folds. The open folds were commonly overturned towards the northwest and having northeast-southwest trending axes. In addition, a northeast-southwest lineation and top-to-west sinistral shear fabrics developed (Braathen *et al.*, 2002; Roberts, 2003; Osmundsen *et al.*, 2006; Robinson and Roberts, 2008). The rocks went from an upper amphibolite facies to low amphibolite facies through this period (Tucker *et al.*, 2004).

The sinistral and top-to-west extension continued into Late Scandian time (390 – 376 Ma), but now turning into semi-brittle to brittle deformation. It was during this period the Støren

Nappe and the Devonian clastic basinal sediments were displaced along the Høybakken detachment with a top-to-southwest extensional shearing with a displacement of 80-100 km. At the same time the MTFC was active with reactivated brittle sinistral shearing creating folds parallel to the extension (Roberts, 2003; Osmundsen *et al.*, 2006).

Methods

Fieldwork

The gathering of data for this thesis was carried out through the months of July, August and September 2015 over 5 weeks in total, where 1.5 weeks were carried out together with Anne Kathrine Svendby. Transportation was mainly done by biking, walking and ferry (between Flakk-Rørvika), and during the fieldwork with Anne Kathrine Svendby a car was used. Camping in tent was done during one week to save time from transportation back and forth between Trondheim and the field area.

The data sampling was first done by the use of maps printed from www.norgeskart.no, a service by the Norwegian Mapping Authority (Kartverket), and a Garmin GPSMAP 64s, and later by a Panasonic ToughbookCF H2 Field with ArcGis 10.0 installed and integrated GPS. Registration of localities, structural measurements and other data gathered was done in BGS SIGMAmobile 2012, a digital field capture system developed by the British Geological Survey that is run together with ArcGis and the Microsoft Office program Access 2007 (<http://www.bgs.ac.uk/research/sigma/home.html>). Pictures were taken with a Nikon D5000 and with the scales being mainly a compass (6.5x8 cm), pencil (about 15 cm), and hammer (height of 28 cm). Structural data were measured with a Harbin Slim-Line Pocket Transit H-DQL-2A/DQL-2A/DQL2A Geological Compass and a Freiburger Geological Stratum Compass. All measurements were of the dip and dip direction of planes and trend and plunge of lines.

Samples were taken from the different lithologies, in total 24 samples for thin section representing 7 samples of amphiboles, 6 aplites, 8 mica schists, one granitic gneiss and two samples from fractures zones (Appendix H). The 6 of the samples of aplites and one from an amphibolite were sampled at a reasonable size to do further petrological work. In addition, an

intermediate layer and three aplites were collected for geochronology. The samples were not oriented.

Map construction and structural interpretation

ArcMap 10.2 and 10.3 from ESRI were used to construct a map of the study area from the gathered data together with the observation points registered in SIGMAmobile from fieldwork.

To analyze the structural data gathered in field, the program Stereonet 9.6.0 by Rick Allmendinger (Cornell University) was used (<http://www.geo.cornell.edu/geology/faculty/RWA/programs/stereonet.html>). Plotting of stereonet of foliations, lineations, fold axis, axial planes and faults were done. The program was also used to do rotation of measurements around a fold axis.

Win-Tensor 5.8.4 by Dr. Damien Delvaux (Royal Museum of Central Africa) was used to do stress inversion analysis of measured faults (http://www.damiendelvaux.be/Tensor/WinTensor/win-tensor_download.html). By registering the fault plane, the slip direction and the sense of shear, a stress field for the formation of the faults can be found.

To stitch photos and make figures the software Adobe Photoshop and Adobe Illustrator and the freeware Inkscape were used.

Sample preparations

Samples for thin sections were cut on a diamond saw at the Geological Survey of Norway (NGU), cut parallel to the lineation and perpendicular to the foliation. Thin sections were prepared at the Norwegian University of Science and Technology (NTNU) at the thin section laboratory at the Department of Geology and Mineral Resources Engineering. All thin sections have a size of 28x48 cm and a thickness of 30 μ m, and a selection was polished.

Polarized light microscopy was done on both a Zeiss Axioskop 40 and an Olympus BX60F-3 at NGU and the identification of the mineral assemblage of the samples was carried out. Pictures were taken with a Zeiss AxioCam MRc5 camera mounted on the Zeiss Axioskop.

Geochemical analysis

The XRF (X-ray fluorescence) method is used to determine mainly the major elements, but also trace element chemistry in the chosen rock samples. This was done at the laboratory at NGU with the instrument PANalytical Axios 4 kW XRF. To do the analyses of the main elements, small glass pills are put together from 0.6 g of the sample material mixed with 4.2 g

lithium tetraborate ($\text{Li}_2\text{B}_4\text{O}_7$). The samples were exposed to heats of 1000°C before melting. The analyzed data is calculated back to the original sample before being exposed to heat. The trace elements were analysed by pressing together small pills consisting of 9.6 g of the sample material and 2.4 g of wax.

The program IgPet – Igneous Petrology software, was used to interpret the data of main and trace elements received from the XRF (<https://www.rockware.com/-product/overview.php?id=102>).

Geochronology

Samples for geochronological analyzes were first crushed and separated at the laboratory at NGU. Conventional magnetic and heavy liquid techniques were used to separate zircons from four samples (AAH_246, AAH_300, AAH_380, DGA_4).

Zircons were extracted from separated fractions with the help of an Olympus SZH10 and Olympus Highlight 2001 binocular and handpicked with tweezers at NGU. The chosen zircons were mounted on a tape attached to a plexiglas. Epoxy was poured over the mounted zircons and the tape and plexiglas were later removed and the epoxy mount polished down to expose the grain centres of the zircons. A 1450 Variable Pressure SEM (Scanning Electron Microscope), LEO Electron Microscopy Ltd, was used to take pictures of the zircons, both with backscatter electrons (BSD) imaging and with cathodoluminescence imaging (SEM-CL) prior to analysis.

LA-ICP-MS (Laser Ablation-Inductively Coupled Plasma-Mass Spectrometry) was performed using a New Wave UP193FX Excimer laser coupled to a Thermo Element XR single collector high resolution ICP-MS at NGU, operated by Øyvind Skår. A $15\mu\text{m}$ wide line scan at a speed of $2\mu\text{m}/\text{sec}$ was used at energies of $4.0\text{ J}/\text{cm}^2$ and a repetition rate of 10 Hz. ca 0.4 l/min. He gas was used as a carrier gas flushing through the sample chamber, mixed with ca 0.9 l/min Ar gas and transported to the ICP-MS. The measurement time was first 30 s of gas blank acquisition and thereafter up to 30 s data acquisition. Masses ^{202}Hg , $^{204}\text{Hg} + ^{204}\text{Pb}$, ^{206}Pb , ^{207}Pb , ^{208}Pb , ^{232}Th and ^{238}U were acquired in a time-resolved counting scanning mode. ^{235}U was recalculated from the natural abundance for $^{238}\text{U}/^{235}\text{U}$ (Steiger and Jäger, 1977). The measured isotope ratios were corrected for element- and mass-bias effects using the zircon standard GJ ($607 \pm 0.4\text{ Ma}$; (Jackson *et al.*, 2004)). The zircon standards 91500 ($1065 \pm 0.3\text{ Ma}$; (Wiedenbeck *et al.*, 1995)) and Temora II ($416.5 \pm 0.22\text{ Ma}$;) were used as control standards, and reference zircons ØS-99-14 ($1797 \pm 3\text{ Ma}$; Skår (2002)), Z6412 ($1160 \pm 1.6\text{ Ma}$;

Methods

unpublished, GSC Ottawa) and the in-house standard T33187 (2674 ± 8 ; unpublished, NGU) were used for standardization. The data were not corrected for common Pb, but the signal from ^{204}Pb is used to exclude analyses containing common Pb. The data reduction was done with the GLITTER® software version 4.4.4 (Van Achterberg *et al.*, 2001) by Torkil Sørli Røhr. U-Pb ages of the zircons are calculated using the ISOPLOT 4.15 software for Microsoft Excel version 2.49 (Ludwig, 2001).

Field results

4.1 Geographical setting

The studied area is located on the Fosen peninsula, in Sør-Trøndelag, Norway (Fig. 4.1a), and stretches from Rødberget in the southwest to the border between the counties of Sør-Trøndelag and Nord-Trøndelag in the northeast (purple line in Fig. 4.1b (Norgeskart.no, 2015)). The area covers about 20 km², with a width from east to west of about 10 km and length from north to south of about 5 km.

Towards the south the mapped area is bounded on its longitudinal axis by the coastline facing Trondheimsfjorden (Fig. 4.1). The outcrops along the coastline are well exposed and scoured by the washing from the sea. The border towards the north was chosen about 2 km inland so that the map provides a section across the NW-SE striking units.

The topography in the area is characterized by moderately steep terrain rising from the fjord up to 320 meters above sea level at Vålheia. Most of the terrain is covered by shrubs and coniferous vegetation in the steeper hills, and where the ground has a low inclination agricultural land dominates. In the area of Statsbygd, Quaternary deposits and agricultural land reveal few outcrops, except for Rødberget in the south (Fig. 4.1b).

The main road stretches along the coast in the eastern part of the mapped area and turns NW into Stadsbygd in the western part (Fig. 4.1b). In addition, a gravel road runs parallel to the shoreline all the way to Statsbygd. There are a few farms and buildings in the steeper terrains around Rørvika (Fig. 4.1b) and towards the northeast within the mapped area. Around Trongen, farm buildings and houses are located in near proximity to the road (Fig. 4.1b). Most of the infrastructure is concentrated in Statsbygd, with houses, stores and industry.

Near S kyråsen (Fig 4.1b) there is a recreational area maintained and used by the inhabitants of the area.



Figure 4.1: a) Geographic map showing location of the studied area (Norgeskart.no, 2015). b) Detailed geographic map over the studied area (Norgeskart.no, 2015).

4.2 Lithological description of mapped units

In this study, the area is subdivided into four large-scale lithological units, namely the Rødberget, Trongen, Rørvika and Varpneset units (Fig. 4.2). The division was done based on most prominent characteristics of mineralogical and textural observations from the field, and not necessarily the most abundant minerals. Moving from west towards the east, a description of the different units follows.

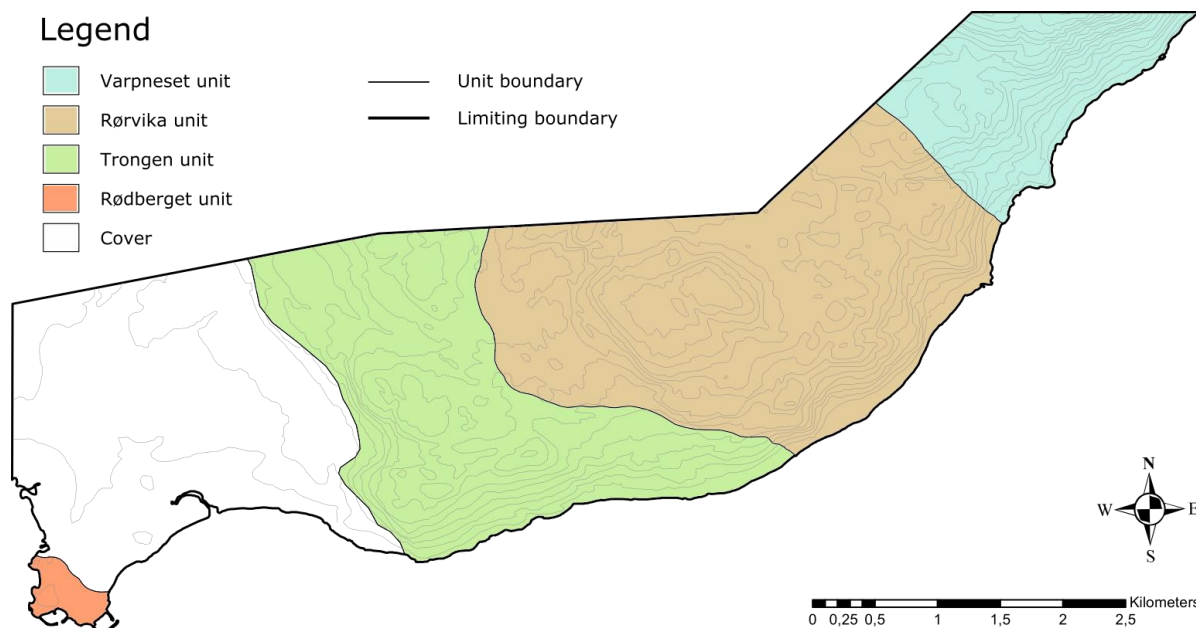


Figure 4.2: Simplified geological map showing the Rødberget, Trongen, Rørvika and Varpneset units.

4.2.1 Rødberget unit

The Rødberget unit crops out in the western part of the studied area at Rødberget (Fig. 5.2; Appendix A). There are no observable boundaries to other rocks, only to vegetation and agricultural land. The Rødberget unit is comprised of easily recognizable Ingdal granitic gneiss, of a strong red to pinkish and greyish colour. The rock is massive and homogeneous, and shows a weak penetrative foliation in some areas (Fig. 4.3a and b). Throughout the rock, there are small variations in grain size, from fine to medium, and in the colour, from strong pink to red, to weak pink and grey. This gives the rock a layered appearance in some areas, especially towards the west, where some layers have pink “augen” in a fine grained pink matrix, alternating with fine grained greyish to pink layers (Fig. 4.3c and d). The augens have a size of about 1-3 cm and a preferred orientation parallel to the foliation.

In several localities, deformed mafic dykes were observed oriented sub-parallel to the foliation of the gneiss. The dykes may be of metamorphosed dolerite and are dark grey to

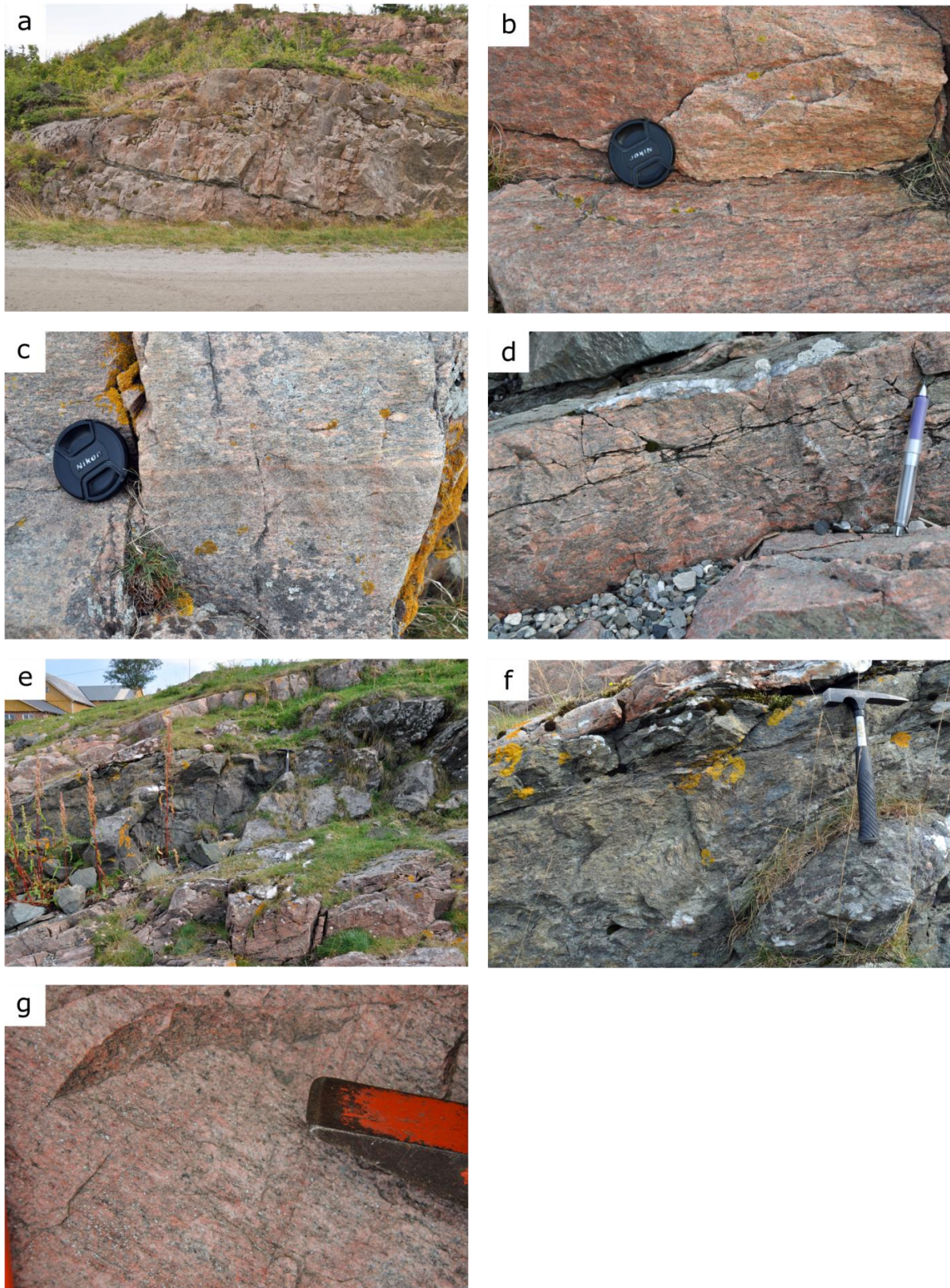


Figure 4.3: a) Outcrop of the characteristic pink Ingdal granitic gneiss. The picture also shows a 15 cm thick mafic dyke cutting the outcrop sub parallel to the weak and penetrative foliation. Loc. no. KSV_63. b) Close-up of the pink Ingdal granitic gneiss. Loc. no. KSV_55. c) The Ingdal granitic gneiss varies in colour from

green in colour (Fig. 4.3e and f). The different dykes vary in thickness, from 15 cm (Fig. 4.3a) to almost a meter (Fig. 4.3e), and lateral extensions that can be observed from 10 to 20 meters. In some places the dykes are folded and show a crenulation cleavage, giving them an undulating appearance (Fig. 4.3f).

The Ingdal granitic gneiss consists of feldspar, quartz, biotite and muscovite. The appearance of the different minerals varies through the outcrops. The quartz is white to grey in colour and is fine- to medium-grained. The feldspar is determinative for the characteristic colour of the gneiss, varying from a strong reddish pink to a weaker pink and grey colour. Normally, the feldspar is found as fine- to medium-grained crystals in a homogeneous matrix, but in some localities there are also 1-2.5 cm augens of feldspar (Fig. 4.3d).

There are minor amounts of both muscovite and biotite to be found in the Ingdal granitic gneiss, varying from about 2-8 % of the rock. Fine grained muscovite and biotite are spread randomly throughout the rock as separate grains (Fig 4.3g). Biotite is also found in zones and layers with an orientation deviant of the foliation and lineation in the rock.

4.2.2 Trongen unit

The Trongen unit crops out in the area around Skyråsen and Trongen and northwest towards Stadsbygd (Fig. 4.2; Appendix A). The landscape of Trongen is dominated by coniferous woods, fields, farms and cabins, which make many outcrops small and hard to find. Along the roads and shore there are well-exposed outcrops without vegetation.

The Trongen unit is the most complex in terms of bedrock diversity, with several types of rock present. The three main lithologies separated on the map are i) garnet-hornblende-muscovite schist (Ghms), ii) quartz-garnet-biotite-muscovite-hornblende schist (Helle), as well as iii) lenses, layers and bigger zones of amphibolitic schist (Ams) (Appendix A).

Garnet-hornblende-muscovite schist (Ghms)

The Ghms is fine- to medium-grained with mm- to cm-sized garnets throughout (Fig. 4.4a). It shows a characteristic brown to golden weathering colour (Fig 4.4a) and is generally

Fig. caption cont. pink to grey and in grain size from small grained to cm sized augens of feldspar. Loc. no. KSV_60. d) Detail of the granitic gneiss below the dyke in e), here with red augens of feldspar showing a preferred orientation parallel to the foliation. Loc. no. KSV_58. e) The granitic gneiss with an 80 cm thick green to grey dyke parallel to the foliation. Loc. no. KSV_58. f) A close-up of the dyke shows the crenulated appearance of the dyke and its greenish colour. Loc. no. KSV_58. g) The muscovite grains are visible on the surface as shiny silver grains. Loc. no. AAH_342.

foliated (Fig. 4.4b) and in places crenulated (Fig. 4.4c). Within the Ghms, quartz lenses and layers are themselves folded and discontinuous, found in some places as isoclinal folds and in other places as quartz blobs. Cm- to m-scale layers and lenses of amphibolitic rocks are folded and boudinaged together with the Ghms at several localities (Fig. 4.4d). In transitional zones to the Helle lithology, the Ghms also contains biotite. In small areas mapped as Ghms garnet is absent.

In the westernmost part of the Trongen unit there is an outcrop along the coast, 170 metres wide, with a rock different from the surrounding Ghms (Locality 348, Appendix A). The rock is penetratively foliated, layered and has a light grey to greenish colour (Fig. 4.4e and f). It contains garnets, quartz, muscovite, biotite and small amounts of hornblende, and it contains finely distributed carbonate throughout. The rock is hard, with a high content of quartz, 50% or more. Moving upwards in the rock column of the outcrop, the rock becomes more fine grained, with the lighter coloured layers containing more quartz whereas the darker increments being richer in biotite. Muscovite is found throughout the section. This rock is not mapped as an own lithology due to the small lateral extent.

Within the Ghms lithology subordinate hornblende-biotite schist (Hbs) occurs. The Hbs is found within the Ghms as lenses from a few cm to more than 10 meters (Fig. 4.5a), or interlayered with the Ghms (Fig. 4.5b). The Hbs is mostly found along the coastline where the outcrops are abundant and clean of vegetation. The Hbs shows a characteristic penetrative foliation, and consists of fine grained quartz, biotite and amphibole. The quartz within the Hbs matrix shows a characteristic fine-grained sugar texture. Pink garnets are present a few places and restricted to specific layers (Fig 4.5c). The garnets show a great variation in size, from 0.3-2 cm in diameter, and show a anhedral to euhedral shape (Fig. 4.5d). Because of the high mica content in the Ghms this rock is less competent than the Hbs, and consequently the Hbs is found also as boudins and lenses within the Ghms (Fig. 4.5e). A boudinaged calc-silicate layer with greenish colour was at one locality observed within the Hbs (Fig. 4.5f). The relationship between Ghms and Hbs can be studied at Oksvika (Locality AAH_322, Appendix A), where Ghms interlayered with Hbs is deformed and folded together (Fig. 4.6).

Quartz-garnet-biotite-muscovite-hornblende schist (Helle)

Helle differs from Ghms in grain size, mineral content and in the general characteristics expressed in the field. Helle is a homogeneous, massive and quartz-rich schist containing garnets, hornblende, muscovite and biotite. It is fine-grained, with a brown to grey

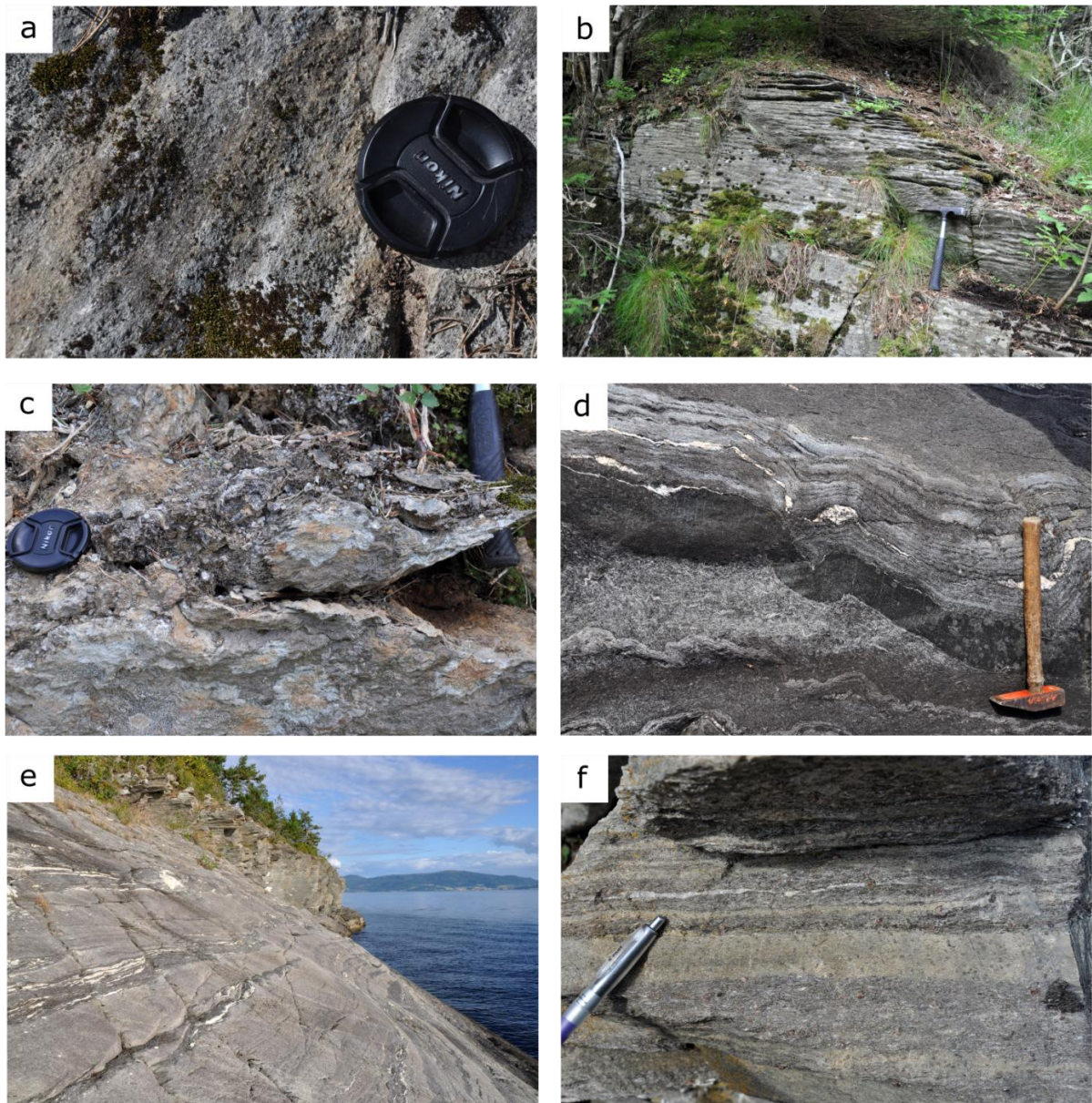


Figure 4.4: a) The Ghms within the Trongen unit has a golden brown to silver weathering colour. The garnets are resistant to the weathering and consequently protrude from the surrounding rock in the process of erosion. Loc. no. AAH_269. b) Due to weathering, the normally weak foliation in the Ghms can be apparent. Loc. no. AAH_340. c) Strongly crenulated Ghms. Loc. no. AAH_327. d) Alternating layers of amphibolitic rock and Ghms folded together. Loc. no. AAH_177. e) Layered and penetratively foliated quartz-rich schist containing garnets. Loc. no. AAH_348. f) Overview of the same rock as in e) showing a clear layering. Loc. no. AAH_348.

weathering colour (Fig. 4.7a). Some places Helle shows a weak foliation, which is often crenulated as well. Quartz veins in Helle are about 1-3 cm thick and are mostly straight and laterally continuous, but may be affected by isoclinal folding (Fig. 4.7b).



Figure 4.5: a) Outcrop of Hbs with big aplite boudin. Loc. no. AAH_305. b) Hbs on the lower half of the picture and Ghms on the upper. The Hbs is straight and penetratively foliated, interlayered with aplites and quartz veins. Also lenses and boudins of Hbs can be observed within the Ghms. Loc. no. AAH_124. c) Hbs with its typical straight penetrative foliation where some layers contain pink, anhedral, and coarse-grained garnets, 0,3-2 cm in diameter. Loc. no. AAH_322. d) Close-up of anhedral and subhedral pink garnets. Loc. no. AAH_120. e) A boudin of Hbs within the Ghms with the sense of shear top to NW. Loc. no. AAH_124. f) Boudins of green rock, possibly representing calc-silicate pods, within the Hbs. Loc. no. AAH_124.

All major outcrops, exposing the rocks representative for the Trongen unit are found in the vicinity of the coastline. The boundary from Helle to Ghms is transitional over a larger area, with a gradual change in grain size and mineral content (Fig. 4.6). The amount of biotite in Helle decreases and the rock becomes less homogeneous, coinciding with a transition in the

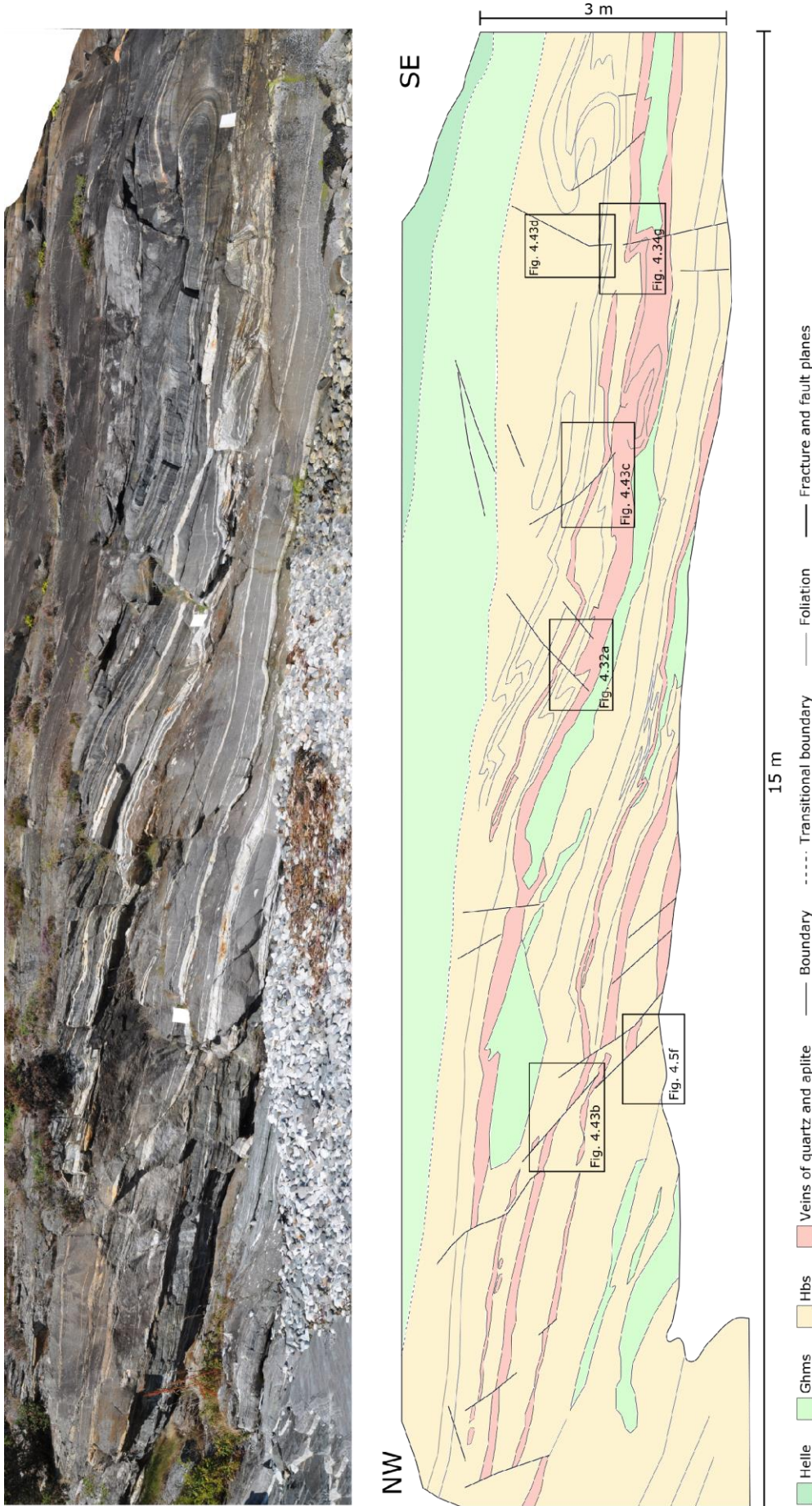


Figure 4.6: Profile of Loc. no. AAH_124 from figure 4.33 (Locality AAH_322, Appendix A). This outcrop shows the transition from Hbs, to Ghms and then into Helle, and the Ghms layers and lenses of Ghms within the Hbs. In addition, ductile and brittle deformation can easily be seen from the outcrop.

quartz veins, changing expression from straight to more folded and deformed as one moves from Helle towards the Ghms.

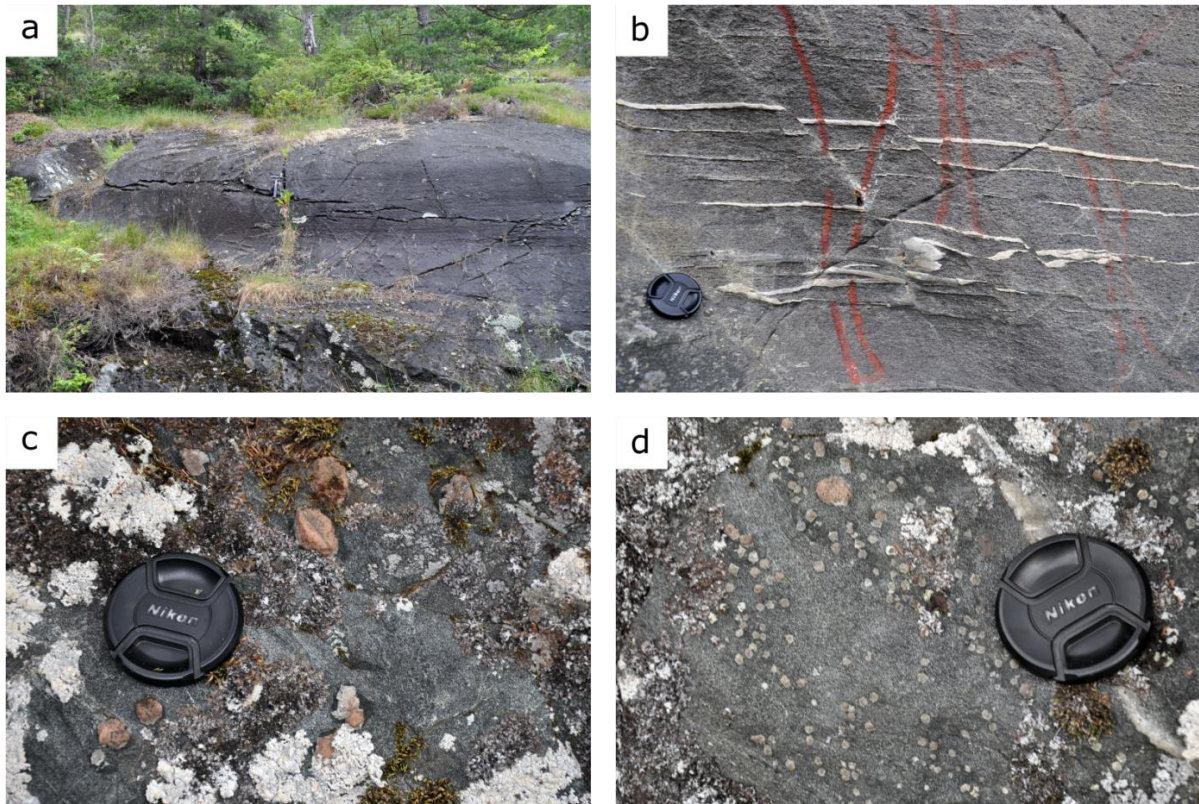


Figure 4.7: a) Helle in a typical outcrop, massive and homogeneous. Loc. no. AAH_314. b) The Helle rock got its name from the type locality at the Helle petroglyph site (petroglyphs visible as red lines). Helle is homogeneous and massive, and contains quartz veins that are both straight and isoclinally folded. Loc. no. AAH_309. c) Within the Helle and Ghms there are zones and lenses of Ams. The Ams contains garnets in zones with varying size, 0.3-2 cm. Loc. no. AAH_106. d) Garnets in Ams. Loc. no. AAH_106.

Amphibolitic schist (Ams)

Ams in the Trongen unit is found as lenses and bigger bodies of varying sizes within the Ghms and Helle (Appendix A). It consists of black amphibole and has a penetrative foliation with thin, 0.2-1.5 cm, parallel quartz veins. In zones and layers anhedral to subhedral 0.3-2 cm sized garnets are found (Fig. 4.7c and d).

Felsic dykes and quartz veins

In addition to the various schistose lithologies described above, the Trongen unit also contains felsic material such as pegmatites, aplites and massive quartz veins (Appendix B). They are all white in colour and can be observed both as boudins or layers varying in size from 10 cm to several meters. The aplites and pegmatites have different appearance in the different

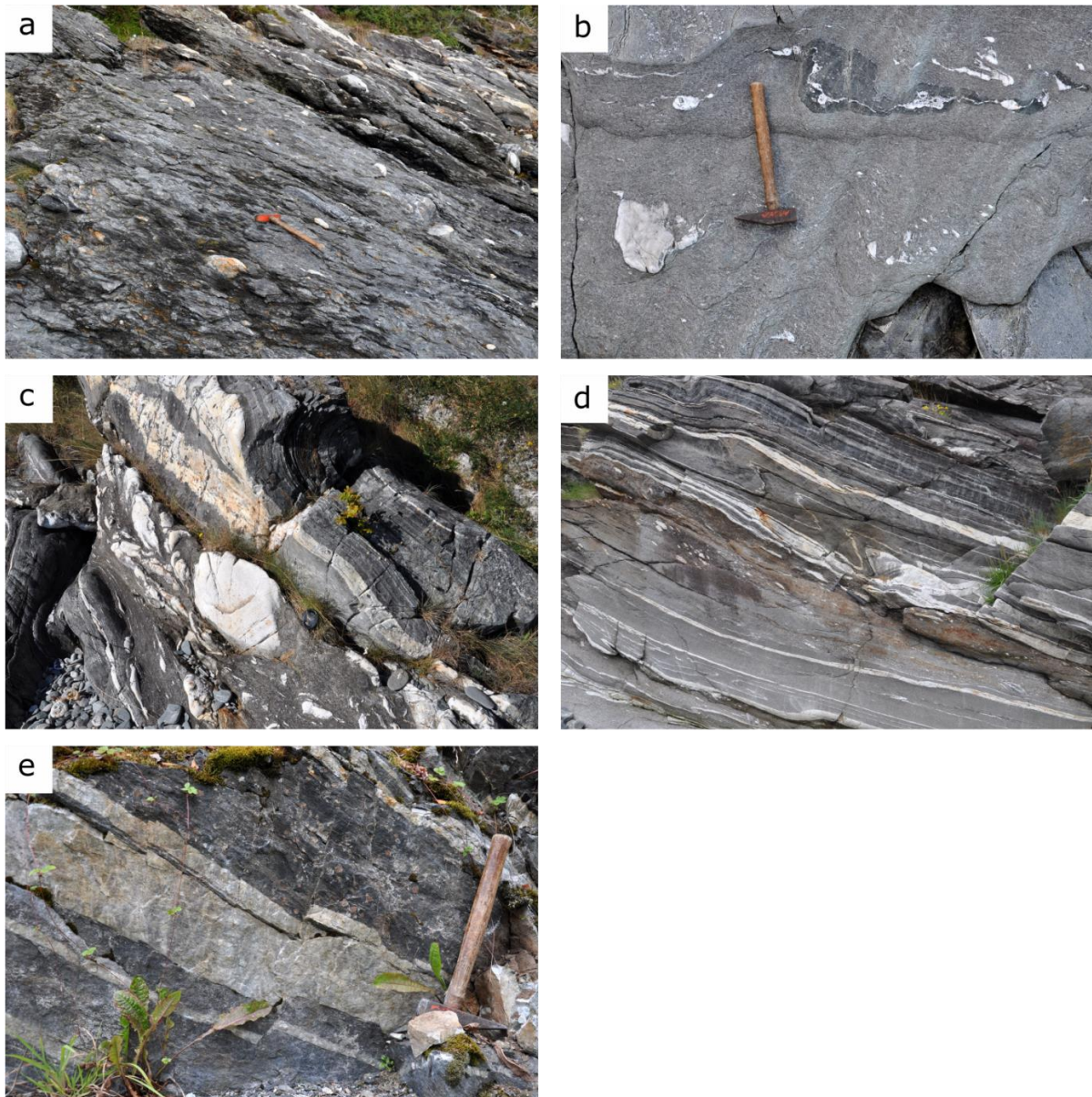


Figure 4.8: a) In Ghms, the aplites and quartz veins appear as blobs. The aplite blobs have a bigger mean size (10-60cm) than the quartz blobs (5-20 cm in diameter). Loc. no. AAH_134. b) Ghms with layers of amphibole and quartz. On the surface of this quartz blob a stretching lineation is visible. Loc. no. AAH_388. c) Ghms with deformed aplite and quartz blobs. The Hbs in the upper part of the picture contains aplite and quartz layers parallel to the foliation. The aplite layers are thicker (5-10cm) than the quartz layers (0.5-3cm). Loc. no. AAH_122. d) Aplite layers parallel to the foliation of Hbs. Also folded together with the Hbs. Loc. no. AAH_124. e) Outcrop of Ams with aplite layer. Loc. no. AAH_190.

rocks, but share quartz, white feldspar and minor biotite and/or hornblende as common constituents. No garnets are found within the felsic rocks in this unit. The Ghms mainly contains quartz veins and aplite blobs varying in size from 10 cm to 60 cm (Fig. 4.8a), and on the surfaces it is possible to measure a stretching lineation (Fig. 4.8b). In the Hbs, the aplites and quartz veins have a different appearance than in the Ghms (Fig. 4.8c). The aplite is boudinaged or interlayered with the Hbs, either as thick boudins (Fig. 4.5a; Fig. 4.8c) or as thin layers (Fig.

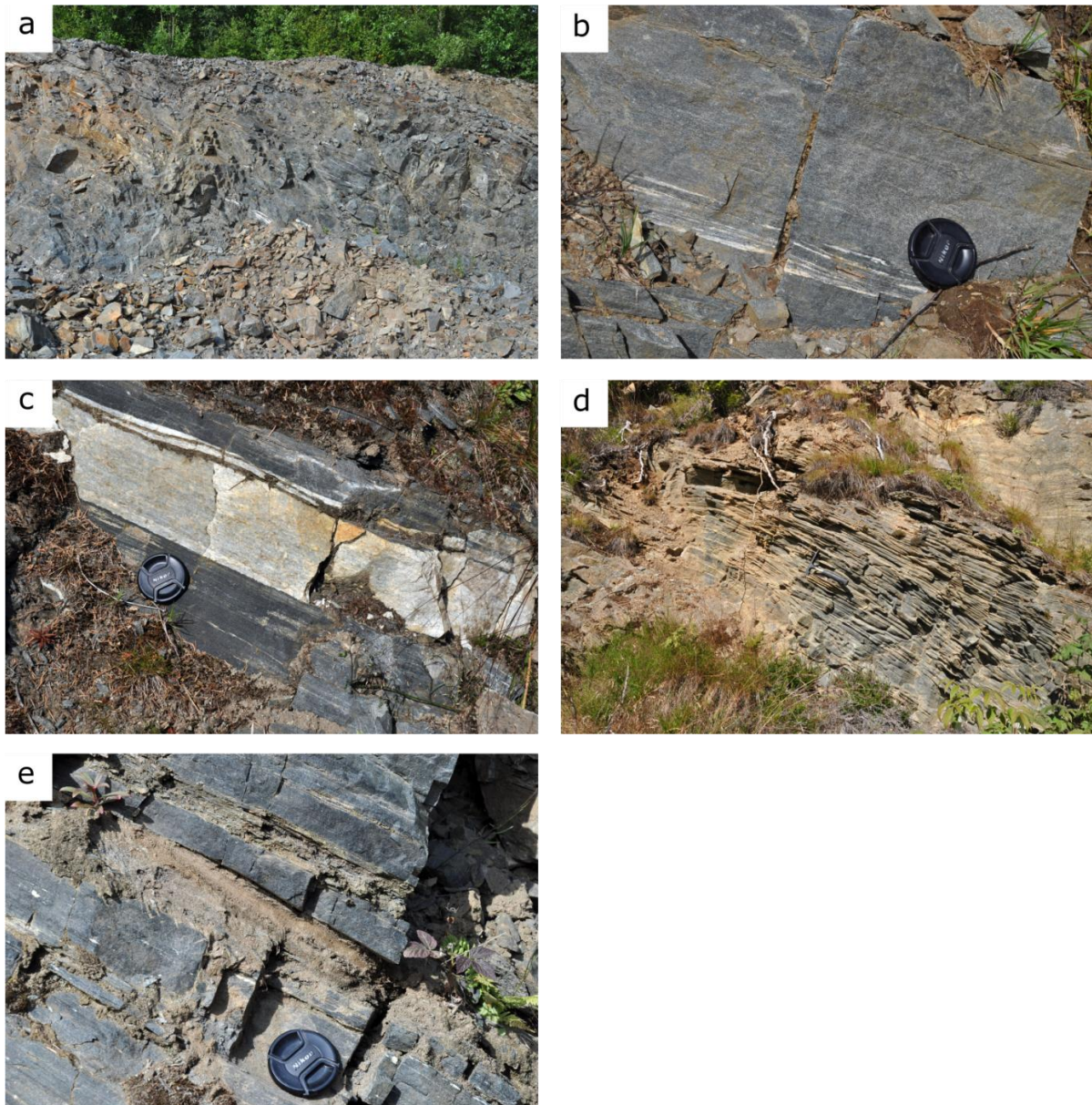


Figure 4.9: a) Outcrop of Ams. Loc. no. AAH_324. b) Close-up of Ams. It is straight and penetrative foliated with thin and deformed quartz veins. Loc. no. AAH_300. c) The Ams alternating with an aplitic layer of almost 20 cm. Loc. no. AAH_301. d) In some areas, the Ams is highly weathered and the foliation becomes very visible. Loc. no. AAH_300. e) Close to Trongen unit Ams alternates with weathered mica rich layers. Loc. no. AAH_300.

4.8d). Quartz veins within the Hbs are parallel to the foliation, but show isoclinal folds in some areas. Aplite was observed in one locality in the Ams. The aplite appears as a continuous layer, 2-15 cm parallel to the foliation (Fig 4.8e). Within the Ams, quartz veins up to a few cm thick were observed at several localities. There was no felsic material observed within Helle, only quartz veins.

4.2.3 Rørvika unit

The Rørvika unit crops out in the central part of the study area, stretching from about half a kilometre northeast of the ferry terminal for about 3 km towards the southwest (Fig. 4.2; Appendix A). The topography is steeper and the best exposed outcrops are found along road cuts and along the shoreline.

The Rørvika unit contains amphibolitic rocks divided into three members based on the amount and characteristics of felsic content present: (i) amphibolitic schist (Ams), (ii) amphibolitic schist with layers and lenses of felsic material (Amfs) and (iii) amphibolitic to intermediate garnet-bearing schist (Amis). One big and a few smaller zones of felsic material within the amphibolitic schists were observed. These tonalitic gneisses were called Fams (felsic zones within the amphibolitic schist) (Appendix A).

Amphibolitic schist (Ams)

Ams is an amphibolitic schist with little to no felsic content (Fig. 4.9a), while Amfs contains more felsic material. The Ams shows a straight and penetrative foliation, the rock is dark grey to almost black and contains mostly amphibole (Fig. 4.9b). Visible streaks of felsic material are present in the rock, generally less than about 5%, and is observed as quartz veins, aplite and pegmatite layers (Appendix B). The felsic layers are parallel to sub parallel to the foliation and have a thickness of about 4-15 cm (Fig. 4.9c). The amphibolitic layers have a thickness of about 5-20 cm. Some outcrops of the Ams are highly weathered and the foliation becomes clearly visible (Fig. 4.9d). Layers of quartz-rich mica schist was found at one locality alternating with amphibole layers close to the boundary of Trongen unit (Fig. 4.9e). The layers of mica schist are 2-10 cm thick, have a brown to grey colour and a high content of weathered mica. In the Ams there were few garnets observed.

Amphibolitic to intermediate garnet-bearing schist (Amis)

The Amis has a straight and penetrative foliation with parallel layers of blackish amphibolite and lighter-coloured intermediate rock (Fig. 4.10a). The amphibolite is dark grey to black, fine- to medium-grained and shows a strong mineral lineation on surfaces. The intermediate rock shows variations in colour, from dark grey to lighter grey, and texture, from being homogeneous and fine grained to medium-grained and with larger feldspar and/or quartz crystals (Fig. 4.10a and b). Locally, the Amis is folded (Fig. 4.10b) and shows similar

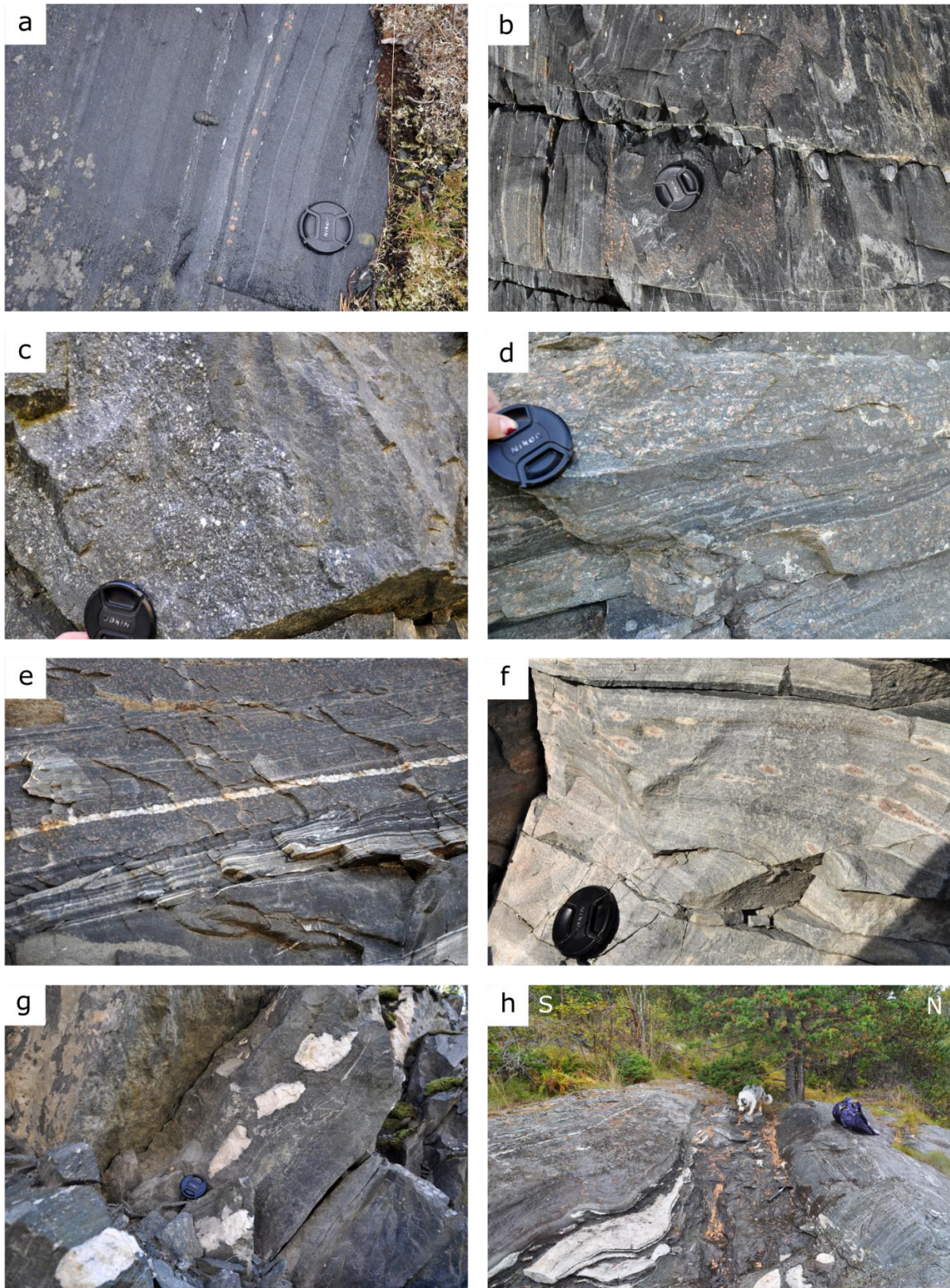


Figure 4.10: a) The Amis shows alternating layers of amphibolitic and intermediate layers. Garnets are restricted to specific layers. Loc. no. AAH_355. b) Folded Amis with mm-sized pink and subhedral to anhedral garnets restricted to layers. Loc. no. AAH_351. c) Zone within the Amis with a porphyritic texture. Loc. no. AAH_367. d) Garnets up to one cm in diameter with thin, 0.1 mm thick, halos concentrated in

porphyritic texture as seen in Amfs (Fig. 4.10c and d), manifested in lenses or layers (3-8 cm) foliated together with the Amis. Garnets occur concentrated along specific layers, mostly in the intermediate strata (Fig. 4.10d, e and f). They usually show an anhedral crystal structure, a light pink colour and vary in size from 0.1-1 cm in diameter. White halos of <1-2 mm are common, and at some localities the halos merged together into covering several garnets (Fig. 4.10f). Quartz veins occur as thin layers and lenses within the Amis (Fig. 4.10a and e). The quartz veins are found both parallel to foliation and cutting it, both appearances can be isoclinally folded and boudinaged. Also pegmatites and aplites are observed as layers parallel to the foliation, occasionally occurring as boudins (Fig. 4.10g and h).

Close to Kleivneset (Locality AAH_232, Appendix A) a lens of mica rich rock can be observed. The lens has a width of about 1.5 metres and an observable length of 4 metres (Fig. 4.10h), contains quartz blobs and has similar characteristics as the Ghms in the Trongen unit (compare Fig. 4.10h to Fig. 4.8a and c). The foliation measured on the two sides of the lens are different from each other, being 225/48 below and 189/12 above.

Amphibolitic schist with layers and lenses of felsic material (Amfs)

The boundary between Ams and Amfs is transitional and the difference between these two rocks is the amount of felsic material present in them. Amfs is, together with Amis, the most abundant rock type in the Rørvika unit, and shows a great variation in appearance (Fig. 4.11). The Amfs shows alternating felsic and black amphibolitic layers and generally a straight and penetrative foliation (Fig. 4.11a). The content of felsic material varies in amount, from about 5-60%. In some areas, the Amfs shows no foliation and is less strained (Fig. 4.11b). In less strained areas, the felsic and amphibolitic layers are folded and mixed together showing primary magmatic textures. In some areas, the Amfs shows a porphyritic texture (Fig 4.11c), having black and white speckles and no foliation. This porphyritic texture appears both as zones and thin layers. The garnets within the Amfs are localized in zones and layers both in the felsic layers and amphibolitic layers, and show great variations in size, from 2 mm to 1 cm in diameter (Fig. 4.11d, e and f). There are no garnets observed in the layers and zones with porphyritic texture. At one locality, millimetre thin layers of calcite were observed (Fig. 4.11g). The lateral

Fig. caption cont. intermediate layers. The layers show small z-folds. Loc. no. AAH_375. e) Pink garnets in both intermediate and amphibolitic layers. Loc. no. AAH_378. f) Intermediate zone of the Amis with anhedral pink garnets. The garnets show elongated and 0.1-0.5 cm thick halos. Loc. no. AAH_374. g) Aplitic and boudinaged vein parallel to the foliation. Loc. no. AAH_263. h) Zone of mica rich rock within the Amis. The rock contains quartz and aplitic elongated blobs and has a brown weathering colour. Loc. no. AAH_231.

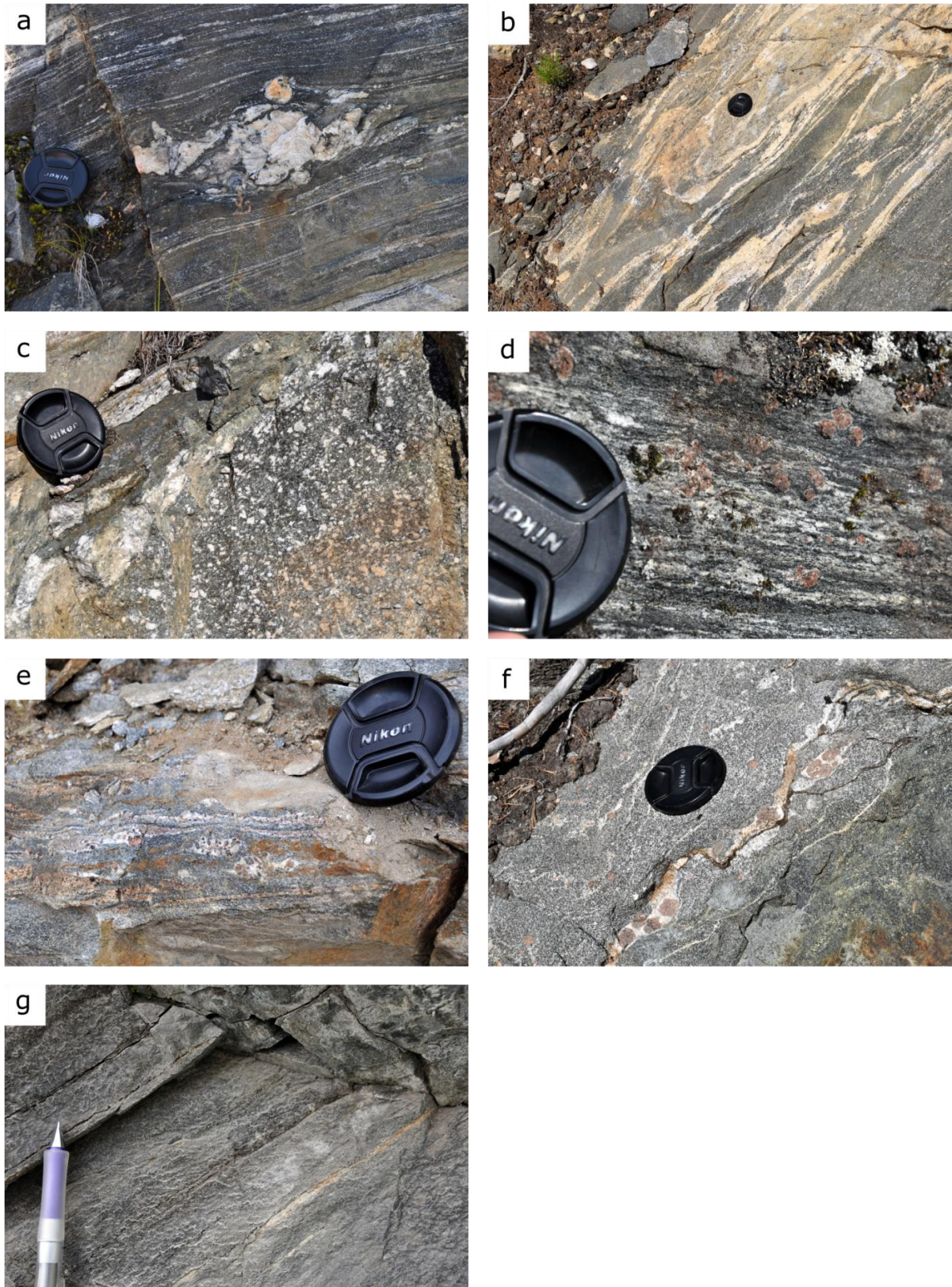


Figure 4.11: a) The Amfs shows a variety in appearance from highly strained and foliated, here with aplitic lens, Loc. no. AAH_238, to b) a less strained and not foliated appearance. Loc. no. AAH_243. c) Zones and layers with porphyritic texture are found within the Amfs. Loc. no. AAH_239. d) Anhedra red garnets, 0.1-1 cm in diameter, with less than 1 millimetre thin halos. Loc. no. AAH_253. e) Garnets, 0.2-0.5cm in

extent of each layer was no more than maximum 25 cm and the calcite shows a strong and orange weathering colour.

Tonalitic gneiss (Fams)

In the western part of the Rørvika unit, massive tonalitic gneiss is found in three zones, one spatially extensive and two more local. The bigger zone has a width of about 100 meters and a roughly estimated length of 1200 meters, while the two smaller zones are 14-16 meters wide and about 110 to 130 meters long (Appendix B). The tonalitic gneisses are fine- to medium-grained and with a white to bluish colour (Fig. 4.12a-e). They contain quartz, feldspar, and small amounts of biotite and/or hornblende. At one location, less than 1 mm sized, dark-red garnets were found throughout the outcrop (Fig. 4.12d).

4.2.4 Varpneset unit

The Varpneset unit crops out in the north-easternmost part of the study area, from Varpneset and northeastwards to the border between the counties of Sør-Trøndelag and Nord-Trøndelag (Fig. 4.1; Fig. 4.2; Appendix A). Most of the mapping was done along roads and the shoreline due to lack of exposures elsewhere.

Hornblende-calcite-quartz schist (Hcqs)

The Varpneset unit shows similar mineralogical characteristics as the Ghms in the Trongen unit, but with important differences in grain size, amount of quartz, the presence of calcite, and the texture. The main rock type within the Varpneset unit is given the name Hcqs (Hornblende-calcite-quartz schist). Hcqs can be identified by its content of quartz, garnet, hornblende, calcite, muscovite and biotite. The Hcqs has a silver luster on fresh surfaces (Fig. 4.13a) and has a layered (Fig. 4.13b) and crenulated appearance (Fig. 4.13c), with more massive layers containing a higher amount of quartz, and more crenulated layers with higher content of muscovite (Fig. 4.13c and d). Together with the layering also variations in grain size occur, where the mica-rich layers show a more coarse grain size (Fig. 4.13a and d). Here hornblende crystals can be up to 2-3 cm long and show both fibrous and prismatic crystal shapes (Fig. 4.13e). Garnets show a dark red to pink colour, depending on the weathering, and vary in size from 0.2-1 cm in diameter. The calcite shows a characteristic brown to orange weathering

Fig. caption cont. diameter, with a pink colour and anhedral shape. They are located within halos grown together parallel to the foliation. Loc. no. AAH_299. f) Big garnets, up to 2 cm in diameter. The garnets are located within a felsic zone. Loc. no. AAH_243. g) Thin calcite veins parallel to the foliation. Lateral extent is maximum 25 cm. Loc. no. AAH_236.

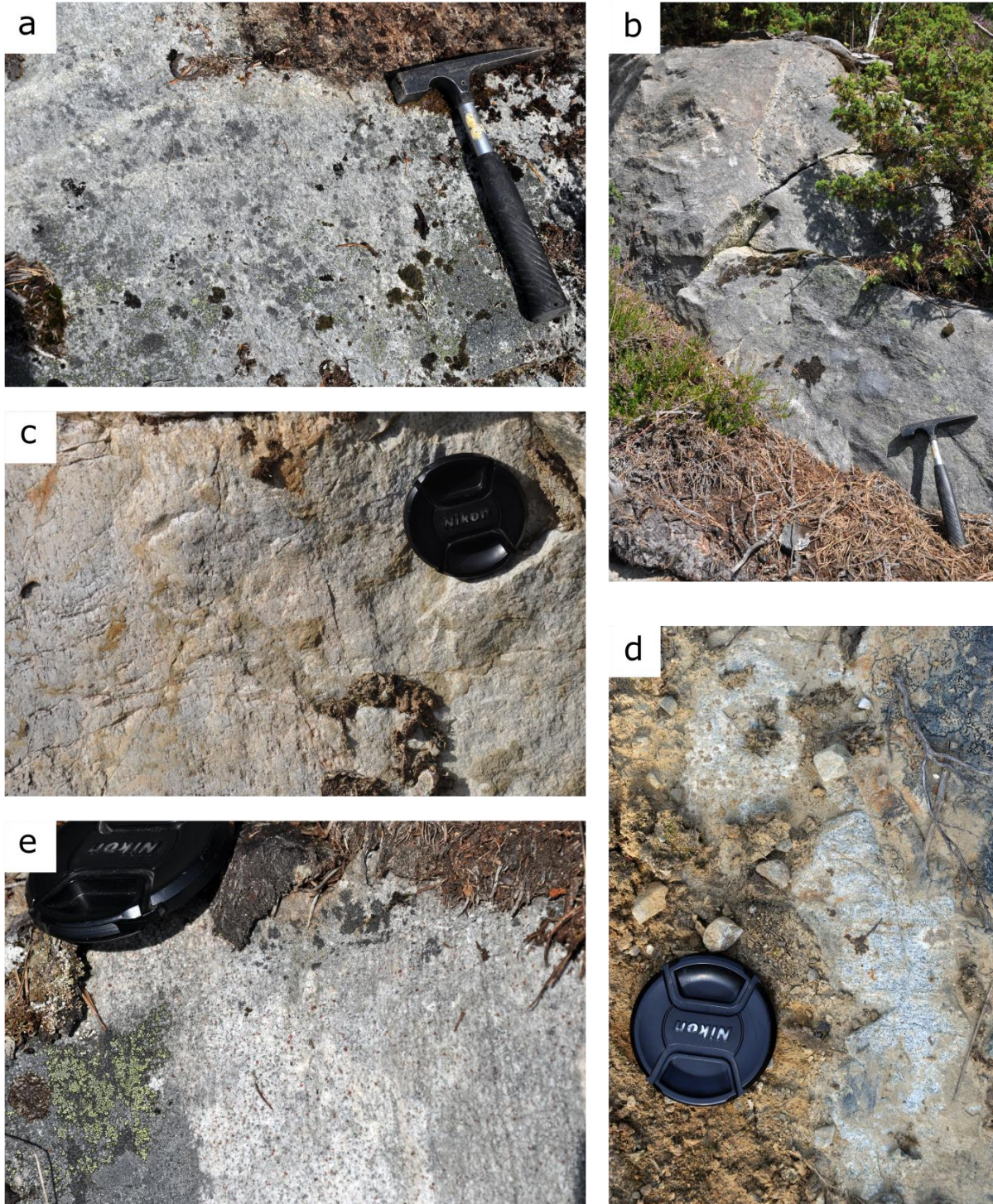


Figure 4.12: a-e) The tonalitic gneisses within the Rørvika unit have a white to light bluish colour and are fine- to medium-grained. Loc. no. AAH_248, AAH_250, AAH_294 and AAH_295. d) Garnets were observed in one outcrop. Loc. no. AAH_249.

colour and appears as small grains throughout the rock and as bigger lenses often together with lenses of quartz (Fig. 4.13f). Most of the bigger lenses along the coastline have weathered out and have left the remaining rock with small pits as evidence of their existence.

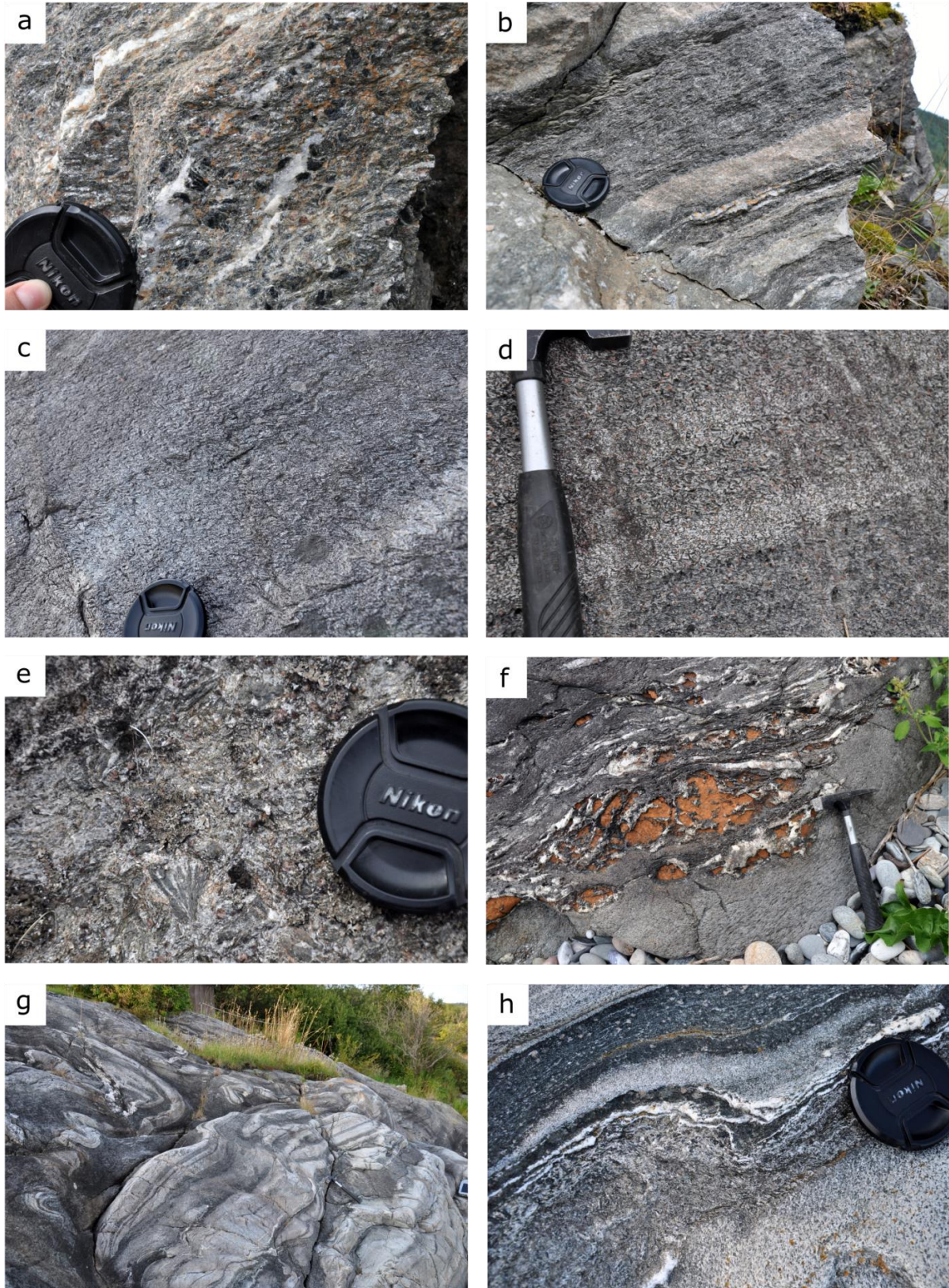


Fig. continues on next page

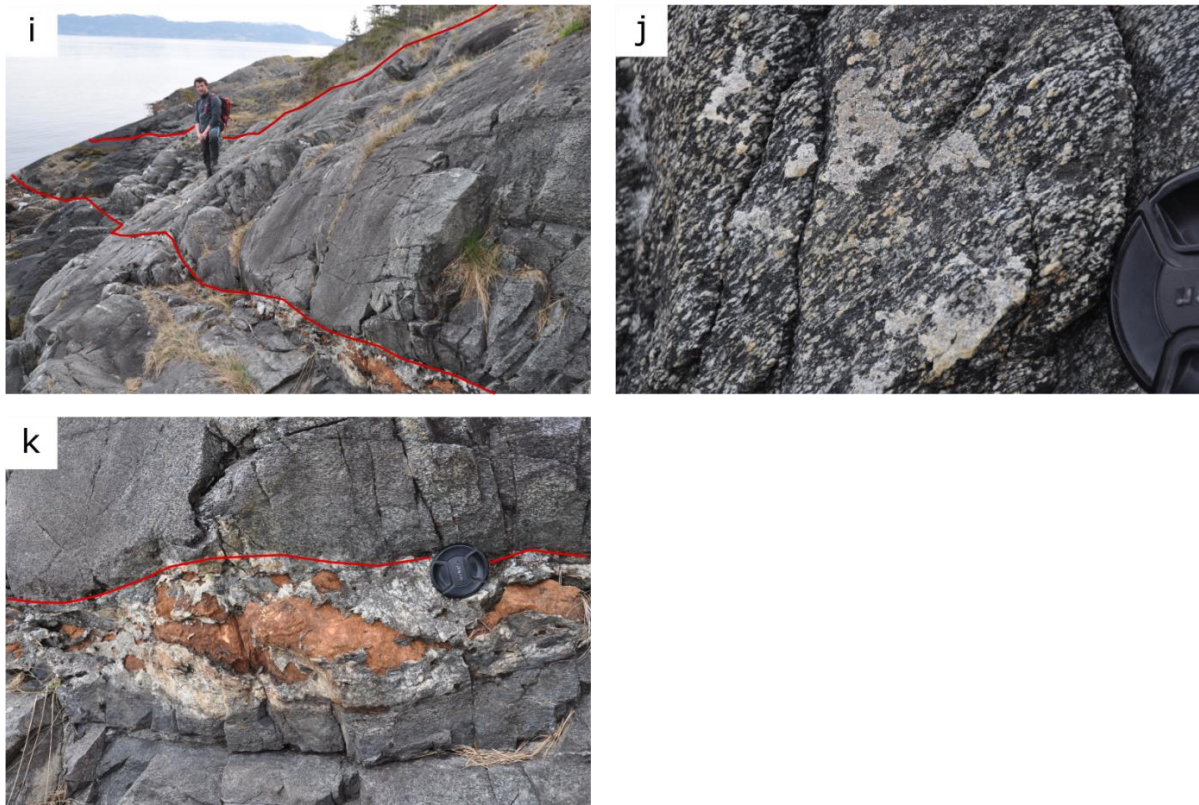


Figure 4.13: a) In the Varpneset unit the Hcqs shows a silver luster and layers with varying amount of muscovite and quartz as well as varying grain sizes. The orange colour on the surfaces originates from the weathering of calcite. Loc. no. AAH_164. b) The Hcqs shows a penetrative and straight foliation and layers varying with quartz- and muscovite content. Loc. no. AAH_165. c) Surface of the Hcqs with a crenulated appearance. Loc. no. AAH_218. d) Simply the variations in grain size can in some places give the rock a layered appearance. This is mostly seen through the hornblende grains, which vary in size from barely being visible with the naked eye to 2.5 cm. Loc. no. AAH_203. e) Amphibole crystals show a fibrous and elongated crystal structure and can measure up to 2.5 cm. Loc. no. AAH_174. f) The Hcqs contains calcite, both as small grains throughout the rock and as larger zones where calcite lenses are found. The calcite has a strong and orange weathering colour and has partly or completely weathered out leaving small caves in the rock. Loc. no. AAH_176. g) Outcrop close to the boundary towards the Rørvika unit. The Hcqs shows a folded and less strained appearance with 5-50 cm thick layers of amphibolite. Loc. no. AAH_221. h) The amphibolitic layers show a dark grey to almost black colour, and some of them contain pink garnets, 0.2-0.6 cm in diameter. Loc. no. AAH_217. i) Dyke parallel to the foliation with a porphyritic texture. The dyke is 2-2.5 metres thick. Loc. no. AAH_403. j) Detail of dyke with porphyritic texture. Loc. no. AAH_403. k) The lower boundary to the Hcqs is divided by an quartz and calcite vein, 10-30 cm thick. The upper boundary is transitional. Loc. no. AAH_403.

A 2-2.5 metres thick dyke with porphyritic texture (Fig. 4.13i) indicates a division of the Hcqs in Varpneset unit, from the dyke and towards the southwest the unit contains more amphibole and less calcite. The dyke has a homogeneous appearance and is of medium grain size (Fig. 4.13j). At the lower boundary between the Hcqs and the dyke, there is a 10-30 cm thick quartz and calcite vein dividing them (Fig. 4.13k). The upper boundary is transitional and it is difficult to find the exact boundary.

Hornblende-quartz schist (Hqs)

In some smaller zones the Hcqs is lacking calcite and thus becoming Hqs. The Hqs, containing quartz, garnet, hornblende, muscovite and biotite, has the same texture as the Hcqs but is differentiated by its lack of the orange tint from calcite.

Close to the boundary to the Rørvika unit, there is a gradual increase in the appearance of amphibolite as lenses or layers alternating with the Hcqs (Fig. 4.13g and h). The amphibolite is folded and deformed together with the Hcqs, and it contains pink garnets 0.2-0.5 cm in diameter.

The Varpneset unit contains quartz veins as layers and lenses, varying in thickness from 1-10 cm. These quartz veins are described in chapter 4.3.3.3.

4.3 Structural observations

The structural observations and measurements taken in the field involve the penetrative foliation as the main planar feature as a reference structure for observations of folds (Appendix C), mineral and elongation lineation (Appendix C), fold axis orientation and fold symmetry (Appendix D) and brittle structures (Appendix E) presented separately for each unit below. The characteristics for each unit and the associated mean measurements are presented in Table 5.1.

4.3.1 Foliation

4.3.1.1 Rødberget unit

The Rødberget unit shows a penetrative foliation from flattening and reorientation of grains. The outcrops are well exposed along the shoreline offering cross-sections through multiple planes of the rock, which makes it possible to get a firm understanding of the dimensional orientation of the foliation in the outcrop (Fig. 4.14a and b).

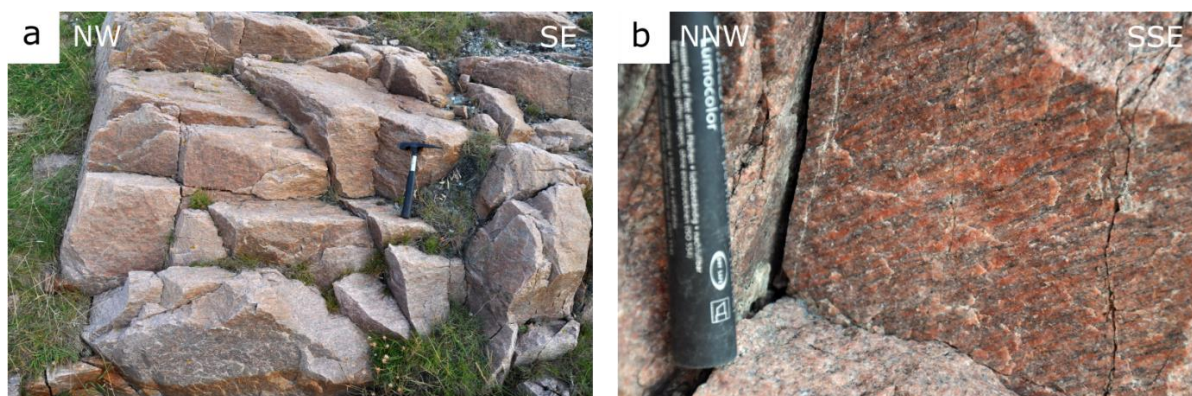


Figure 4.14: a) Example of a well-exposed 3D outcrop where the foliation can be readily measured. Loc. no. KSV_55. b) Detailed aspects of the foliation. Loc. no. KSV_56.

The foliation has a shallow dip towards the northeast (Fig. 4.15). All but one measurement show a coherent direction of the foliation. The deviant measurement (marked with a green line in Figure 4.15) originates from a measurement taken on a surface with a weak and therefore potentially misleading foliation. However, the poles for the foliations show smaller differences, and the deviant foliation can also be rotated. The mean dip direction/dip for the foliations without the exception mentioned above is 026/18.

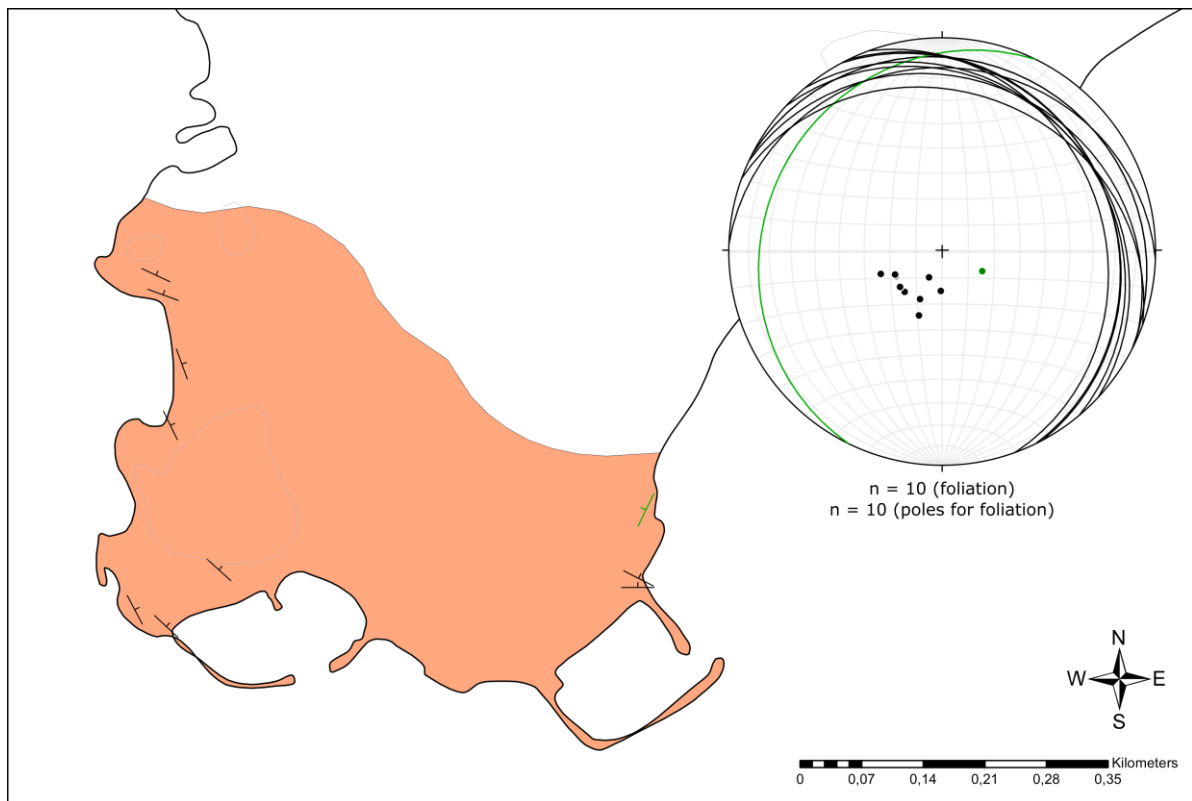


Figure 4.15: Map over Rødberget unit detailing location of all measured foliations. The foliations show a dip direction towards the northeast (black) with the exception of one deviant measurement marked by a green line. The locality of the measurement differing from the other is situated in the eastern part of the unit.

4.3.1.2 Trongen unit

The foliation appearance in Trongen varies with rock types. Hbs shows a strong platy and straight schistosity (Fig. 4.16a) whereas in the Ghms, the foliation gets less prominent due to undulation of the main planar feature (Fig. 4.16b and c). With an increasing content of amphibole in the Ghms, the foliation also gets a stronger appearance (Fig. 4.16d). Helle has due to its homogeneous texture in general only a weakly visible penetrative foliation, but with quartz veins present the foliation can become more apparent (Fig. 4.7b). In some outcrops, Helle shows crenulation cleavage.

The foliation in the Trongen unit is divided into five groups based on dip and dip direction (Fig. 4.17); i) a main foliation with a shallow dipping trend towards the northeast to southeast (black, Fig. 4.17). The mean dip direction and dip for the main foliation dataset is 120/19. It is interpreted that the very weakly dipping layers with a dip direction towards the west and southwest are showing this same main foliation that has been locally rotated.

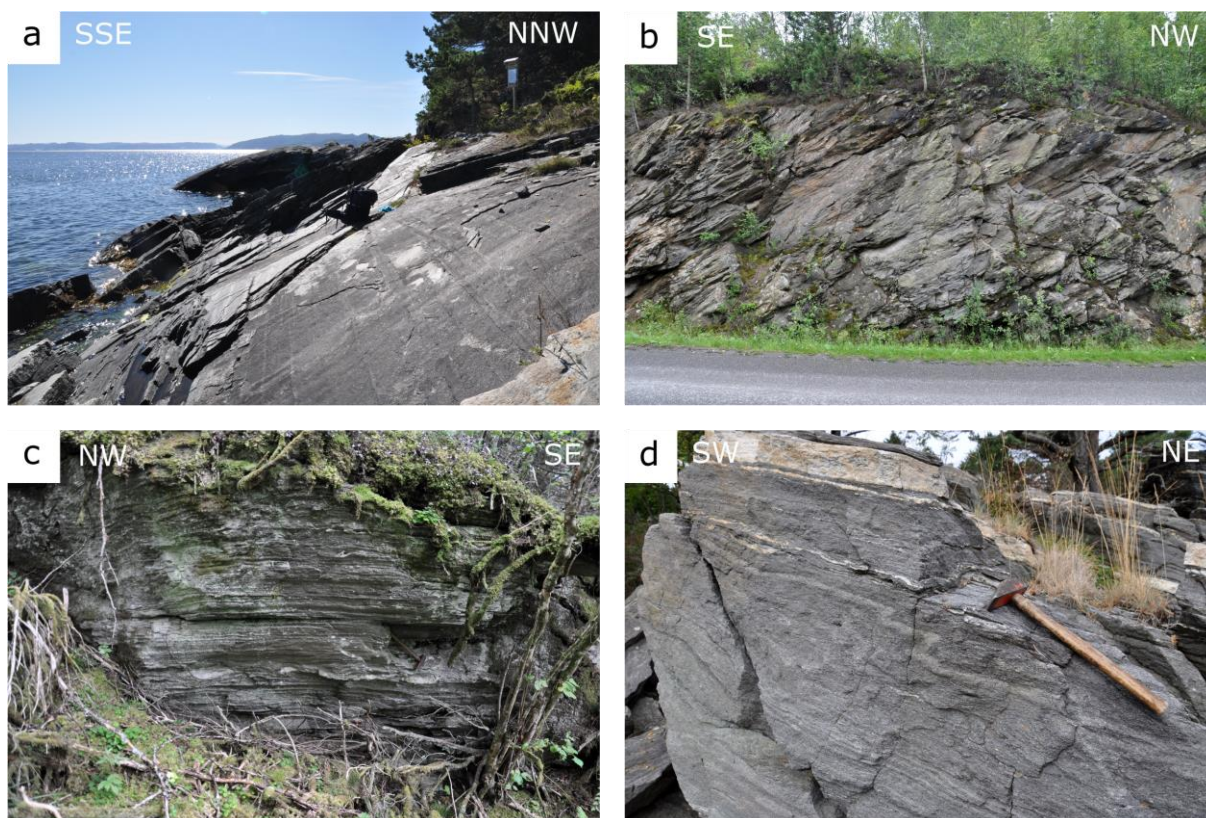


Figure 4.16: a) Straight foliation in an outcrop of Hbs. Loc. no. AAH_322. b) Outcrop of Ghms. The foliation has a dip directed towards the south-southeast. Loc. no. AAH_327. c) Weathering of the Ghms makes the foliation visible. Loc. no. AAH_195. d) Outcrop of an amphibole rich Ghms with thin layers of Hbs. The outcrop shows a strong foliation and small NE-vergent folds. Loc. no. AAH_141.

Several foliation measurements deviating from the main foliation orientation can be assigned to four groups. ii) Three measurements show a steep dip towards the east-northeast (blue, Fig. 4.17). iii) Within the Ams, six measurements show steep dips towards the southeast (orange, Fig. 4.17). iv) One group of foliations (green, Fig. 4.17) deviate from the main foliation due to the northwest to north dip direction and varying dip angle, from shallow to moderately steep. They are all located along the coastline in the most western part of Trongen unit (Fig. 4.17). v) Two foliations were measured from a small outcrop that might not be in place and can therefore be misleading (purple, Fig. 4.17).

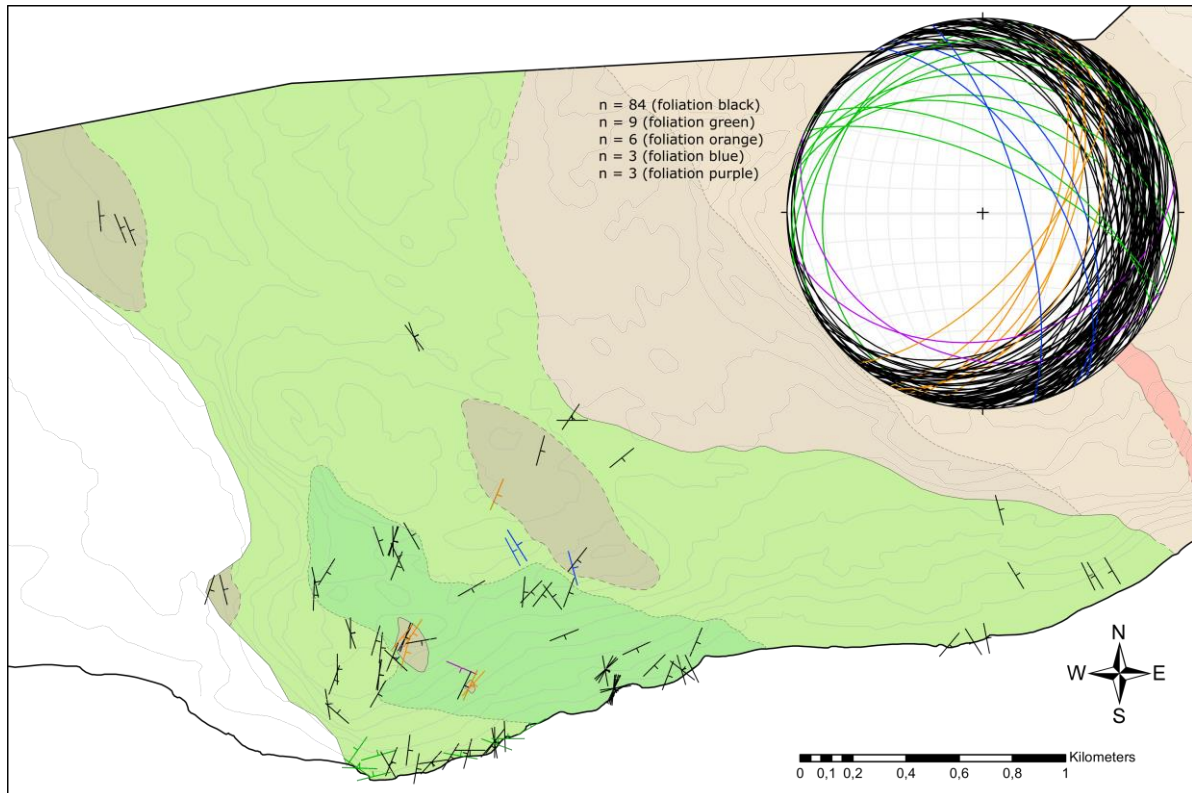


Figure 4.17: Overview of all measured foliations within the Trongen unit. The areas without measurement are due to lack of outcrops because of agricultural land or forest. The colour of the different sets of foliations matches the colours of the different sets in the stereonet. There are five groups of foliations, i) a main foliation with shallow dip (black), ii) steep dip towards the east-northeast (blue), iii) moderate dip towards the southeast (orange), iv) moderate dip towards the northwest (green), and v) unreliable foliations (purple).

4.3.1.3 Rørvika unit

Foliation from Kleivneset, just northeast of the ferry terminal are here not included with measurements from Rørvika unit due to the need of a more detailed study of the Kleivneset area. This detailed study of Kleivneset follows in chapter 4.3.4.3.

The foliation in all Rørvika lithologies is penetrative and shows a strong planar feature throughout the rock. It is enhanced in the Amfs and Amis by compositional banding with felsic and amphibolitic layers (Fig. 4.18a and b).

The foliation is divided into four groups based on orientation: i) a main foliation with a shallow to moderate dip towards the southwest to southeast (black, Fig. 4.19). The mean dip direction and dip is 222/21. ii) A group of foliations with a sub-vertical orientation and steep dip towards the southwest and northeast (red, Fig. 4.19), and with a mean dip direction and dip of 181/77. iii) Foliation concentrated mainly in the western part of Rørvika unit with a moderate dip towards the east-northeast (blue, Fig. 4.19), and a mean foliation of 078/34. iv) A group of foliations with a moderate dip towards the west and west-southwest (green, Fig. 4.19),

all located within the Amfs. The dip angle varies from shallow to moderate and the mean foliation is 258/41.

One exception (purple dotted line, Fig. 4.19) has a steep dip with a dip direction towards the southeast.

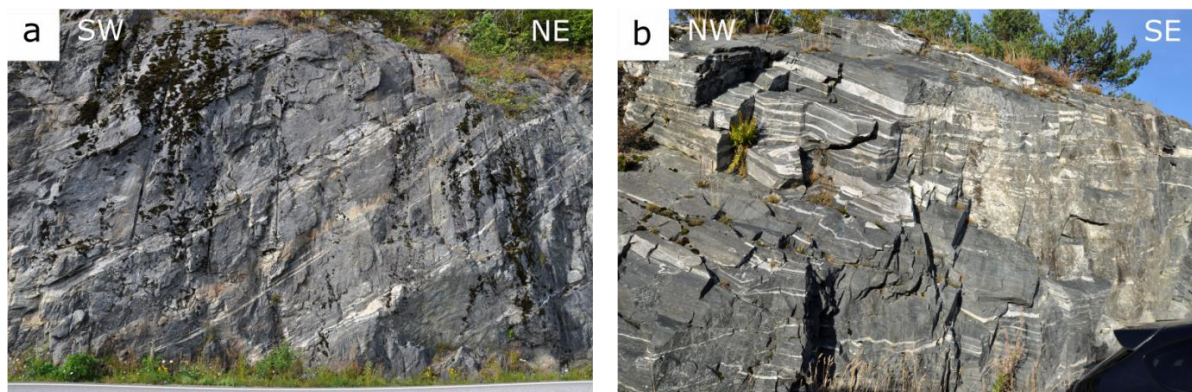


Figure 4.18: a) Foliation in the Amis dipping towards the southwest (black, Fig. 4.19). Loc. no. AAH_236. b) Foliation in Amis with dip direction towards the south-southeast (black, Fig. 4.19). Loc. no. AAH_379.

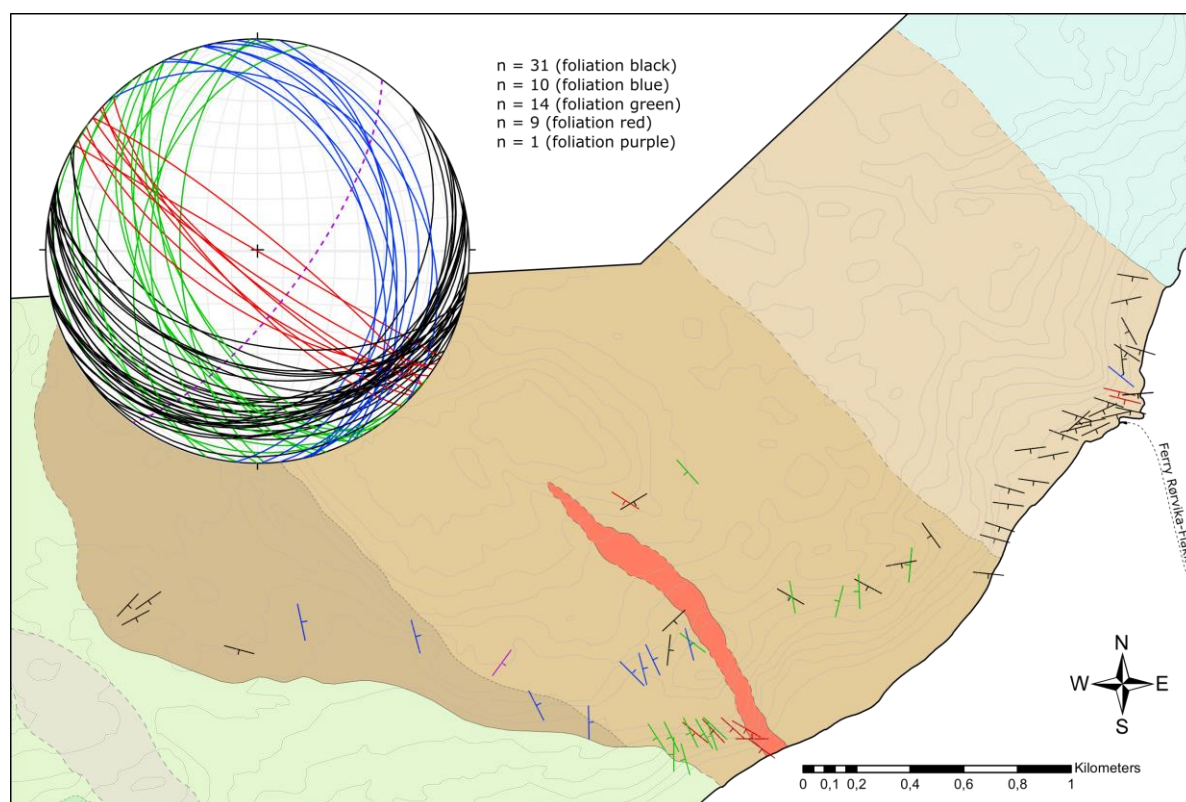


Figure 4.19: Rørvika unit with measured foliations. The foliations are divided into four main groups (see text for more explanation). In addition there is one exception marked in purple. The colours of the foliations on the map coincide with the colours of the planes in the stereonet.

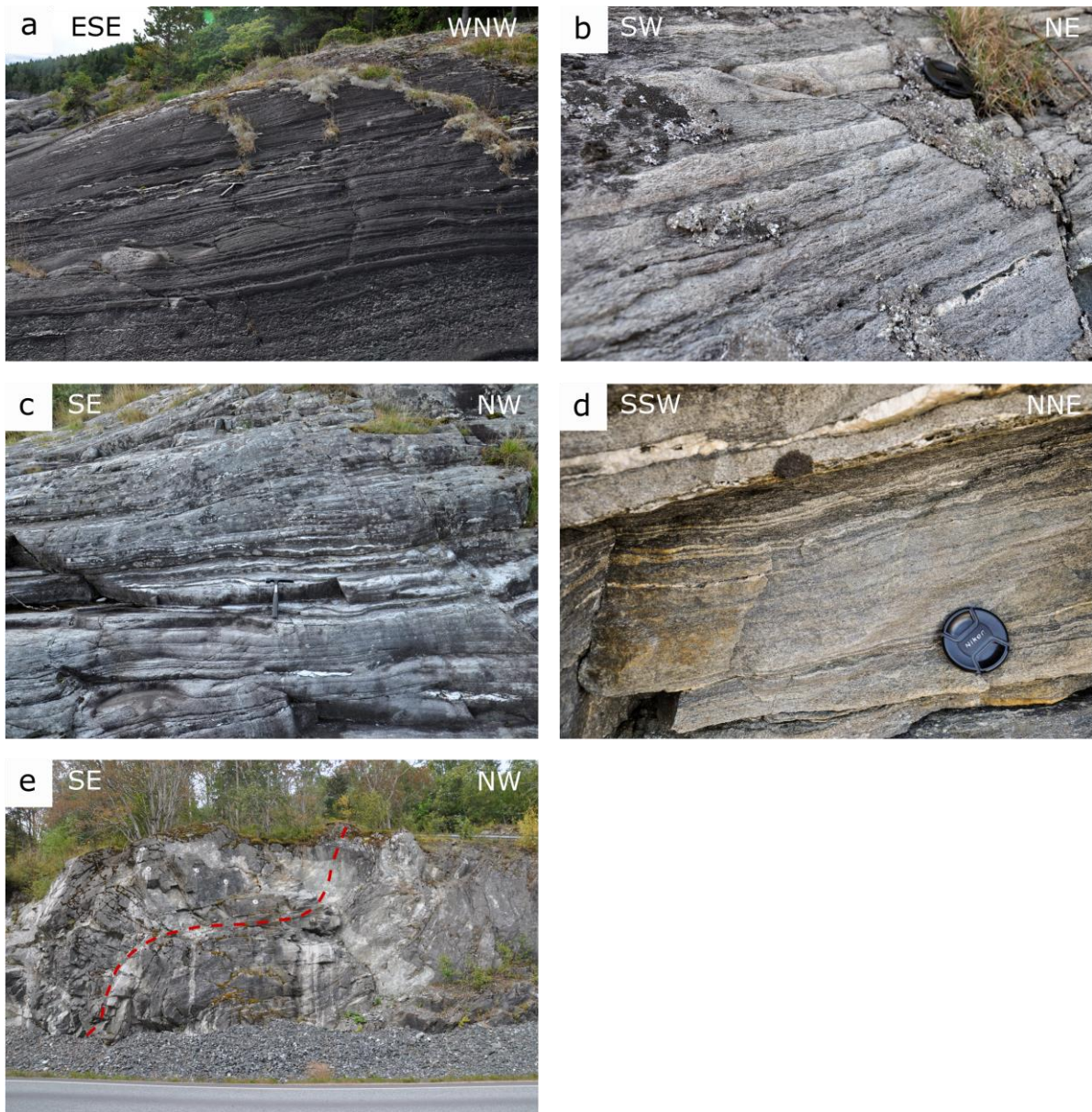


Figure 4.20: a) Foliation on a weathered surface of the Hcqs showing a dip direction towards the southwest, away from the photographer's position. Loc. no. AAH_171. b) Foliation in the Hcqs showing compositional layering with dip direction to southwest. Loc. no. AAH_216. c) The foliation on weathered surfaces further to the west where the unit contains amphibole layers. Dip direction to southeast. Loc. no. AAH_220. d) Foliation on surface less affected by weathering. Loc. no. AAH_216. e) Larger fold giving a steep dip to the foliation on the flanks. Outcrop is about 5 metres high. Loc. no. AAH_165.

4.3.1.4 Varpneset unit

The rocks in the Varpneset unit display a straight and penetrative foliation best visible along the coast due to weathering and the compositional banding (Fig. 4.20). This makes the layers rich in quartz stand out, making the foliation even more evident (Fig. 4.20a and b). Towards the southwest the of Varpneset unit, where the Hcqs gets richer in amphiboles, the

penetrative foliation becomes more obvious (Fig. 4.20c and d). The Hcqs can also show a crenulated appearance in mica rich layers.

In the southwestern and central part of the unit, the foliation has a low to moderate dip towards the southwest (black, Fig. 4.20). In the northeastern part of the area the direction of the foliation changes to a shallow dip towards the southeast to east. The mean dip direction and dip of the main foliation with dip towards the southwest is 230/24, and the mean dip and dip direction for all foliations measured is 148/19. Some of the foliation measured show a steep dip towards the northeast or southwest and are thought to be part of larger folds (purple, Fig. 4.21; Fig. 4.20e). There are two more exceptions to the trend in the Varpneset unit (Fig. 4.20). The red group with steep dips and with dip directions towards the east-southeast is most likely part of a transitional zone where the foliation changes dip direction. The foliation of the green group have a shallow dip with dip direction towards the east and are both located on the boundary to Rørvika unit.

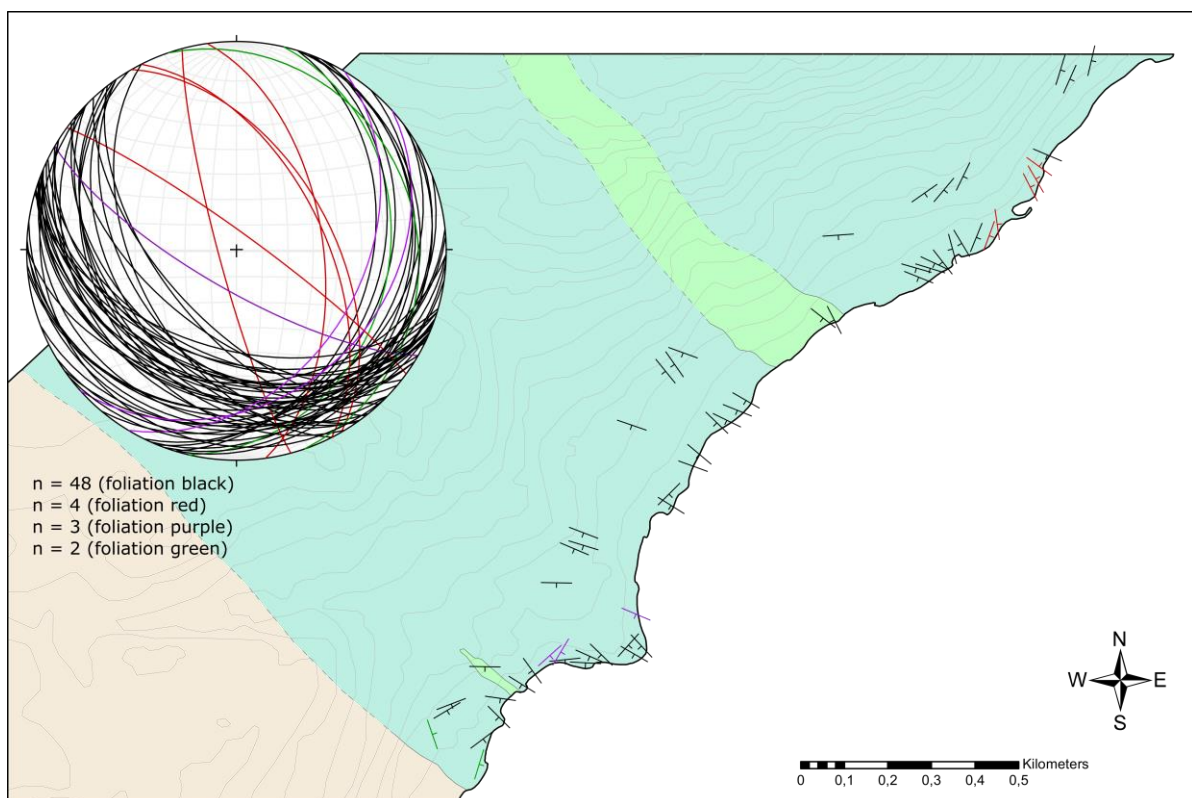


Figure 4.21: Measured foliations from the Rørvika unit with the main foliation (black) displaying a shallow to moderate dip towards the southwest and a moderate dip towards the east-southeast close to the boundary to Nord-Trøndelag County in the northeast of the unit. Three sets of measurements different from the main trend (red, purple and green) with a deviant dip direction from the main foliation.

4.3.2 Mineral lineation

4.3.2.1 Rødberget unit

The Ingdal granitic gneiss of the Rødberget unit shows a mineral lineation seen on surfaces as penetrative mineral lineation, consisting of stretched quartz/feldspars and aligned biotites (Fig. 4.22). The lineation has a shallow plunge towards the northeast (Fig. 5.21), with the mean mineral lineation of 058/08.

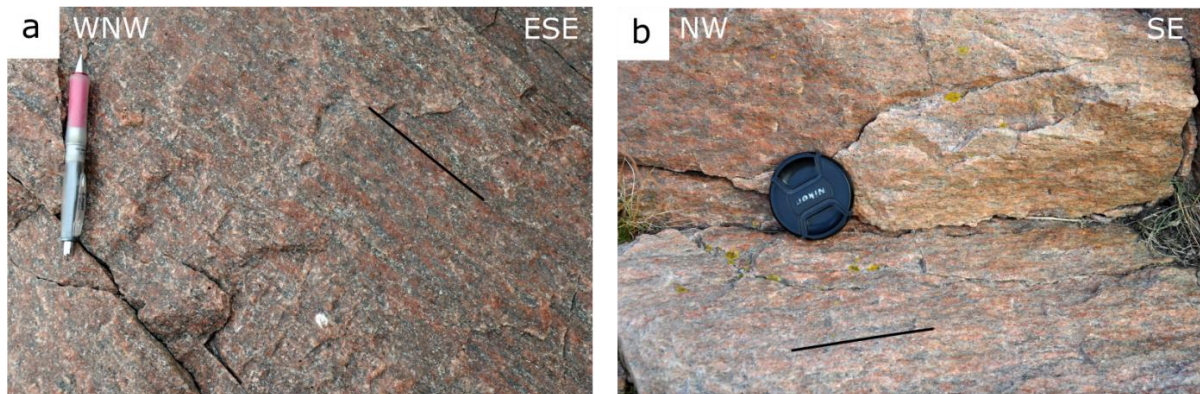


Figure 4.22: a) Lineation in granitic gneiss from the Rødberget unit, highlighted by black line. Loc. no. KSV_55. b) Lineation in the Ingdal granitic gneiss from Rødberget unit. Black line is parallel to the lineation. Loc. no. KSV_55.

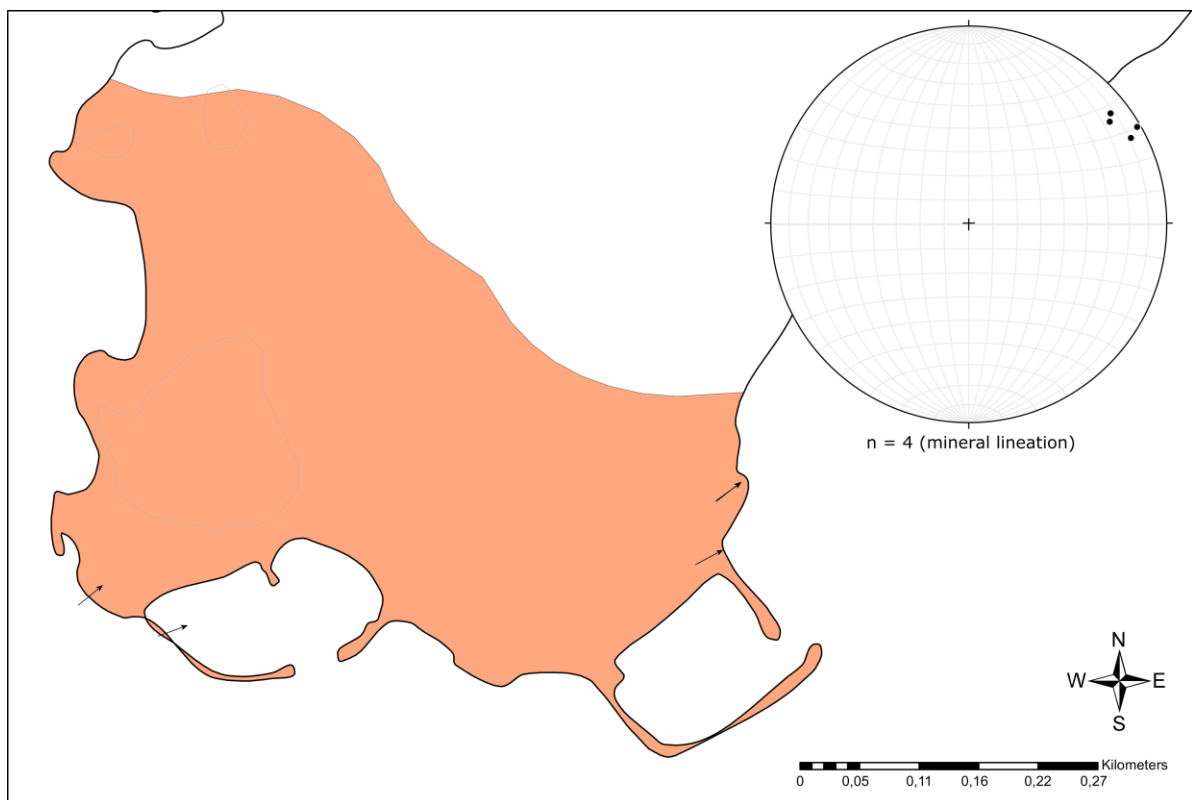


Figure 4.23: Map of locations of measured lineation in the Rødberget unit and corresponding stereonet highlighting lineations. The lineations exhibit a trend towards the northeast and with low plunge.

4.3.2.2 Trongen unit

Lineations in the Trongen unit comprise mineral lineations and elongation lineations. Ghms does not display any obvious lineations due to the undulating foliation. The mineral lineations are represented by aligned hornblende crystals exposed on surfaces of the Ams and Hbs (Fig. 4.24a; Fig. 4.25 – black), and the elongation lineations are represented by stretched quartz veins and quartz blobs within the Ghms (Fig. 4.24b, c and d; Fig. 4.25 - orange).

The main trend of the foliation is towards the northeast to southeast (Fig. 4.25). Excluding the deviant measurements, the mean trend and plunge, for the mineral lineation and elongation lineation together, is 109/22.

There are two sets of exceptions to the main trend, the first characterized by a shallow plunge towards the north (red, Fig. 4.25). One measured lineation with a shallow plunge to the northwest (green, Fig. 4.25) is assumed to be part of the main mineral lineation towards the east-southeast.

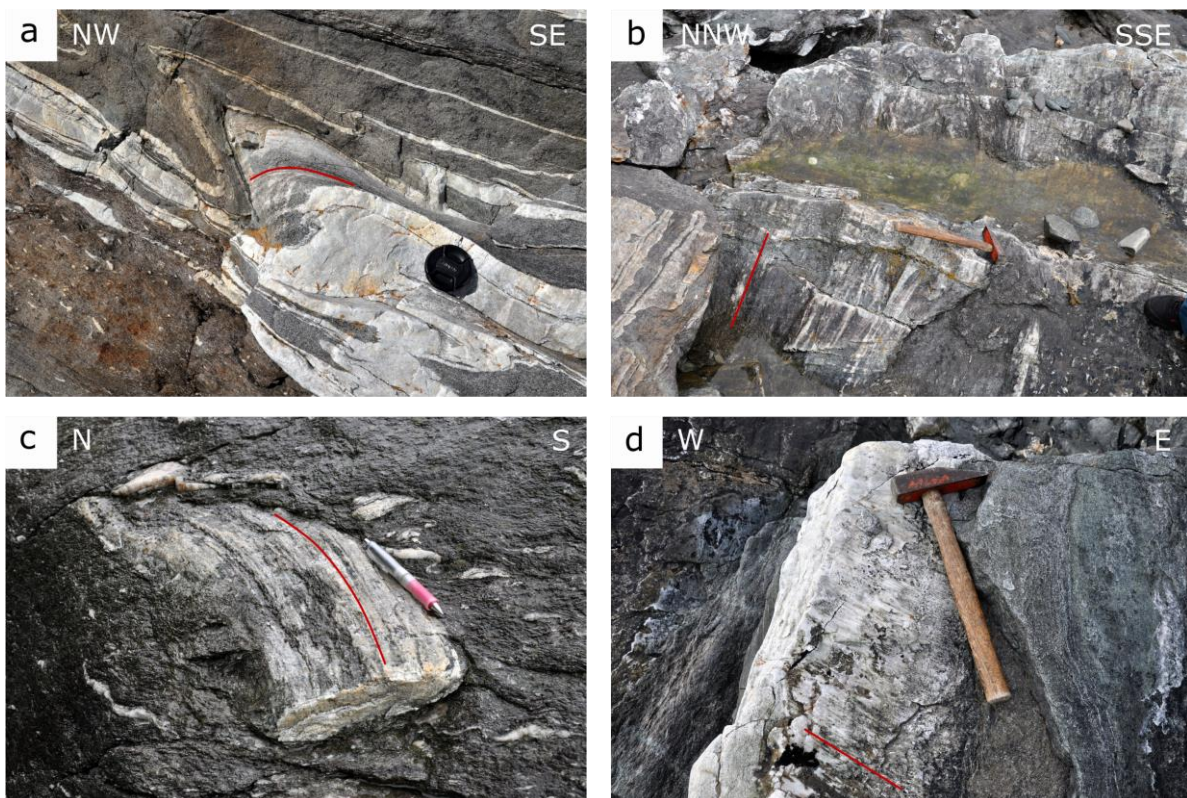


Figure 4.24: a) Mineral lineation on the surface of a folded aplite, drawn red line enhances the mineral lineation. Loc. no. AAH_124. b) Elongation lineation on the surface of large quartz lens, red line enhances the lineation. Loc. no. AAH_128. c) Elongation lineation on the surface of a quartz blob, red line enhances the lineation. Loc. no. AAH_127. d) Elongation lineation on the surface of an aplite layer, red line enhances the lineation. Loc. no. AAH_349.

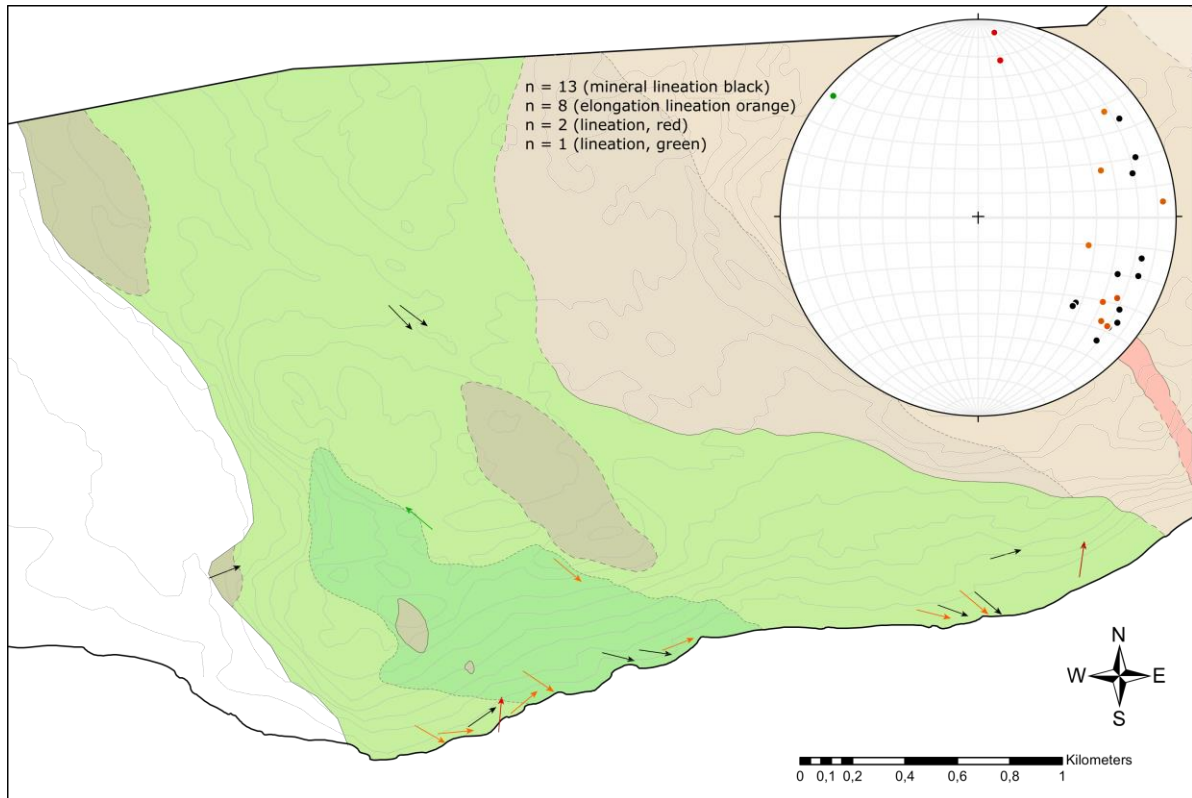


Figure 4.25: Overview map of mineral lineations (black) and elongation lineations (orange) with two groups of deviant measurements marked with red and green. The green one is assumed to be part of the main lineation towards the southeast. The colours of the measured lineations in the stereonet corresponds to the colours used on the map.

4.3.2.3 Rørvika unit

The mineral lineation within the Rørvika unit is represented on foliation planes by elongated and oriented hornblende crystals (Fig. 4.26a and b). A few quartz veins show elongation lineation on the border to surrounding amphibolitic rock corresponding to the trends of the mineral lineation (orange, Fig. 4.27), but it is less apparent than in the Trongen unit. Excluding the three excepting lineations with dip to south and southwest (blue, Fig. 4.27), the mean trend and plunge for Rørvika unit is 125/16.

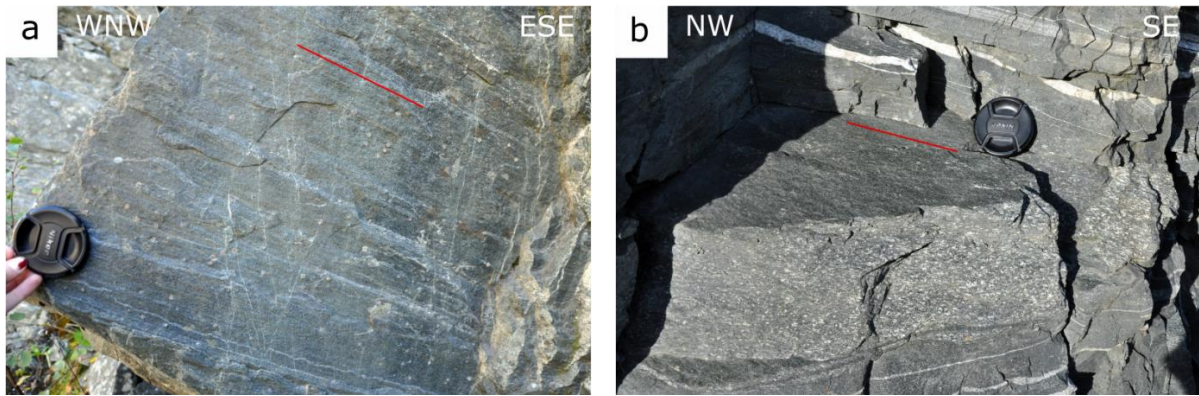


Figure 4.26: a) Mineral lineation of hornblende crystals on a surface with pink 0.5 cm big garnets, within the Amis. The black line indicates the direction of the lineation. Loc. no. AAH_364. b) Mineral lineation of hornblende crystals within Amis on the surface of a layer with porphyritic texture. The red line indicates the direction of the lineation. Loc. no. AAH_377.

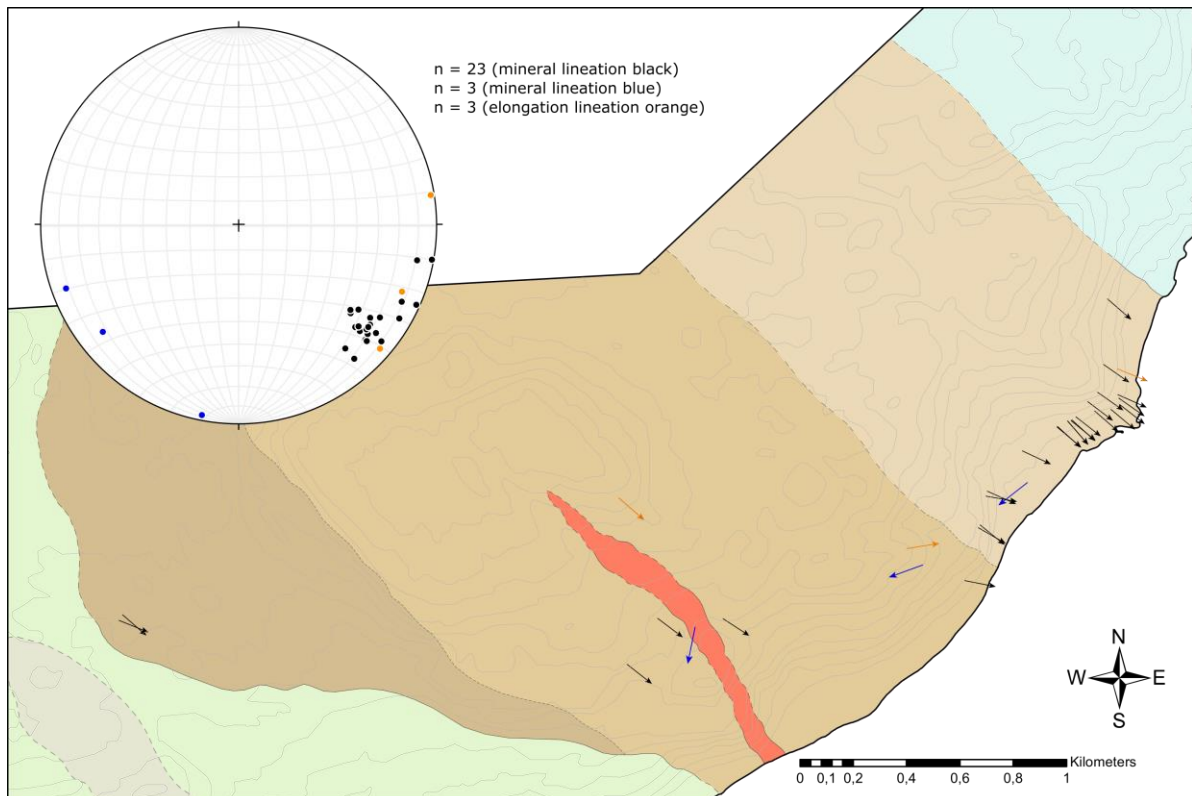


Figure 4.27: Map over the Rørvika unit with overview of the measured lineations. Orange arrows indicate elongation lineations measured on quartz layers, black arrows are mineral lineations and one blue arrows represents a mineral lineations deviant from the main trend. The colours of the measured lines in the stereonet coincide with the colours of the arrows on the map.

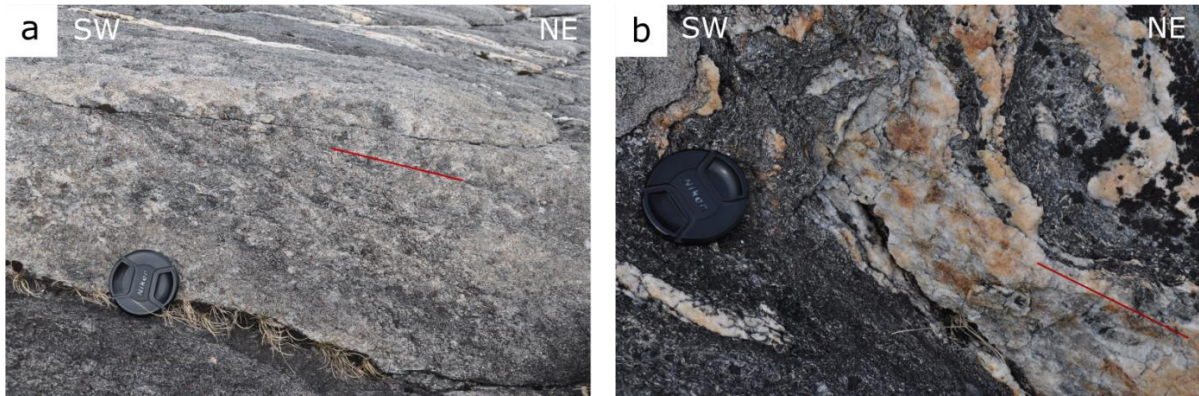


Figure 4.28: a) Weathered surface where oriented amphibole crystals exhibit a mineral lineation. The lineation is enhanced by the red line in the picture. Loc. no. AAH_402. b) Elongation lineation weakly visible on the surface of a quartz vein. The red line enhances the lineation. Loc. no. AAH_404.

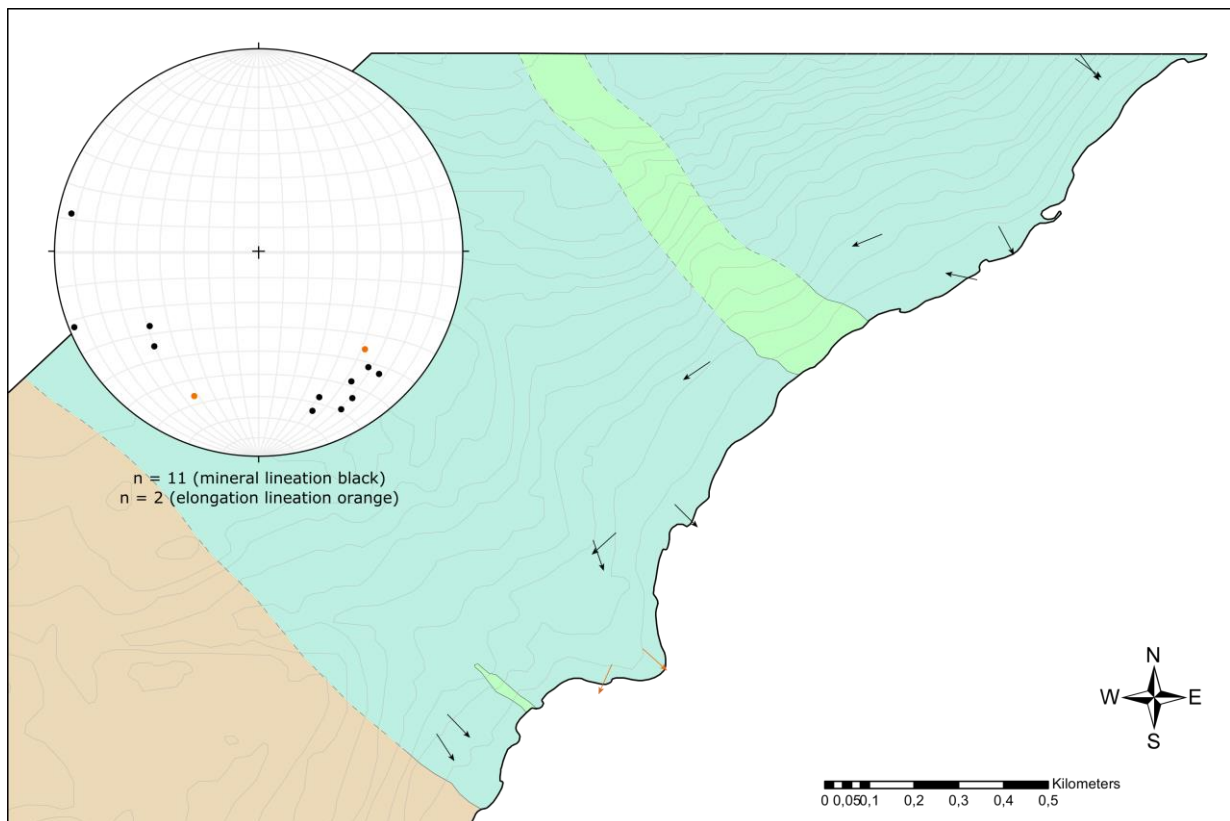


Figure 4.29: Map with an overview of all mineral lineations and elongation lineations measured within the Varneset unit. The mineral lineations are represented by black arrows and the elongation lineation by orange ones. The colours of the arrows coincide with the colours used in the stereonet.

4.3.2.4 Varpneset unit

A general lack of clear lineations within the Varpneset unit prevented a more detailed assessment and explains the relatively low number of mineral and elongation lineation measurements in comparison to the other units. The lineation was poorly visible due to strongly weathered surfaces and larger mineral grains with no preferred orientation.

The mineral lineation represented by aligned amphibole crystals (Fig. 4.28a; black, Fig. 4.29) and the elongation lineation are seen on the surface of a quartz vein (Fig. 4.28b; orange, Fig. 4.29). In general, the trend for the lineation in this unit is towards the south-southeast with a low plunge, and the mean trend and plunge for all measured lineations Varpneset unit is 172/21.

4.3.3 Fold systems

In the study area four distinct fold systems folding the main foliation and compositional banding were observed: i) SW-vergent folds (red, Fig. 4.30a), ii) NE-vergent folds (green, Fig. 4.30b), iii) NW-vergent folds (orange, Fig. 4.30c), iv) SE to E-vergent folds (purple, Fig. 4.30d) and v) symmetric folds (blue, Fig. 4.30e). The symmetric folds (blue, Fig. 4.30) are also representatives for the folds where the sense of vergence could not be deduced due to poor exposure. It should be noted that the folds studied are those where the main planar foliation itself is folded, and does not include intrafolial folds.

The Rødberget unit was not included in this subchapter due to the absence of any fold system.

4.3.3.1 Trongen unit

Within the Trongen unit, folds occur mainly within the Ghms and Hbs. Illustrative examples are found many places along the shoreline, where the outcrops are abundant and barren of vegetation (Fig. 4.32). Due to the strong planar foliation and interlayered quartz veins and aplites in the Hbs, folds are easily recognizable (Fig. 4.32a and b). In the Ghms, where the foliation is more undulating and less pronounced, the folds are observed with the help of deformed quartz veins, aplites, and pegmatites (Fig. 5.32c). Ghms and Hbs are often found in proximity to each other, either with thin layers or zones of Ghms within the Hbs, (Fig. 4.32d), or as Hbs as layers and zones within the Ghms (Fig. 4.32e and f). It can be observed at several locations that Ghms is preserved in the hinge zones of folded Hbs (Fig. 4.32f).

Analysing the direction of all studied folds within the Trongen unit, a clear and consolidating SW-vergent symmetry for the majority of the folds becomes evident (red, Fig. 4.31a, Appendix D). This also means that looking towards the north they show an s-fold symmetry. The axial planes of the SW-vergent folds dip towards the northeast and east, and the fold axes have a low to moderate trend towards the southeast (red, Fig. 4.31b). The group called SW-vergent folds are found throughout the Trongen unit (Fig. 4.32a-f; Appendix D).

At one location within the Trongen unit, close to the boundary towards the Rørvika unit (Appendix D), the observed axial plane dips towards the northeast and shows a NE-vergence (green, Fig. 4.31a; Fig. 4.32g). The corresponding fold axis (green, Fig. 4.31b) is part of the main NW-SE trending system.

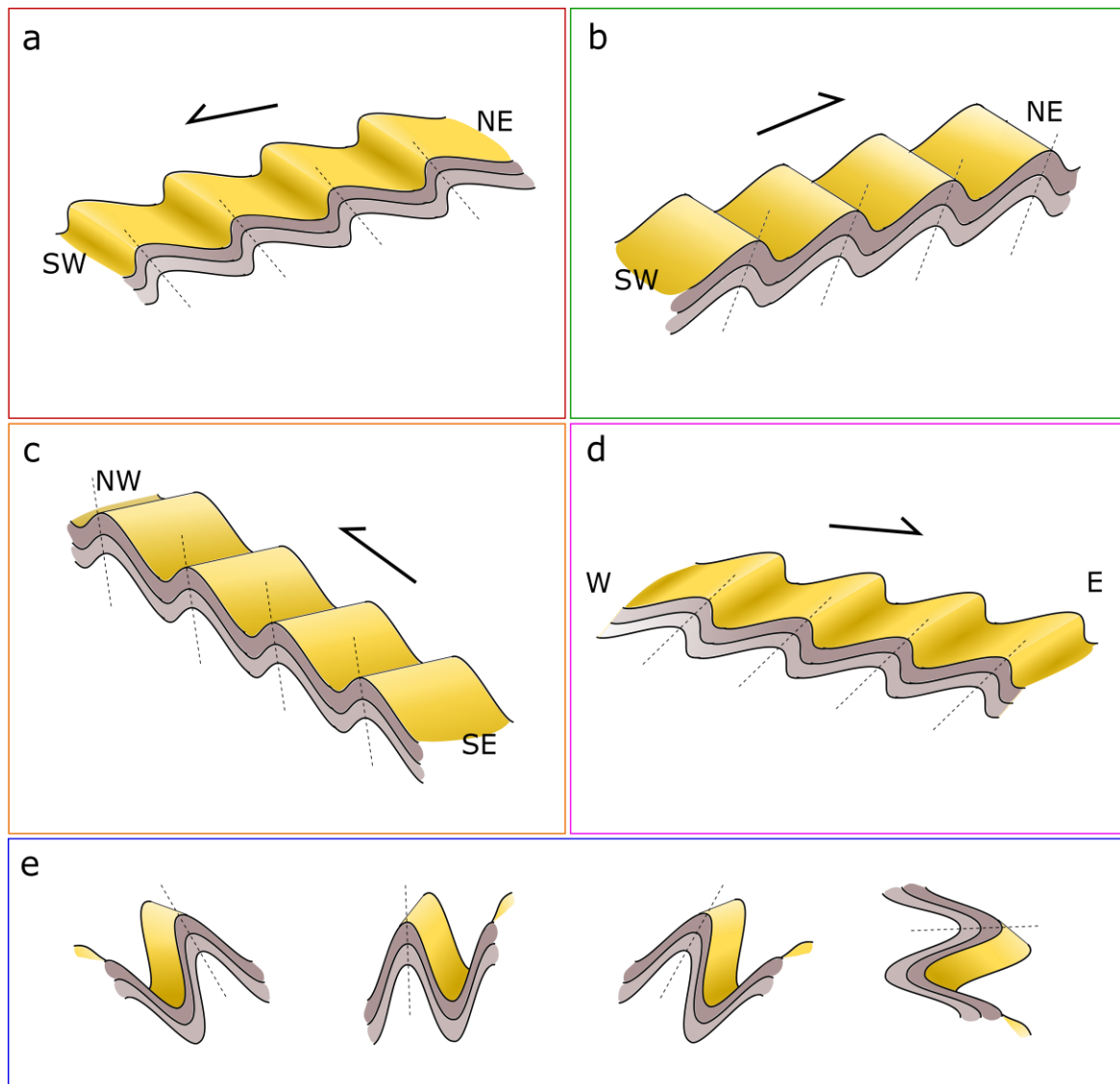


Figure 4.30: a) Schematic illustration of the SW-vergent folds (red). b) Schematic illustration of the NE-vergent folds (green). c) Schematic illustration of the NW-vergent folds (orange). d) Schematic illustration of the SE to E-vergent folds (purple). e) Schematic illustrations of examples of the symmetric folds (blue).

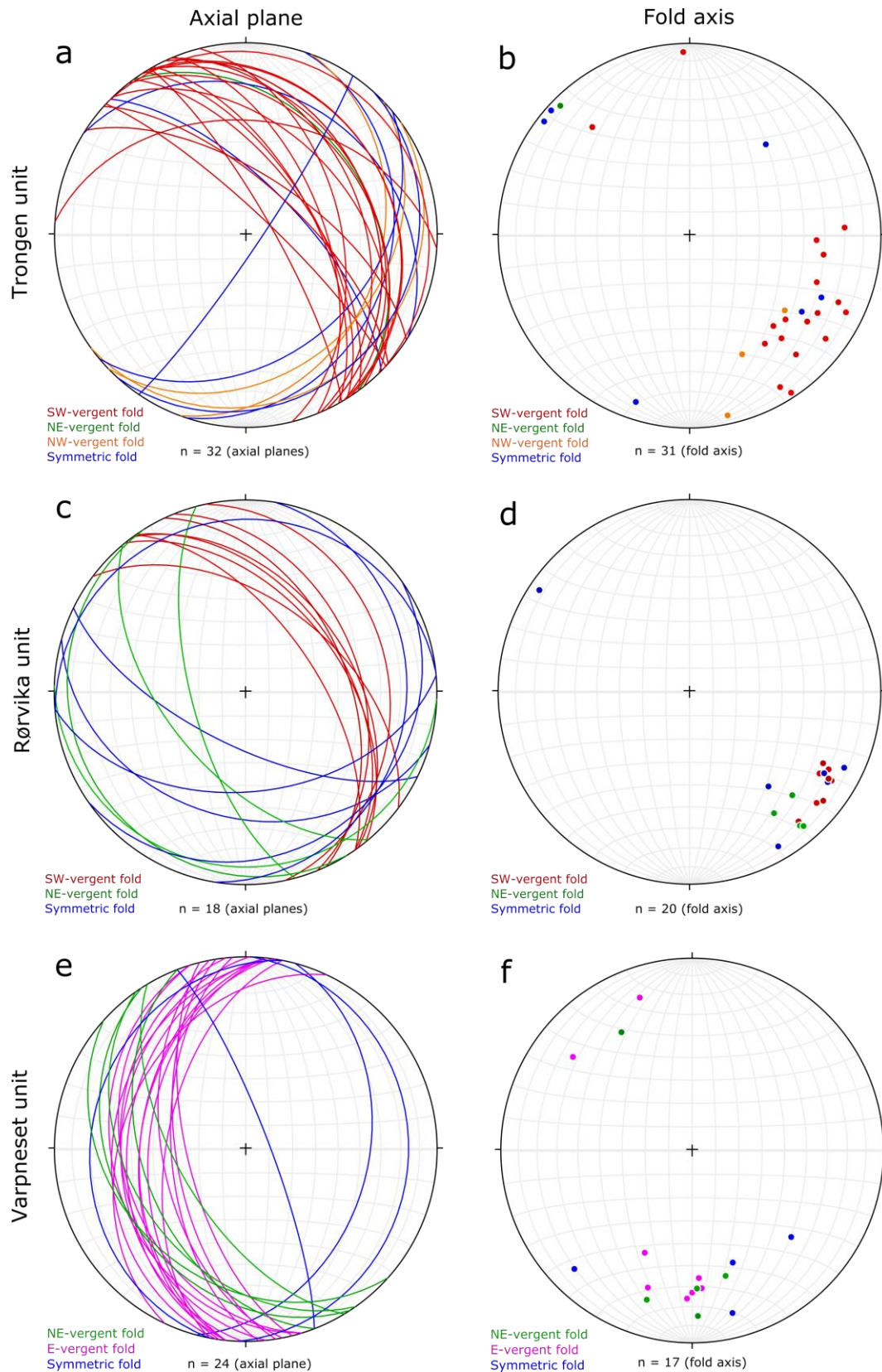


Figure 4.31: Stereonets of axial plane and fold axis from different units. Red colour indicating SW-vergent fold, green colour indicating NE-vergent fold, orange colour indicating NW-vergent fold, purple indicating SE to E-vergent fold, and blue the symmetric fold. a) Axial planes from Trongen unit. b) Fold axes from Trongen unit. c) Axial planes from Rørvika unit. d) Fold axes from Rørvika unit. e) Axial planes from Varpneset unit. f) Fold axes from Varpneset unit.

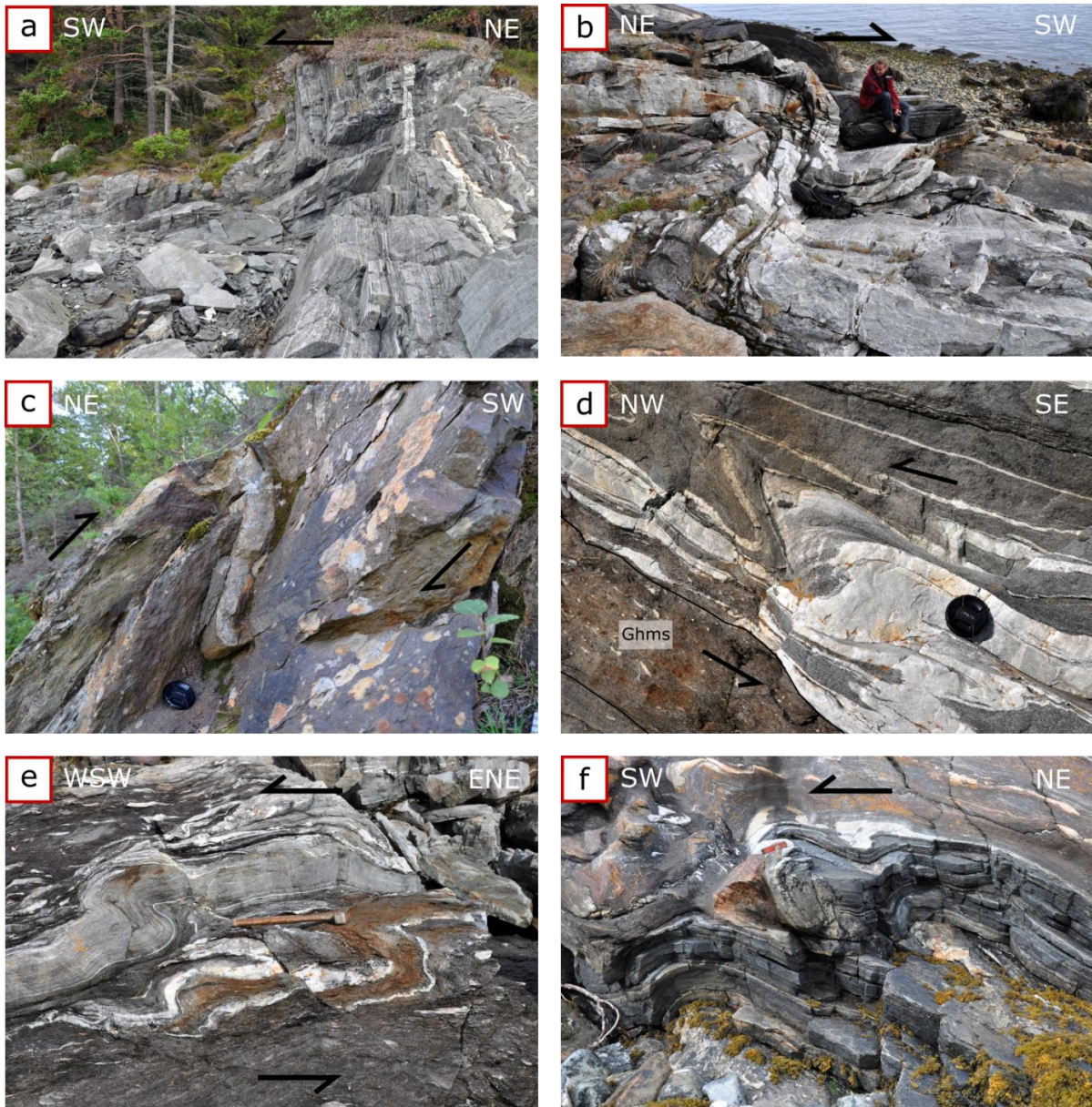


Figure 4.32: The colour on the box on each picture coincides with the type of fold shown in the picture, respectively red colour indicating SW-vergent folds, green colour indicating NE-vergent folds, orange representing the NW-vergent folds, and blue colour indicating symmetric folds. a) SW-vergent fold in Hbs. Loc. no. AAH_322. b) A larger zone of Hbs within Ghms folded with a SW-vergence. Loc. no. AAH_349. c) SW-vergent folded aplite in Ghms. Loc. no. AAH_327. d) SW-vergent fold within the Hbs. Beneath a 40 cm thick layer of Ghms can be noted. Loc. no. AAH_124. e) WSW-vergent folded layer of Hbs within Ghms. Loc. no. AAH_129. f) SW-vergent folded zone of Hbs within Ghms. Ghms is preserved in the hinge zone of the fold. Loc. no. AAH_140. g) NE-vergent fold in Ghms. Loc. no. AAH_119. h) NW-vergent folded quartz veins within the Ghms. Loc. no. AAH_341. i) Symmetric fold in Ghms. Loc. no. AAH_323. j) Symmetric folded Hbs and quartz vein within Ghms. Later cut by a fault with a 40 cm offset. Loc. no. AAH_177. k) Symmetric folded Hbs layer in Ghms. Loc. no. AAH_177. l) Symmetric folded pegmatite. The Ghms around shows the same clear folding due to the high content of amphibole and many quartz layers present. Loc. no. AAH_185.



Fig. continued from previous page

In addition, three NW-vergent folds are found in the Trongen unit (orange, Fig. 4.31a). There is no noticeable difference in the fold axis orientation between this group of folds and the other groups (orange, Fig. 4.31b), and they are represented both by deformed quartz veins (Fig. 4.32h) and by folds in the Hbs.

There are several folds where a vergence cannot unambiguously be assigned, as some are apparently symmetric and others are heavily eroded in such a way that vergence cannot be deduced. The symmetric folds show varying axial planes and fold axes (blue, Fig. 4.31a), and are observed as folded quartz veins in the Ghms (Fig. 4.32i), folded Hbs interlayered with the Ghms (Fig. 4.32j and k), and as folded pegmatite layers (Fig. 4.32l).

Oksvika, within the Trongen unit, is a good place to study folds representative for the entire unit. Oksvika is at locality AAH_322 (Appendix A) along the shoreline. Along the edges of a small pebble-covered bay, lithologies representative for the Trongen unit are well exposed in outcrops kept clean by constant wave-action.

The bay is situated within the Helle lithology and shows exposures of Ghms and Hbs, and the relationship between these three lithologies. Here several big open folds with axial planes towards the northeast can be observed. The largest folds are found at locality numbers AAH_120, AAH_121 and AAH_122 (Fig. 4.33). The open SW-vergent fold on locality AAH_120 is seen through the folding of the Hbs (Fig. 4.34a and b) with a plunge of the fold axis towards the southeast. The Hbs is interlayered with quartz veins and aplite layers, consequently folded together. The same can be said for the locality 121 and 122 (Fig. 4.34c and d). In the hinge zone of these two folds Ghms is preserved (Fig. 4.34c). At locality 123, a gentle fold with undulating fold flanks shows the same plunge in the fold axis towards the southeast, but no vergence could be deduced (Fig. 4.34e and f).

On the NE wall of the profile at locality number 124 (Fig. 4.33), there are several smaller folds observable (Fig. 4.6). These are open to tight folds of mostly Hbs (Fig. 4.24a and Fig. 4.34g) and Ghms that can be seen in thin layers and zones giving parts of the outcrop a brownish colour compared to the characteristic black Hbs (Fig. 4.6). This outcrop displays the transition from Hbs interlayered with Ghms into Ghms, then, and on the far top the transition into Helle (Fig. 4.33 and Fig. 4.6).

The outcrop on the SW wall of Oksvika at locality number 322 shows the same characteristic as on locality 124. A gradual transition from Hbs to Ghms and then Helle can be observed. The outcrop contains folded Hbs with lenses of interlayered Ghms (Fig. 4.34h). Within the Ghms, quartz veins have been tightly folded with an incline directed towards the northeast (Fig. 4.33 and Fig. 4.34i).

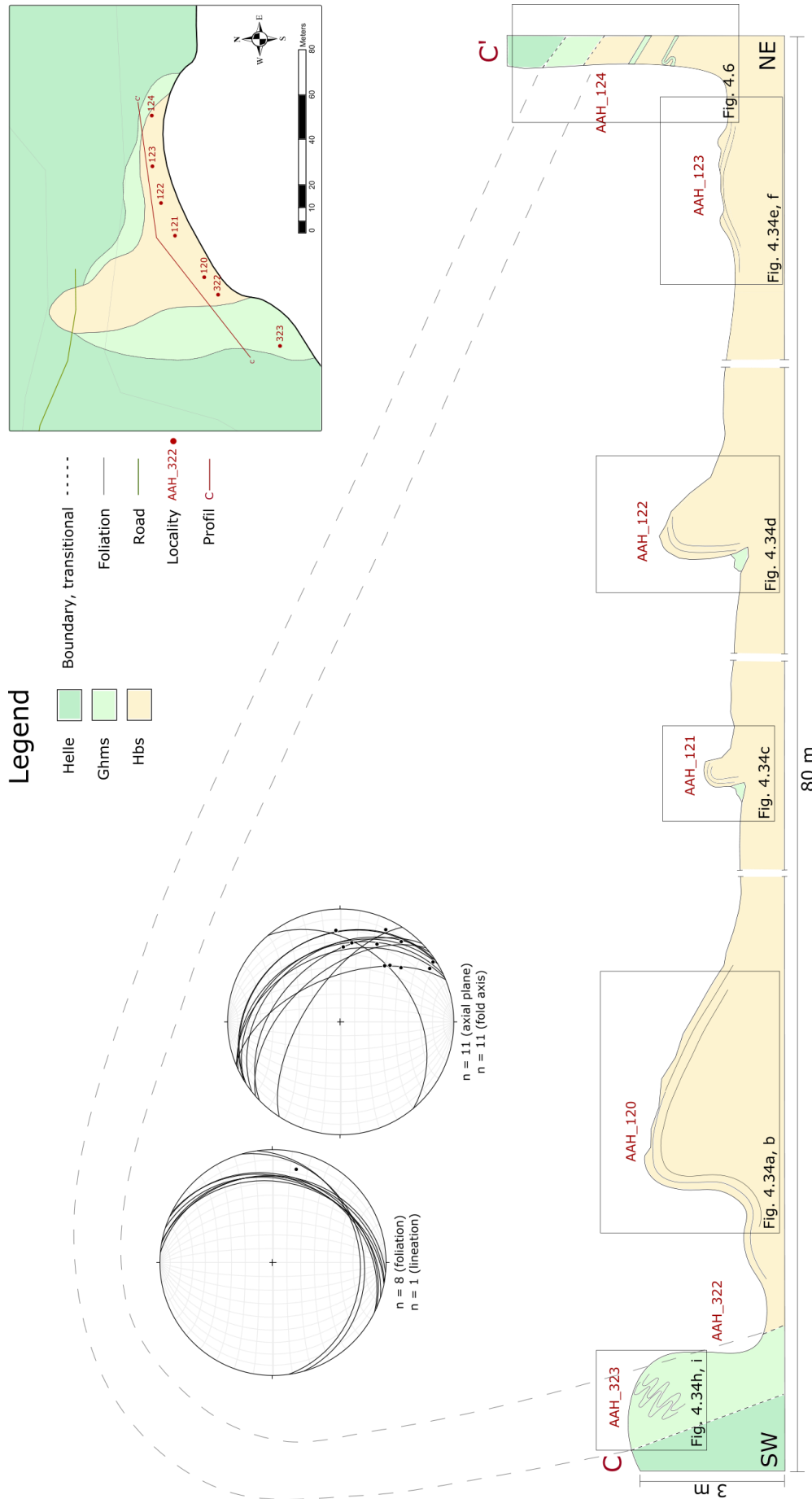
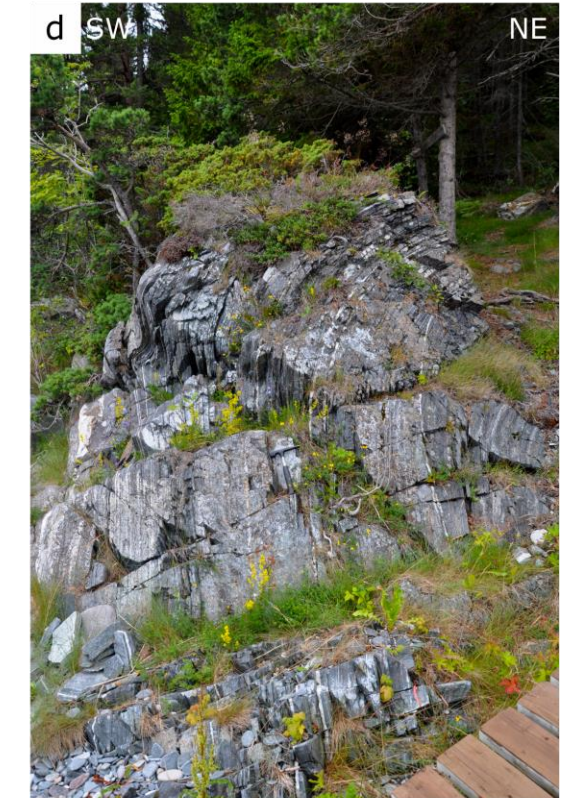


Figure 4.33: Profile over Oksvika with locality numbers and stereonet for the foliations and mineral lineation, axial planes and fold axis, and fault planes measured in the bay. Note that the profile has an approximate scale. Map with accurate length of the profil in upper right corner.

Field results



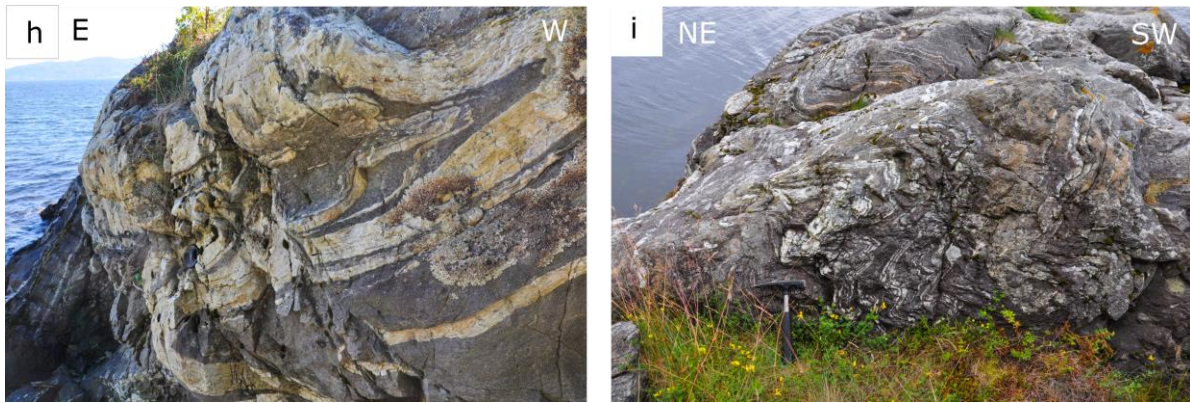


Figure 4.34: a) Folded Hbs on locality AAH_322 seen from northwest. b) Folded Hbs on locality AAH_322 seen from southeast. c) Folded Hbs on locality AAH_122. Note the Ghms preserved in the hinge zone. d) Folded Hbs on locality AAH_123. e) Gentle folded Hbs at locality AAH_123. The gentle fold show undulations on the flanks. f) Same fold as in e, just seen from southeast. g) At locality AAH_124 Ghms and Hbs are interlayered and folded together. This fold shows a vergence to west-southwest. h) Folded Hbs at locality AHH_322 with vergence to the SW. i) Between locality AAH_322 and AAH_323 there is a transitional boundary into Ghms. Within this zone of Ghms (locality AAH_323), quartz veins are folded with a vergence to southwest.

Folded Ghms is more difficult to observe in the field. At the Fagerli outcrop, a roadcut between Rørvika and Stadsbygd (Locality AAH_327, Appendix 1), folds related to Ghms can be observed. Judging by the lichen and trees growing on and along the outcrop, it must be fairly old. The outcrop is about 200 meters long and stretches out in an SE-NW direction. To the southeast, the outcrop is dominated by foliated and folded Ghms with its characteristic brown weathering colour. The inclined folds are open to tight with a steeply dipping axial plane towards the northeast (Fig. 4.35). The fold axis has a trend towards the southeast with a moderate plunge (Fig. 4.35). The folds can be seen in the Ghms itself (Fig. 4.35a and b), and through folding of quartz veins with a thickness at a few centimetres (Fig. 4.35c and d).

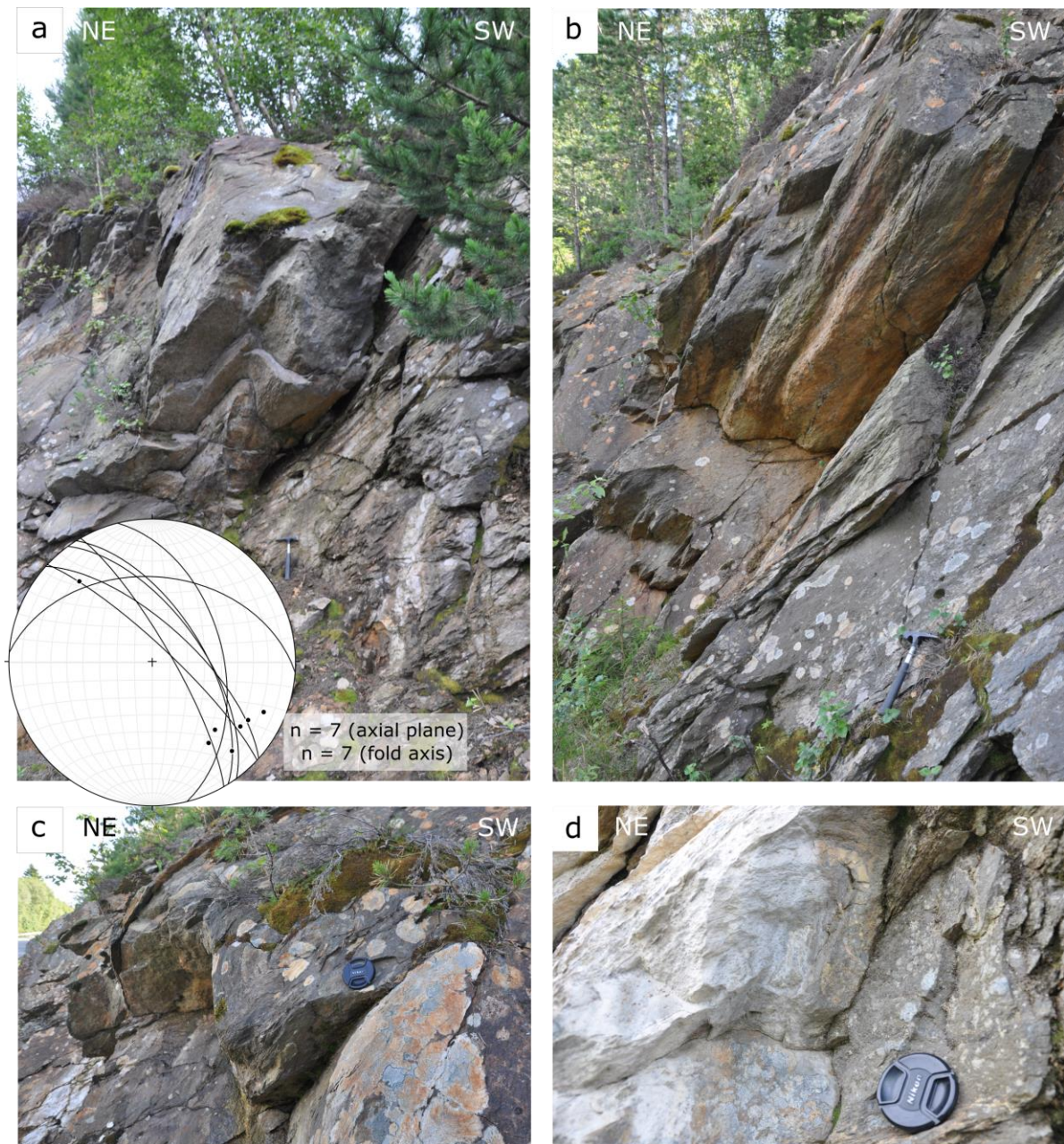


Figure 4.35: Examples of folds from the Fagerli outcrop, all showing a vergence towards the southwest. The stereonet shows the measured axial planes and fold axis. a and b) Folded Ghms. c and d) Folded Ghms with quartz veins. Loc. no. AAH_327.

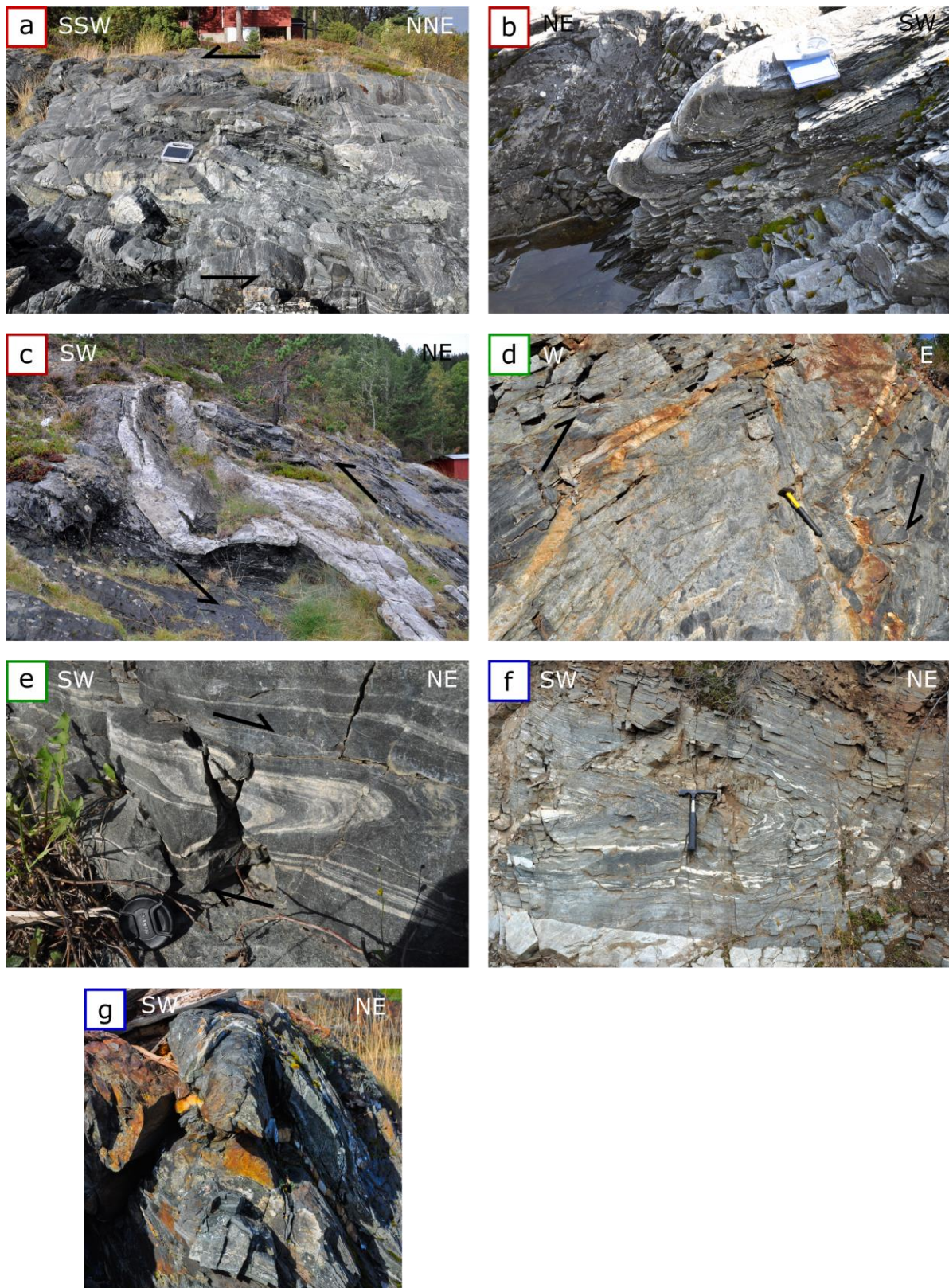


Figure 4.36: The colour on the box on each picture correlates with the type of fold shown in the picture, respectively red colour indicating SW-vergent folds, green colour indicating NE-vergent folds, and blue colour indicating symmetric folds. a) SW-vergent folds in Amis. Loc. no. AAH_351. b) SW-vergent fold in Amis. Loc. no. AAH_351. c) And a SW-vergent fold within Amfs. Loc. no. AAH_353. d) NE-vergent fold in the Amis. Loc. no. AAH_380. e) NE-vergent fold in the Amis. Loc. no. AAH_373. f) Symmetric fold in Amfs. Loc. no. AAH_148. g) Symmetric and upright fold in Amis. Loc. no. AAH_232.

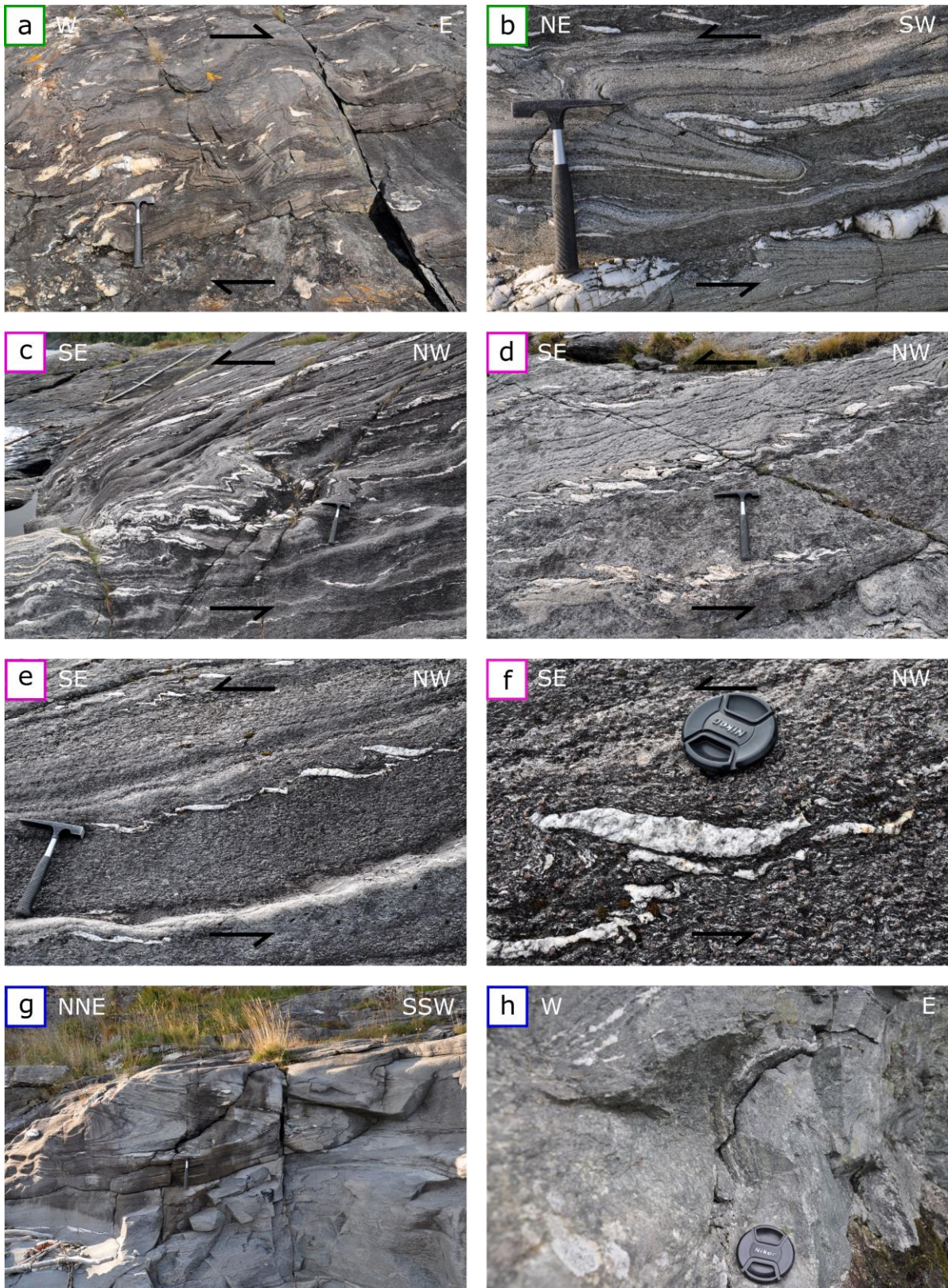


Figure 4.37: The colour on the box on each picture corresponds with the type of fold shown in the picture, respectively green colour indicating NE-vergent folds, purple colour indicating SE-vergent folds, and blue colour indicating symmetric folds. a) NE-vergent fold in Hcqs with alternating layer being more amphibolite-rich. The outcrop contains lenses and layers of quartz parallel to the foliation. Loc. no. AAH_206. b) NE-vergent and

4.3.3.2 Rørvika unit

In the Rørvika unit, folds can be observed through folding of the clear and planar foliation in the amphibolitic rocks. Interlayered quartz veins and aplites are folded together with the amphibolitic rocks. Open to tight folds are found within all the three amphibolitic lithologies of the Rørvika unit (Appendix D). The general vergence of the folds from east to west in the unit varies from being mainly SW-vergent (Fig. 4.36a-c) to NE-vergent (Fig. 4.36d and e).

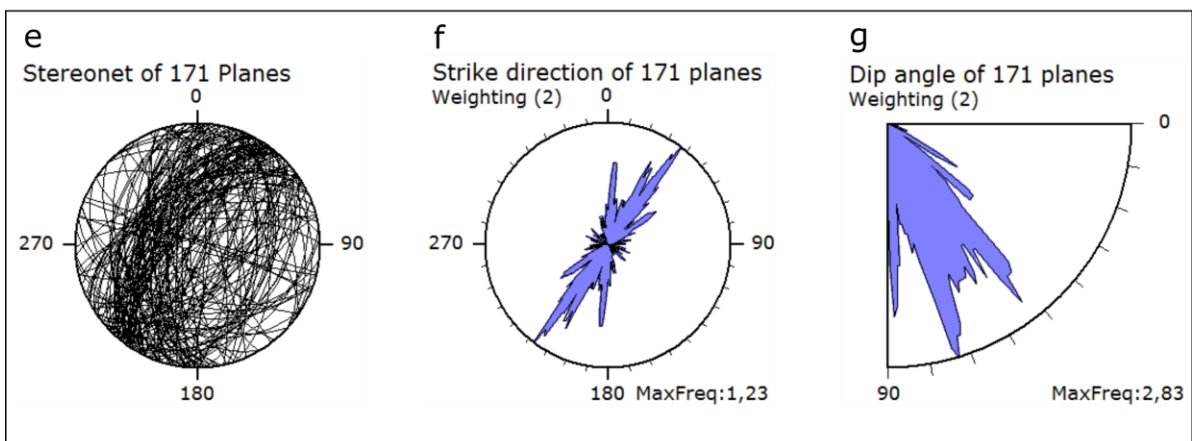
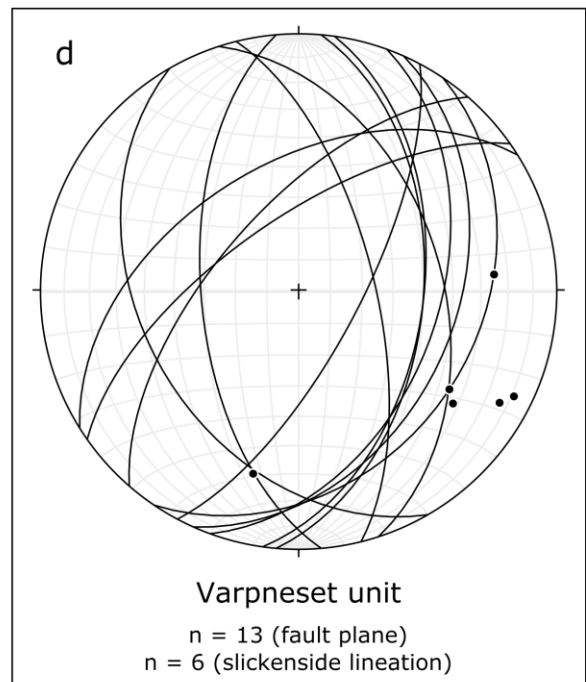
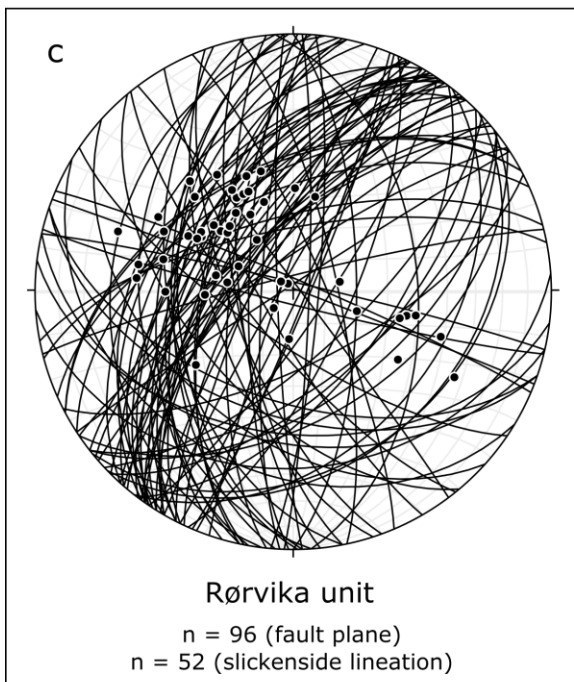
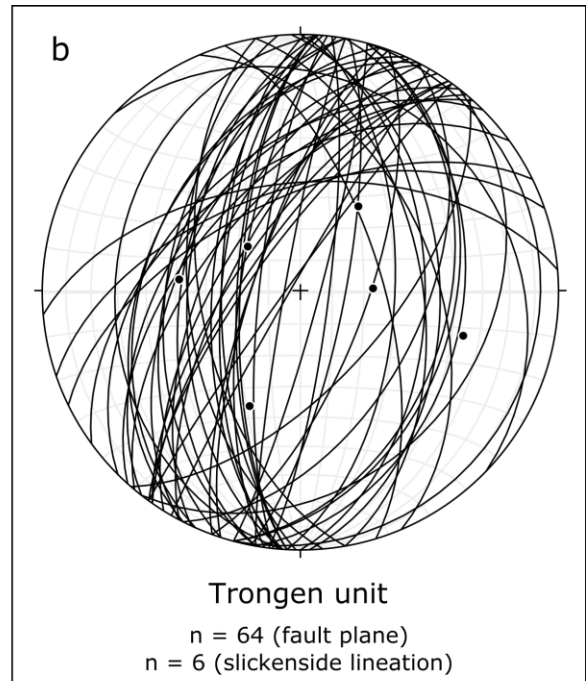
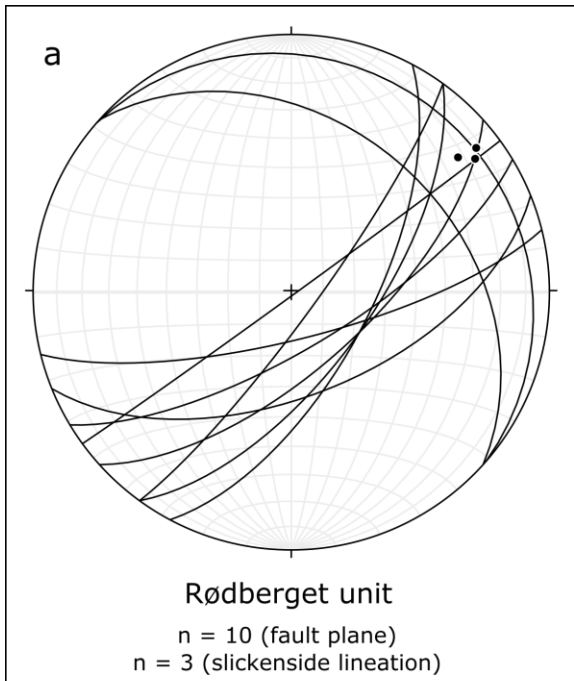
The SW-vergent (Fig. 4.36a-c) folds have axial planes with dip direction towards the northeast (red, Fig. 4.31c) and the fold axes show a trend to the southeast (red, Fig. 4.31d). The NE-vergent folds (Fig. 4.36d and e) have axial planes with a steep to shallow dip and a dip direction mainly towards the southwest (green, Fig. 4.31c) and the fold axes show the same trend as for the SW-vergent folds, with a low plunge towards the southeast (green, Fig. 4.31d).

In addition, several symmetric folds are present in the Rørvika unit (Fig. 4.36f and g), showing both axial planes with dip towards the southwest and northeast (blue, Fig. 4.31c). All the symmetric folds have a fold axis with a trend towards the southeast (blue, Fig. 4.31d). As mentioned above, some of these folds might be part of bigger NE- or SW-vergent folds.

4.3.3.3 Varpneset unit

The fold system in the Varpneset unit changes characteristics from southwest to northeast corresponding to a change in the Hcqs. In the southwest, the Hcqs shows layers with a higher content of amphiboles and the rock exhibits folding of the foliated layers (Fig. 4.37a and b). Towards the northeast, Hcqs enclose abundant 1-6 cm thick quartz veins with strong accommodation of shear and a more homogeneous rock with less pronounced foliation and layering. The fold system is thus identified with the help of these sheared quartz veins (Fig. 4.37c and d). Because of the competence of the quartz veins, they have split during shearing, leaving quartz “duplexes” (Fig. 4.37e). At a closer look (Fig. 4.37f) the folding of also the Hcqs gets apparent.

Fig. caption cont. tight fold in Hcqs. Loc. no. AAH_217. c) Deformed quartz veins indicating shear towards the southeast. Loc. no. AAH_172. d) SE-vergent folds in quartz veins within the Hcqs. Loc. no. AAH_400. e) Sheared quartz-veins with vergence towards the southeast. It is only the veins showing an apparent sense of shear, the surrounding rock exhibits an apparent planar foliation. Loc. no. AAH_172. f) Close-up of the sheared quartz veins. The surrounding Hcqs is deformed and folded together with the quartz veins on a small scale. Loc. no. AAH_172. g) A symmetric fold with a sub-horizontal axial plane in Hcqs. Loc. no. AAH_218. h) Symmetric fold in close proximity to the boundary towards the Rørvika unit. Loc. no. AAH_157.



The axial planes of the folds in northeast have a dip towards the west-southwest (green, Fig. 4.31e, Appendix D) and are part of the NE-vergent fold system. The fold axis of these folds have a low plunge towards the south (green, Fig. 4.31f). The SE to E-vergent fold system display axial planes with a dip towards the west (purple, Fig. 4.31e). The fold axis for both the NE-vergent and SE to E-vergent fold systems show a general trend towards the southwest to southeast, with three deviant measurements with the fold axis trending northwest (Fig. 4.31f). The symmetric folds observed in Varpneset unit show a dip direction either to the east or to west (blue, Fig. 4.31e; Fig. 4.37 g and h), with a fold axis varying in trend towards the south-southeast to southwest (blue, Fig. 4.31f).

4.3.4 Brittle structures

Brittle structures are present in all the units of the studied area (Fig. 4.38; Appendix E). Some of the faults show a semi ductile character, and these are here included among the brittle structures.

4.3.4.1 Rødberget unit

In the Ingdal granitic gneiss (Locality 15KSV_55 and AAH_346) most of the brittle faults have a steep dip towards the southeast (Fig. 4.38a; Appendix E). Some faults are asymmetric and contain brecciated rock in the fault zone (Fig. 4.39a and b). The boundary to the host rock is sharp on one side and gradually moves into less deformed host rock on the other side (Fig. 4.39c). The fragment size within the fault zone varies from millimetre size close to the boundary, to 8 cm and increases in size towards the less deformed host rock (Fig. 4.39c and d). The bigger and undulating fracture zones show smaller and parallel fractures in close proximity, both of antithetic and synthetic character. Within the fault zones mineralisation of quartz, epidote, calcite and some chlorite is found on and in between the brecciated rock. The quartz mineralisation can be found alone (Fig. 4.39e) or together with epidote (Fig. 4.39f). Where quartz and epidote co-occur, it seems like the quartz is coating the epidote, indicating that quartz formed at a later stage after the epidote had already crystallized. Some surfaces show a characteristic glazed and shiny appearance resulting from the coating of epidote and quartz (Fig. 4.39g). The calcite has a white and flaky occurrence and is found only on some of the

Figure 4.38: Overview of the measured fault planes and slickenside lineations from a) Rødberget unit, b) Trongen unit, c) Rørvika unit, and d) Varpneset unit. e) A plot showing all measured fault planes. f) Rosediagram enhancing the strike direction for the measured fault. A southwest-northeast strike dominated. g) Rosediagram showing the distribution of the dip for all measured fault planes. A dip of about 54-74° dominates.

Field results

fault planes (Fig. 4.39h), and can in appearance be compared to the calcite mineralisation in the quarry (chapter 4.3.4.3).





Figure 4.40: At several locations along the shoreline faulted outcrops can be found. From the faulted quartz veins one can deduce apparent movement along the faults. Picture is taken at locality AAH_180 and shows an outcrop with a set of apparent normal faults.

4.3.4.2 Trongen unit

Brittle structures in the form of fractures and faults are abundant within the Trongen unit, especially in the Hbs and Ams. Where the fractures are well exposed, the fault rock and mineralisation can be studied. Fault mineralisations observed are quartz, epidote, and chlorite, with epidote being the most abundant. In a few localities slickensides are readily observed, and in other localities quartz veins show an offset and hence the sense of shear on the fault (Fig. 4.40).

Figure 4.39: a) Fault zones within the Rødberget unit have a steep dip towards the southeast. Loc. no. KSV_55. b) Some of the larger faults show brecciated Ingdal granitic gneiss. Loc. no. AAH_346. c) The breccia has fragments varying in size from a few mm and up to about 8 cm, increasing in size towards the centre of the fault zone. Loc. no. KSV_55. d) Fragments within a brecciated fault zone. Loc. no. KSV_55. e) Quartz mineralisation within a fault zone. To the right in the picture the intact rock can be seen. The grain sizes of the fragments are small close to the edge and increases in size towards the centre of the zone. Where the fragments are smaller, more quartz mineralisation occurs. Loc. no. AAH_346. f) Quartz and epidote mineralisation together on a fault surface. The quartz appears to have mineralized at a later stage than the epidote. Loc. no. KSV_55. g) A fault surface with a glazed and shiny appearance. Under the “glazing”, structural characteristics typical for slickenside lineations can be conjectured. Loc. no. KSV_55. h) The mineralisation of calcite is coarse, white and flaky. Loc. no. KSV_56.

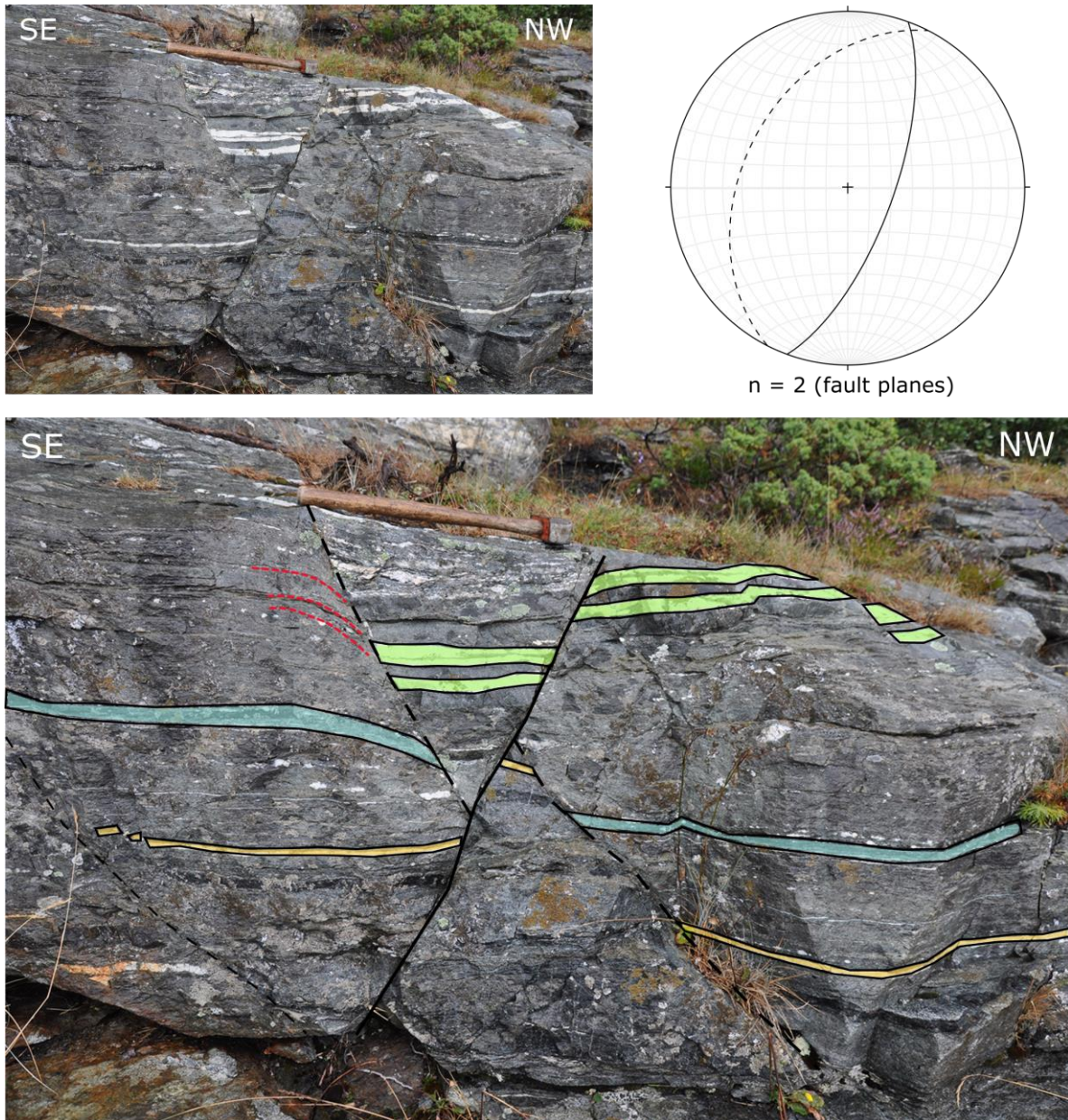


Figure 4.41: A northwest (dotted line) and a southeast (solid line) dipping fault. The NW-dipping fault is cut by the SE-dipping fault, indicating a relative age relationship between these two sets of faults. Picture is taken at locality AAH_126.

Mostly the faults show a moderate to steep incline with dip towards the southeast or northwest (Fig. 4.38b; Appendix E). However, localities in the north of the unit exhibit a steep dip direction facing more to the west and to the east, while closer to the shoreline in the south the dip direction is more similar to the quarry, towards the northwest and southeast.

A locality where the relationship between the northwest and the southeast dipping faults can be studied indicates that the NW-dipping faults are older than the SE-dipping faults (Fig. 4.41). However, it is not possible to say anything more precise about the timing of these two events.

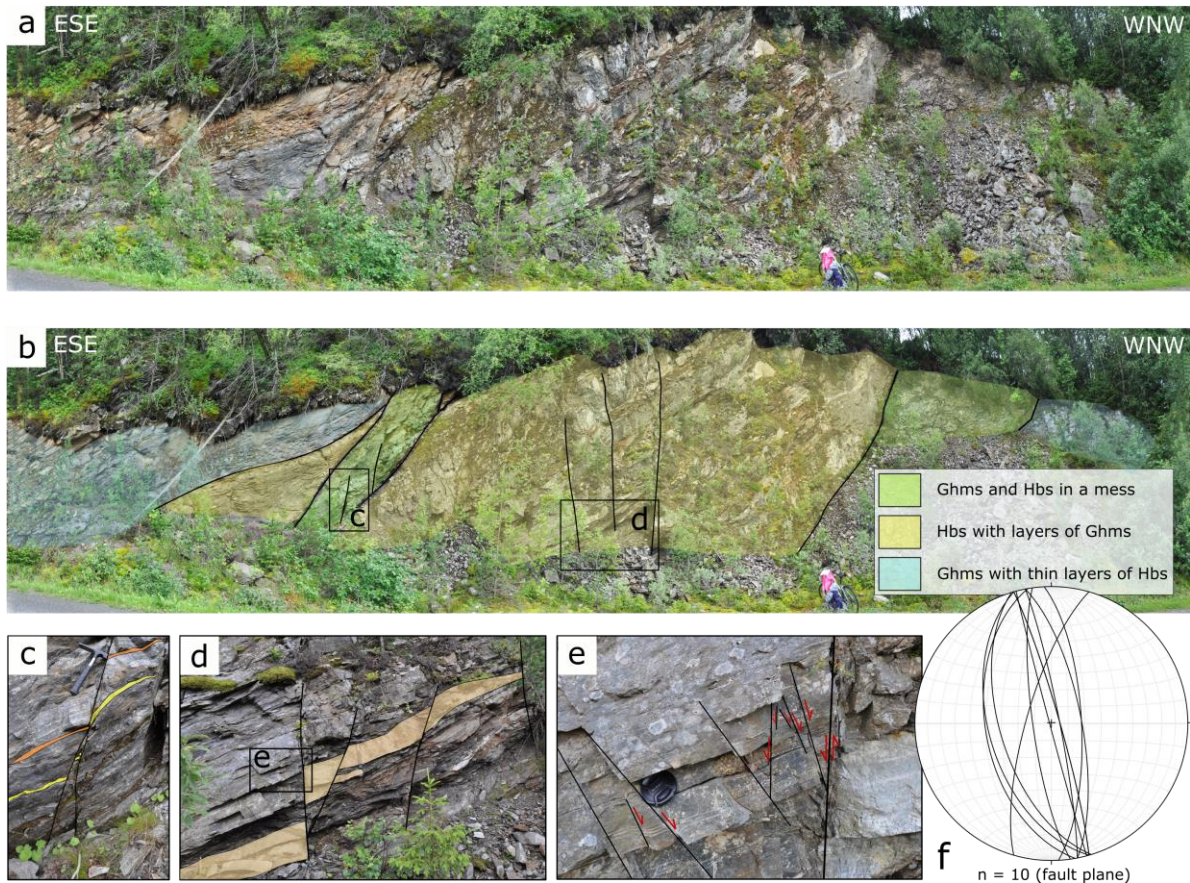


Figure 4.42: Sets of brittle structures from the Fagerli outcrop (Locality AAH_327, Appendix A). a) Overview of the most west-northwest part of the Fagerli outcrop. b) This part of the outcrop can be divided into three parts, Ghms with thin alternating layers of Hbs, Hbs with layers of Ghms, and Ghms and Hbs together in a fault rock. c) Detail from the outcrop showing a brittle normal fault, down the east. d) Detail from the Fagerli outcrop. A set of normal faults with down to the east. e) Detail from d) with a set of several faults with apparent normal movement, both down towards the east and towards the west. f) The stereonet displays an overview of the brittle faults showing up/down characteristics found in the Fagerli outcrop. Red represents the brittle fault planes with a normal movement and blue represents reverse brittle faults.

At the Fagerli outcrop (Locality AAH_327, Appendix A) a larger fault zone can be observed. The outcrop consists of Ghms, Hbs and fault rock and no folds can be observed in this part of the outcrop (Fig. 4.42a). A more Hbs rich zone of the outcrop is alternating with zones where Ghms and Hbs are deformed together in a fault rock (Fig. 4.42b). Within this part of the Fagerli outcrop there are several brittle faults indicating normal movement (Fig. 4.42d and e). The normal fault shows down towards both the east and west, all with a steep dip.

In Oksvika (Locality AAH_322, Appendix A), the brittle structures show similar trends to the brittle structures described above, with a steep to moderate dip towards the northwest and southeast. No slickenside lineations could be measured, but due to the quartz veins parallel to the foliation of the Hbs (Fig. 4.6), an apparent movement can be deduced. In general, the faults observed are normal with a down movement either to the northwest (Fig. 4.43a) or down

towards the southeast (Fig. 4.43b and c). The offsets of the faults are less pronounced in the down-to-northwest faults with about 3-10 cm, while the down-to-southeast faults have offsets of about 10-40 cm. The faults tend to fade out in the Ghms layers within the Hbs (Fig. 4.43d), indicating that Hbs is more competent than the Ghms.

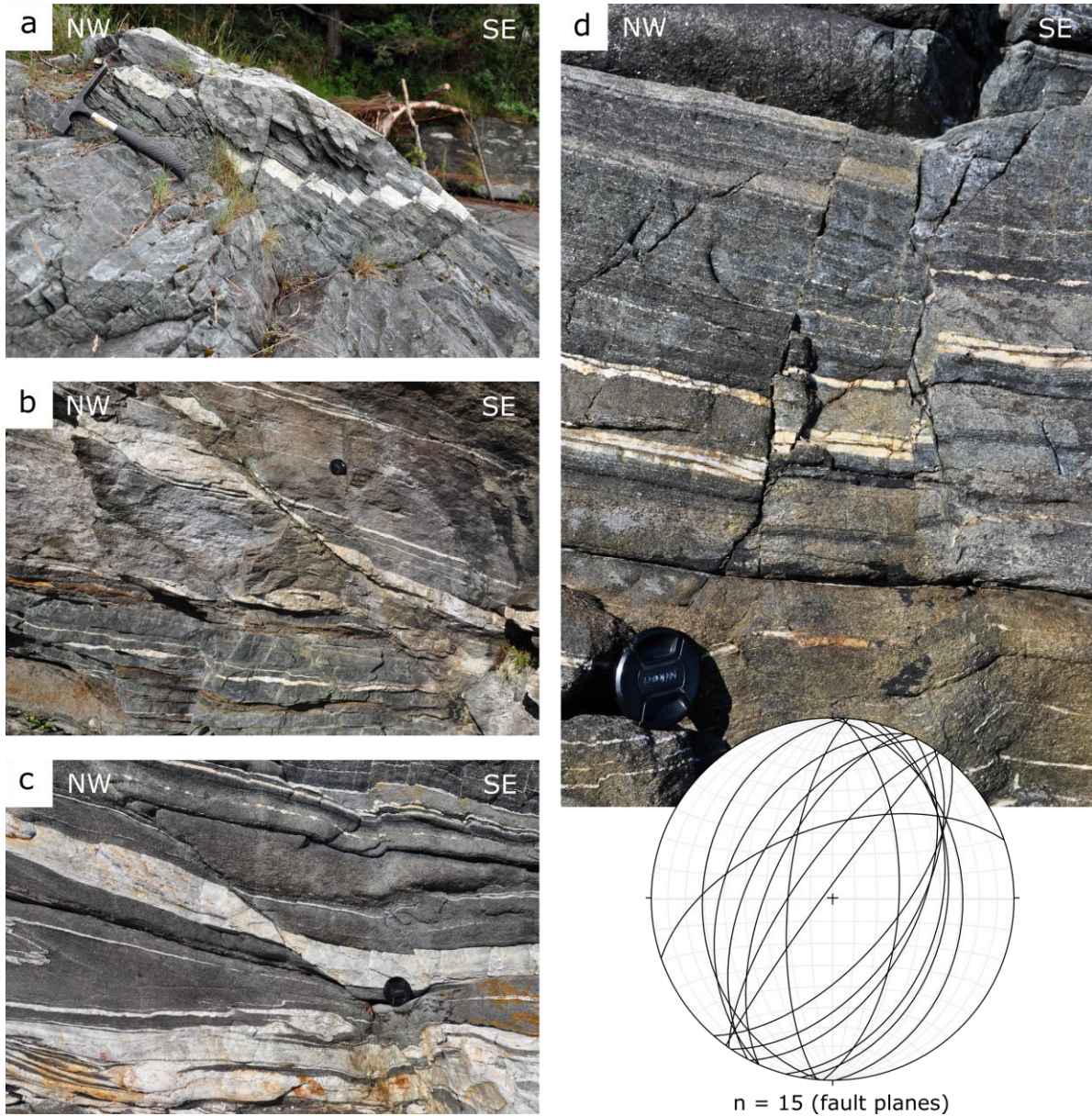


Figure 4.43: The outcrops of Oksvika (locality AAH_322, Appendix A) exhibit faults with an offset due to the different lithologies present. Stereonet shows the fault planes measured in the outcrops. For an overview and locality of picture, see Fig. 4.6. a) Faults in the Hbs at locality AAH_124. Mica rich layers can be observed from the brownish weathering colour and the faults tends to fade out into Ghms layers. k) Fault in Hbs, locality AAH_124, with an offset of 17 cm. The Hbs layers show earlier folding. l) Fault in Hbs, locality AAH_124. The offset and the apparent movement along the fault can be seen from the cutting of the quartz veins. The Offset is about 60 cm.

4.3.4.3 Rørvika unit

The brittle structures in the Rørvika unit show similar strikes as the ones in the Trongen unit, namely steep fault planes with a dip towards the northwest and towards the southeast (Appendix E). Yet, there are some exceptions with steep N-NE and S-SW dipping faults.

Similar to findings from the Tronget unit, quartz veins and pegmatite or aplite dykes make it possible to decide a relative movement along the fault planes in the Rørvika unit (Fig. 4.44).

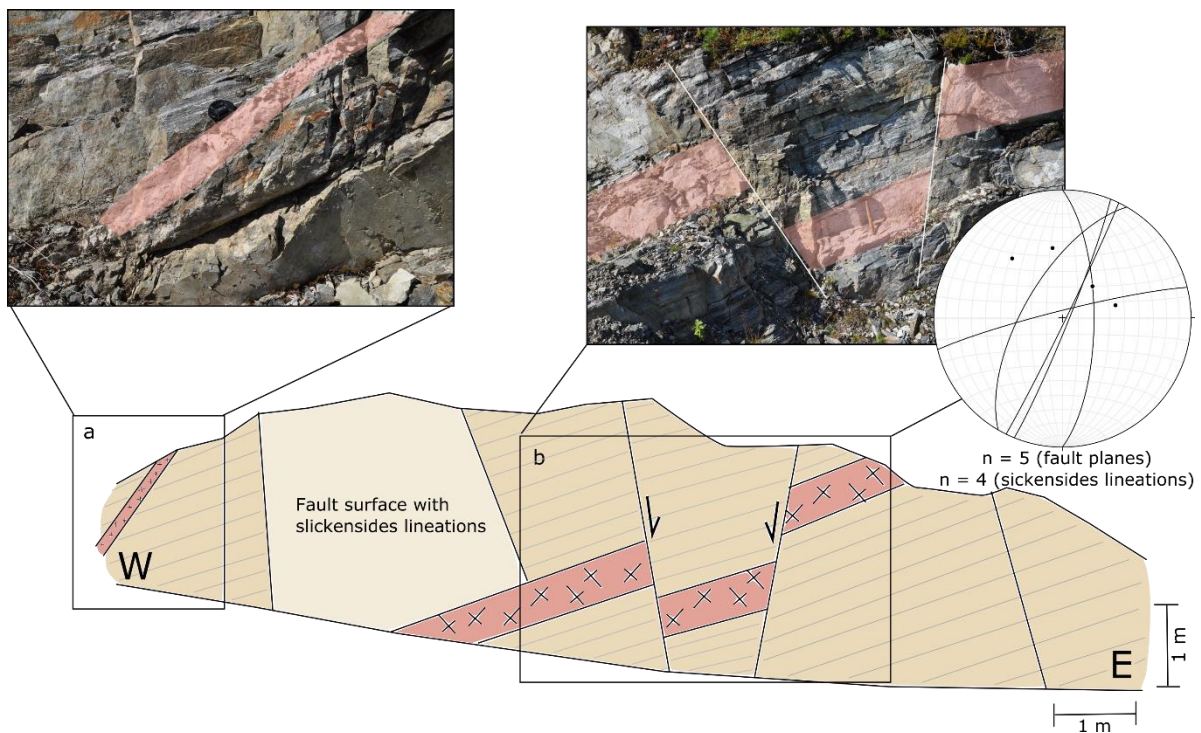


Figure 4.44: Outcrop in the Amfs with two aplite dykes. The larger dyke is faulted showing a graben structure. The offset is about 90 cm for the western fault and 70 cm for the eastern. The larger pegmatite dyke is parallel to the foliation whereas the smaller pegmatite crosscuts the foliation. Loc. no. AAH_238.

Just north of the Rørvika ferry terminal, at Kleivneset (Locality AAH_232, Appendix A), complex brittle-ductile structures make this locality interesting to describe in more detail. It is located within the Amis of the Rørvika unit, just along the shoreline where the outcrops are good and highly visible, affected by the wave action and tide, and easily accessible from the ferry terminal (Fig. 4.45).

The Amis has a straight and penetrative foliation and is affected by folding. Looking at a profile from southwest to northeast, the area can be divided into three parts, *a*, *b* and *c*, to more easily describe the observations (Fig. 4.45). The southern part [*a*] of this locality is

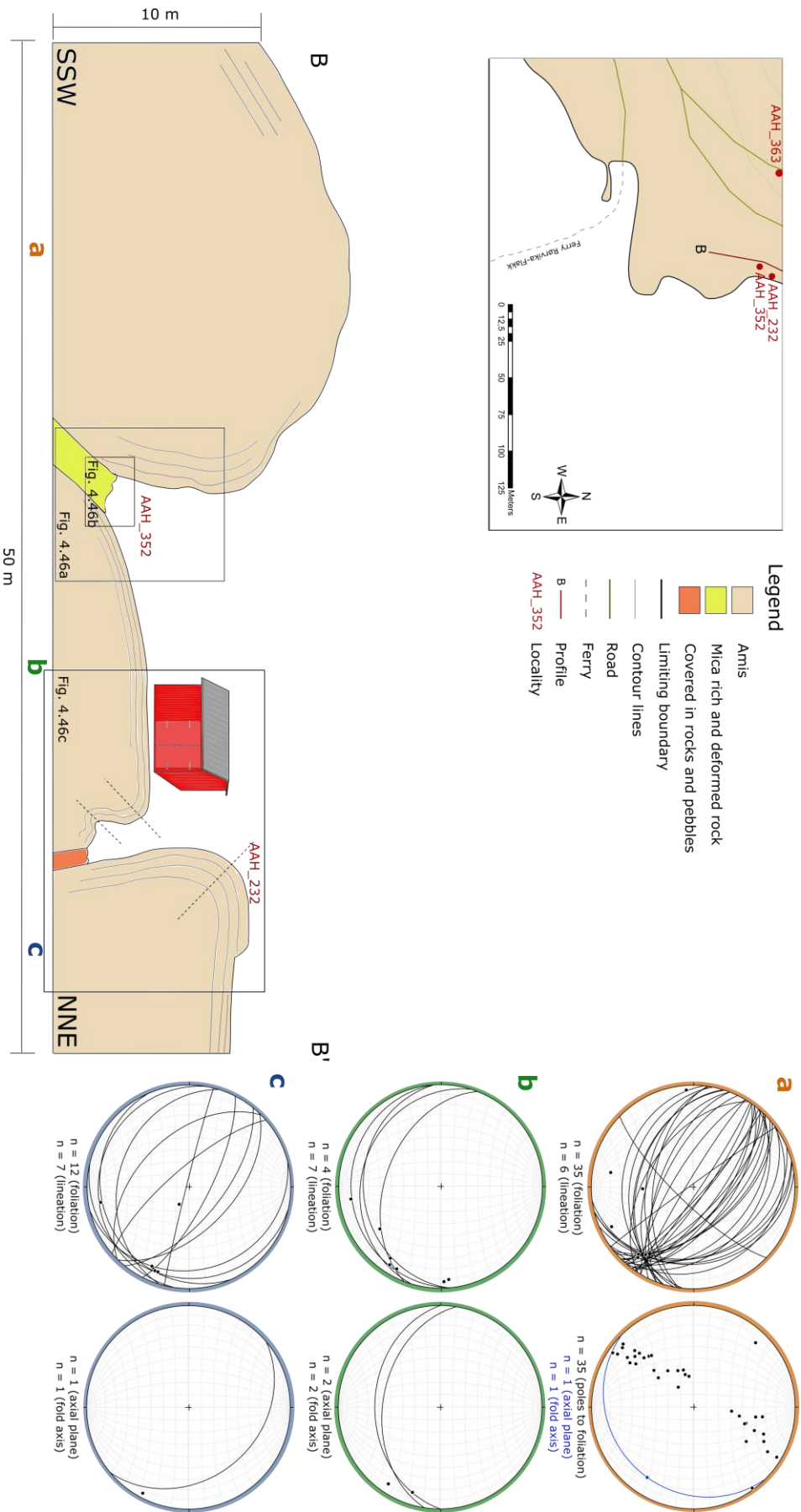


Figure 4.45: A schematic SSW-NNE profile over Kleivneset (locality AAH_232, Appendix A), located within the Amis in Rørvika unit. The area is divided into three parts, a (orange), b (green) and c (blue), each with corresponding stereonet over foliation and mineral lineation, and axial plane and fold axis. The axial plane and the fold axis for the fold in part a was found through a pi-plot. Also note that the scales on this figure are an approximation of the reality. The red numbers coincide with the localities on the map in the upper left corner.

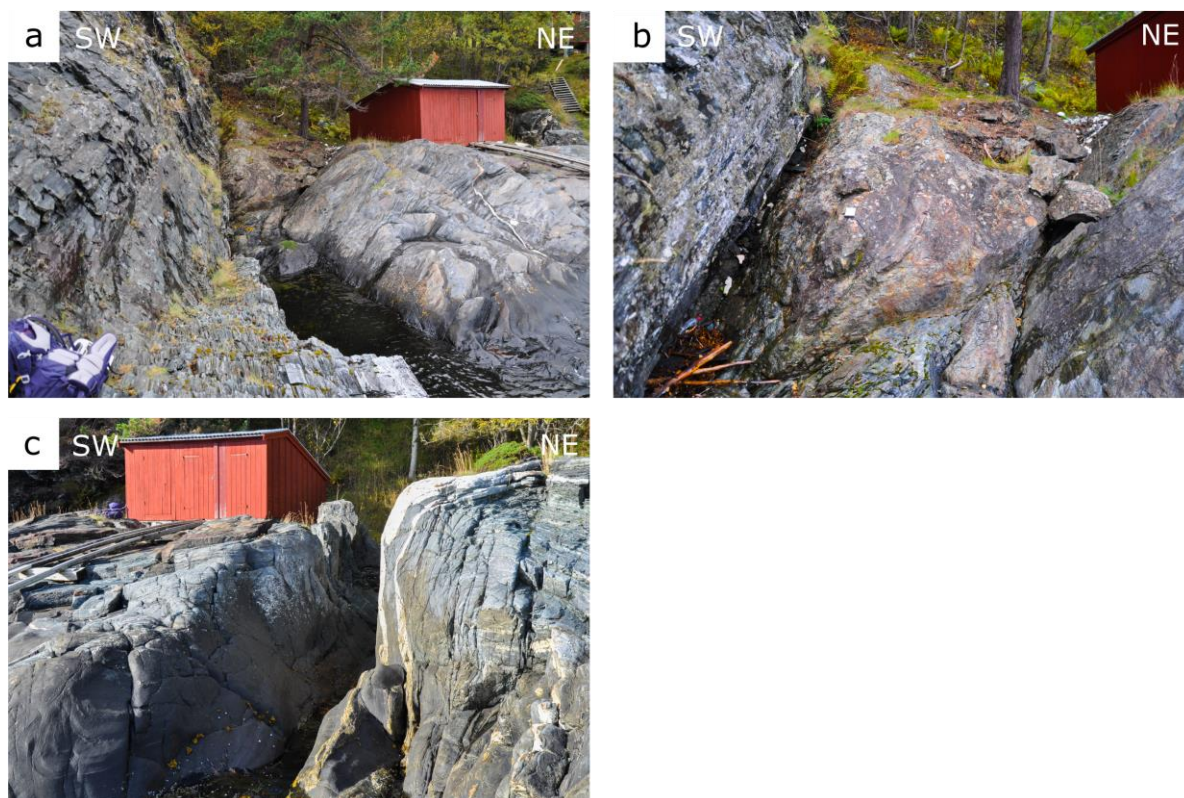


Figure 4.46: Detailed pictures of geological features from Kleivneset as indicated in figure 4.45. a) Overview of the boundary between part a and b. b) Close-up of a highly deformed mica rich rock on the boundary between part a and b. c) Boundary between part b and c. N-vergent folds from part b and SW-vergent folds from part c visible.

dominated by an antiform where fold axis and axial plane were found with the help of a pi-plot (a, Fig. 4.45). The measured foliations indicate an axial plane dipping towards the southeast and a fold axis with shallow plunge with a trend towards the southeast (Fig. 4.45).

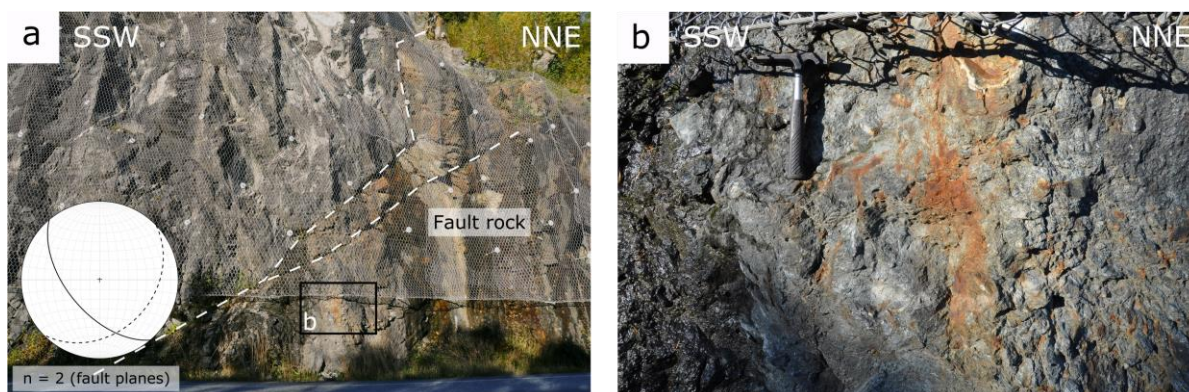


Figure 4.47: a) Overview of the fault from locality AAH_363 (Fig. 4.45). The stippled line in the stereonet correlates with the stippled fault plane in the picture. The other fault plane in the stereonet is measured outside the picture to the north-northeast. b) Detail from fault rock, locality AAH_363.

On the boundary between the southern part [a] and the middle part [b], a highly deformed and mica rich rock is observed (Fig. 4.45; Fig. 4.46a). The material of the rock is homogeneous and fine grained with a brown to golden weathering colour (Fig. 4.46b).

In part [b], there is a strong and penetrative foliation with dip direction towards the south-southwest (b, Fig. 4.45). The dip of the foliation is shallow, but with a slight increase towards the south-southwest of the outcrop. An amphibole mineral lineation shows a trend of the lineation that rotates through the outcrop, from east to south (Fig. 4.45).

The boundary between the middle part [b] and the northern [c] is an opening between a SW-vergent fold and what seems to be a NE-vergent fold (Fig. 4.45; Fig. 4.46c). The exact boundary between the two folds could not be seen because it is covered in gravel and rocks, and partly beneath the tidal mark.

On locality AAH_363 (Fig. 4.45), a 4-5 meter thick fault zone was observed where the fault rock showed the same characteristics as the mica-rich rock at locality AAH_352 except for being more coarse grained (Fig. 4.47a and b). Fault planes on each side of this fault zone measured 136/33 (stippled line, Fig. 4.47a) and 230/56 (full line, Fig. 4.47a), from the south-southwest to north-northeast. The complicated structures on Kleivneset are thought to relate to these fault planes.

Detailed study of brittle structures in a quarry

Many brittle faults were measured throughout the studied area, but the mineralization and sense of movement were not systematically observed. A more detailed study of a quarry (Location AAH_324, Appendix A) where different sets of fractures, faults, slickenside lineations and the sense of slip of the plane could be observed, was done in addition.

The quarry is found within Ams and contains a few pegmatites, all running parallel to the foliation (Fig. 4.48; Appendix E). Measurements were only taken from those fault surfaces that show both slickenside lineation and a sense of slip. That means that fracture sets from the quarry not meeting these criteria were overlooked. The measurements taken in the quarry could then be compared to measurements from the entire studied area (Appendix E).

Measurements were divided into different groups based on the minerals found on the fault surface (Fig. 4.49). The minerals on the surfaces are i) epidote (Fig. 4.49b), ii) epidote together with chlorite (Fig. 4.49c), iii) epidote together with quartz (Fig. 4.49d), and iv) calcite (Fig. 4.49e). Together with the calcite (Fig. 4.49e) quartz, chlorite and epidote were also found.

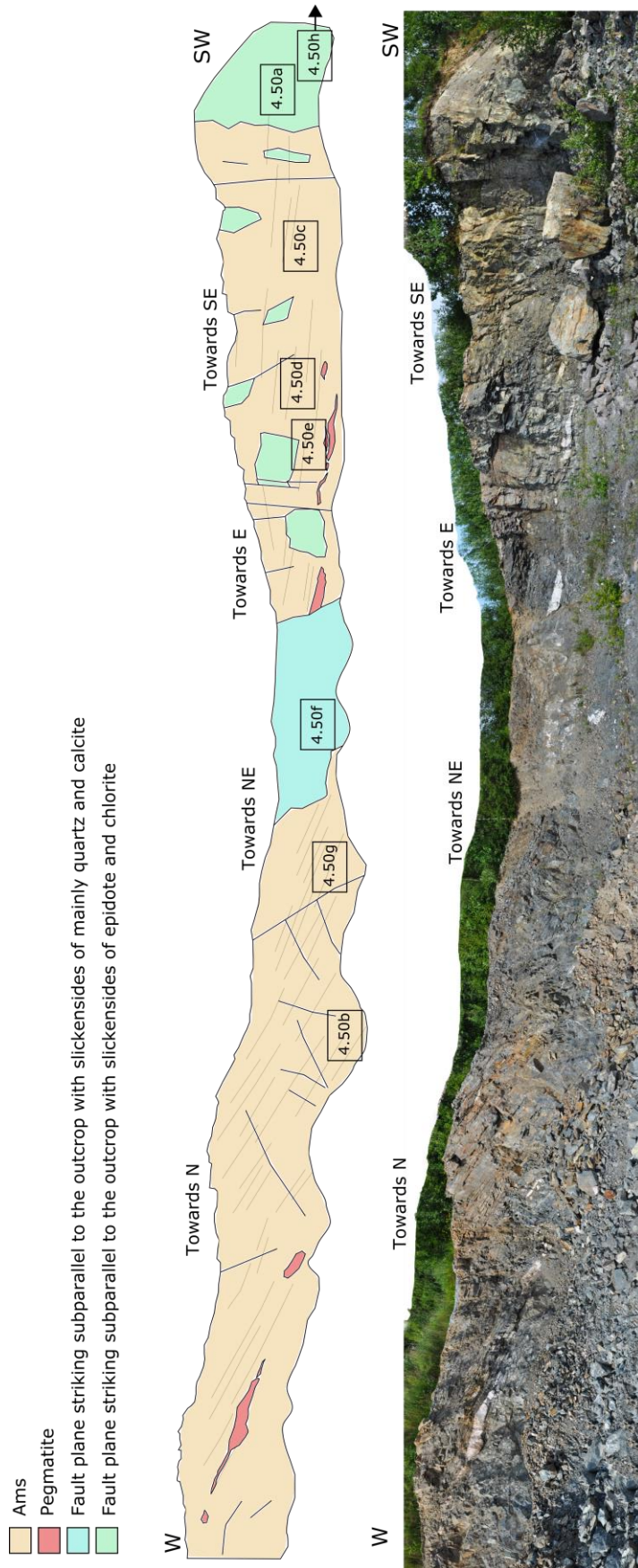


Figure 4.48: Overview profile of the quarry situated within Ams in the Rørvika unit, locality number AAH_324 (Appendix A). Two deformed pegmatites (pink) can be seen running parallel to the foliation. Several larger fault zones running subparallel to the outcrop with different mineralisations are marked of in the blue and green areas. The black lines indicate larger faults and the numbered squares indicate the location of images presented in Figure 4.50. Note that the quarry is three-dimensional, which means that the flattened profile stretches from west and all the way around towards southwest.

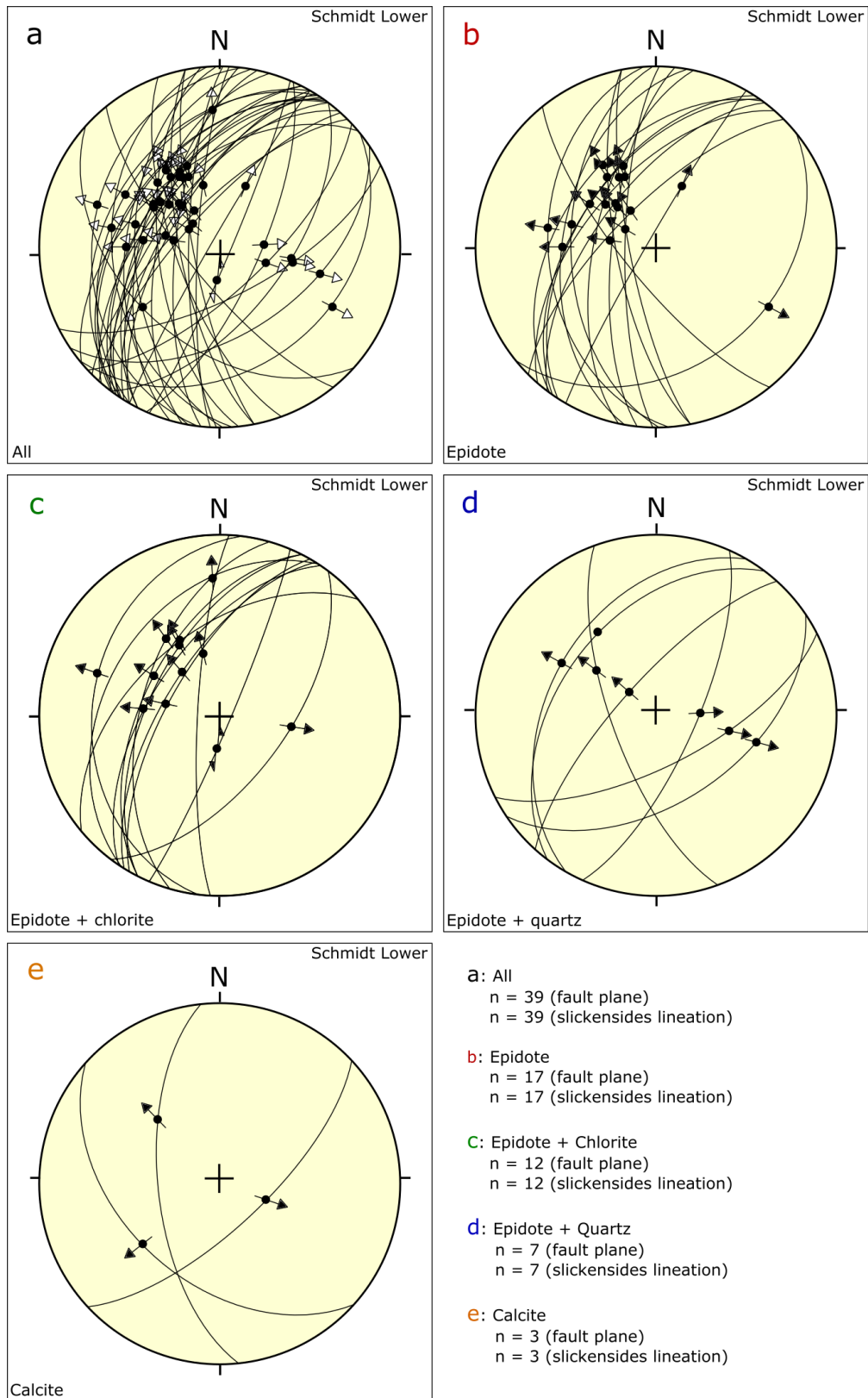


Figure 4.49: Stereonets showing the measured fault planes that also show slip direction and sense of slip (black arrows). The arrows indicating direction of slip. a) All measured faults. b) Faults with epidote mineralisation. c) Faults with mineralisation of epidote and chlorite together. d) Faults with mineralisation of epidote and quartz together. e) Faults with calcite mineralisation. Note that the calcite was found on faults also showing mineralisation of epidote, chlorite and quartz.

Fault planes where epidote is present show a light green colour and a strong slickenside lineation (Fig. 4.50a). Throughout the quarry, several zones of millimetre-thin fractures with a NE-SW direction can be observed (Fig. 4.50b). The planes themselves cannot be seen, but the light green colour in the fracture indicates epidote on the fracture planes. This corresponds with the faults measured with epidote on the surface (Fig. 4.50b).

Where chlorite occurs beside epidote, the colour shifts to dark green with a light green undertone (Fig. 4.50c). A consistent observation within the study area is that when these two minerals occur together, a thin layer of chlorite is found over the epidote, indicating that the chlorite crystallized at a later stage than the epidote. Some of the epidote- and chlorite-coated surfaces have a polished appearance and look almost shiny (Fig. 4.50d). Both the fault planes with epidote and the planes with epidote and chlorite strikes subparallel to the outcrop; the bigger ones are shown in Figure 4.48.

On some of the fault surfaces quartz is also present together with epidote, which gives the surface a white to very light green colour (Fig. 4.50e). On several of the surfaces with quartz, the slickenside lineations are absent because the surface is polished and no lineation can be observed.

The calcite at the fault surfaces appear as bigger crystals concentrated in bigger fracture zones together with brecciated rock (Fig. 4.50f). On the larger fault surface with calcite (Fig. 4.48), mineralization of quartz and calcite shows an elongated and lineated appearance together with the brecciated rock (Fig. 4.50g). There were only three fault planes with the calcite mineralization observed in the quarry, all found in close proximity to each other. Calcite on a fault plane has only been observed in Rødberget unit except from in this quarry.

Just south of the quarry, there is a small zone where the Ams contains many thin pink felsic layers (Fig. 4.50h). The felsic layers nicely show offsets of 2-4 cm across thin brittle faults.

4.3.4.4 Varpneset unit

In the Varpneset unit the brittle structures show straight fault planes with little or no slickenside lineations on the planes (Fig. 4.51a and b). The few slickenside lineations observed has mineralisation of chlorite. The measured faults have a low to steep dip towards the northwest and southeast, as well as a few with a dip towards the northeast and southwest (Fig. 4.38d; Appendix E). Slickenside lineation observed show mainly a moderate plunge towards the southeast. It was not possible to deduce the sense of movement along the faults.

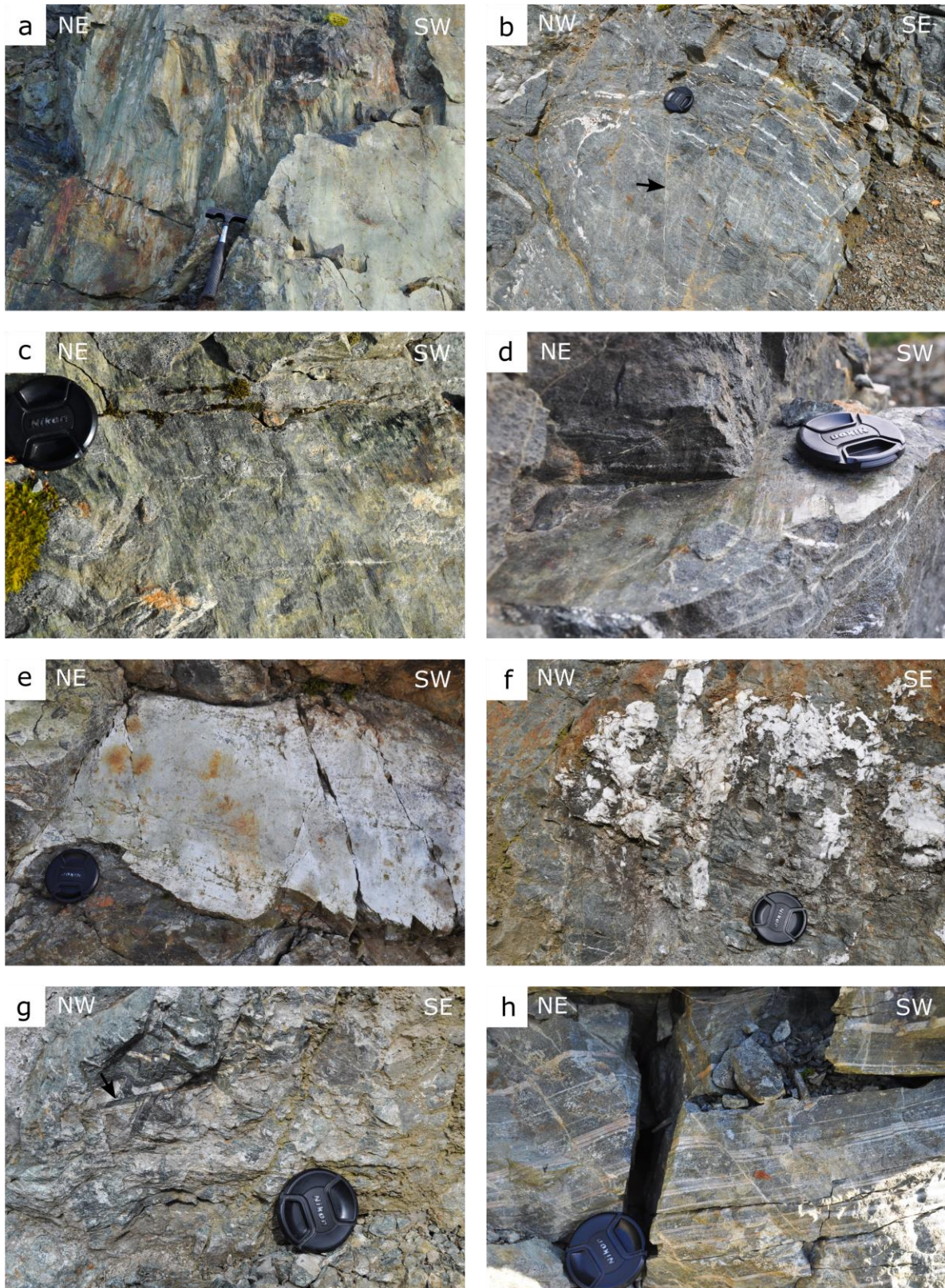


Figure 4.50: Detailed pictures from the quarry, locality AAH_324. Location for the pictures can be seen in figure 4.49. a) Epidote mineralisation on fault also showing slickenside lineations and sense of slip. b) SW-NE-striking fractures with epidote mineralisation (black arrow). c) Fault surface with epidote and chlorite mineralisation. d) Polished fault surface with epidote and chlorite mineralisation. e) Fault plane with quartz and

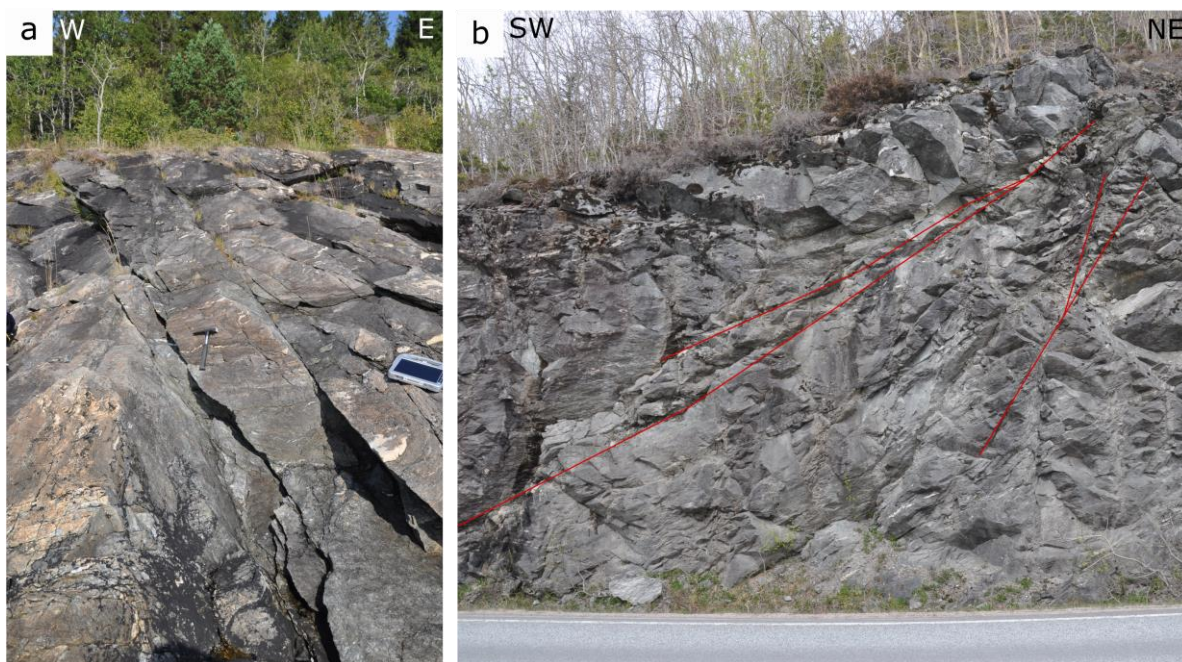


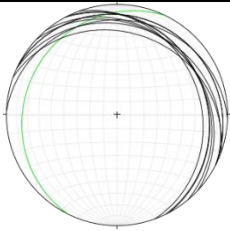
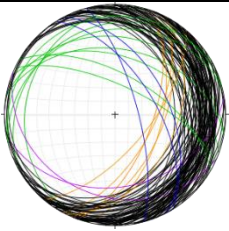
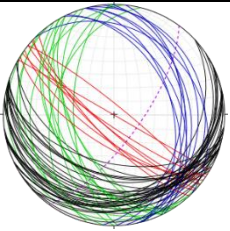
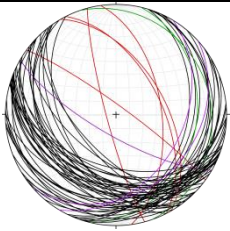
Figure 4.51: a) Brittle fault in the Hcqs. Loc. no. AAH_207. b) Brittle fault in the Hcqs. Loc. no. AAH_389. Red lines highlighting the fault planes.

Fig. caption cont. epidote (upper left corner) mineralisation. f) Calcite on fault surface. g) Elongated and lined quartz and calcite mineralisation on a brecciated fault surface (black arrow). h) Faulted Ams where pink felsic layers show offsets of 1-4 cm.

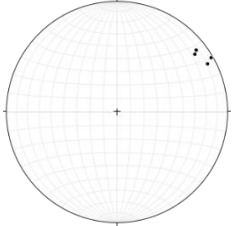
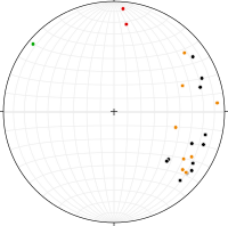
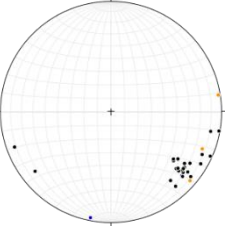
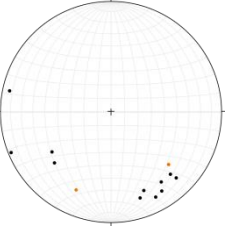
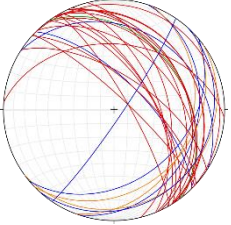
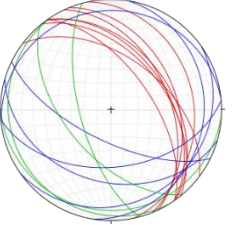
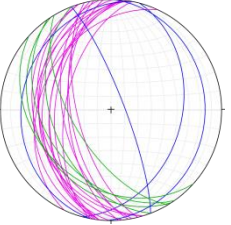
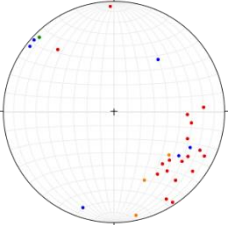
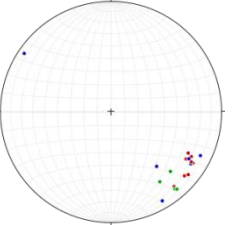
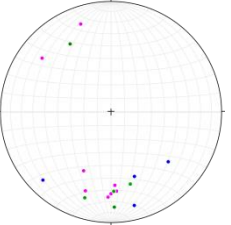
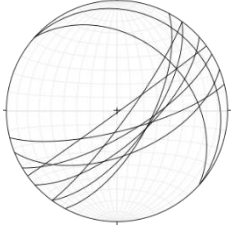

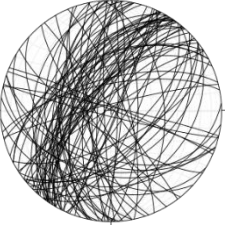
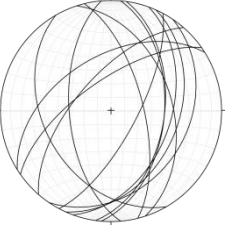
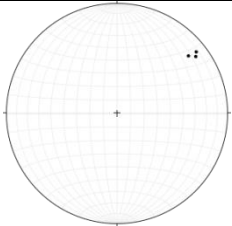
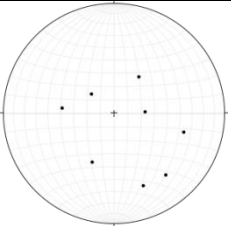
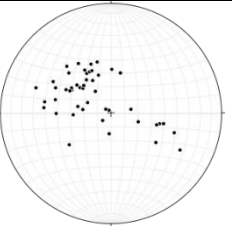
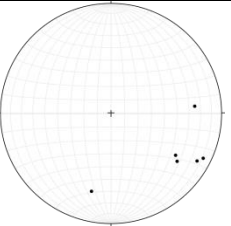
Summary and structural model

The previous chapter provided a description of foliations, mineral and elongation lineations, fold axes and axial planes, and brittle structures. This chapter summarizes these measurements in a table, profile and a 3D model of the described area.

Table 5.1: Summary of the lithologies and structures from the studied area. Details in chapter 4.

Unit	Rødberget unit	Tronggen unit	Rørvika unit	Varpneset unit
Lithologies	Ingdal granitic gneiss	Ghms, Helle and Ams	Ams, Amis, Amfs and Fams	Hcqs and Hqs
Field characteristics	<ul style="list-style-type: none"> - Strong pink colour - Weak penetrative foliation - Subparallel mafic dykes 	<ul style="list-style-type: none"> - Brown to silver luster - Rich in garnet and mica - Strong deformation - Amphibolitic bodies and lenses 	<ul style="list-style-type: none"> - Strong penetrative foliation - Black amphibolite with pink garnets in zones - Pegmatites and aplites present 	<ul style="list-style-type: none"> - Orange weathering colour - Silver luster - Coarse grained layers - Calcite present
Foliations	 n = 10	 n = 105	 n = 65	 n = 57
Mean foliations	026/18	120/19	Black: 222/21 Red: 181/77 Blue: 078/34 Green: 258/41	148/19

Summary and structural model

Unit	Rødberget unit	Tronggen unit	Rørvika unit	Varpneset unit
Mineral lineations and elongation lineations	 n = 4	 n = 24	 n = 29	 n = 13
Mean lineation	058/08	109/22	125/16	172/21
Axial planes	-	 n = 32	 n = 18	 n = 24
Fold axes	-	 n = 31	 n = 20	 n = 17
Fold vergence	-	SW, NE, NW and symmetric	SW, NE and symmetric	NE, SE-E and symmetric
Fault planes	 n = 10	 n = 64	 n = 94	 n = 13
Slickenside lineations	 n = 3	 n = 6	 n = 52	 n = 6

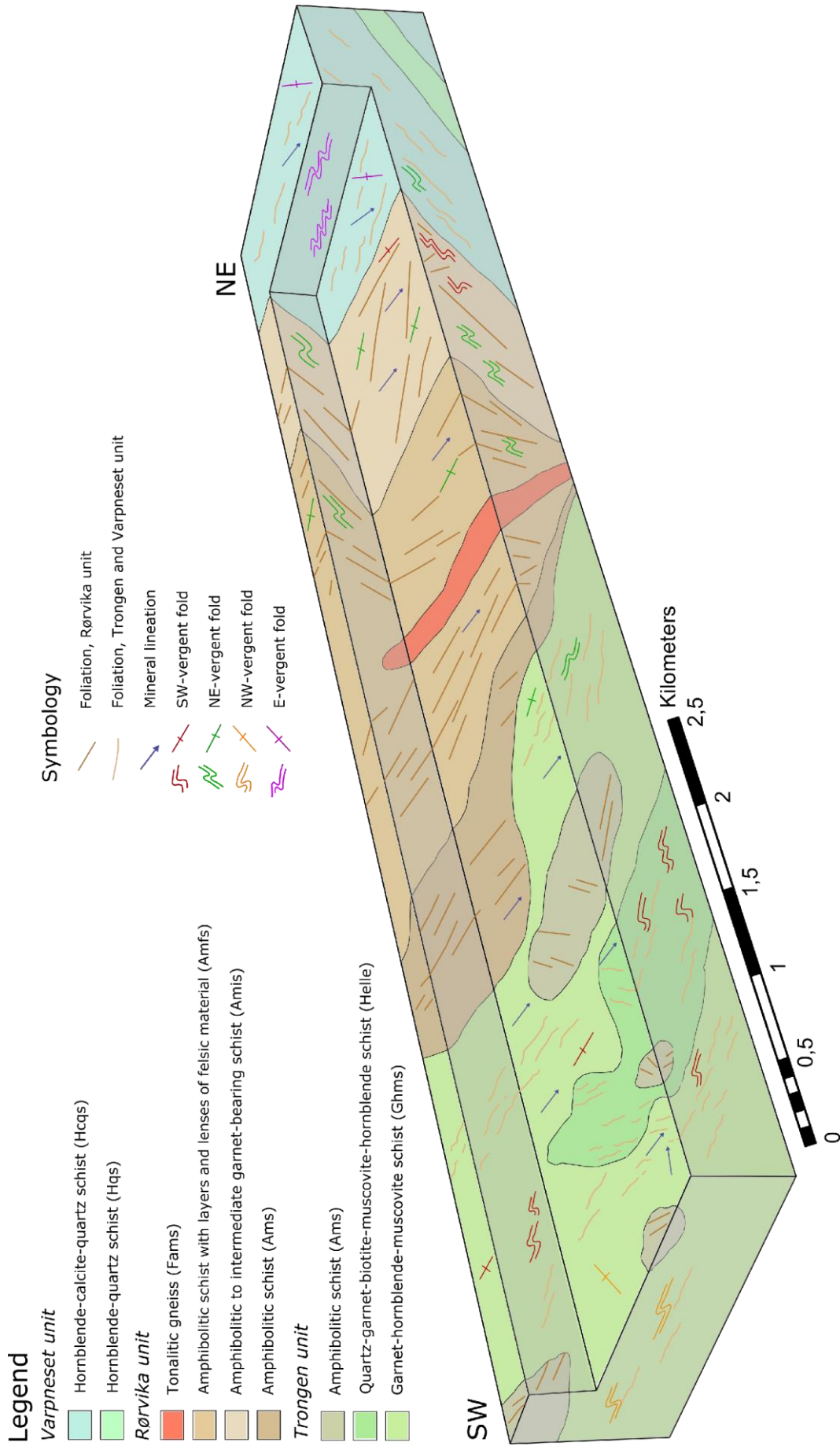


Figure 5.1: Schematic 3D sketch of the transect stretching from southwest to northeast.

Based on the structural data above a block diagram (Fig. 5.1) and a profile of the transect (Appendix F) was made to get a better understanding of the overall structural development of the area. Note that the brittle structures are excluded from both.

Petrography, geochemistry and geochronology

6.1 Petrographic description of lithologies

A total of 24 samples of the different lithologies were collected in the field and thin sections were made from a representative selection of these (Appendix G; Appendix H). Note that the thin sections are not oriented.

6.1.1 Rødberget unit

The Rødberget unit consists of the Ingdal granitic gneiss (Appendix H, KSV_55). On a microscopic level this rock has a seriate interlobate texture and consists of mainly anhedral quartz and feldspars with a grain size ranging from 0.01-2 mm in diameter. Elongated quartz and feldspar aggregates, together with the oriented and platy mica grains, give the rock its foliation (gneissosity).

The feldspars found are microcline and plagioclase. Some grains show deformation twins that are lenticular with pointy terminations. Plagioclase with albite twins (Fig. 6.1a) and microcline with microcline twins (Fig. 6.1b) can be observed. Some of the feldspar also displays exsolution lamellae due to mineral breakdown (Fig. 6.1c). Poikiloblastic feldspars can have inclusions of both quartz and muscovite (Fig. 6.1d). The quartz grains show undulose extinction (Fig. 6.1e), deformation bands (Fig. 6.1e), subgrains (Fig. 6.1f), and sutured boundaries (Fig. 6.1f).

Fault rocks within Rødberget unit (Appendix H, KSV_55b) have a sharp boundary to the host rock (Fig. 6.2a) and contain secondary minerals of calcite and quartz and fragments of

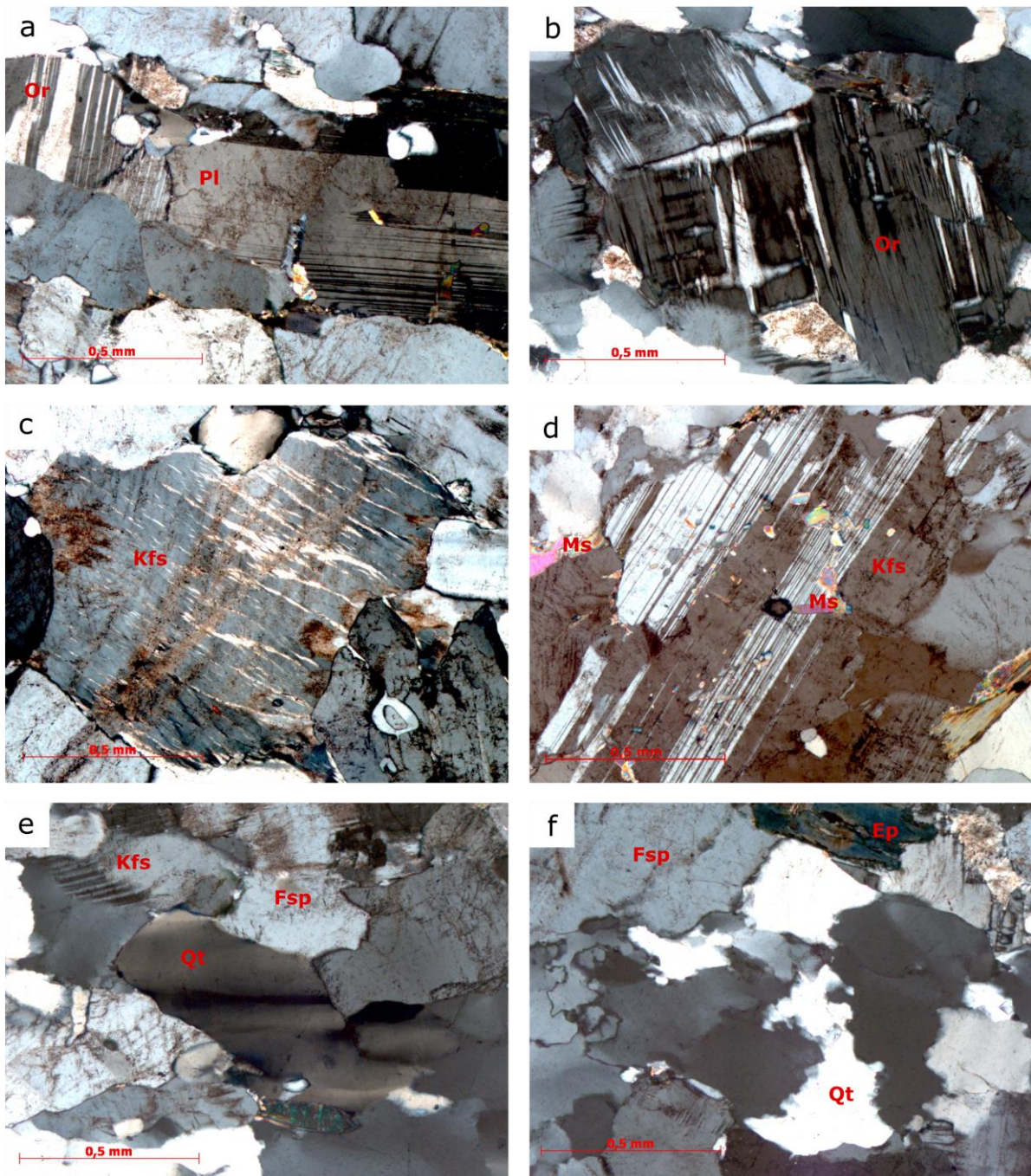


Figure 6.1: Photomicrographs from the Rørdberget unit. a) Albite twins in a plagioclase grain. From KSV_55, 10x and XPL. b) Microcline twinning. From KSV_55, 10x and XPL. c) Exsolution lamellae in a feldspar grain. From KSV_55, 10x and XPL. d) Plagioclase grain with muscovite inclusion and albite twinning. From KSV_55, 10x and XPL. e) Deformation bands and undulose extinction in quartz. From KSV_55, 10x and XPL. f) Sutured quartz grain boundaries and subgrains. From KSV_55, 10x and XPL.

the host rocks with a size from 0.1-1 mm (Fig. 6.2a and b). The most abundant mineral is calcite, which is found both as a fine grained matrix and as larger, 0.5-1.5 mm, anhedral to subhedral grains with twinning (Fig. 6.2c). The quartz in the matrix of the fault rock is very fine grained and is concentrated in zones (Fig. 6.2d). These zones are situated in between highly prismatic

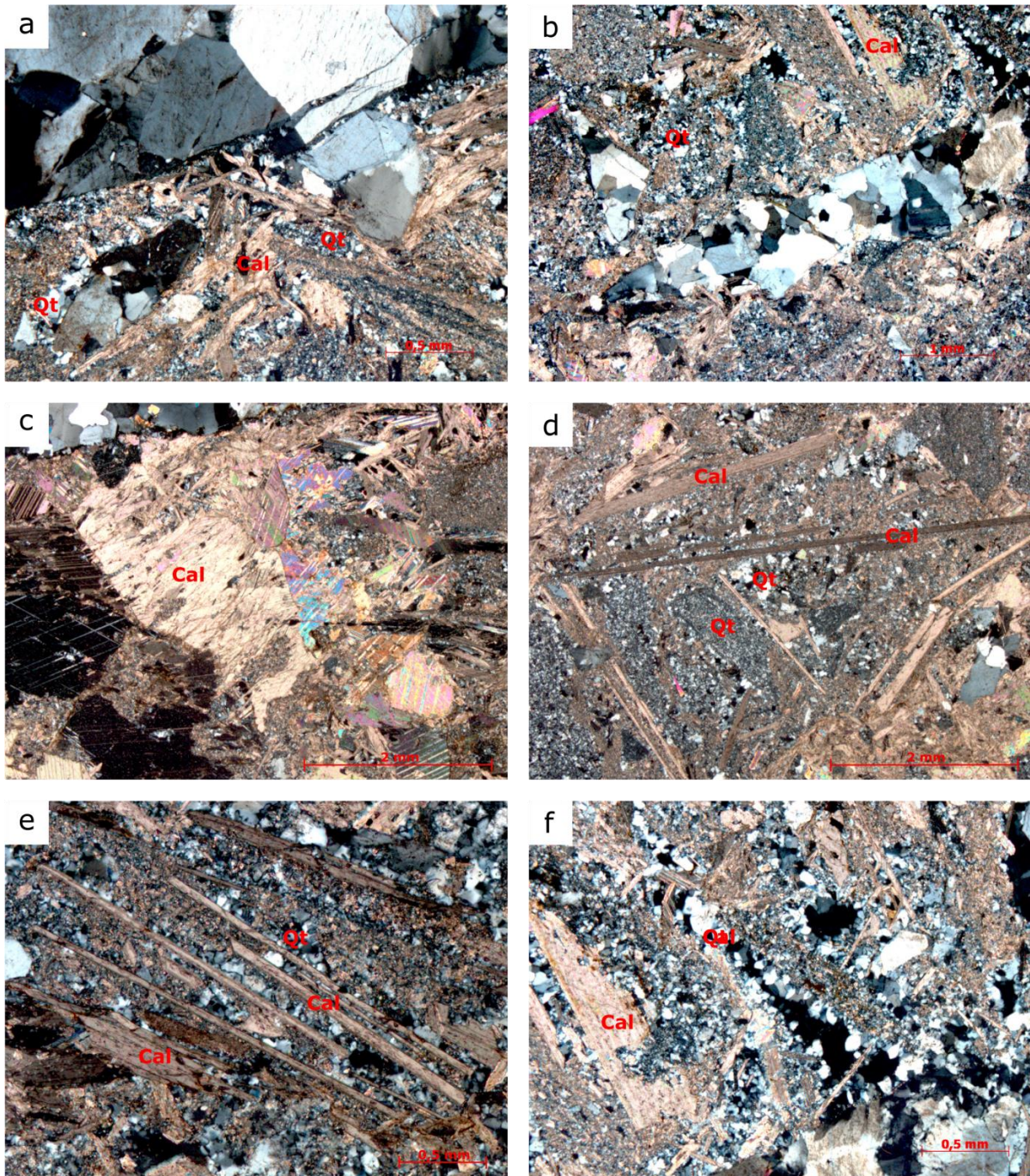


Figure 6.2: Photomicrographs from the Rørdberget unit. a) Boundary between host rock and fault rock is sharp. The fault rock contains larger clasts of the host rock, as well as porphyroblastic and elongated calcite and fine grained matrix of quartz and calcite. From KSV_55b, 10x and XPL. b) Large clast of host rock, 3 mm long, in a matrix of quartz and calcite. From KSV_55b, 5x and XPL. c) Porphyroblastic calcite in the fault zone. The calcite grains show both parallel twinning (lower right in picture) and cross-cutting twinning (left in picture). From KSV_55b, 2.5x and XPL. d) Prismatic calcite grains in the matrix restricting the areas with quartz rich matrix. From KSV_55b, 2.5x and XPL. e) Same as in d). From KSV_55b, 10x and XPL. f) Where empty voids have been present in the fault zone, the quartz has grown larger than in the surrounding matrix and with crystal surfaces and terminations. From KSV_55b, 10x and XPL.

and elongated calcite grains (Fig. 6.2d and e). Where there are voids in the fault rock present, the quartz has had space to grow larger and with crystal surfaces and terminations (Fig. 6.2f).

6.1.2 Trongen unit

The Trongen unit consists of mica schists and amphibolitic schist, together with aplites with tonalitic composition, all affected by metamorphism of lower to middle amphibolite facies. A common characteristic throughout the unit for the mica schist is the feldspar- and quartz-rich matrix with an equigranular to inequigranular fine-grained and polygonal fabric.

Garnet-hornblende-muscovite schist (Ghms)

The Ghms contains feldspar, quartz, hornblende, biotite, muscovite, garnet, clinozoisite, epidote and chlorite, with variations in content from west to east. In the western area, the Ghms shows a finer grain size, none to a few and small (0.1-1mm) garnets, a significant content of chlorite, epidote and clinozoisite, and abundant sericite (AAH_128 and AAH_141, Appendix H). Towards the east the garnets grow bigger, up to 1-2 cm in diameter, the content of biotite increases, and calcite appears (AAH_147 and AAH_278, Appendix H).

In the westernmost area, the chlorite shows a strong purple interference colour (Fig. 6.3a and b). It appears as parallel blades of varying size, as single crystals, or it has grown at the expense of hornblende (Fig. 6.3c and d) and garnets (Fig. 6.3e and f). The bladed chlorite is poikiloblastic with inclusions of epidote (Fig. 6.3b), and its orientation gives the rock its foliation. Also, in the western area, the feldspars are highly affected by sericite (Fig. 6.3a and d).

Towards the east and northeast, the content of chlorite is dramatically decreased and the rock becomes coarser grained, and biotite and garnets are more abundant. The content of hornblende is varying as subhedral porphyroblasts (Fig. 6.4a and b). Sericite is affecting the feldspars (Fig. 6.4c) and the micas are oriented (Fig. 6.4d and e) representing the foliation. Calcite is found in very fine-grained aggregates (Fig. 6.4f).

The poikiloblastic garnets within the Ghms are synkinematic, which can be seen through the sigmoidal-shaped inclusion trails (S_1 , Fig. 6.5). The micas foliated around the porphyroclastic garnets show coaxial ϕ -type deformation (S_2 , Fig. 6.5).

Quartz-garnet-biotite-muscovite-hornblende schist (Helle)

Helle has the same mineral content as the Ghms, but is more homogeneous in its appearance, both at macroscopic and microscopic level (AAH_350, Appendix H). The foliation is continuous and made up by oriented micas (Fig. 6.6a). A new set of foliated biotite (S_2 , Fig. 6.6a) is overprinting the direction of an older generation of biotite (S_1 , Fig. 6.6a) with a divergent orientation oblique to the newer.

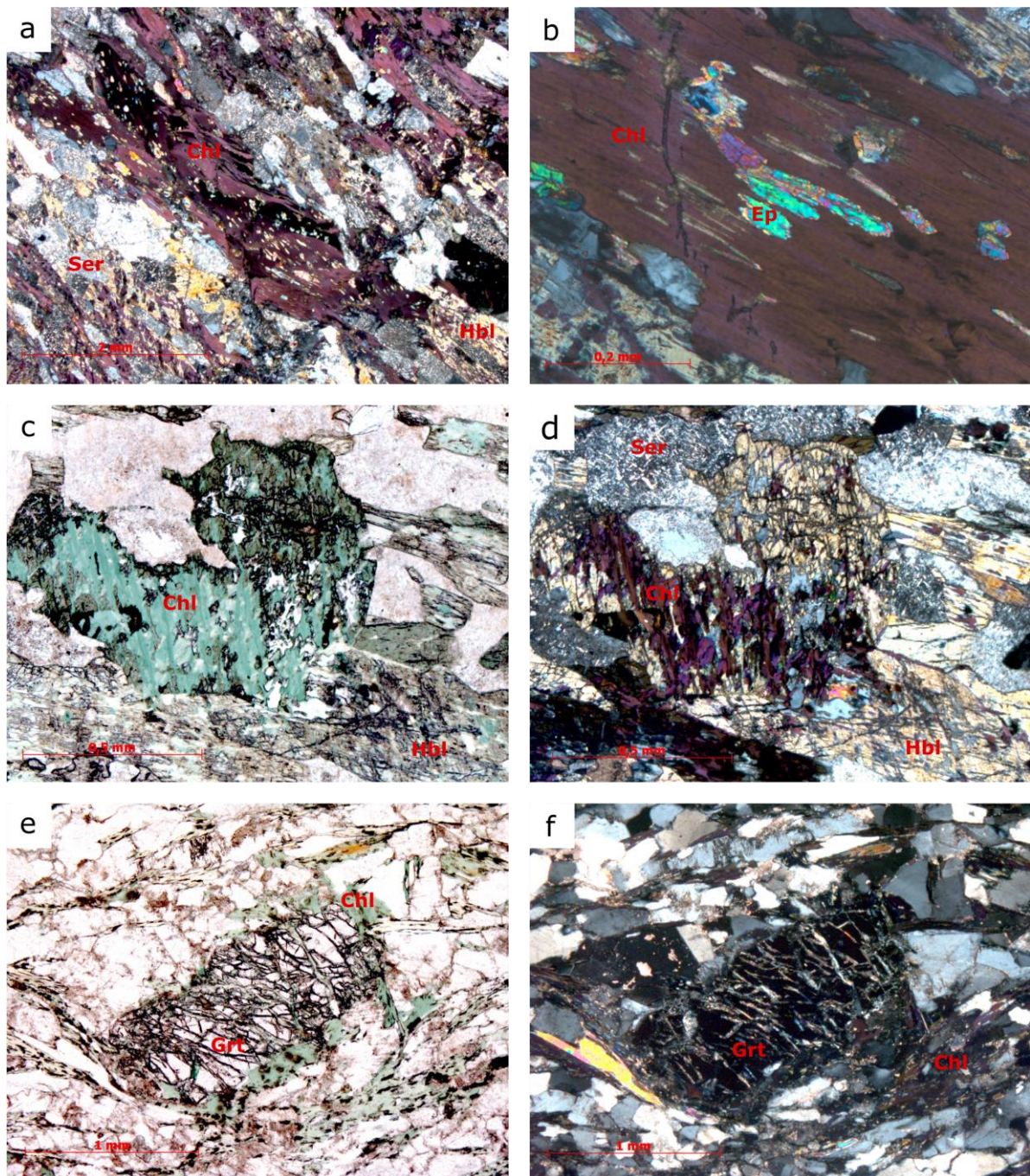


Figure 6.3: Photomicrographs from the Trongen unit. a) Purple, poikiloblastic and bladed chlorite grain, surrounded with plagioclase affected by sericite, and partly replaced hornblende. From AAH_128, 2.5x and in XPL. b) Purple and poikiloblastic chlorite with elongated and parallel inclusions of epidote. From AAH_128, 20x and in XPL. c) Hornblende (cleavage {011} and {110}, and green to pale green pleochroic) partly replaced by chlorite (strong green to bluish colour). From AAH_128, 10x and in PPL. d) The same as c), XPL. Hornblende (cleavage {011} and {110}, and yellow 1.order interference colour) replaced by chlorite (strong purple colour), surrounded by plagioclase with sericite. e) Porphyroblastic garnet and chlorite (green colour). From AAH_141, 5x and in PPL. f) The same as e), XPL. Porphyroblastic garnet and chlorite (purple interference colour).

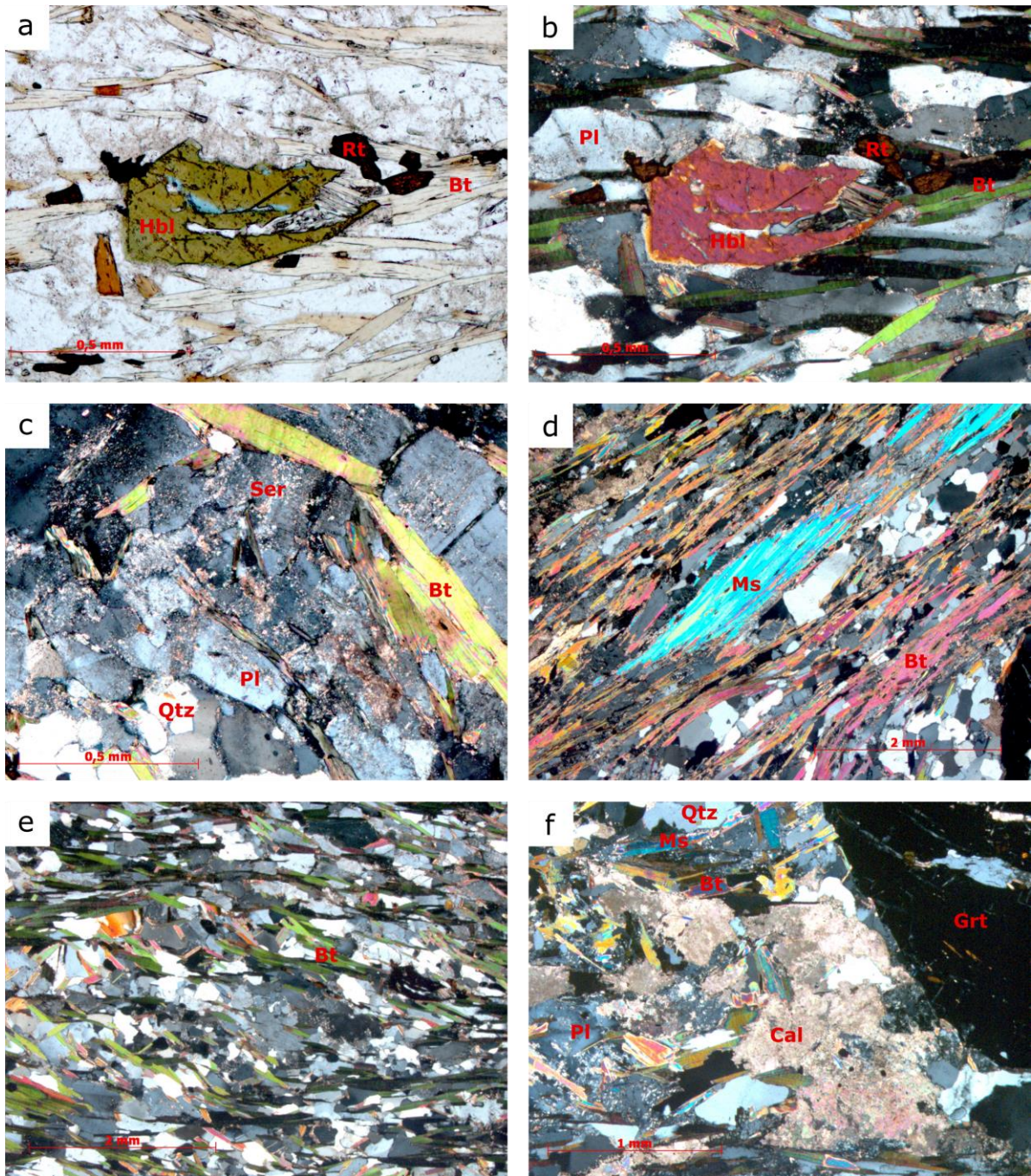


Figure 6.4: Photomicrographs from the Trongen unit. a) Anhedronal hornblende parallel to foliation. From AAH_278, 10x and in PPL. b) The same as a), XPL. c) Plagioclase with sericite. From AAH_278, 10x and in XPL. d) Parallel and foliated muscovite and biotite. From AAH_147, 2,5x and in XPL. e) Crenulated biotite. From AAH_278, 2,5x and in XPL. f) Calcite aggregate close to garnet porphyroblasts. From AAH_147, 5x and in XPL.

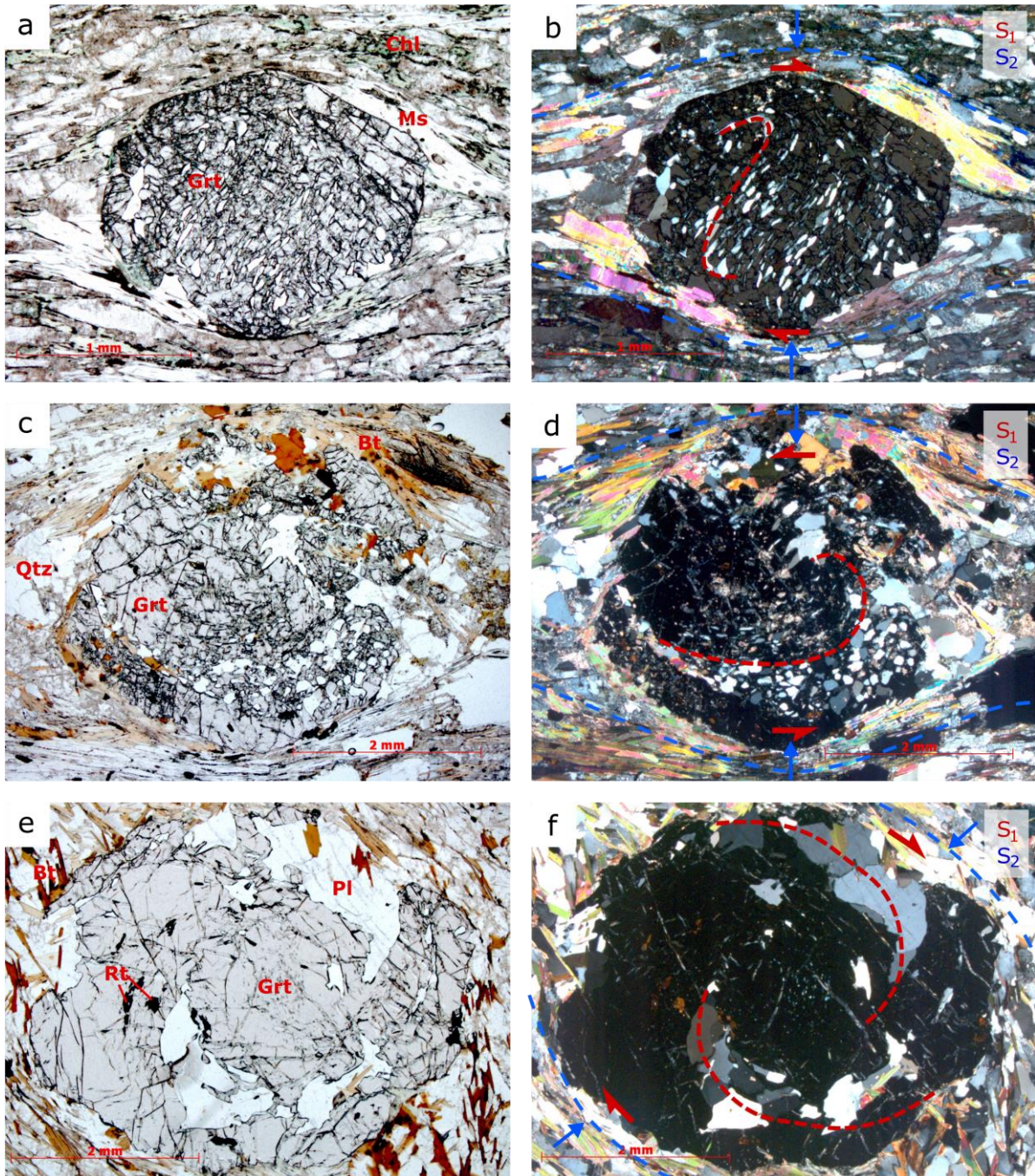


Figure 6.5: Photomicrographs from the Trongen unit. a) Synkinematic garnet from AAH_141, 5x, and in PPL. b) The same as a), XPL. Primary growth during deformation (red, S₁) and secondary deformation (blue, S₂). c) Synkinematic garnet from AAH_147, 2.5x, and in PPL. d) The same as d), XPL. Primary growth during deformation (red, S₁) and secondary deformation (blue, S₂). e) Synkinematic garnet from AAH_278, 2.5x, and in PPL. f) The same as e), XPL. Primary growth during deformation (red, S₁) and secondary deformation (blue, S₂).

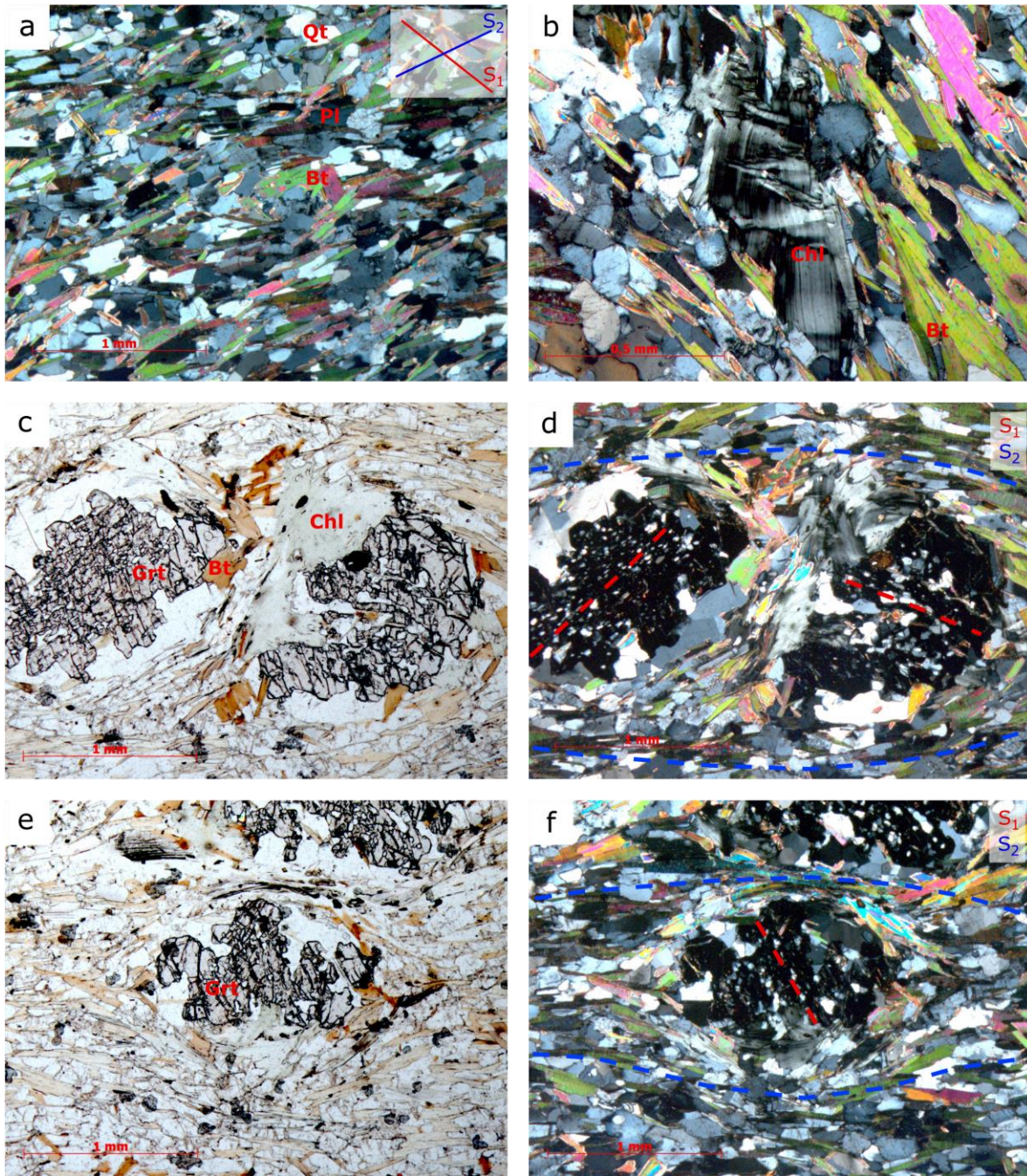


Figure 6.6: Photomicrographs from the Trongen unit. a) Matrix of the Helle lithology with biotite showing two different orientations, S_1 and S_2 . From AAH_350, 5x, and in crossed polarized . b) Mg-chlorite with kink bands. From AAH_350, 10x, and in crossed polarized . c) Pre- or synkinematic and poikiloblastic garnet split in to with inclusions of two different orientations. Mg-chlorite between the two pieces of garnet. From AAH_350, 5x, and in PPL. d) Same as c), XPL. Inclusion trails during growth (red, S_1) and the secondary deformation (blue, S_2). e) Pre- or synkinematic and poikiloblastic garnet. From AAH_350, 5x, and in PPL. f) Same as e), XPL. Inclusion trails during growth (red, S_1) and the secondary deformation (blue, S_2).

Mg-rich chlorite is found as a few single grains in the matrix showing kink bands (Fig. 6.6b), and close to and within fractures of the garnets (Fig. 6.6c and d).

Within Helle, the garnets show pre- or synkinematic trends with deformed inclusion trails (S_1 , Fig. 6.6d and f) and showing ϕ -type deformation (S_2 , Fig. 6.6d and f). The garnets are highly fractured and poikiloblastic with inclusion of quartz, rutile, muscovite and chlorite.

Amphibolitic schist (Ams)

Ams (AAH_305, Appendix H), which is found throughout Trongen unit in bodies of varying size, contains equigranular polygonal hornblende porphyroblasts (Fig. 6.7a) and an inequigranular interlobate matrix consisting of hornblende, feldspar and quartz (Fig. 6.7b). It is foliated with oriented subhedral hornblende grains and a fine-grained matrix. Subhedral to euhedral and rhombic titanite is abundant and oriented parallel to the foliation (Fig. 6.7c and d).

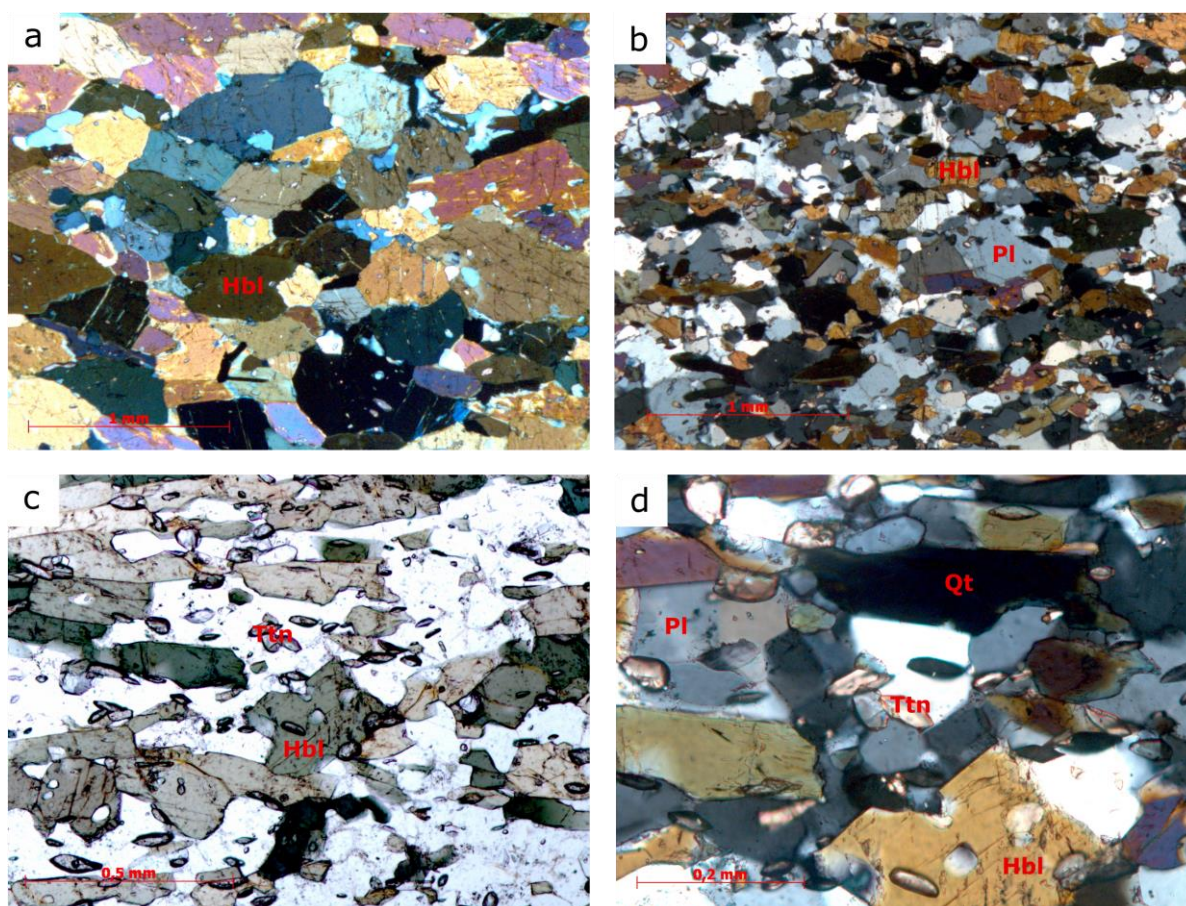


Figure 6.7: Photomicrographs from the Trongen unit. a) Porphyroblastic and equigranular hornblende from AAH_305. 5x and in XPL. b) Matrix consisting of feldspar, hornblende, titanite and quartz. From AAH_305, 5x and in XPL. c) Subhedral and rhombic titanite in matrix. From AAH_305, 10x and in PPL. d) Subhedral and rhombic titanite in matrix. From AAH_305, 20x and in XPL.

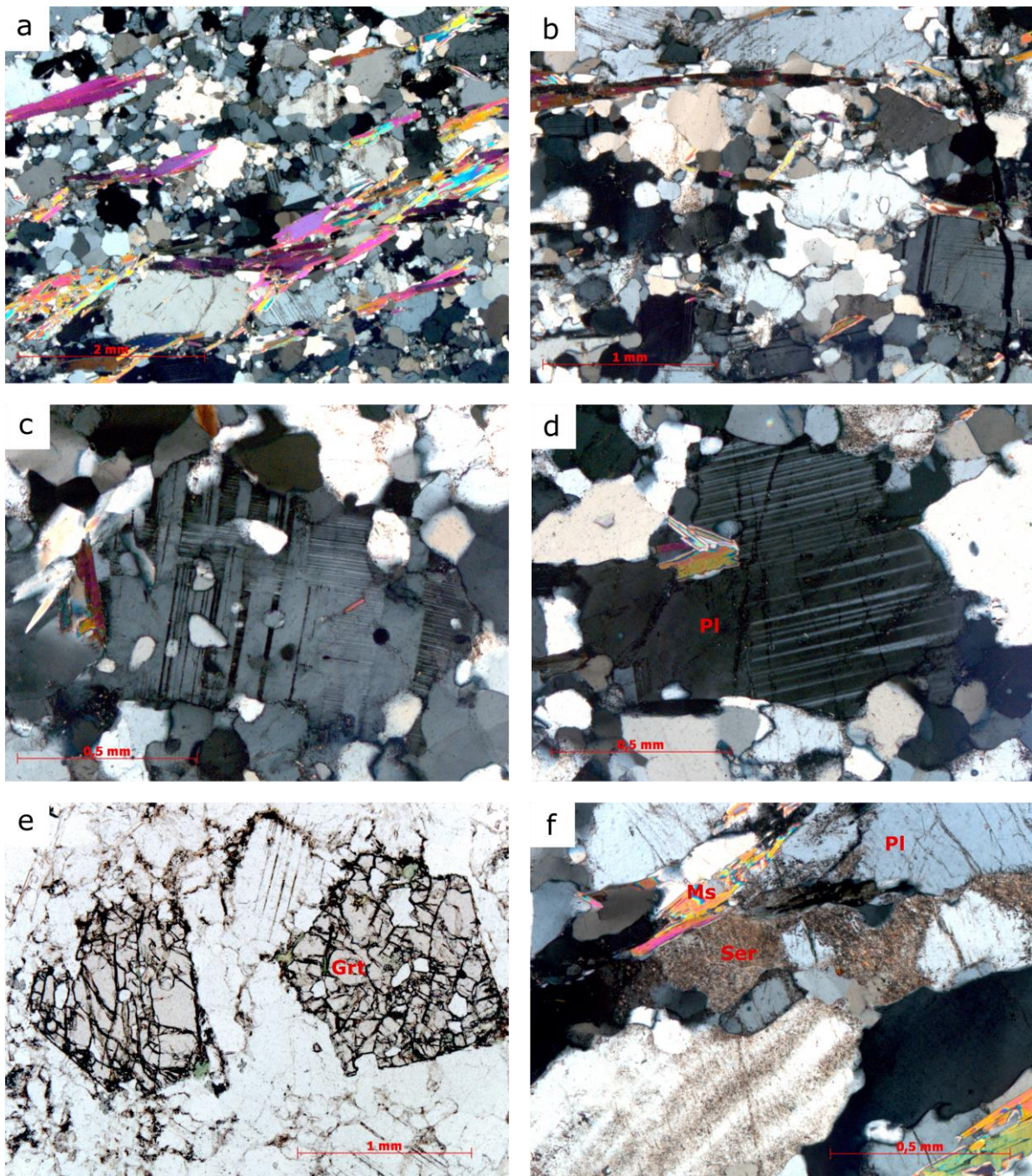


Figure 6.8: Photomicrographs from the Trongen unit. a) Oriented muscovite giving the rock a weak foliation. The matrix exhibits a mantle and core texture. From AAH_185, 2.5x, and in XPL. b) Matrix consisting mainly of feldspar with oriented and acicular biotite grains giving the rock a weak foliation. From AAH_185, 5x and in XPL. c) Microcline twinning of feldspar. From AAH_185, 10x, and in XPL. d) Polysynthetic twinning in plagioclase. From AAH_185, 10x, and in XPL. e) Subhedral and poikiloblastic garnets with inclusions of mainly feldspar. From AAH_185, 5x, and in PPL. f) Sericite affecting the plagioclase and oriented muscovite. From AAH_349, 10x, and in XPL.

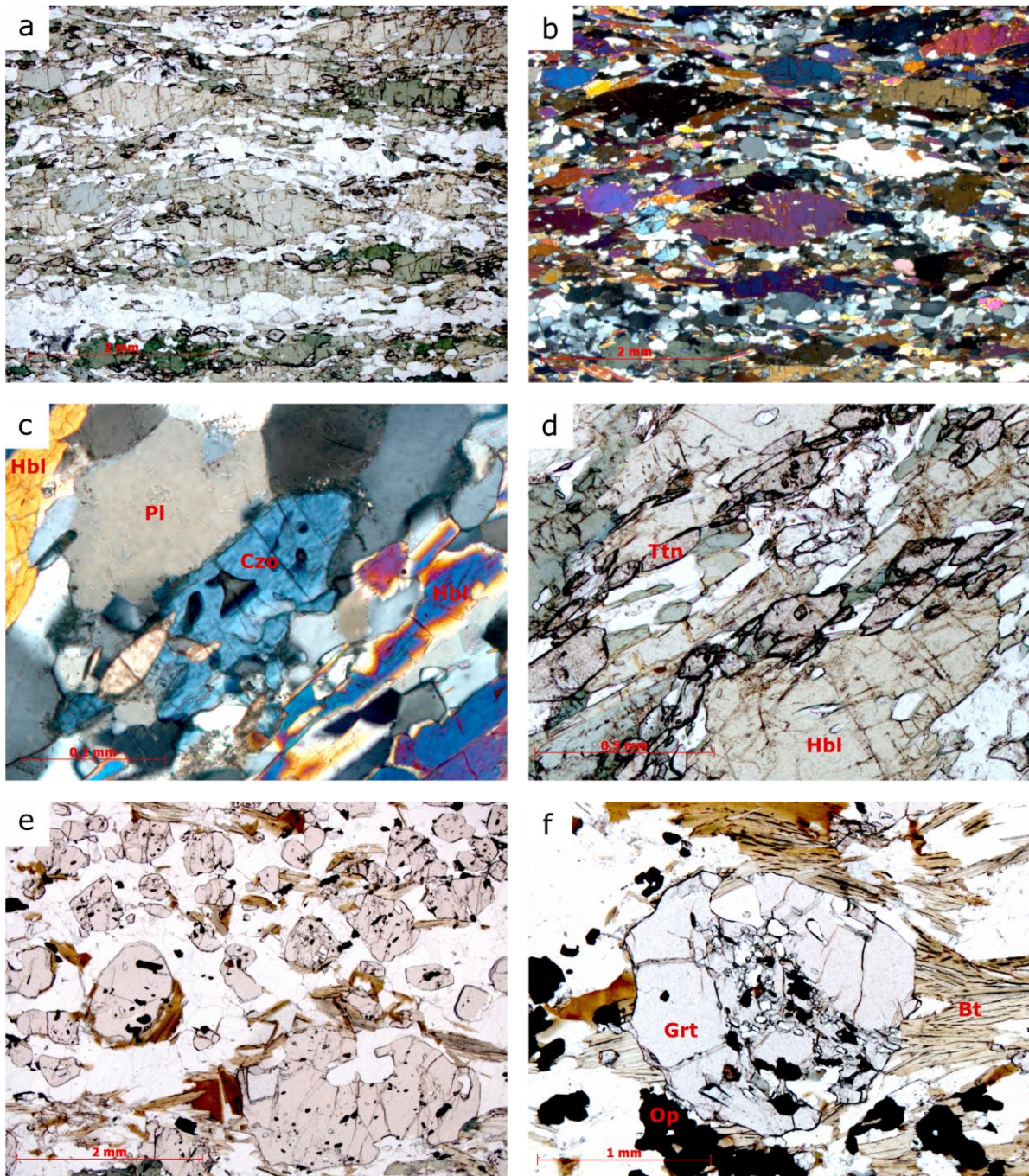
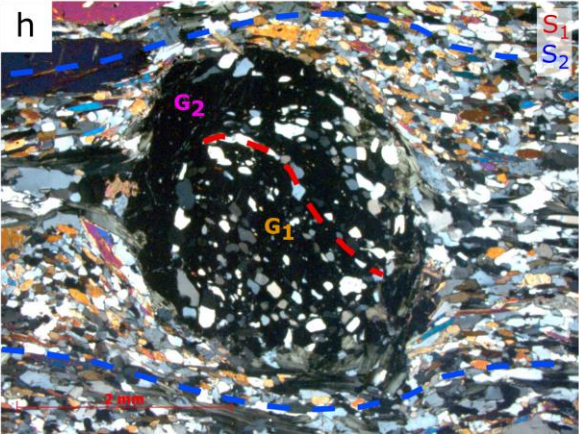
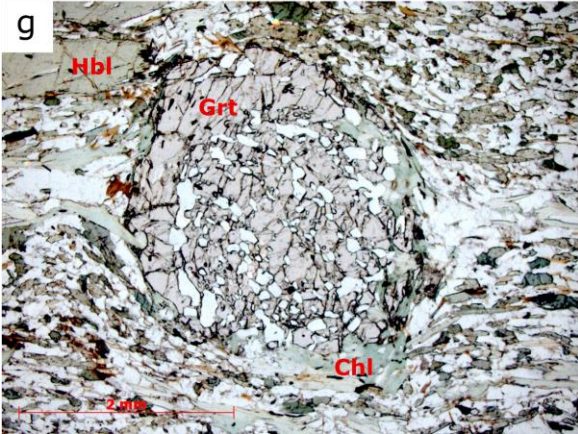
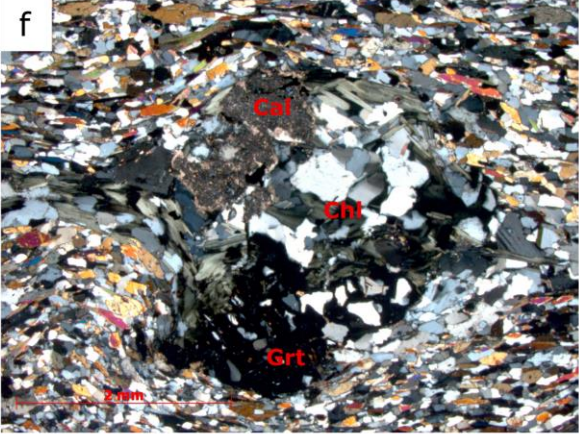
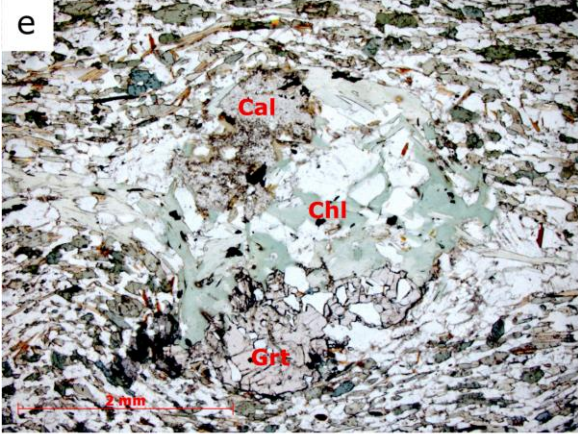
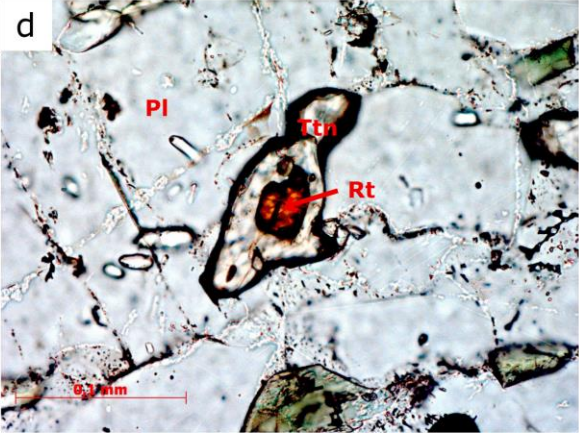
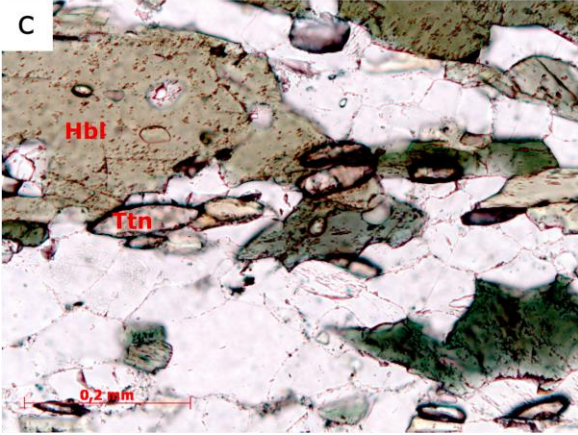
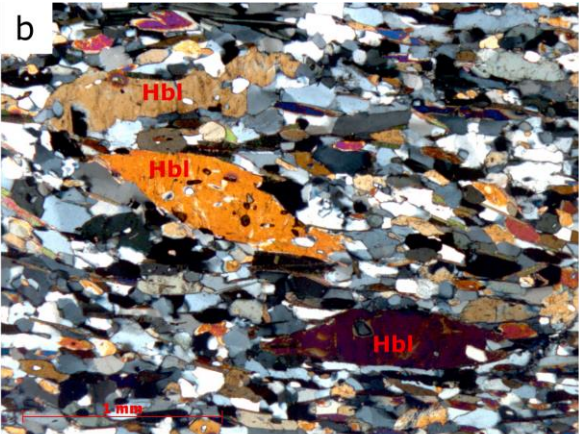


Figure 6.9: Photomicrographs from the Rørvika unit. a) Porphyroblastic hornblende in an equigranular polygonal matrix of hornblende, plagioclase and quartz. The hornblende is elongated and oriented parallel to the foliation. Subhedral titanite concentrated in layers parallel to the foliation. From AAH_281, 2.5x, and in PPL. b) Same as a), XPL. c) Clinozoisite in a matrix of hornblende, plagioclase and quartz. From AAH_281, 20x, and in XPL. d) Subhedral and rhombic titanite grains parallel to the foliation and concentrated in zones. From AAH_281, 10x, and in PPL. e) In a very few zones garnet can be observed concentrated within zones rich in biotite. The garnets are anhedral and contain inclusions of rutile and opaques. From AAH_303, 2.5x, and in PPL. f) The garnets are anhedral, concentrated in biotite-rich zones, and contain inclusions of rutile and opaques. From AAH_303, 5x, and in PPL.



Felsic dykes

Within the Trongen unit, several aplitic dykes (AAH_185 and AAH_349, Appendix H) are observed. They show a weak foliation through the parallel orientation of micas (Fig. 6.8a and b) and feldspar grains with both microcline (Fig. 6.8c) and polysynthetic twinning (Fig. 6.8d). A very few garnets have been observed (Fig. 6.8e). They are poikiloblastic and subhedral to euhedral with chlorite in fractures. Sericite is observed in a few feldspars (Fig. 6.8f).

6.1.3 Rørvika unit

The amphibolitic rocks of the Rørvika unit show a strong and penetrative foliation and are rich in hornblende. Hornblende is found both as part of the fine-grained matrix and as porphyroblasts.

Amphibolitic schist (Ams)

Ams is rich in hornblende, and together with feldspar, quartz and biotite it makes up the matrix of the rock (AAH_303 and AAH_281, Appendix H). Parallel oriented hornblende porphyroblasts constitute the foliation (Fig 6.9a and b), together with elongation of quartz and feldspar (Fig. 6.9b).

Clinozoisite with blue interference colour is parallel to the foliation (Fig. 6.9c). Subhedral to euhedral rhomboid titanite, also oriented parallel to the foliation, occurs together with hornblende (Fig. 6.9d).

Porphyroblastic garnets with inclusions of feldspar, quartz and opaques are identified within zones containing less hornblende (Fig. 6.9e and f). These zones with garnets are also rich in biotite, and one can see the growth of garnet on the expense of biotite.

Figure 6.10: Photomicrographs from the Rørvika unit. a) Porphyroblastic and subhedral garnets in a matrix of equigranular hornblende, feldspar and quartz. Tabular hornblende grains are parallel to the foliation. From AAH_158, 2.5x, and in XPL. b) Porphyroblastic hornblende parallel to the foliation. Matrix of equigranular hornblende, feldspar and quartz. From AAH_158, 5x, and in XPL. c) Rhombic and subhedral titanite grains, about 0.1 mm big, parallel to the foliation. Concentrated in zones and layers. From AAH_232, 20x, and in PPL. d) Anhedral titanite grain with inclusion of rutile. From AHH_347, 40x, and in PPL. e) Anhedral garnet partly replaced by Mg-chlorite and calcite with ϕ -type deformation. From AAH_158, 2.5x, and in PPL. f) Same as e), XPL. Anhedral and porphyroblastic garnet partly dissolved and replaced by Mg-chlorite and calcite with ϕ -type deformation. g) Porphyroblastic and poikiloblastic garnet with a ϕ -type deformation. The garnet show replacement to chlorite on the edges. From AAH_158, 2.5x, and in PPL. h) Same as g), XPL. Porphyroblastic and poikiloblastic garnet showing two stages of growth. The first stage of growth, G_1 , was synkinematic, S_1 . The second stage of growth does not indicate under what conditions it grew. A newer foliation, S_2 , is oblique to S_1 .

Amphibolitic to intermediate garnet-bearing schist (Amis)

Amis contains mainly hornblende, feldspar and quartz, with varying amount of garnet and micas (AAH_232, AAH_374 and AAH_158, Appendix H). It is foliated and layered with porphyroblastic garnets concentrated in layers and zones (Fig. 6.10a). The foliation is mainly made up by oriented hornblende grains (Fig. 6.10a and b). The matrix consists of fine grained equigranular to inequigranular polygonal to interlobate hornblende, feldspar and quartz (Fig. 6.10a and b). Hornblende is found as fine grains in the matrix and as porphyroblasts (Fig. 6.10b).

Abundant subhedral to euhedral rhombic titanite is found concentrated in layers and zones (Fig. 6.10c). They are oriented parallel to subparallel to the foliation, and some titanites are found with anhedral cores of rutile (Fig. 6.10d).

Garnets are anhedral to subhedral, poikiloblastic with inclusions of mainly quartz and feldspar (Fig. 6.10e-h), and can show halos of quartz and feldspar, and in areas chlorite and calcite (AAH_374, Appendix H). Mg-chlorite and calcite can be observed as porphyroblasts in the matrix or related to garnets (Fig. 6.10e). Some garnets show two stages of growth, the first (G₁, Fig. 6.10h) showing a synkinematic inclusion trails (S₁, Fig. 6.10h), and the second one (G₂, Fig. 6.10h) showing less inclusions.

Amphibolitic schist with layers and lenses of felsic material (Amfs)

The Amfs contains outcrops with porphyritic texture (AAH_253, Appendix H). Porphyroblasts of hornblende (Fig. 6.11a) and plagioclase (Fig. 6.11b) float in an inequigranular polygonal to interlobate matrix consisting of plagioclase, hornblende, quartz, epidote and opaques (Fig. 6.11c and d). The porphyroblasts are anhedral to subhedral and vary in size from 1-15 mm, and some plagioclase porphyroblasts show inclusions of prismatic clinozoisite (Fig. 6.11e). The plagioclase can show polysynthetic twinning and sericite (Fig. 6.11b).

Tonalitic gneiss (Fams) and aplites

The tonalitic rocks of the Rørvika unit, both Fams (AAH_149 and AAH_246, Appendix H) and aplitic dykes (AAH_300, Appendix H), contain mostly quartz and plagioclase, with small amounts of oriented biotite (Fig. 6.12a and b), clinozoisite, epidote (Fig. 6.12c) and chlorite (Fig. 6.12d). The chlorite exhibit a strong and blue interference colour. The texture is seriate interlobate, with a core and mantle texture (Fig. 6.12a and b). The plagioclase can be partly replaced by sericite (6.12e) and can show polysynthetic twinning (Fig. 6.12f).

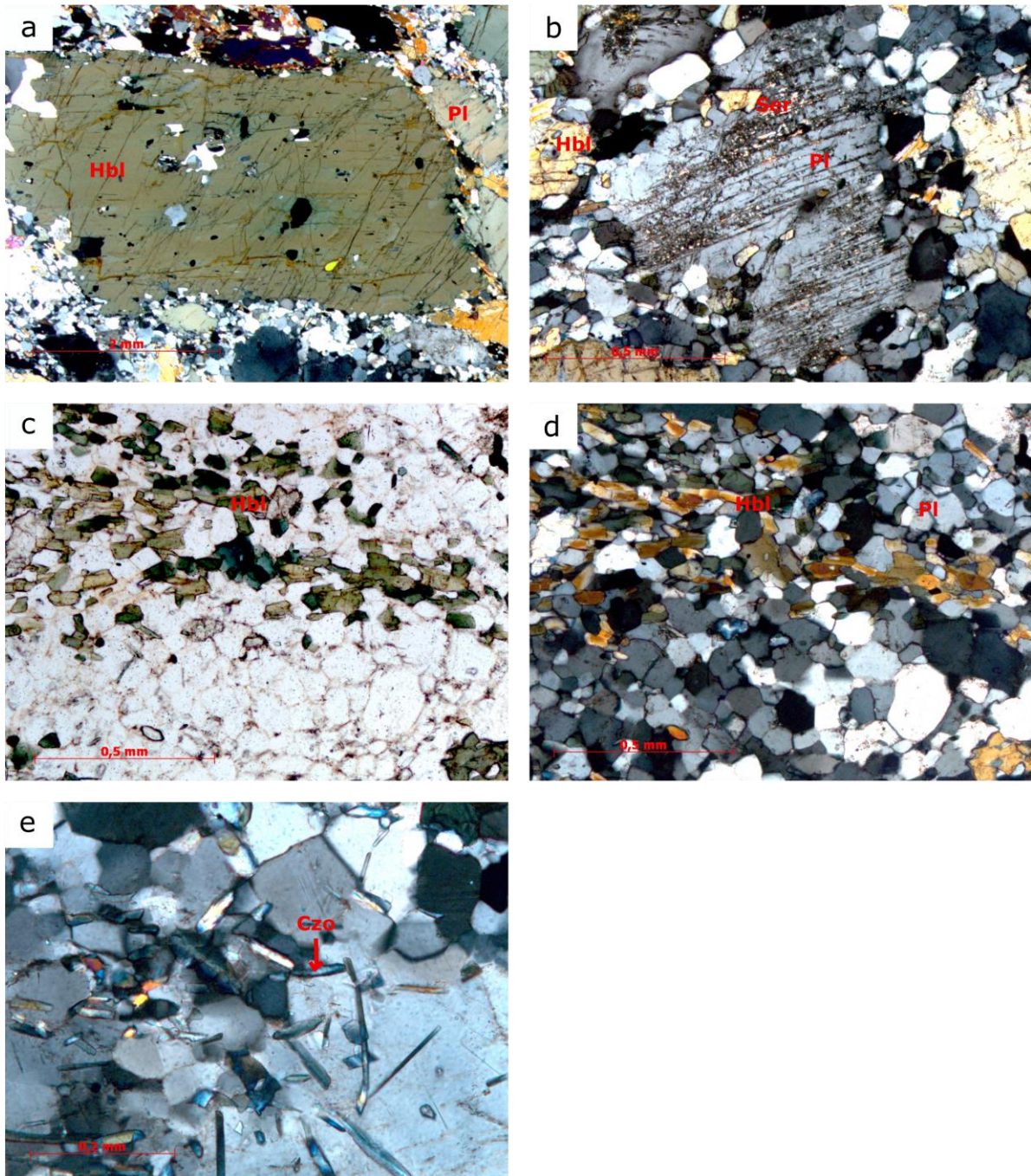


Figure 6.11: Photomicrographs from the Rørvika unit. a) Porphyroblastic and subhedral hornblende in an inequigranular polygonal to interlobate matrix consisting of hornblende, plagioclase and quartz. From AAH_253, 2.5x, and in XPL. b) Porphyroblast of plagioclase affected by sericite. From AAH_253, 10x, and in XPL. c) Matrix consisting of inequigranular to equigranular hornblende, plagioclase and quartz. From AAH_253, 10x, and in PPL. d) Same as c), XPL. e) Porphyroblastic plagioclase with inclusions of clinozoisite, also partly occurring in the plagioclase in the matrix. The clinozoisite are prismatic expressing no preferred orientation. From AAH_253, 20x, and in XPL.

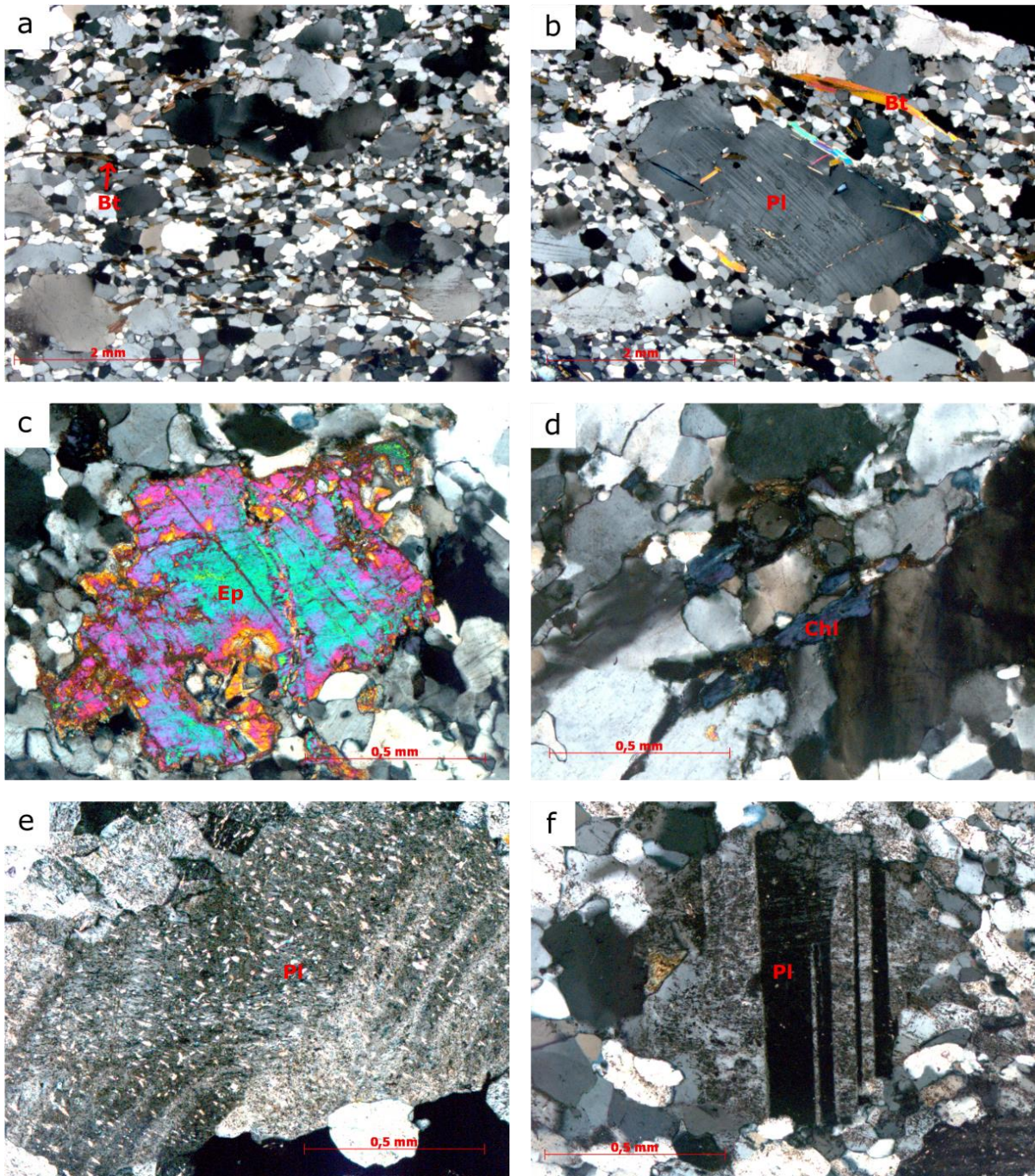


Figure 6.12: Photomicrographs from the Rørvika unit. a) Core and mantle texture of plagioclase and quartz. Oriented and subparallel biotite grains make up a weak foliation. From AAH_246, 2.5x, and in XPL. b) Porphyroblastic plagioclase grain with inclusions of biotite in a seriate interlobate matrix. From AAH_246, 2.5x, and in XPL. c) Epidote grain in the quartz and plagioclase matrix. From AAH_149, 10x, and in XPL. d) Chlorite with blue interference colour. From AAH_149, 10x, and in XPL. e) Plagioclase grain affected by sericite. From AAH_300, 10x, and in XPL. f) Plagioclase grain showing polysynthetic twinning. From AAH_300, 10x, and in XPL.

Fault rock

Fault rocks within Rørvika unit (AAH_324, Appendix H) show thin and irregular fault cores, while the rock around is affected by the faulting through fractures. The rocks surrounding the immediate fault zone contain epidote (Fig. 6.13a) and clinozoisite (Fig. 6.13b), all in a fine grained matrix. The entire rock is affected by sericite (fig. 6.13c). In the fault core itself, the rock is crushed and contains small fragments of the host rock and fine grained chlorite (Fig. 6.13d).

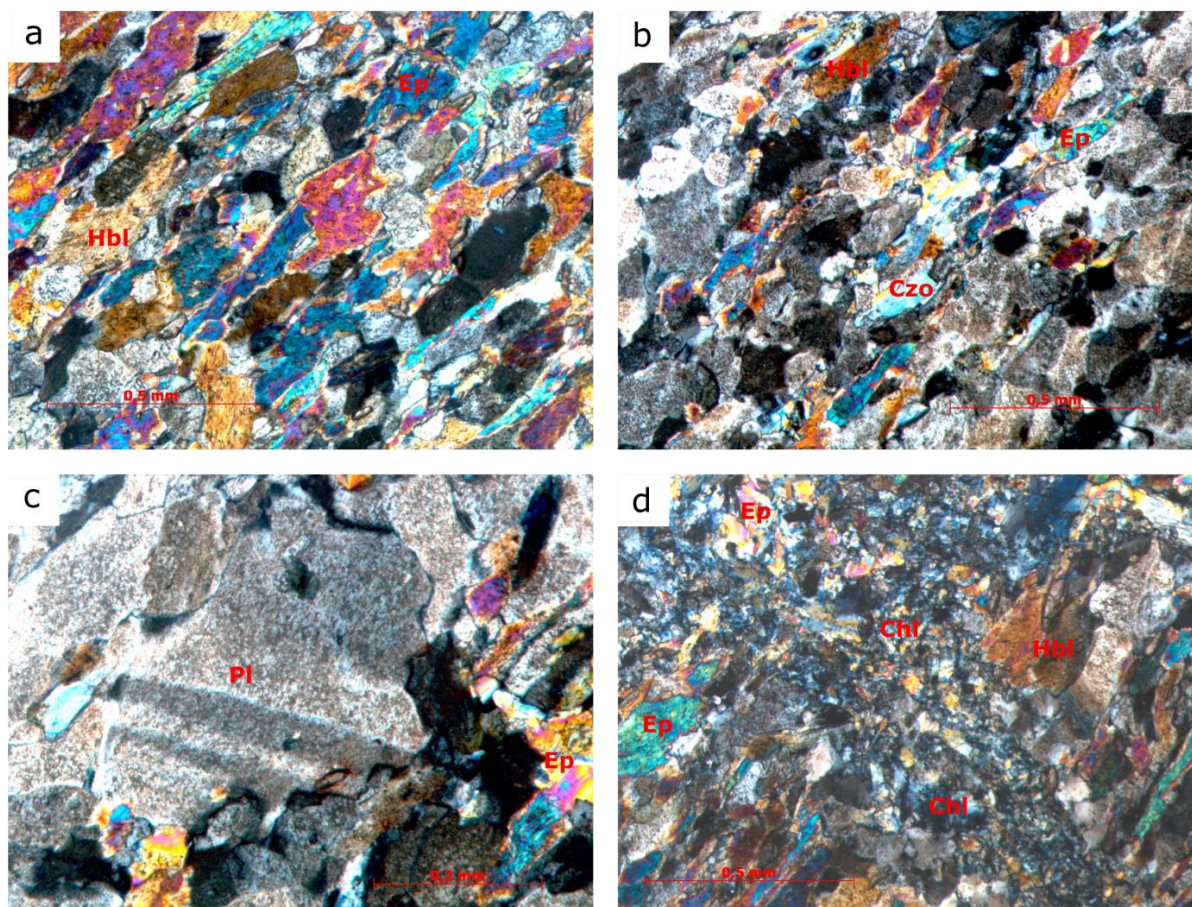
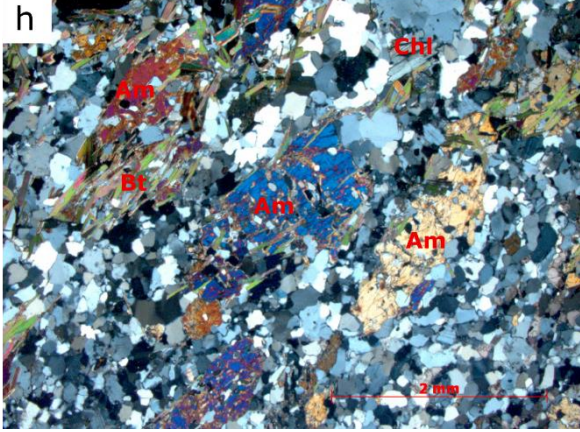
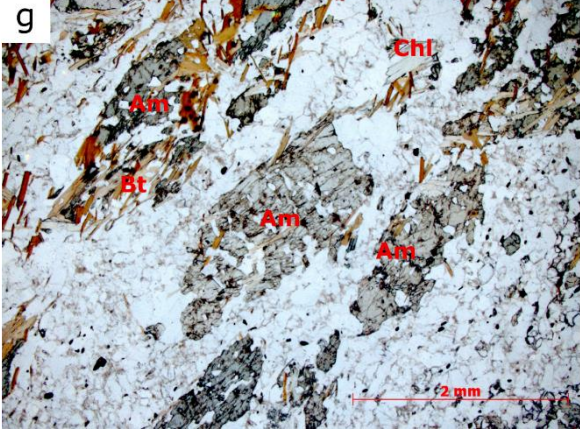
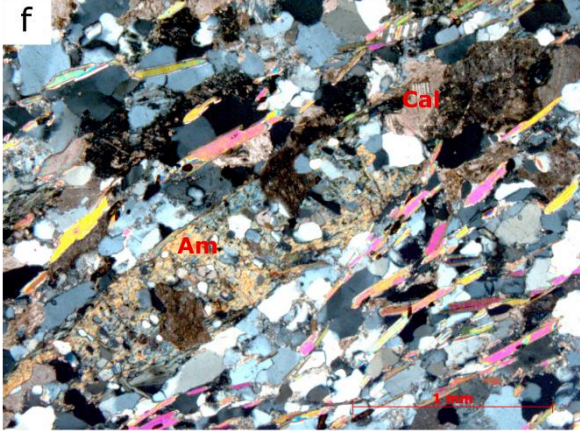
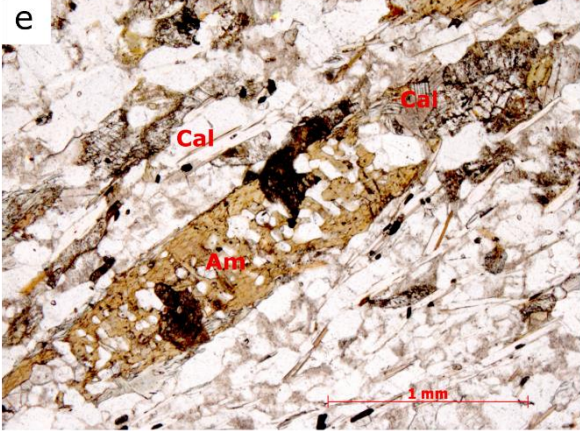
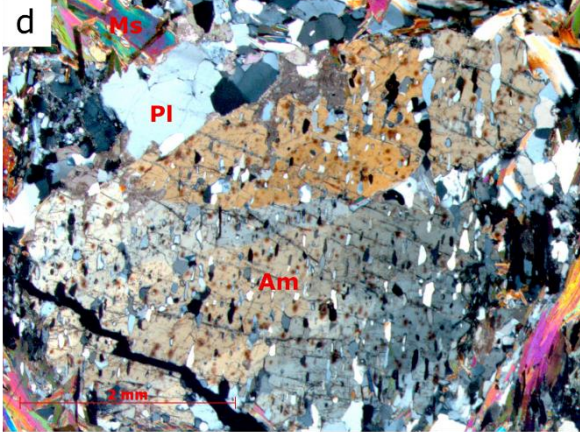
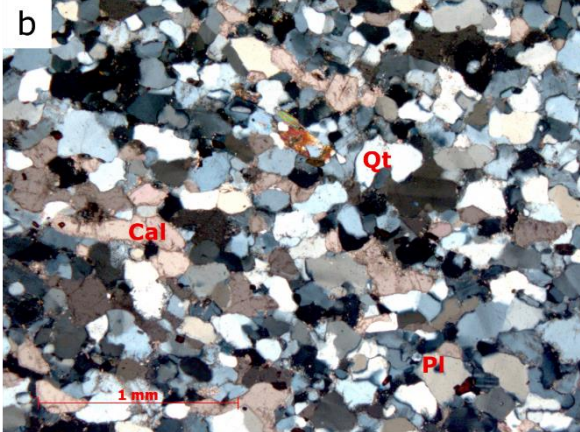


Figure 6.13: Photomicrographs from the Rørvika unit. a) Matrix of feldspar, hornblende and epidote in near proximity to a fault core. From AAH_324, 10x, and in XPL. b) Matrix also contains small amounts of clinozoisite. From AAH_324, 10x, and in XPL. c) The entire rock is highly affected by sericite. From AAH_324, 20x, and in XPL. d) Within the fault core, the rock is crushed, containing fragments of the host rock and fine grained chlorite. From AAH_324, 10x, and in XPL.

6.1.4 Varpneset unit

Hornblende-calcite-quartz schist (Hcqs)

The Hcqs (AAH_162, AAH_164 and AAH_165, Appendix H) is medium to coarse-grained with porphyroblasts of garnet, muscovite, and amphibole in an equigranular polygonal to interlobate matrix consisting of feldspar, calcite and quartz (Fig. 6.14a and b). Bladed



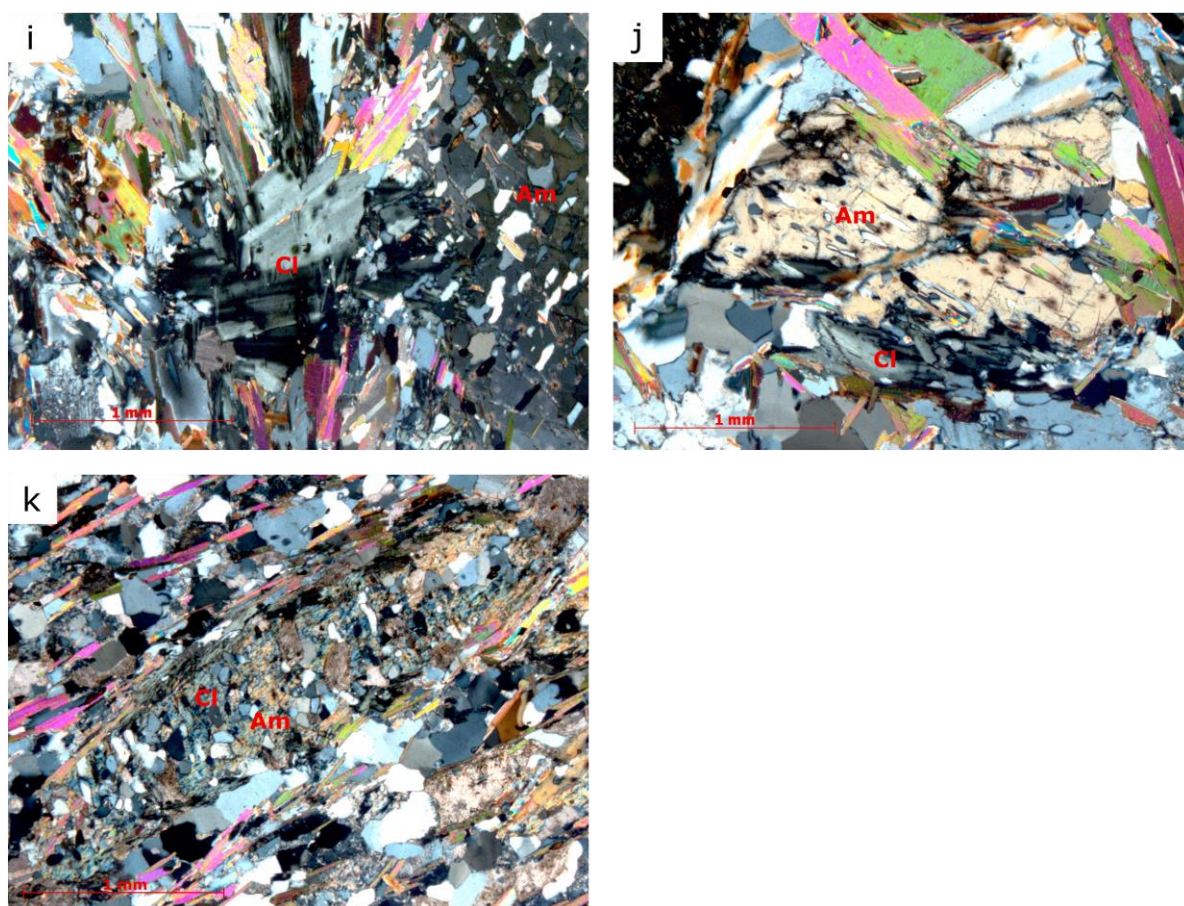
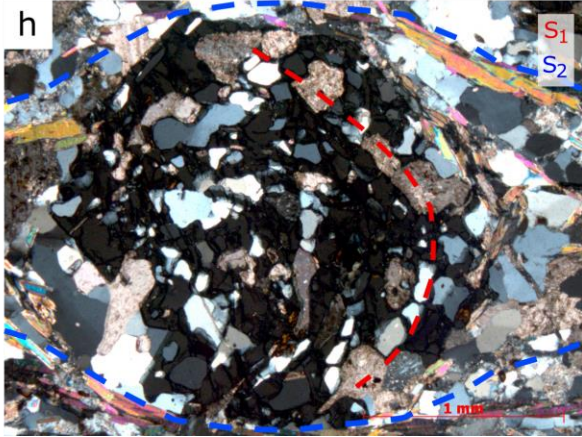
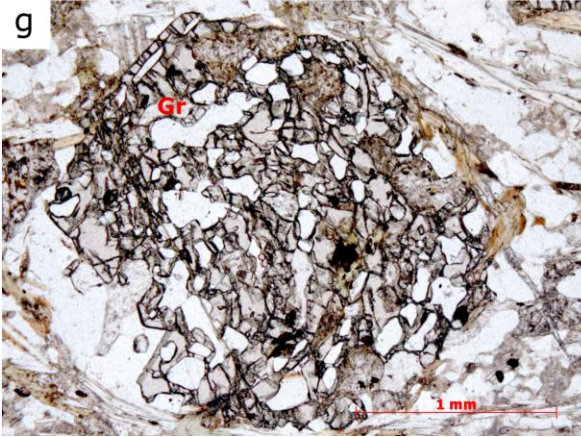
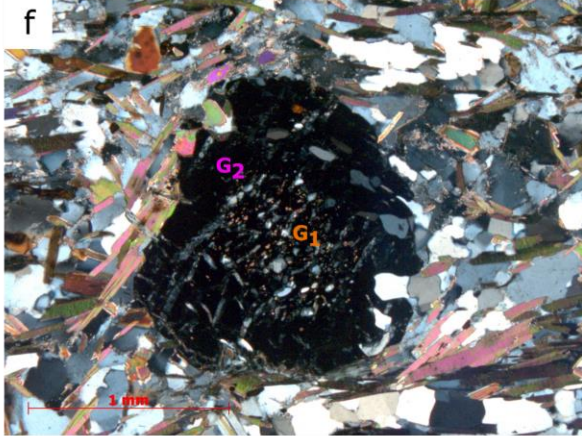
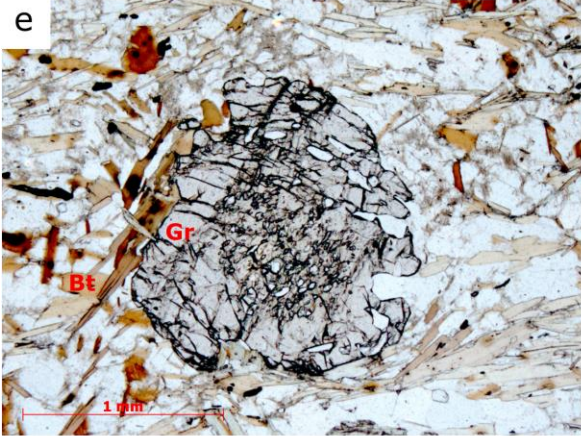
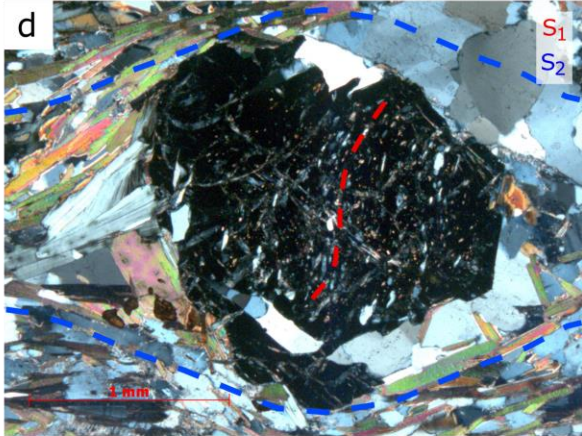
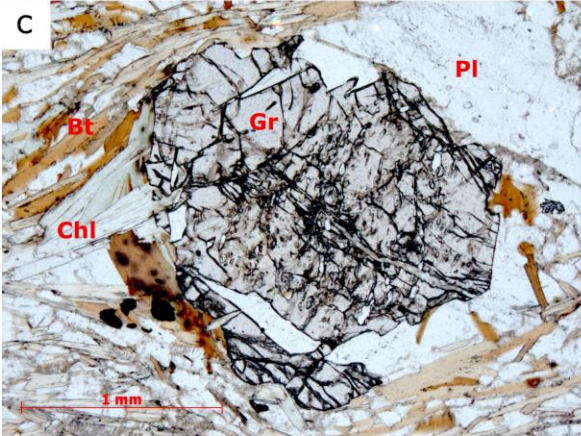
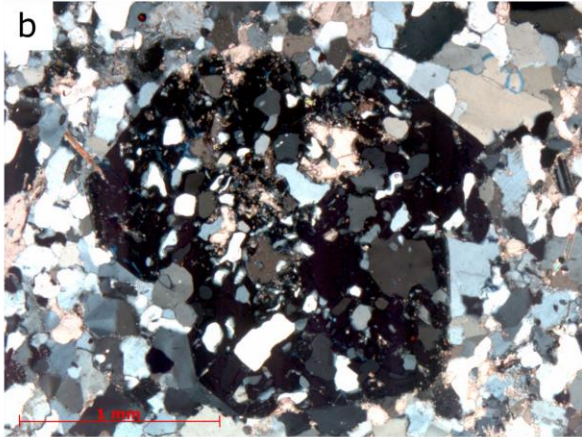
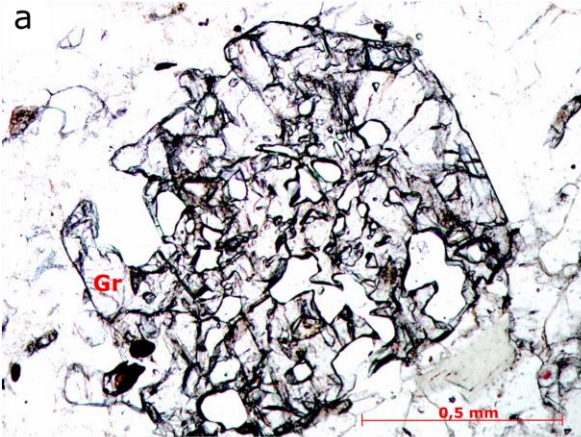


Figure 6.14: Photomicrographs from the Varpneset unit. a) Matrix of the Hcqs consisting of feldspar, quartz and calcite in an inequigranular polygonal to interlobate texture together with oriented and acicular biotite grains being parallel to the foliation. From AAH_162, 2,5x and XPL. b) Matrix with equigranular polygonal to interlobate feldspar, quartz and calcite. From AAH_165, 5x and XPL. c) Acicular biotite showing two preferred directions of orientation. From AAH_165, 2,5x, and in PPL. d) Poikiloblastic amphibole with low interference colours. From AAH_164, 2,5x, and in XPL. e) Bladed and poikiloblastic amphibole parallel to the foliation partly replaced by calcite and chlorite. From AAH_162, 5x, and in PPL. f) Same as e), XPL. Bladed and acicular amphibole with low interference colours partly replaced by calcite and Mg-chlorite. g) Anhedral to subhedral porphyroblastic amphiboles in a matrix of feldspar, quartz, calcite and biotite. From AAH_165, 2,5x, and in PPL. h) Same as g), XPL. Anhedral to subhedral amphiboles with interference colours of second order. i) Mg-chlorite related to a poikiloblastic amphibole with low interference colours. From AAH_164, 5x, and in XPL. j) Amphibole with low interference colour partly replaced by Mg-chlorite on the edges. From AAH_164, 5x, and in XPL. k) Bladed and poikiloblastic amphibole with low interference colours parallel to the foliation. The amphibole is replaced by Mg-chlorite. From AAH_162, 5x, and in XPL.

micas and amphibole crystals give the rock its foliation. The zones rich in biotite show biotite with two preferred orientations, giving the thin section an appearance of undulose foliation (Fig. 6.14c).

The amphiboles within Varpneset unit display two different types of appearances. The first shows elongated, subhedral and bladed amphiboles with low interference colours, highly poikiloblastic and partly replaced by calcite and some chlorite (Fig. 6.14d, e and f). The



inclusion trails of these amphiboles can have a small oblique angle to the foliation (Fig. 6.14d). The second type of amphibole is anhedral and elongated, and shows interference colours blue and reddish of second order (Fig. 6.14g and h), contains less inclusions and is replaced by other minerals to a less extent.

Mg-chlorite with a grey interference colour and a fibrous texture is found related to the amphibole grains with low interference colour. The chlorite occurs as grains next to amphibole (Fig. 6.14i), or within the amphibole grains (Fig. 6.14j and k).

Hcqs show a layered appearance in the field, with alternating layers rich in amphibole and biotite, and layers where these minerals are virtually absent (AAH_165, Appendix H). On a microscopic level the layering shows a transitional zone moving from the biotite- and amphibole-absent part, into a zone dominated by amphibole and with an increasing amount of biotite towards a thicker zone consisting of mainly biotite. Within the different zones there are also changes in the appearance of garnets, from highly fractured and poikiloblastic garnets in the zone absent of biotite and amphibole (Fig. 6.15a and b), to a more massive look nearly free of poikiloblasts in the biotite zone (Fig. 6.15c-f). In addition, some garnets show synkinematic inclusion trails with quartz, feldspar and calcite (S_1 , Fig. 6.15d and h), and two stages of growth (G_1 and G_2 , Fig. 6.15f). The first stage (G_1 , Fig. 6.15f) shows a poikiloblastic texture with inclusion trails oblique to the direction of the foliation. The second stage (G_2 , Fig. 6.15f) displays few and bigger inclusions with inclusion trails different from the core of the garnet.

Figure 6.15: Photomicrographs from the Varpneset unit. a) Poikiloblastic and subhedral garnet in a matrix consisting of feldspar, quartz and hornblende. From AAH_165, 10x, and in PPL. b) The same as a), XPL. c) Garnet in a matrix consisting of feldspar, quartz, calcite and abundant oriented biotite. From AAH_165, 5x, and in PPL. d) The same as c), XPL. Showing synkinematic deformation, S_1 , in the central part with small inclusion trails in a sinuous shape. The inclusion trail shows a direction oblique to the main foliation, S_2 . e) Garnet showing a minor poikiloblastic tendency in a matrix consisting of quartz, feldspar, calcite and biotite. From AAH_165, 5x, and in PPL. f) The same as e), XPL. Garnet showing two stages of growth, the first stage, G_1 , showing small inclusion trails oblique to the main foliation of the thin section. The second stage, G_2 , contains less but larger inclusion trails, also with a direction different from the main foliation of the thin section. g) Poikiloblastic and subhedral to euhedral garnet in a matrix consisting of quartz, feldspar, calcite and some muscovite. From AAH_162, 5x, and in XPL. h) The same as g), XPL. Poikiloblastic garnet with inclusion trails in a sinuous shape showing synkinematic deformation, S_1 . The orientation of the inclusions is different from the main foliation, S_2 , of the thin section.

6.2 Geochemistry

7 samples from the Trongen and Rørvika unit were gathered for geochemical analysis on the XRF of main elements and trace elements.

6.2.1 Felsic aplites

Six samples from aplites were prepared for XRF and analysed (Appendix I), two samples from within the Ghms lithology in the Trongen unit (green, Fig. 6.16), one sample from the Ams lithology in Rørvika unit (blue, Fig. 6.16), two samples from the Fams unit in the Rørvika unit (red, Fig. 6.16), and one sample from an aplitite in the Amfs lithology in the Rørvika unit (red, Fig. 6.16). The resulting main elements from the XRF analysis are shown in the Harker diagrams in figure 6.17, and the data is plotted in diagrams showing rock type (Fig. 6.18a) and Shand's Index (Fig. 6.18b). All aplites plot as calc-alkaline rocks in the AMF-diagram (Fig. 6.18c).

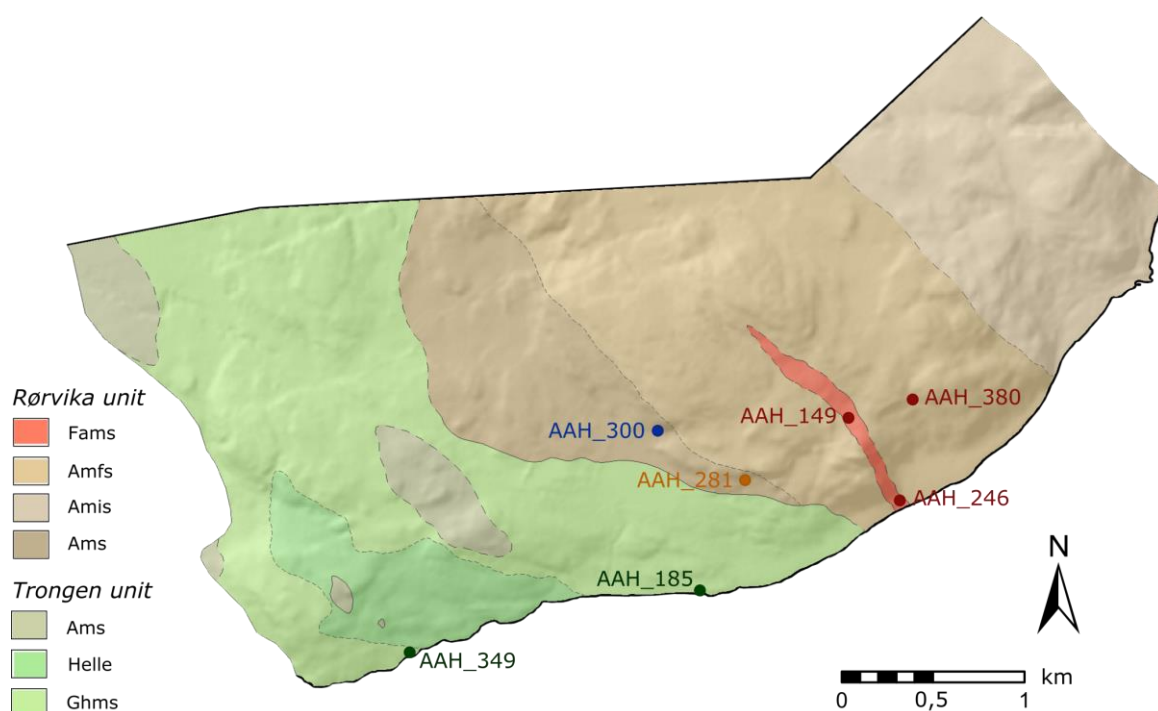


Figure 6.16: Overview of Trongen and Rørvika unit with location of samples analysed outlined. The colours on locations are consistent with the colour coding in the following figures.

Felsic dyke within Ghms, Trongen unit

From the Harker plots (Fig. 6.17), the samples of aplites from within the Ghms show a high content of SiO_2 , from 72.5-74.5 wt%. Plotting the other main elements from these two samples show a lower content of Al_2O_3 , higher content of K_2O , and a lower content of Na_2O compared to the other samples. The other elements show more or less a horizontal linear

relationship to the other samples. The samples plot within the field of granite in the discrimination diagram from Middlemost (1994) (Fig. 6.18a). Plotting the aluminium content by using Shands Index (Maniar and Piccoli, 1989), places the samples from the Trongen unit as peraluminous (Fig. 6.18b).

Felsic dyke within Ams, Rørvika unit

The sample from the aplite within the Ams has a lower content of SiO₂ than the other samples collected, of about 69 wt% (Fig. 6.17). The Harker diagrams show little variations from the other samples, except for a higher content of Al₂O₃ and Na₂O. The sample does not contain MnO. Plotting the sample in the discrimination diagram (Middlemost, 1994) places the rock as a quartz monzonite (Fig. 6.18a). From Maniar and Piccoli (1989) it is shown that the sample lies on the boundary between being classified as a metaluminous and peraluminous rock.

Fams and felsic dyke within the Amfs, Rørvika unit

The three samples of Fams and the aplite dyke within the Amfs lithology in Rørvika unit show similar characteristics on the Harker diagrams (Fig. 6.17). The SiO₂ content is about 71 wt% and the samples show a higher CaO content compared to the other samples from the Rørvika and Trongen units. Also, compared to the other samples, this group of felsic rocks show a medium content of Al₂O₃, K₂O and Na₂O. From Middlemost (1994) the rocks are classified as granite, but very close to the boundary to granodiorite (Fig. 6.18). The samples are characterized as peraluminous even though they are close to being metaluminous (Fig. 6.19).

6.2.2 Ams

There was only taken one sample from the amphibolites in the study area for further geochemical analysis. The sample was taken in the Ams representing a black and homogeneous amphibolite. In the discrimination diagram from Le Bas *et al.* (1986) it plots as basalt (Fig. 6.19a). From the spider diagram (Fig. 6.19b) the sample shows a lower value for mobile elements and a stable linear relationship for immobile elements. A u-shaped depletion around potassium (K) and an a-shape enrichment around Cerium (Ce) can be observed. It can be argued that the sample shows similarities to a MORB (mid-ocean ridge basalt) (Winter, 2010) with the relative flat curve and with a general increasing trend for the mobile elements. This is supported by the discrimination diagram (Pearce and Cann, 1973) that plots the Ams as an ocean-floor basalt (Fig. 6.19c). However, with just one sample it is difficult to make any more specific statements.

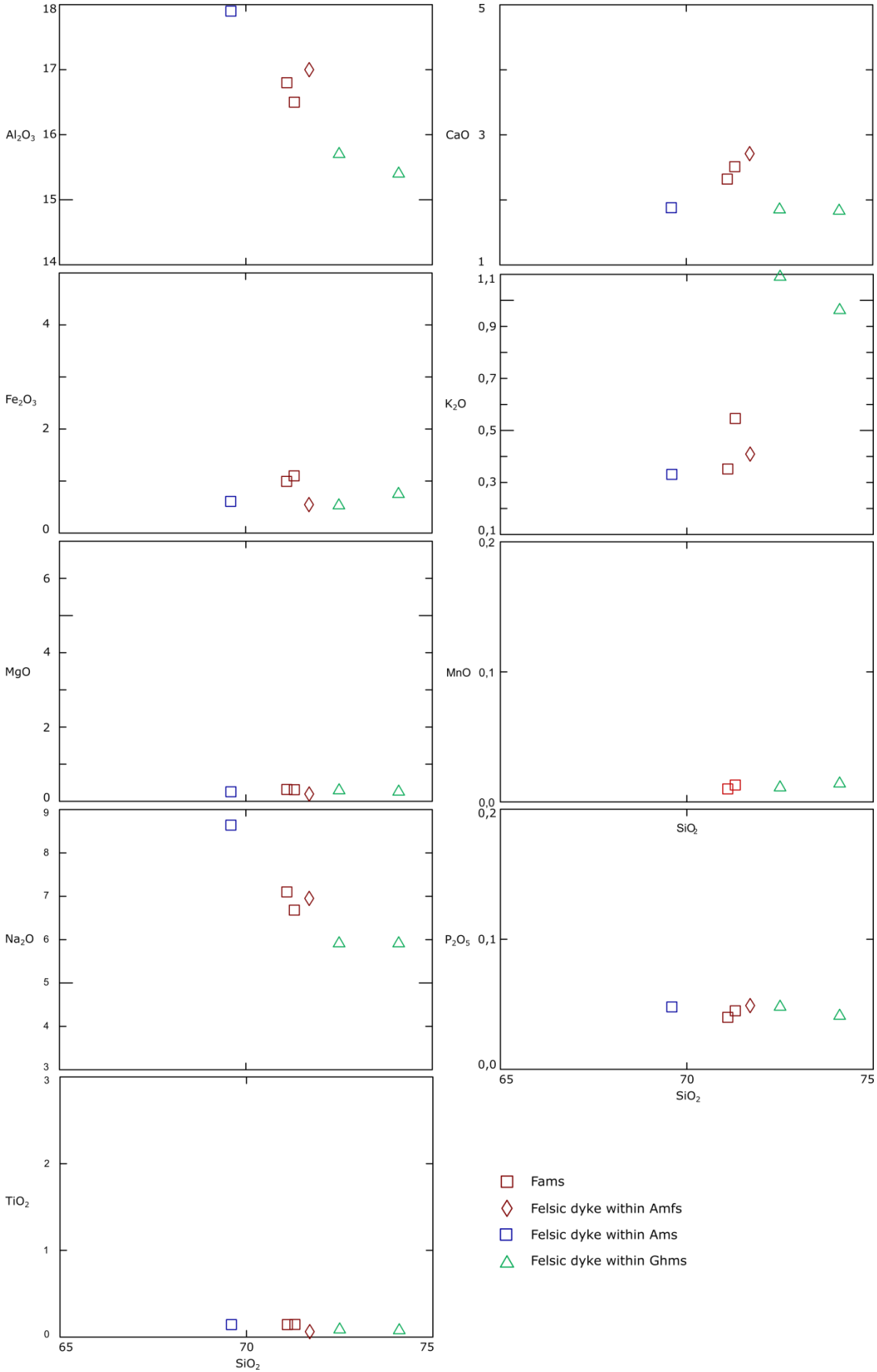


Figure 6.17: Harker diagrams showing the wt% of SiO₂ plotted against the other main elements in the samples.

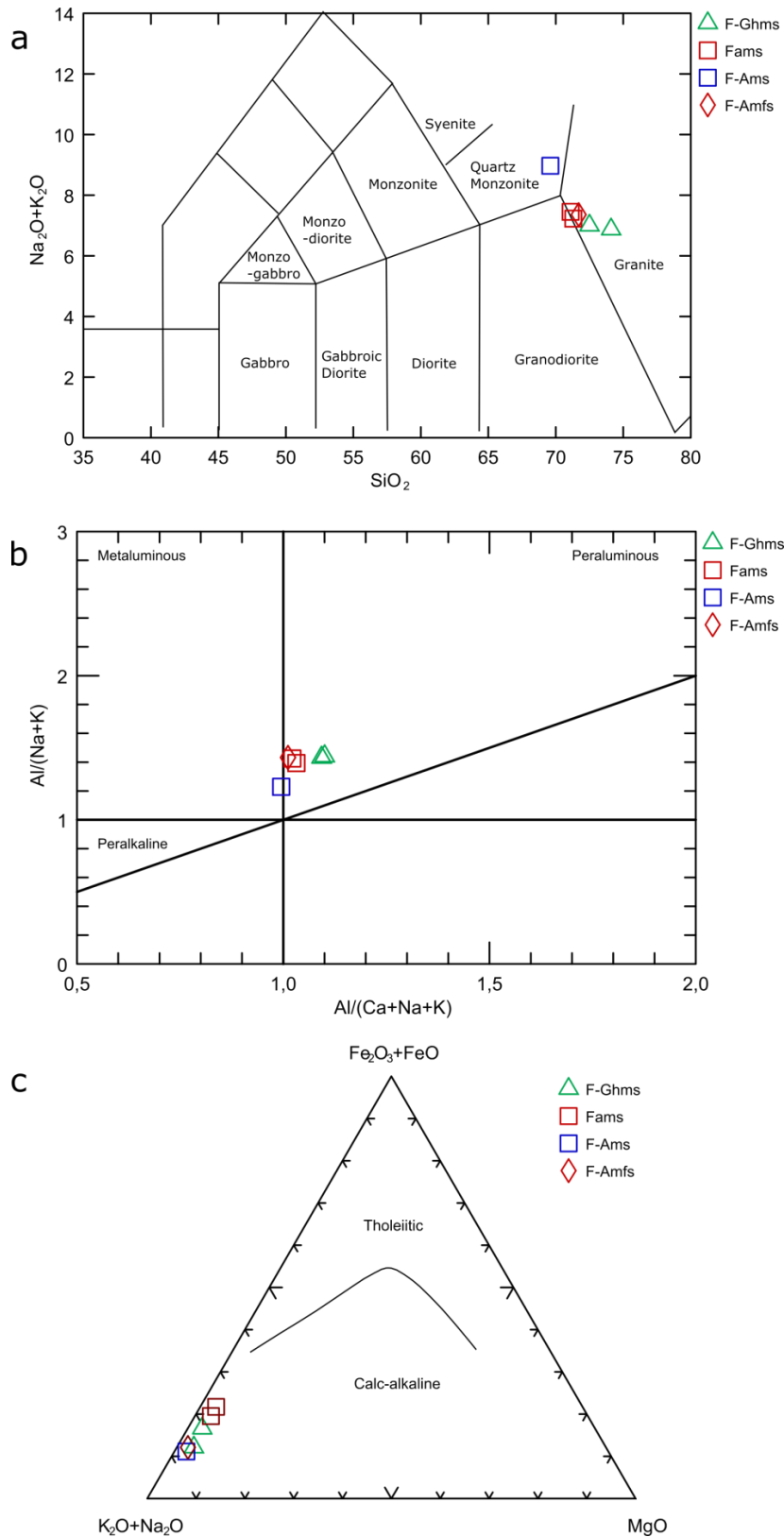


Figure 6.18: a) Discrimination diagram for classifying of granitoids (Middlemost, 1994). All except one sample plot as granite on the boundary to granodioritic composition. The aplite sampled in Ams show a composition of quartz monzonite. b) Shand's Index (Maniar and Piccoli, 1989). All samples plot in the peraluminous field except the sample from Ams that plot on the boundary to being metaluminous. c) AFM diagram placing all the aplite as calc-alkalines (Irvine and Barager, 1971).

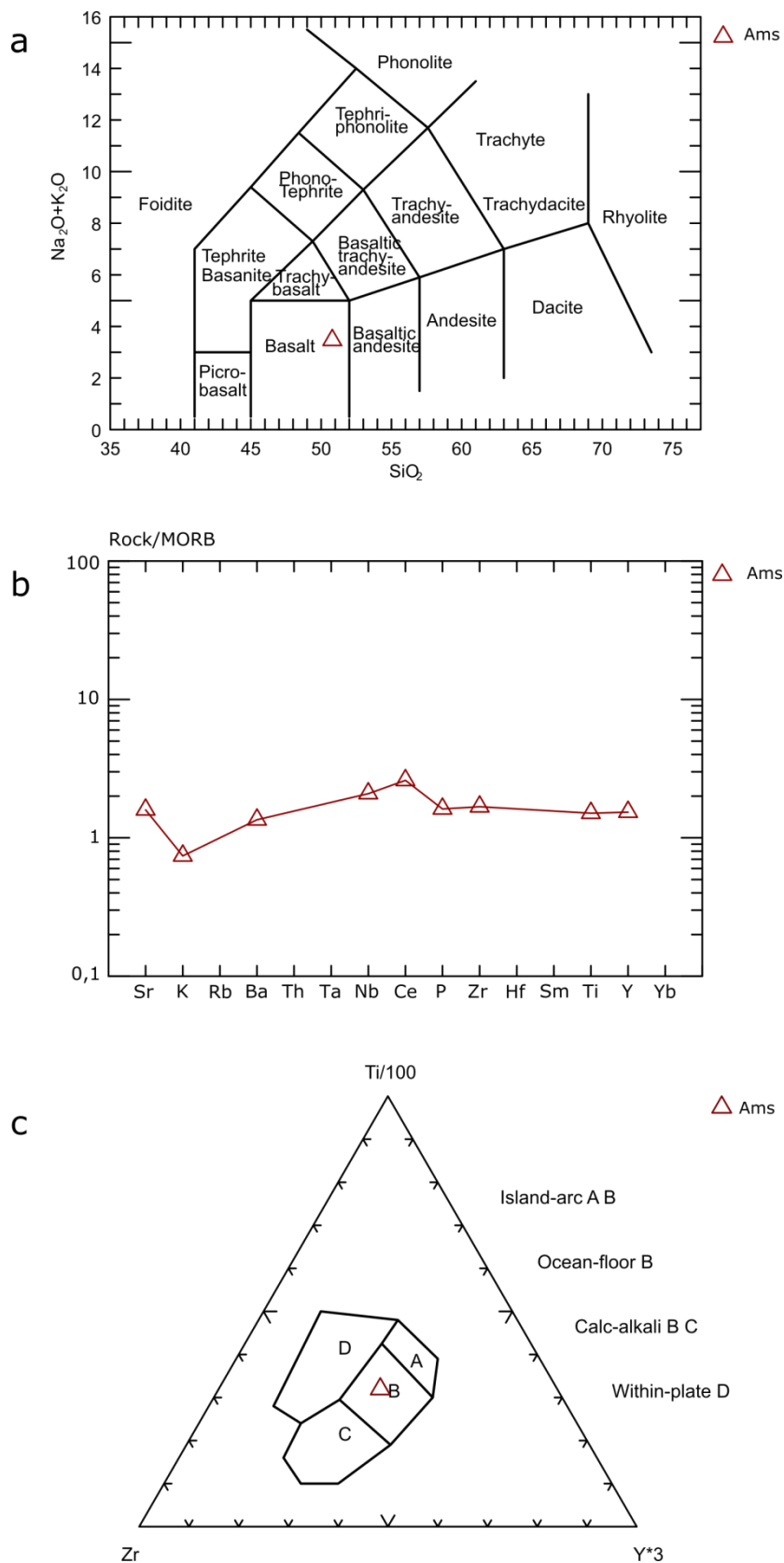


Figure 6.19: a) Discrimination diagram for basalt (Le Bas *et al.*, 1986). The Ams plot as a basalt. b) Spider diagram of the sample from Ams (Pearce, 1983). c) Discrimination diagram for basalt from Pearce and Cann (1973). The Ams plots as an ocean-floor basalt.

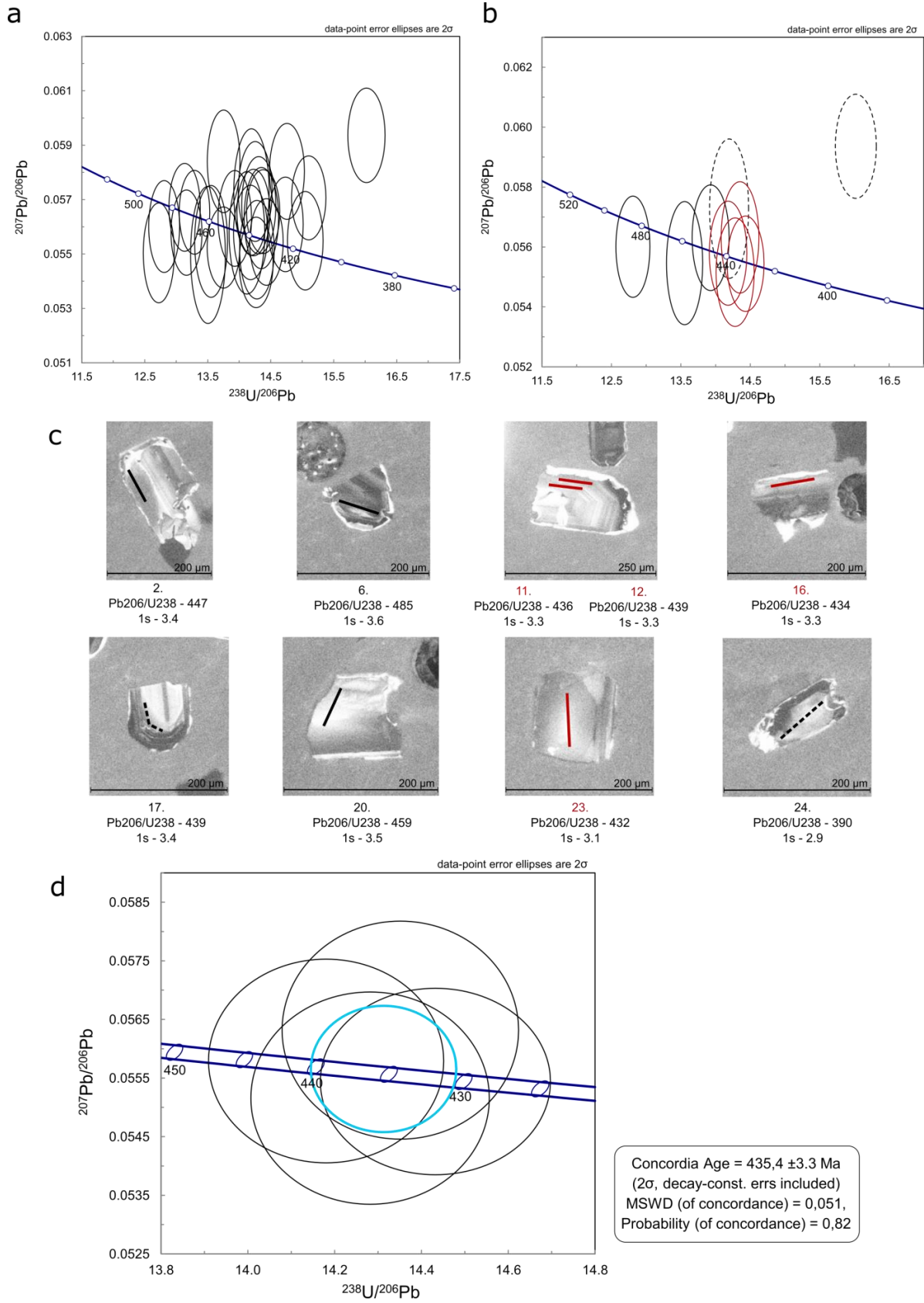
6.3 Geochronology

Three samples from aplites in the Rørvika unit were chosen for geochronological analysis (AAH_300, AAH_246 and AAH_380, Appendix G). The aplites chosen were found within the Ams and Amfs lithologies and characterized by the fine grain size and a high content of quartz and feldspars, which was also confirmed through microscope study. These aplites were chosen for U-Pb dating with the wish to compare the felsic dykes in the study area with dating of similar dykes in other tectonostratigraphic units such as the Seve and Gula nappe complexes (Dunning and Grenne, 2000; Tucker *et al.*, 2004; Ladenberger *et al.*, 2013). The zirconium content (Zr) in these samples from XRF-analysis (Appendix I) is sufficient (>100 ppm) to expect to find zircons in the sample. However, after mineral separation, there were too few zircons found in the samples to continue with the geochronological analysis.

In addition to the aplite samples, one intermediate layer from the Amis lithology was chosen for U-Pb dating (DGA_4). This sample was taken from the ferry-terminal at Rørvika. The Amis is a layered rock with dark amphibolite interlayered with felsic foliation-parallel dykes and intermediate layers. The sample chosen for geochronology was from an intermediate layer with garnets, but unfortunately no geochemical analysis was done on this sample.

The zircons from this sample can be described as belonging to two different groups, one being prismatic with sub-angular to angular corners and one being rounded with irregular shapes. Zircons of sizes from 90-300µm were picked from both groups. Later, when pictures with SEM-CL were taken of the mounted zircons it was clear that the rounded groups thought to be zircons were not. Element identification analyses showed that these grains were titanites. In total 311 grains were mounted where 236 grains in the end proved to be zircons. The prismatic and angular zircons from the sample show a very low CL emission indicating a high content of uranium (U: 67-3767 ppm). The grains have a fractured and broken appearance and some show oscillating zonations with a slightly darker core. Some of the grains were highly metamict and were not used for analysis.

For the analysis, the grains with the highest CL-emission were chosen, hence the lowest content of uranium. This was due to complications doing analysis with a high U-content from the machine set-up and too high estimates of $^{206}\text{Pb}/^{238}\text{U}$ and $^{207}\text{Pb}/^{235}\text{U}$ are given. In total, 26 analyses were targeted (Fig. 6.20a) (Appendix J) where 9 could be used for further analysis (Fig. 6.20b). For the remaining 17 analyses the detector was overloaded and the data unreliable. From the 9 reliable analyses, two were >10% discordant, and three analyses older



than the main cluster of four analyses (Fig. 6.20b, c). The cluster of the four youngest analyses yielded a Concordia age of 435.4 ± 3.3 Ma (Fig. 6.20d; MSWD = 0.051).

Figure 6.20: a) All samples analysed plotted in a Terra-Wasserburg diagram. b) Terra-Wasserburg diagram where unreliable analyses are excluded. Two dotted ellipsoids represent analyses which are >10% discordant. The four red ellipsoids are enhanced in d). c) Zircons from the amphibolite from Rørvika unit. The zircons show oscillating zonation and low CL-emission indicating a high content of uranium. Line indicate where analyses with 15 μm beam were taken. Zircon number 11, 12, 16 and 23 overlap on Concordia and were chosen to calculate a U-Pb age, marked red, sample 17 and 24 correlate with the dotted ellipsoids in b), and the remaining 4 samples were excluded for the age calculation since they are slightly older than the main cluster. d) Terra-Wasserburg diagram of analyses 11,12,16, and 23 yielding an U-Pb Concordia age of 435.4 ± 3.3 Ma.

Discussion

The area of interest was divided into four units based on the characteristics of different lithologies, from west to east being Rødberget unit, Trongen unit, Rørvika unit, and Varpneset unit. The following discussion focuses in a first part on identifying the protoliths for these rocks, discussing their metamorphic history and trying to answer the question of what tectonostratigraphic level these mapped units belong to. In a second part, the structural development of the study area is discussed in more detail.

7.1 Protolith identification, metamorphic history and tectonostratigraphic correlation

7.1.1 The Rødberget unit – a piece of Baltoscandian basement

The Rødberget unit, consisting of the characteristic Ingdal granitic gneiss that contains mostly quartz, feldspars, and some biotite and muscovite, was first mapped by Ramberg (1973) as a “rather homogeneous granitic gneiss”. Later, Tucker *et al.* (1986) and Tucker and Krogh (1988) described the rock as a basement granitic gneiss rich in microcline that was structurally intercalated with schistose and stratified nappe units. Through U-Pb zircon and titanite dating of the rock, ages of 1652.9 ± 1.7 and 396.1 ± 4.9 Ma were given. The oldest age was interpreted as the age of granite crystallization and the lower age as the time of regional medium to high-grade metamorphic resetting as an influence of the Caledonian orogeny (Tucker *et al.*, 1986).

In the Rødberget unit dark to green dykes parallel to the foliation were observed. There are no similar dykes described elsewhere on the northern side of the Trondheimsfjorden. Tucker *et al.* (2004) described mafic dykes observed in the allochthonous Mesoproterozoic basement of the Risberget Nappe. In addition, (Hollocher *et al.*, 2007) suggested that both the Sætra Nappe and the basement of Risberget Nappe are cut by the same dyke system emplaced during Late Neoproterozoic. Whether the mafic dykes in Rødberget unit can be correlated to the mafic dykes on the southern side of the fjord cannot be determined here.

To the west of the Rødberget unit, just west of the study area, a large outcrop of feldspathic quartzite is documented belonging to the Sætra Nappe (Ramberg, 1973; Robinson and Roberts, 2008). In the map of Robinson and Roberts (2008) this nappe is thought to extend all the way around the Rødberget unit also to the eastern side. In this study no outcrops of this quartzite have been observed within the study area due to high degree of cover and the presence of it is still uncertain.

7.1.2 The Trongen unit – Gula or Seve nappe complex?

The Trongen unit, comprising the mica schists called Ghms and Helle, and the amphibolitic rocks Hbs and Ams, is a highly deformed unit containing both deformed aplites and pegmatites and quartz veins. Trongen unit was on the maps by Wolff (1976, 1978) interpreted to be part of the Gula Nappe (Fig. 1.1), later supported by Robinson and Roberts (2008) (Fig. 1.2a). However, Gee (1985) and Corfu *et al.* (2014) interpreted the rocks to be part of the Seve Nappe Complex (Fig. 1.2b and Fig. 2.2).

The main lithology Ghms is rich in garnets and mica and contains varying amounts of hornblende. It is interpreted to represent a sedimentary protolith, and because of the high quartz content it is reasonable to assume a considerable continental source for this sediment. Small amounts of calcite are found from petrographic studies throughout the Trongen unit in the Ghms, indicating some carbonate input during the deposition of these rocks. The amphiboles could have a source from eroded volcanic rocks or could be a result of a metamorphic reaction involving calc-silicates. West in the unit, at locality 348 (Appendix A), the Ghms shows a strong layered character rich in quartz, pointing to an increased influence of continentally-derived material. This rock contains fine-grained carbonates throughout and has a greenish colour, suggesting that this was originally a calc-silicate or marl.

The amphibolitic Hbs found in close relation to the Ghms is believed to be derived from eroded basaltic sources. The lenses of Ams in the Ghms either represent basaltic flows within the original Ghms sediment or they represent pieces of the Ams of the Rørvika unit that has through a complex deformational history ended up as lenses in the Trongen unit. Hull and Adamy (1989) interpreted the Ams in the mica schist as metamorphosed basaltic flows, but it was also suggested that they could be dykes or sills from the central amphibolites, here called Rørvika unit.

Similar rocks as in the Trongen unit are described from the Gangåsvann area, Orkdal (Fig. 2.2), where it was observed a garnet-hornblende-mica schist and amphibolites with lenses

and sheets of felsic trondhjemite (Peacey (1963); Johnsen (1979)). The unit was named Gangåsvann Group and was described as containing amphiboles absent of relict igneous textures. The rocks were found above quartzites and basement gneisses. Later, Kollung (1990) recognized similar rocks in the Surnadal-Orkdal district (Fig. 2.2), and assigned them to the Surna Nappe. The upper part of this nappe was described as mica schist with a brown weathering colour due to high biotite content. Garnets are common and the mica schist contains in places hornblende. Similar mica schist units have been described by others (Gee, 1985; Krill, 1985; Rickard, 1985), under different names like Blåhø Nappe, Skjøtingen Nappe and Essandsjø Nappe in various parts of Mid-Norway. These nappes have later been correlated with the Seve Nappe Complex (Gee *et al.* 1985).

The Trongen unit has earlier been interpreted as part of the Gula Group, which mainly consists of calcareous metasandstones, ribbon chert, graphitic schist, amphibolites, and pelitic schist (Nilsen, 1978). From this study it was not found rocks similar in appearance to descriptions from the Gula Nappe, and lithologically the Trongen unit resembles more the units related to the Seve Nappe Complex. From the observations done in this study and descriptions above, it is believed that the Trongen unit is part of the Seve Nappe Complex related to the outer margin of the Baltican continent. The high grade amphibolite facies metamorphism and the resemblance to other described areas support this theory.

7.1.3 The Rørvika unit –Støren Nappe or Seve Nappe Complex?

The massive amphibolites of the Rørvika unit have earlier been linked to the Støren Nappe and put in relation to the greenstones of the same nappe on the southern side of Trondheimsfjorden (Fig. 2.2). The amphibolites of the Rørvika unit have been thought to be part of a local synform on the eastern limb of a larger north-south striking antiform with the Rødberget unit in the centre (Fig.1.1 and Fig. 1.3).

Lithological and metamorphic considerations

The amphibolites of the study area are divided into three lithologies based on the appearance in the field: (1) Ams with little felsic content and with a transitional boundary to 2) Amfs, being a massive amphibolite with high amount of felsic material interlayered, and 3) Amis with an intermediate component. Garnets can be observed in all lithologies, less in the two first. All the amphibolites of the Rørvika unit are interpreted to be affected by high-grade amphibolite facies metamorphism. Robinson and Roberts (2008) mentioned that the Støren and Seve Nappe Complex could be distinguished based on the general metamorphic grade and the content of

garnet; the Støren Nappe containing low to medium grade rocks with no to just a few garnets, not bigger than 2-3 mm, while the Seve Nappe Complex has a higher grade of metamorphism and contains many and coarse garnets. The rocks of the Støren Nappe south of Trondheimsfjorden are usually described as affected by greenschist facies metamorphism (Slagstad, 2003), while Hollocher *et al.* (2012) pointed out that the metamorphic grade of the Støren Nappe increases towards the west in mid-Norway to lower amphibolite facies. More evidence is needed to decide an affinity of the Rørvika unit.

Geochemical considerations

Hollocher *et al.* (2012) sampled mafic volcanics from the Støren Nappe on the Fosen peninsula west of the study area for geochemical analysis. Basaltic amphibolites were described as greenish to grey with internally fine-grained and homogeneous boudinaged layers, and are interpreted as deformed pillow lavas and lava flows. Two gabbroic rocks are of special interest since they were found on the western side of the antiform (Fig. 1.1) that Rørvika has been interpreted to be a part of (NG, Fig. 7.1a and Fig. 7.2). Comparing the geochemistry of the samples from Hollocher *et al.* (2012) with the Ams from the Rørvika unit (Fig 7.1a), it is clear that the Ams is not related to the non-cumulative gabbros from the same interpreted body of the Støren Nappe. In general, the samples from Hollocher *et al.* (2012) plot as volcanic island basalts (Fig. 7.2), and they show a depleted Nb-trend in the Spider diagram (Fig. 7.1a), characteristic for subduction zone related basalts. The sample from Ams does not show this depleted Nb-trend (Fig. 7.1a) and plots as ocean floor (Fig. 6.19c) and mid-ocean ridge basalts (MORB) (Fig. 7.2). Two samples of intermediate MORB-like basalt (IM, Fig. 7.1a) show similar trends as the sample from Ams, but with a u-shape above the Nb-value, whereas the Ams shows an a-shape geometry. Hollocher *et al.* (2012) related all the samples from the study, basalts and gabbros, to the Støren Nappe and ophiolites in this nappe, and argued that this was supported by the presence of gabbros and the lack of metamorphosed sediments. Similar trends of subduction zone related basaltic rocks are found from the Bymarka gabbros (Slagstad, 2003). However, from this study there is one out of two samples of what is called a low-level gabbro (LLG, Fig. 7.1a and Fig. 7.2) that plots similar to the Ams. This gabbro shows a MORB-character but field relations and a light rare earth element (LREE) pattern suggest that it is part of an ophiolite, field relations that Ams does not show. Comparing the trace element composition of these dykes with the Ams does not show a good fit (Fig. 7.1a). However, in discrimination diagrams, these samples from dykes of the Seve and lower nappes show an overall more similar trend as the Ams, plotting mainly as MORB (Fig. 7.2).

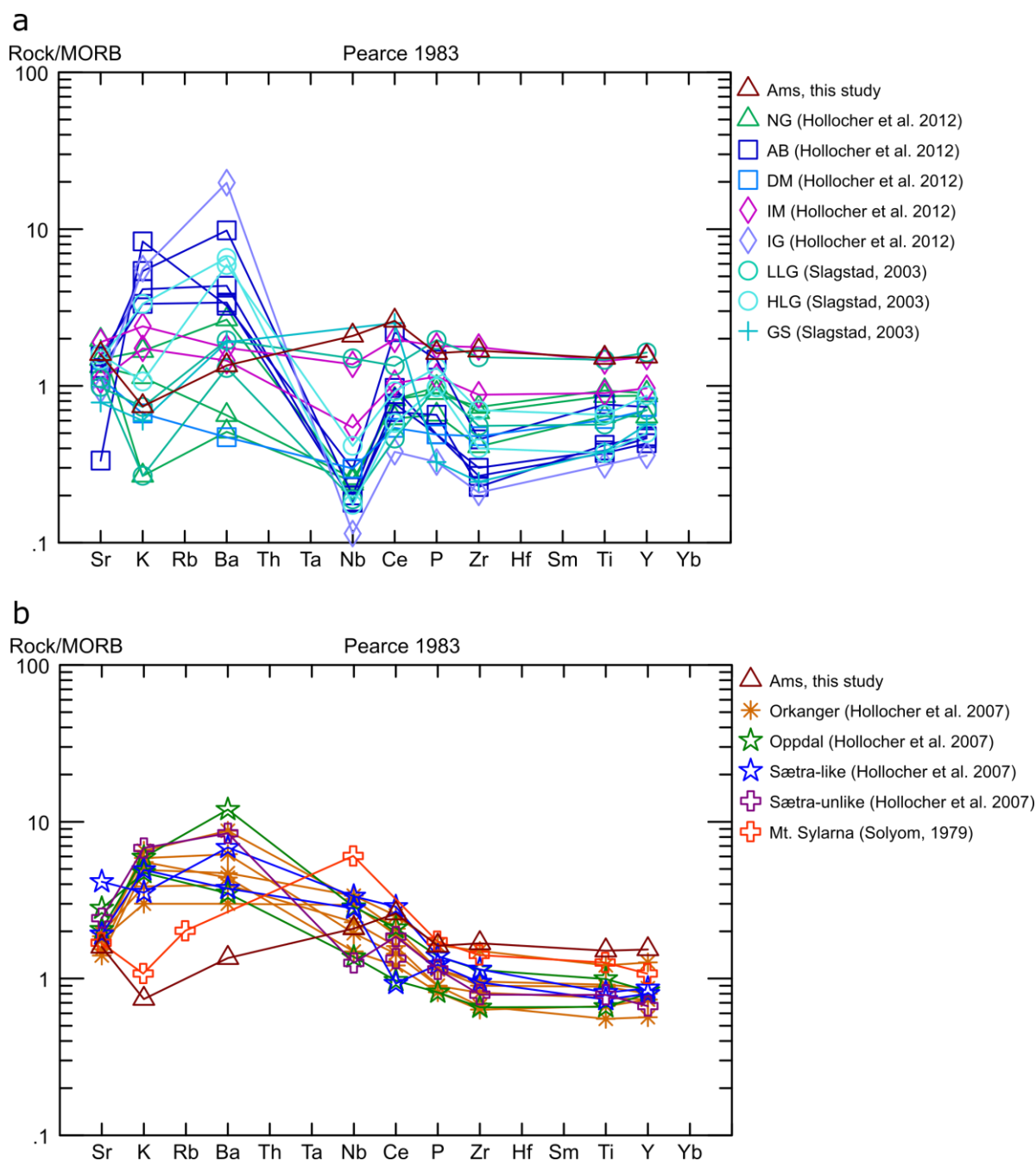


Figure 7.1: a) Spider diagram Rock/MORB normalized (Pearce, 1983) of trace elements from XRF from Ams and relevant samples from Hollocher *et al.* (2012) (Støren Nappe) and Slagstad (2003) (Støren Nappe). b) Spider diagram Rock/MORB normalized (Pearce, 1983) of trace elements from Ams and relevant samples from Hollocher *et al.* (2007) (Risberget Nappe) and Solyom *et al.* (1979) (Seve Nappe Complex). It should be noted that the samples from the literature is done with different methods (Hollocher *et al.* (2007) and Hollocher *et al.* (2012), LA-ICP-OES (inductively coupled plasma optical emission spectrometry) and LA-ICP-MS; Slagstad (2003), XRF and LA-ICP-MS; Solyom *et al.* (1979), mainly XRF) and only the same trace elements as obtained from the Ams were included in the Spider diagram, excluding the sample from Solyom *et al.* (1979), where also Rb is included. NG = non-cumulative gabbro; AB = arc basalt-like amphibolite; DM = depleted MORB-like amphibolite; IM = intermediate MORB-like amphibolite; IG = intermediate gabbro; LLG = low-level gabbro; HLG = high-level gabbro; GS = greenstone; MORB = mid-ocean ridge basalt; VAB = volcanic arc basalt; WPB = within-plate basalt.

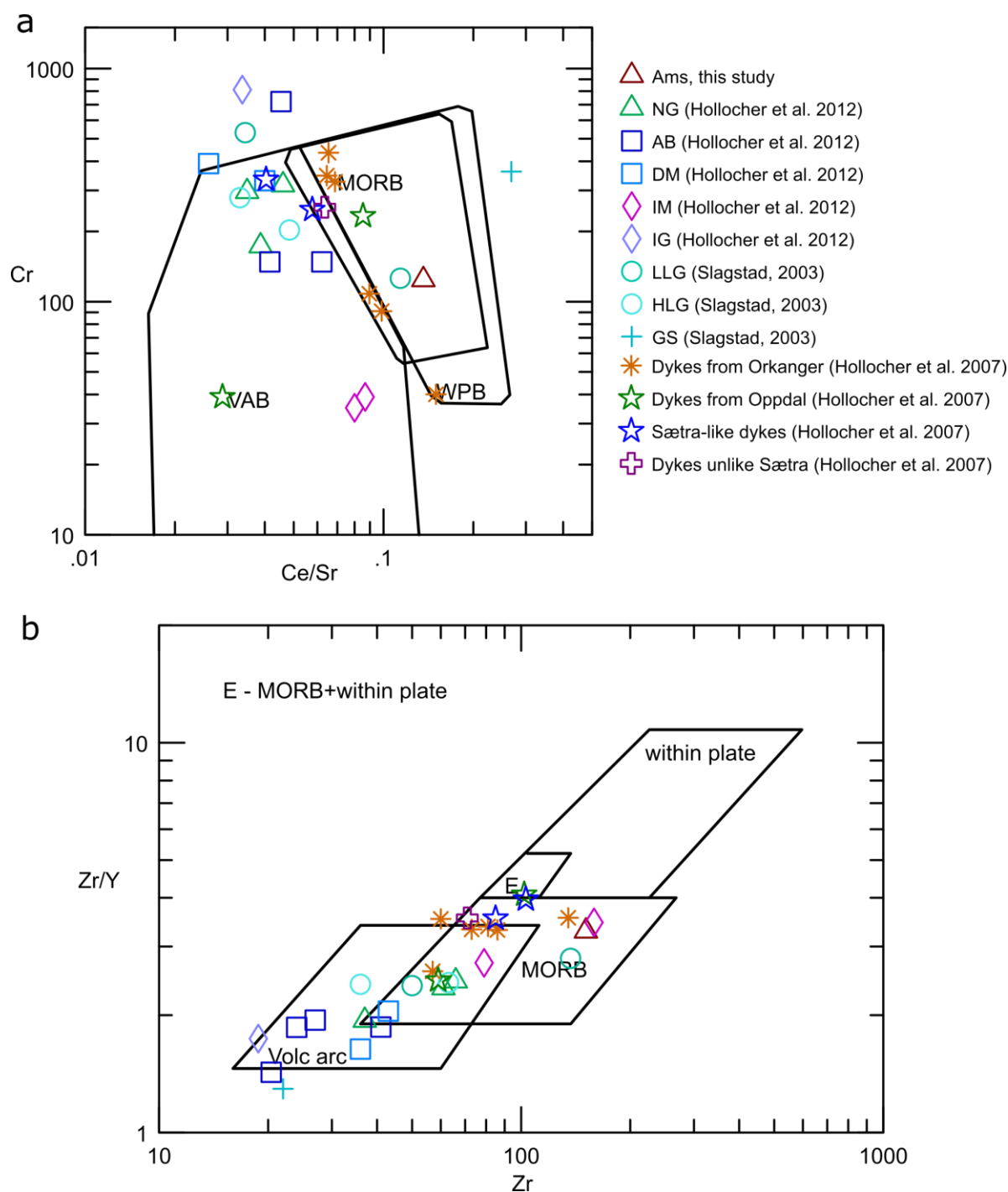


Figure 7.2: a) Discrimination diagram for basalts (Pearce, 1982). Ams plot as a MORB. b) Discrimination diagram for basalts (Pearce and Norry, 1979). AMS plot as a MORB. NG = non-cumulative gabbro; AB = arc basalt-like amphibolite; DM = depleted MORB-like amphibolite; IM = intermediate MORB-like amphibolite; IG = intermediate gabbro; LLG = low-level gabbro; HLG = high-level gabbro; GS = greenstone; MORB = mid-ocean ridge basalt; VAB = volcanic arc basalt; WPB = within-plate basalt.

A dyke swarm studied in the Risberget Nappe (Hollocher *et al.*, 2007) shows a different trend in spider diagram (Fig. 7.1a) and discriminations diagrams (Fig. 7.2b) than the Ams, and is also interpreted to be of another source. Solyom *et al.* (1979) analysed amphibolites interpreted to belong to the Seve Nappe Complex on Mt. Sylarna (Fig. 2.2) on the boundary

between Central Norway and Sweden. From this study just a mean value of the samples taken were presented and few trace elements were listed. Still, the trend in the spider diagram shows similar trends as the Ams (Fig. 7.1b) and it plots as MORB and ocean floor basalt. This sample from the Seve Nappe Complex is the closest correlation to the Ams, but still, one sample is not enough to make any strong conclusions. More sampling and geochemical analysis would be needed to make a more thorough investigation and a conclusion on the affinity of the Rørvika unit cannot be based solely on this sample.

Geochronological considerations

The U-Pb zircon dating of the Amis revealing an age of 435.4 ± 3.3 Ma gives a better clue of the affinity of these amphibolites. Similar ages have been documented from northern and Central Norway in granitic and mafic plutonic rocks (Kirkland *et al.*, 2005; Corfu *et al.*, 2006; Nilsen *et al.*, 2007; Corfu *et al.*, 2011) and in central Norway in calc-alkaline plutonic rocks (Tucker *et al.*, 2004), none, however, from lithologically similar rocks as the Amis. In contrast, Ladenberger *et al.* (2013) documented comparable ages in related lithologies, where zircons from garnet migmatites and leucogranites from the Åreskutan Nappe of the Seve Nappe Complex were dated with secondary ionization mass spectrometry. An age of 442 ± 4 Ma was given from the garnet migmatite, and felsic segregations, occasionally with garnets, within a migmatitic amphibolite yielded 436 ± 2 Ma, which is the rock that resembles the Amis in appearance. Related leucogranites revealed ages of 442 ± 3 and 441 ± 4 Ma. The age from the segregation in the amphibolite overlaps within error with the ages revealed from the garnet migmatite and was interpreted by the author to be of the same event. This minor difference in age might be due to different responses from different lithologies when exposed to metamorphism (Ladenberger *et al.*, 2013). Majka *et al.* (2012) found similar ages (439 Ma) in migmatitic paragneisses containing garnet and sillimanite in the Åreskutan area (Fig. 2.2) of Central Sweden.

Metamorphic considerations

The rocks described and dated by Ladenberger *et al.* (2013) are similar in appearance to the lithologies from this study area, though of a higher metamorphic grade (granulite facies) and consequently a somewhat different mineral assemblage reflecting this. It is interpreted that exhumation from eclogite facies metamorphism caused decompressional melting and migmatization in granulite facies, and dehydration melting of hornblende in the amphibolites. This was the same interpretation also given by Majka *et al.* (2012). From geothermobarometry

calculations and thermodynamic modelling (Klonowska *et al.*, 2014) it was found peak pressure conditions for the Åreskutan Nappe of 24-32 kbar at temperatures of 700-720°C. For similar lithologies in the Trondheim region it was found pressures up to 11-12 kbar and temperatures of 700-725°C (Hacker and Gans, 2005) and a more recent study yielded PT conditions of 600-700°C and pressures of 10-16 kbar (Weigand *et al.*, 2016). Hartel and Pattison (1996) documented that dehydration melting of amphiboles could take place at 9 kbar and 685-735°C, though experimental work showed that temperatures up to 850°C were needed. The reaction described was in need of plagioclase, hornblende and quartz to form a felsic melt, diopsid and garnets. The diopsid can later have been affected by retrograde metamorphism and the creation of chlorite. With this in mind it can be assumed that the Amis has been exposed to temperature and pressure high enough to form a dehydrate melt, and as a result forming intermediate layers within the amphibolite with restitic garnet from the partial melting. This reaction could have been brought about by the presence of metasediments and fluids released from them (Ladenberger *et al.*, 2013).

Both Majka *et al.* (2012) and Ladenberger *et al.* (2013) documented ages around 455 Ma, which is similar to a 459 Ma age found in this study (Fig. 6.20, analysis 20). Majka *et al.* (2012) interpreted this to be part of the prograde metamorphic phase.

The geochemistry of Ams in the Rørvika unit cannot directly be related to any analysis done in the Støren Nappe, and because of the lack of enough good data from similar basaltic rocks in the Seve Nappe Complex it cannot be decided from the geochemistry alone which nappe the Ams would fit. The U-Pb age of 435.4 ± 3.3 Ma in the Amis of the same unit strongly supports that the amphibolitic rocks of Rørvika unit belong to the Seve Nappe Complex together with the Trongen unit. This is further supported by lenses of Ghms found within the Ams and Amis of Rørvika unit (AAH_290 and AAH_231). As a conclusion based on the metamorphic grade, suggestions from geochemistry of the Ams and U-Pb zircon age, the Rørvika unit is thought to be part of the Seve Nappe Complex, and not the Støren Nappe as interpreted before. The basaltic amphibolites can have been formed as a result of mafic volcanism due to the opening of the Iapetus Ocean in the Neoproterozoic.

7.1.4 Varpneset unit

The Varpneset unit, comprising high grade metamorphic mica schist, shows similar composition as the Trongen unit to the west. The main difference between the mica schist of this unit and the Trongen unit is the high content of calcite and quartz, and the layering

throughout the unit showing coarse and prismatic amphiboles and larger garnet in the Varpneset unit.

The high content of quartz could indicate a continental derived source and the abundant calcite shows an original environment rich in carbonates. The strong layering often seen with variations on the grain size of garnet and amphibole can be a result of originally differently distributed elements/minerals which cause different nucleation behaviour of metamorphic minerals. Towards the Rørvika unit to the west there is an increasing content of amphibole present in the Hcqs, which could be interpreted as a higher influx of basaltic derived sediments or flows of basaltic material. The dyke with porphyritic texture indicates the latter.

Through petrographic studies garnets showing synkinematic deformation and two stages of growth are observed and amphiboles later being replaced by calcite and chlorite. This points towards a system being exposed to high grade metamorphism, upper amphibolite facies, which is later affected by retrograde metamorphism.

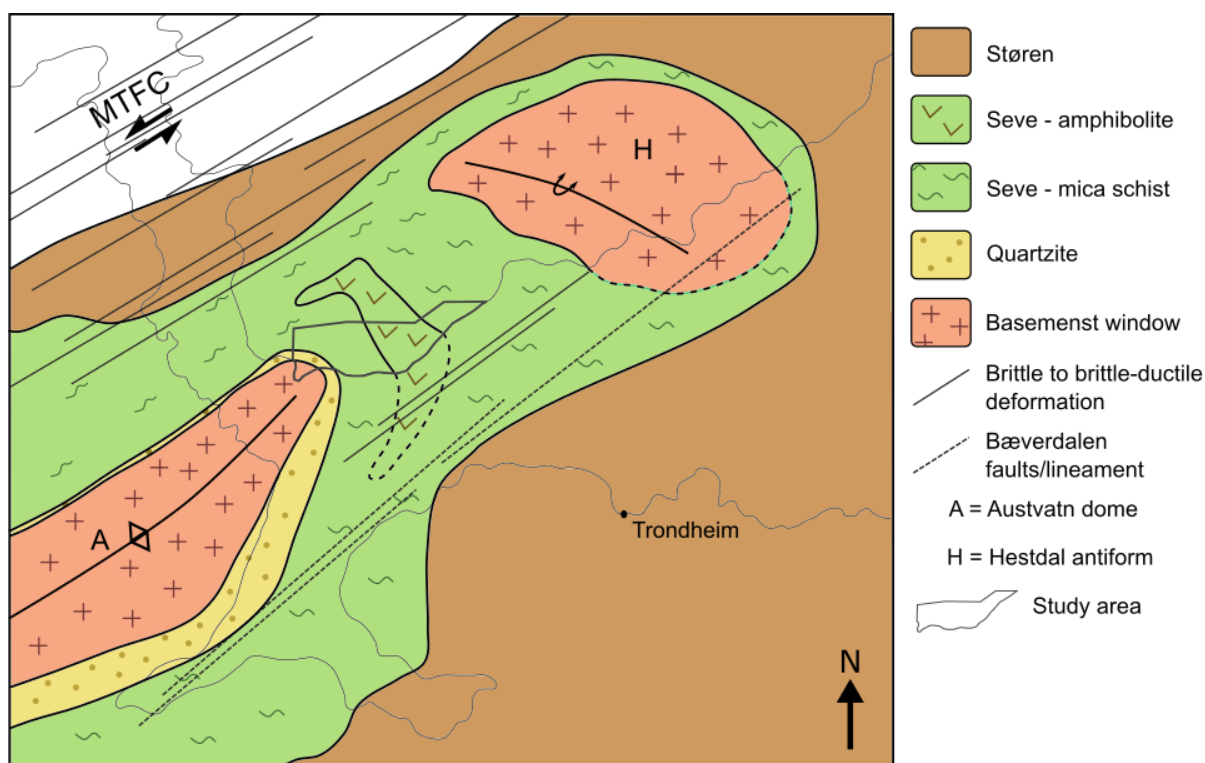


Figure 7.3: Interpreted map over the Trondheim area, including the study area. The study area is marked as part of the Seve Nappe Complex and Rødberget unit as part of a basement window.

Lithologies similar to the Varpneset unit have been described from the Trondheim region before (Peacey, 1963; Johnsen, 1979; Tucker, 1986; Hull and Adamy, 1989) as Vanvik Group and Gangåsvann Group, all being related to rocks similar to the mica schists of the Trongen unit. These units have later been correlated with the Seve Nappe Complex

(Tucker *et al.*, 2004). Johnsen (1979) concluded that the protolith for the mica schist containing calcite would have been a lime-bearing clay, and Kollung (1990) noted that the mica schist contained lenses of pure limestone. Of more recent descriptions, Ladenberger *et al.* (2013) described lithologies from the lower part of the Seve Nappe Complex from central Sweden as a calcareous metasedimentary rock in a succession with related amphibolites and mica schist.

Ambom (1980) described similar lithologies in the Lower Seve Nappe Complex in the Åreskutan area (Fig. 2.2) in Central Sweden. This lower nappe is affected by amphibolite facies, and the lithologies consist of, from bottom to the top, metapsammite and mica schist and some calcareous material, amphibolites and metadolerites, and on the top calc-silicates. Based on these lithological descriptions, it is most likely that the Varpneset unit, together with the Trongen and Rørvika units, is part of the Seve Nappe Complex (Fig. 7.3).

7.1.5 The significance of aplites

Aplitic dykes are found in abundance, mainly in the Trongen and Rørvika units (Appendix B), where they appeared as cm to metre thick dykes, deformed boudins and blobs, and larger bodies (Fams in Rørvika unit).

All the granitic aplites sampled and analysed show similar trends in the various plots (Fig. 6.18), the only variations seen it from the main element plot in Figure 6.17. It can be argued that these differences are a result of fractionation and that the aplites are most likely from the same source. From the AFM-diagram (Fig. 6.18c), they all plot as calc-alkaline rocks, and all being slightly peraluminous, on the boundary to metaluminous. From Barbarin (1999) and Winter (2010) rocks with these characteristics could be interpreted as either I-type or S-type volcanic related to a continental arc or a continental collision setting. From petrographic studies many of the analysed samples contain both muscovite and biotite, which can strengthen the theory of a S-type magmatic source (Winter, 2010). More data is however needed of preferentially trace elements, to investigate this further and to be able to compare it with relevant literature.

Geochemical considerations

There was not found any geochemical data from similar aplites in the Seve Nappe Complex in the literature. In the Gula Nappe (Dunning and Grenne, 2000) and the Støren Nappe (Slagstad, 2003) trondhjemites were documented fitting the description of the aplites in this study. Plotting these data together with the aplites analysed in this study in a spider diagram (Fig. 7.4a) normalized to chondrites (Thompson *et al.*, 1982), they show similar trends for the immobile

elements. The discrimination diagram plots the trondhjemites from the Gula and Støren nappes as quartz monzonite and granodiorite (Fig. 7.4b) and in the Shand's Index all the samples plot on the boundary between peraluminous and metaluminous as the samples in this study (Fig.7.4c).

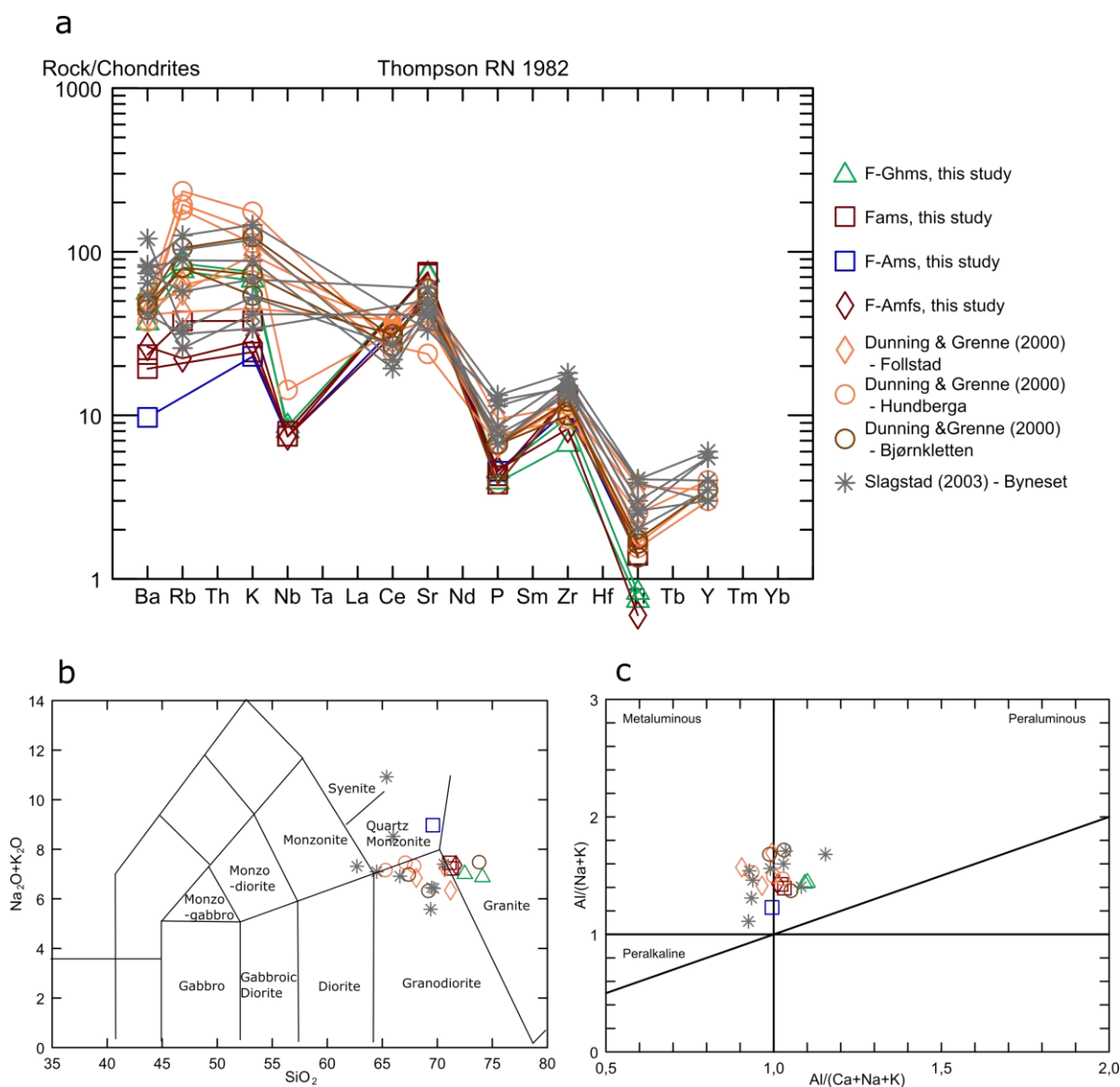


Figure 7.4: a) Spider diagram normalized to chondrites (Thompson *et al.*, 1982). The plot includes the aplites from the study area together with analysis done by Dunning and Grenne (2000) and Slagstad (2003) of trondhjemites. b) Discrimination diagram for granitoids (Middlemost, 1994) showing the same sample as in a). In general, the trondhjemites plot in a close range around a granitic to granodioritic to quartz monzonitic content. c) Shand's index (Maniar and Piccoli, 1989). Same samples as in a) where all plot close to the boundary between metaluminous and peraluminous trends.

Geochronological considerations

Even though the aplites from this study have no geochronological constraints, age data from similar dykes from various units in the region will be discussed.

Dunning and Grenne (2000) interpreted the trondhjemites from Central Norway to be a result of partial melting of crustal rocks at garnet-amphibolite facies metamorphism. U-Pb zircon age of this trondhjemite was set to 432 ± 3 Ma. The Byneset trondhjemite from Bymarka, Trondheim (Fig. 2.2), being similar in appearance as the aplites of this study, was interpreted to be a result of partial melting of a garnet-bearing mafic rock derived from an island arc or ocean floor stacked up on the continental margin at 468-467 Ma (Slagstad, 2003; Slagstad *et al.*, 2014).

Both Hull and Adamy (1989) and Kollung (1990) mentioned tonalitic to granitic trondhjemite dykes intruding similar mica schist and amphibolite sequences in Central Norway as the ones studied in this work, but they were not further described. Nordgulen *et al.* (2002) did geochronological analyses on a granitic dyke containing muscovite, biotite and garnet and a fine grained biotite tonalite intruding Skjøtingen (Seve) Nappe in the northern Central Norway. The zircons from the dykes gave Early Silurian U-Pb ages (430 ± 4 Ma and 436 ± 2 Ma). Similar ages were found by Tucker *et al.* (2004) (431 ± 2.9 Ma) and by Ladenberger *et al.* (2013) (430 ± 3 Ma and 428 ± 4 Ma) in the Seve Nappe Complex, where foliated pegmatites were interpreted to represent an event of metamorphism in the nappe complex and a minimum age for the commencement of the Caledonian thrusting.

The aplites from the study area are from this interpreted to correlate with pegmatites/trondhjemites of an age around 430 Ma with a source from partial melt of garnet-bearing mafic rocks in a setting where nappes were stacked up on a basement. This strengthens the theory of the units belonging to the Seve Nappe Complex, known for containing abundant of felsic dykes compared to the Støren Nappe where very few can be observed (NGU, unpublished mapping). It could be suggested that the trondhjemites from the Gula Nappe are from the same source as the tonalitic pegmatites/aplites from the Seve Nappe Complex, but this is not a discussion for this work.

7.2 Ductile structural evolution

In the following, the ductile evolution of the study area will be discussed. First, a few comments on the foliations, lineations and fold axes will be made. Then the proposed theory of the Rørvika unit in the centre of a synform is a starting point for the structural model of the

area, and taking into account new knowledge from the study area, this theory is discussed and the evolution of the area is put into a regional context.

7.2.1 Comments on foliation, lineation and fold axes

The main foliation: overprinting an older fabric?

The three larger units, Trongen, Rørvika and Varpneset, show a general trend in the foliation from west to east with a dip towards mainly east and southwest. Several lines of evidence indicate that the prevailing foliation seen today has overprinted an older foliation, and that there has earlier been at least one more important phase of deformation and folding. From petrographic studies all three units show garnets with sigmoidal inclusion trails with a different direction than the main foliation. Because of the shape of the inclusions it is clear that the garnets have formed synkinematically in a system under the influence of shear and high temperatures. Also biotite grains showing one early and a later preferred orientation in the Trongen unit is evidence of several phases of deformation. However, due to the high grade of deformation in the studied units, there were not found many evidences of this earlier deformation in the field and the discussion hereafter focuses on the main structural trends of the dominating, younger foliation.

Fold-axis parallel mineral lineations

The observation of the southeast trending mineral lineation within the area for this study was also done by Seranne (1992), then interpreted to be remaining, but deviant, structures from the Caledonian top-to-NE shearing. Robinson and Roberts (2008) later explained this observation with relations to a larger synformal structure in Surnadal (Fig. 2.2) where similar trends were related to a back-folding of a fold limb. These interpretations were not put in to a context with related structures for the study area and none of the interpretations mentioned is thought to be an explanation for the structural development.

The documented trend of mineral lineations parallel to the fold axes can be a clue to the overall development of the area. Generally, in a compressive or extensional simple shear regime with moderate displacement one would expect to see mineral lineations perpendicular to the fold axis. In the study area on the other hand, the mineral and elongation lineations show a more or less consistent trend parallel to the fold axes in the Trongen, Rørvika and Varpneset units (Table 5.1). Similar relationships were observed in the Caledonides further south (Robinson, 1995; Krabbendam and Dewey, 1998). According to Grujic and Mancktelow (1995), this is a characteristic that can be observed in many orogenic belts and where the degree

of strain has been high. The Rødberget unit is excluded from this discussion due to the deviant mineral lineation and the fact that there is no fold axis observed to compare the event of stretching with.

Cobbold and Quinquis (1980) and Skjernaa (1980) suggested that the fold axis and the mineral/elongation lineation might be parallel to sub parallel because of a passive rotation of the fold axis during continued shear. This would require high strain and a homogeneous deformation of passive folds, and a development of sheath folds would be normal, which is not observed in the study area. Grujic and Mancktelow (1995) did experimental studies showing that the fold axis and the lineation could actually form parallel to each other. This was shown to be possible in a system where there was a high effective viscosity contrast between folded layers, a non-plane strain condition, and a constrictional factor with a component of extension parallel to the fold axis. Their study showed that if these conditions occurred, parallel lineations and fold axes could form during deformation and the proposed model is illustrated in Figure 7.5. Relating this to the study area, several of the factors needed are present. The incompetent mica schist compared to the stronger rocks, such as amphibolite layers, aplite dykes and quartz veins gives the viscosity contrast mentioned above. The constrictional factor is given through the more massive and competent basement windows to the northeast and southwest of the area (Fig. 7.3). Because of the complicated ductile development of the Caledonides, it is not reasonable to suggest a plane strain regime.

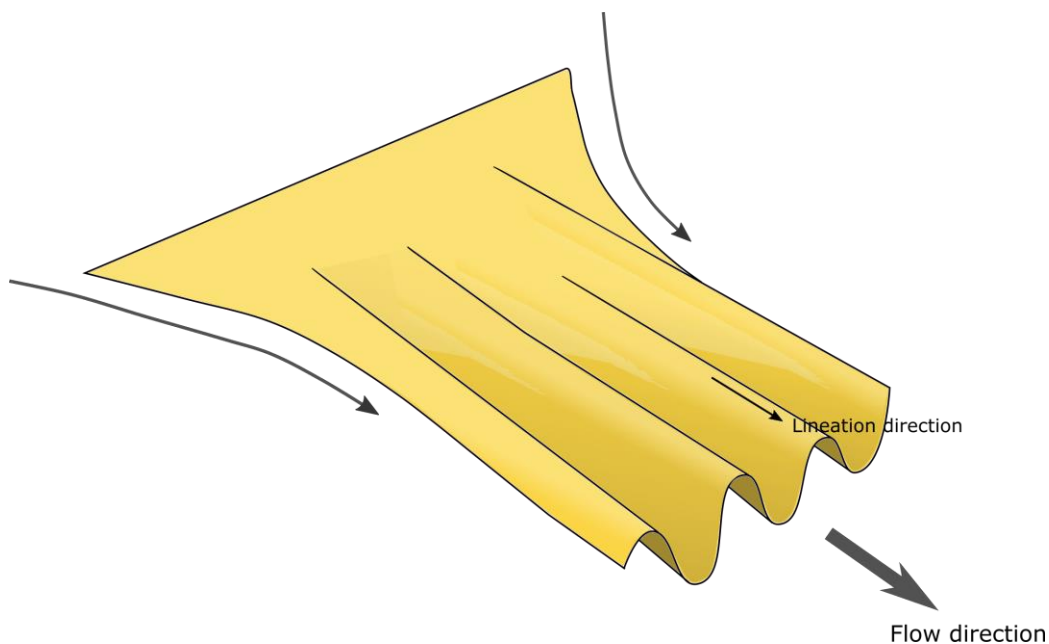


Figure 7.5: Schematic sketch of a possible model that could form mineral/elongation lineations parallel to fold axes.

Variances in mineral lineation orientation: due to later folding?

In Oksvika, a SW-vergent fold with amphibole mineral lineation bent around with an oblique angle to the fold axis was observed (Fig. 4.24), indicating at least locally that the event of folding is younger than the formation of the regional mineral/elongation lineation trend. Mineral lineation deviant from the main lineation could consequently be due to the folding of lineations around the fold axis. Similar observations have been made by Krabbendam and Dewey (1998) where an amphibolite facies lineation was folded around east-west trending folds giving an overall north-south shortening of an area related to a sedimentary basin in Western Norway. This shortening has also affected the overlying Devonian basin and was interpreted as synchronous with vertical thinning and east-west extension in a late period of the orogenic evolution.

With this as the basis, mineral and elongation lineations in the Trongen and Varpneset unit showing an offset from the main lineation were rotated around an axis of rotation (Fig. 7.6). This interpretation includes an azimuth of rotation axis, plunge of rotation axis and the magnitude of rotation. For the Trongen unit the azimuth of rotation axis and the plunge of the rotation axis were found through a mean value of SW-vergent fold axes from the unit, consequently giving the values of 140° and 25° . The magnitude of rotation was set to 90° as a result of an approximation of the angle between main foliation and foliations deviant from this. The rotation (Fig. 7.6a) shows that all lineations in the unit may in fact be part of the same system with a low to moderate plunge towards the southeast.

The same procedure was done for the Varpneset unit, with the azimuth of rotation and the plunge of the rotation axis found to be 180° and 30° as a mean of the fold axes from the unit. The magnitude of rotation was set to 150° , found from an approximation of the differences in foliation close to where the mineral lineations were measured. The resulting main lineation for the Varpneset unit after the rotation (Fig. 7.6b) is shown to be towards the southeast with a low to moderate plunge.

Doing this rotation, it is assumed that the event of folding postdates the formation of the mineral lineation. Most of the measured mineral/elongation lineations that are deviant from the main lineation trend were found in outcrops where no folds were observed, but the foliation of the outcrop shows smaller or larger offsets from the main foliation trend. East in the Rørvika and in the Varpneset units, the main foliation pattern shows a trend in strike that could resemble larger plunging folds (Fig. 4.19 and 4.21) with a fold axis parallel to the axis of the smaller fold

systems, as also indicated from Oksvika in the Trongen unit (Fig. 4.33). The deviant foliations in the Trongen, Rørvika and Varpneset units could therefore be interpreted as larger open-to-close folding formed under the same event as the smaller scale folds observed throughout the study area.

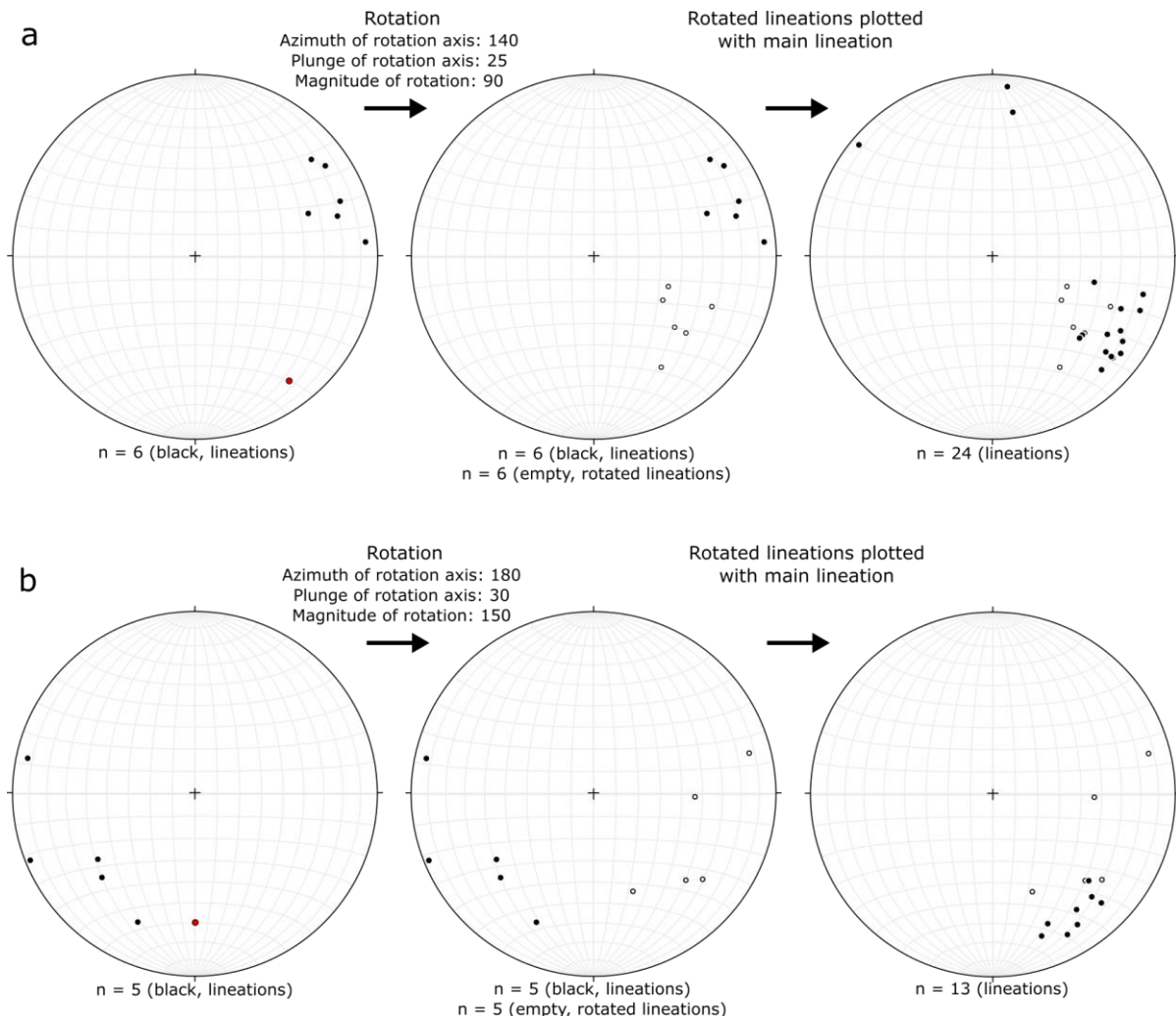


Figure 7.6: a) Rotation of lineations measured in Trongen unit. The first stereoplot shows the deviant lineations that will be rotated, and the red dot indicating the rotation axis. The second stereoplot shows these together with the rotated lineations based on the azimuth of rotation axis at 140° , plunge of rotation axis of 25° and magnitude of rotation at 90° . The final stereoplot shows the rotated lineations together with the main trending group from Trongen unit. b) The stereoplots show the same procedure as in a) for lineations in Varpneset unit. The azimuth of rotation axis used was 180° , the plunge of the rotation axis was 30° , and the magnitude of rotation was set to 150° . The red dot in the first stereoplot indicate the rotation axis.

Nevertheless, from Figure 4.24a a fold with pre-existing amphibole mineral lineation can be observed. This observation, together with the rotation of the lineation outliers above, indicates that locally the folding occurred after the event of stretching, at least for the Trongen unit. Since the trend of lineation for Trongen, Rørvika and Varpneset are the same; it could be assumed that this predating lineation is the case for all three units. Donath and Parker (1964)

showed that if the fold axis was parallel to the pre-existing lineation, the lineation would also be parallel after the folding, which is the case for the measurements of lineation and fold axis in this study. However, the relative age of the stretching event and the folding event can be discussed, and they might very well be part of the same regional event.

7.2.2 Large-scale structural models

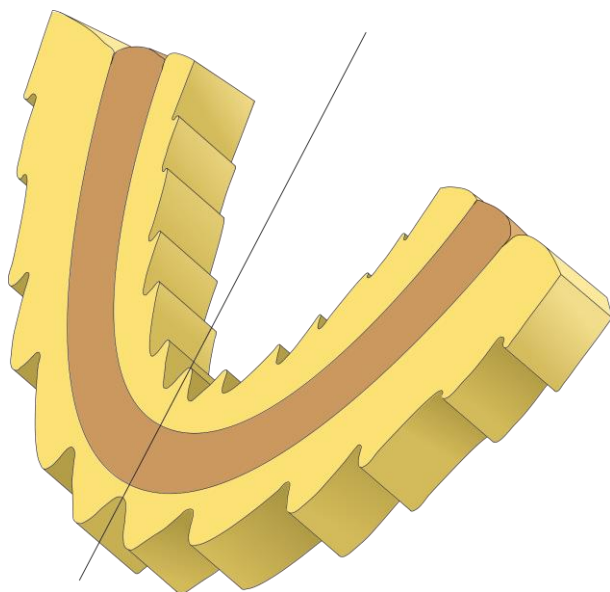
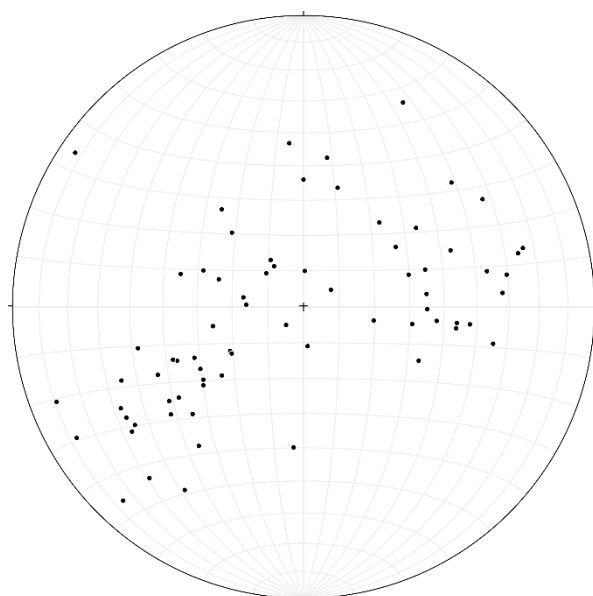


Figure 7.7: Schematic sketch of a synformal fold with related parasitic folds. Note the shallow dip of the main folded layer in the center of the synform compared to the flanks of the synform.



n = 74 (poles, axial planes)

Figure 7.8: Overview plot of all the axial planes measured in Trongen, Rørvika and Varpneset unit.

The Austvatn basement antiform

The Rødberget unit in the west shows a foliation and mineral lineation deviant from the other units from the study area (Table 5.1). The foliation with a low dip towards the northeast and the mineral lineation with a very low plunge also to the northeast, indicate that this unit is influenced by other processes than the other mapped units or show a different response to the same processes. The homogeneous and massive appearance of the granitic gneiss could easily be understood as a reason to this, compared to the more incompetent mica schist and amphibolites. Seranne (1992) and Tucker (1986) described upright northeast-southwest striking folding of the basement, creating regional-scale antiforms including the Austvatn dome that Rødberget unit is interpreted to be a part of (Fig. 7.3). The Austvatn dome is thought to be a non-cylindrical upright fold that narrows out towards the northeast. The Rødberget unit represents then the northern tip of this large-scale antiform and the measurements

taken could be from the hinge zone of this structure. The expected foliations and lineations would then coincide with the measured structures from this study, a foliation with dip towards the northeast and a lineation trending in the same direction.

The Rørvika amphibolites: in the hinge of a large-scale synform?

Earlier work indicates that the Rørvika amphibolites lie within the hinge of a larger synform (Fig. 1.1 and Fig. 1.3) (Wolff, 1976; Wolff, 1978), a theory that is at first sight supported by the observations from foliations measured during this study to the east and west of Rørvika unit dipping towards these central amphibolites. However, in the Rørvika unit the dip of the foliation increases, showing a wedge shape (Fig. 5.1 and Appendix F), while in a synform it is expected that the dip would decrease towards the centre (Fig. 7.7). This observation makes it difficult to interpret the Rørvika unit as lying within a synform. In addition, the small scale folds observed throughout the study area point against a model of a Rørvika synform. Together with a synform, smaller parasitic folds should appear (Fig. 7.7) with fold axes and axial planes parallel to the fold axis and axial plane of the main fold. The axial planes in the study area show large variations in dip (Fig. 7.8) from mainly southwest to northeast, and together with the increasing dip of the foliation towards the centre of the Rørvika unit, the theory of the area as a synform has to be discarded.

Alternative model: the Rørvika amphibolites at the core of an extruding wedge?

Rather than the area being part of a synform, the foliations and the vergence and axial planes of the folds strongly suggest that the study area has an overall wedge shape (Fig. 7.9). In a forming wedge it would be natural for the steepest dipping foliations and axial planes to occur in the centre, with a progressive decrease both ways from the centre. The axial planes measured (Fig. 7.8) show a wide spread of dip from low to high supporting this theory. The parallel lineations and fold axes further indicate that this wedge system has experienced a deformation with a large compressive component in northeast-southwest direction and a less compressive to extensive component in the northwest-southeast direction. The folds could be formed as a result of the formation of the wedge itself, or in combination with the model proposed in Figure 7.5, where a flow of the rock masses perpendicular to a compressive regime would enhance the formation of flow-parallel folds. The vergence of the observed folds is then thought to be an evidence of the movement of the rock masses in the wedge, in the southwestern part of the area verging mainly southwest and in the northeastern part of the area northeast to the east.

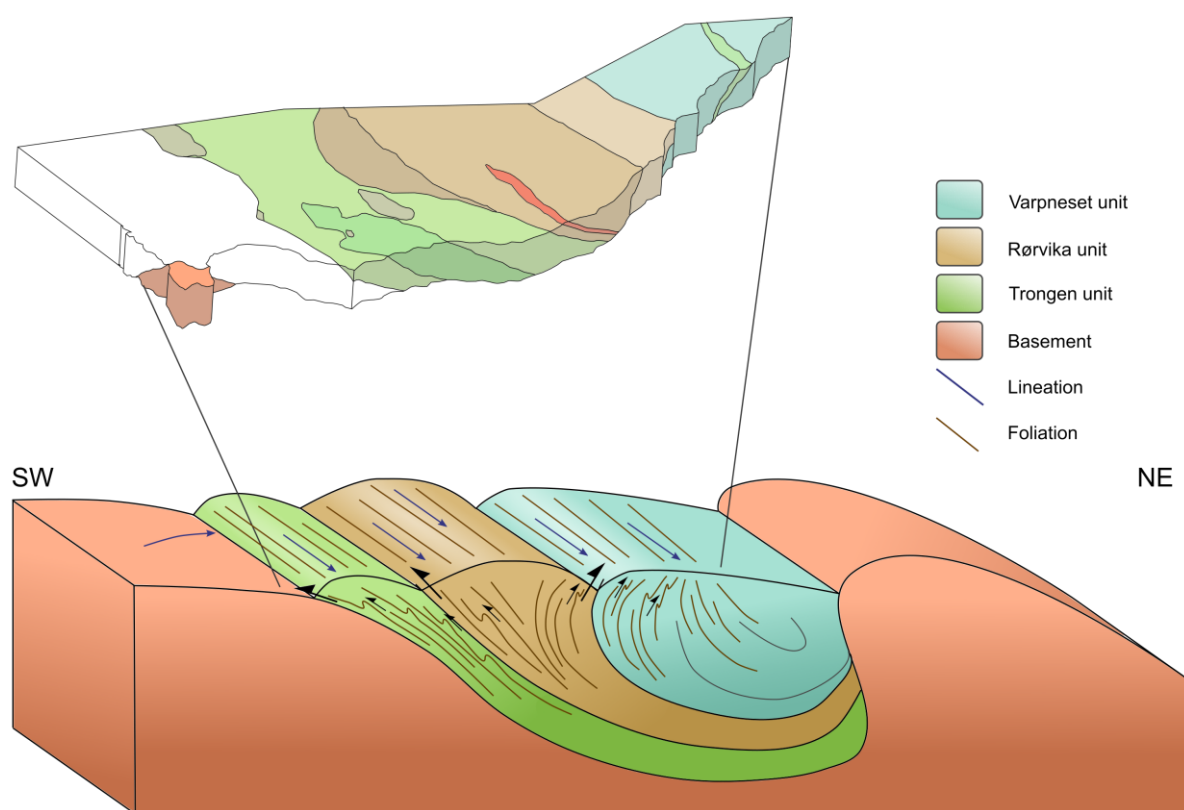


Figure 7.9: Schematic sketch of the interpretation of the present structural situation of the study area. The lithologies are part of a larger wedge situated between the two basement windows of Austvatn dome and Hestdal antiform.

Formation of the wedge in a regional context: buckling versus rotation model

In order to explain the formation of such a wedge and its surroundings two possible models are proposed: (1) an obstacle and buckling model and (2) a rotation model. For a better understanding of these models, the tectonic basement windows in the area need a closer look.

As mentioned above the Rødberget unit is part of a basement antiform called Austvatn dome (Fig. 7.3, Fig. 7.10; Tucker, 1986). Several similar basement antiforms are exposed in central Norway, with related synforms and with a fold axis trending northeast-southwest. It is thought that these antiforms formed during a late stage of the Caledonian orogeny with upright folding. Seranne (1992) showed that this folding was contemporaneous with the sinistral movement along the MTFC. However, the basement window northeast of the study area has a different orientation (Fig. 7.3). Hull and Adamy (1989) and Heim (1993) described this basement window and called it Kjerringklumpvinduet (Heim, 1993) or Hestdal antiform (Hull and Adamy, 1989), consisting of metagranitoids, migmatitic gneisses and porphyritic granite gneiss similar to the Ingdal granite gneiss. Structurally the Hestdal antiform is interpreted as an

overturned antiform with the fold axis trending mainly northwest-southeast, perpendicular to the fold axis trend in the Austvatn dome (Fig. 7.3, Fig. 7.10; Hull and Adamy, 1989). With these perpendicular basement dome orientations in mind, the two models for development are proposed.

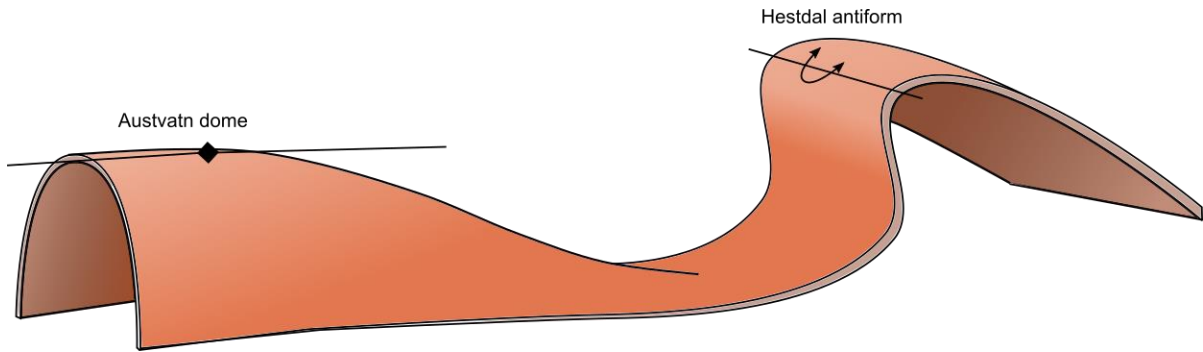


Figure 7.10: Schematic illustration of the relationship between the two basement windows of Austvatn in the southwest and Hestdal in the northeast.

The first model, “Obstacle and buckling model” (Fig. 7.11), shows a starting point at just after 400 Ma when the MTFC was in its early stages (Osmundsen *et al.*, 2006). The two basement windows of Hestdal antiform and Austvatn dome formed contemporaneously as a result of a northeast-southwest stretching and a top-to-SW ductile shearing along the MTFC to the west of the area (Osmundsen *et al.*, 2006). For some reason, possibly pre-existing heterogeneities in the basement, the Hestdal window formed with a perpendicular fold axis orientation and acted as an obstacle for further deformation of the lithologies between the two domes. During continuous movement along the MTFC and the simultaneous exhumation of the domes, the nappes in between the two basement windows were lifted and compressed, creating a wedge between them. In the early stages of the development, the wedge and the related structures started forming with a northwest-southeast striking orientation, and it was first in the very late stages of the evolution that it got affected by rotation in the northwesternmost part. The Hestdal antiform would in the late stages have undergone high amounts of shear and the antiform got overtilted (Hull and Adamy, 1989).

The second model, “Rotation model” (Fig. 7.12), shows a starting point at about 430-400 Ma, in the latest stages of the emplacement of the Caledonian Nappes (Roberts, 2003). In this model, the basement windows were exhumed during the Scandian compression with fold axes parallel to mineral/elongation lineations, due to orogen-parallel flow in the hinterland of the Scandian collision. At the onset of the MTFC a rotation of the Hestdal antiform and the Nappes north of the antiform started due to the sinistral movement along the larger fault complex to the west. As this rotation continued, the Seve Nappe Complex situated in between

the Hestdal antiform and the Austvatn dome was slowly compressed and rotated together with the basement antiform. In the later stage of the sinistral shear along the MTFC, the Hestdal antiform started to get overtilted, further increasing the compression on the Seve Nappe Complex in between the two basement windows.

From both models it is interpreted that the Hestdal antiform functioned as a “protection” for the forming wedge in between the two basement windows, preventing the study area to become even more deformed into structures parallel to the MTFC.

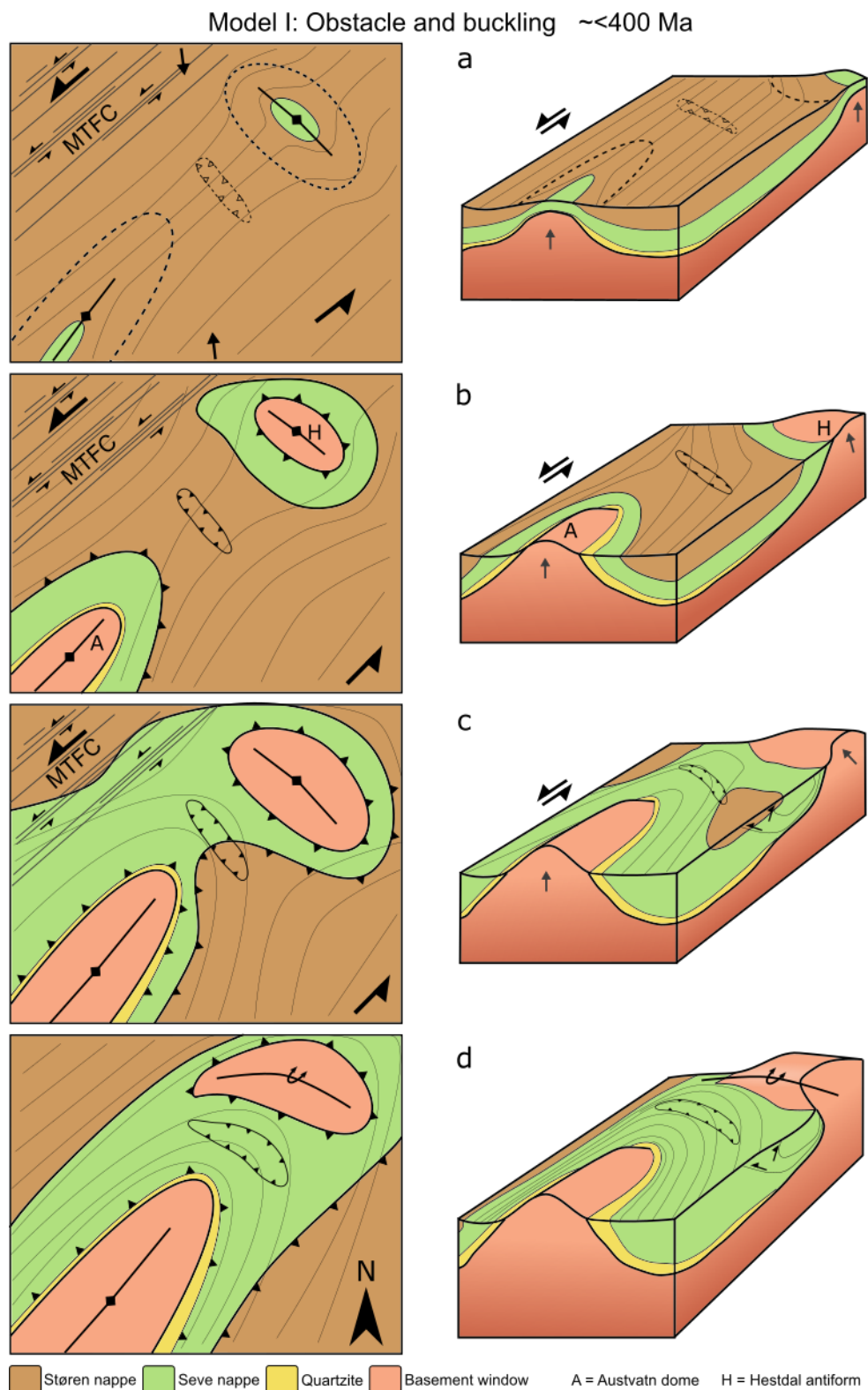


Figure 7.11: Sketch of a possible model for the development of the study area and the region around. The model is called the “obstacle and buckling”-model and is based on a starting point at 400 Ma or younger where the two basement windows got exhumed related to the activity along the MTFC with perpendicular fold axis. As the exhumation, and also the sinistral strike-slip deformation along the fault complex progressed, the Seve Nappe Complex between the two basement windows experienced a northeast-southwest compression forming a pop-up wedge. The high amounts of shear resulted in a overtilting of the Hestdal antiform northeast of the study area.

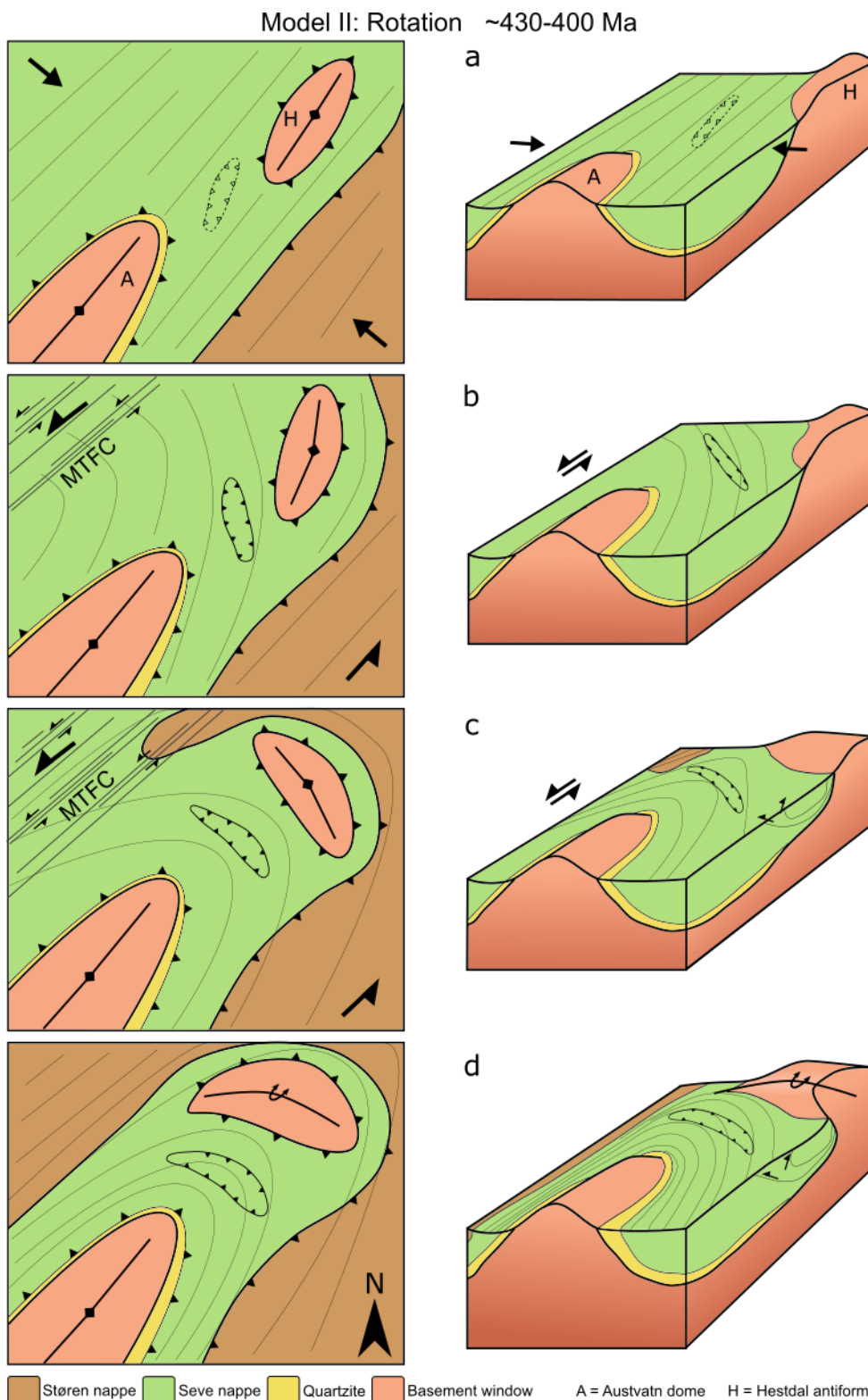


Figure 7.12: Sketch of the second proposed model for the development of the area. After the northwest-southeast compression of the Caledonian orogeny, the two basement windows of Austvatn and Hestdal were situated as two parallel antiforms in the terrain. With the onset of the deformation along the MTFC, a progressive rotation of the Hestdal antiform and the study area took place. With related compression and overtilting of the Hestdal window, a wedge was formed between the two basement antiforms.

7.3 Brittle structural evolution

This part of the discussion focus on the observations and development of the brittle structures observed in the study area.

Stress inversion indicating dominant NW-SE extension

The brittle structures of the study area show an overall extensional character with faults trending mainly northeast to southwest, even though some measurements deviate from this showing a northwest-southeast to a north-south striking trend (Fig. 4.38). From the quarry in the Rørvika unit, stress inversion was done in the program Win Tensor (Fig. 7.13a), and it shows that the overall stress field for all measured faults in the quarry has been exposed to more or less horizontal extension with the largest axes of stress, σ_1 , being vertical and the smallest axes of stress, σ_3 , being horizontal trending from northwest to southeast (Fig. 7.13a). The same is shown dividing the measurements into the different groups based on the mineralization introduced in chapter 4.3.4.3, respectively mineralizations of 1) epidote (Fig. 7.13b), 2) epidote and chlorite (Fig. 7.13c), 3) epidote and quartz (Fig. 7.13d) and 4) calcite. For the group containing calcite it was obtained too few measurements in the quarry to do a stress inversion for the group alone.

It should be noted from this stress inversion that a few measurements had to be left out to obtain a misfit angle of less than 30°. Ranalli (2000) documented that the highest angle of reactivation on a pre-existing surfaces of weakness is 30° compared to the ideal orientation of the surfaces, and 30° degrees is therefore put as a threshold value for possible fracture sets acting together doing the stress analysis.

Extensional brittle tectonics from Central Norway has earlier been documented by many authors (Seranne, 1992; Braathen *et al.*, 2002; Osmundsen *et al.*, 2006). The major brittle structure in the area, the MTFC is dominated by sinistral strike-slip movement, accompanied by northeast-southwest extension along the Høybakken detachment. Grønlie *et al.* (1991) and Redfield *et al.* (2005a) documented later reactivation and normal extensional dip-slip along the MTFC in Late Mesozoic to Early Cenozoic and consequently a northwest-southeast extension.

Northwest-southeast brittle extensional deformation has earlier been documented by Bunkholt (2006) and Bekkedal (2015) elsewhere in Central Norway. It was suggested that this northwest-southeast extension deviating from the main northeast-southwest extension studied above the Høybakken detachment in central Norway by Bunkholt (2006) can be a result of the

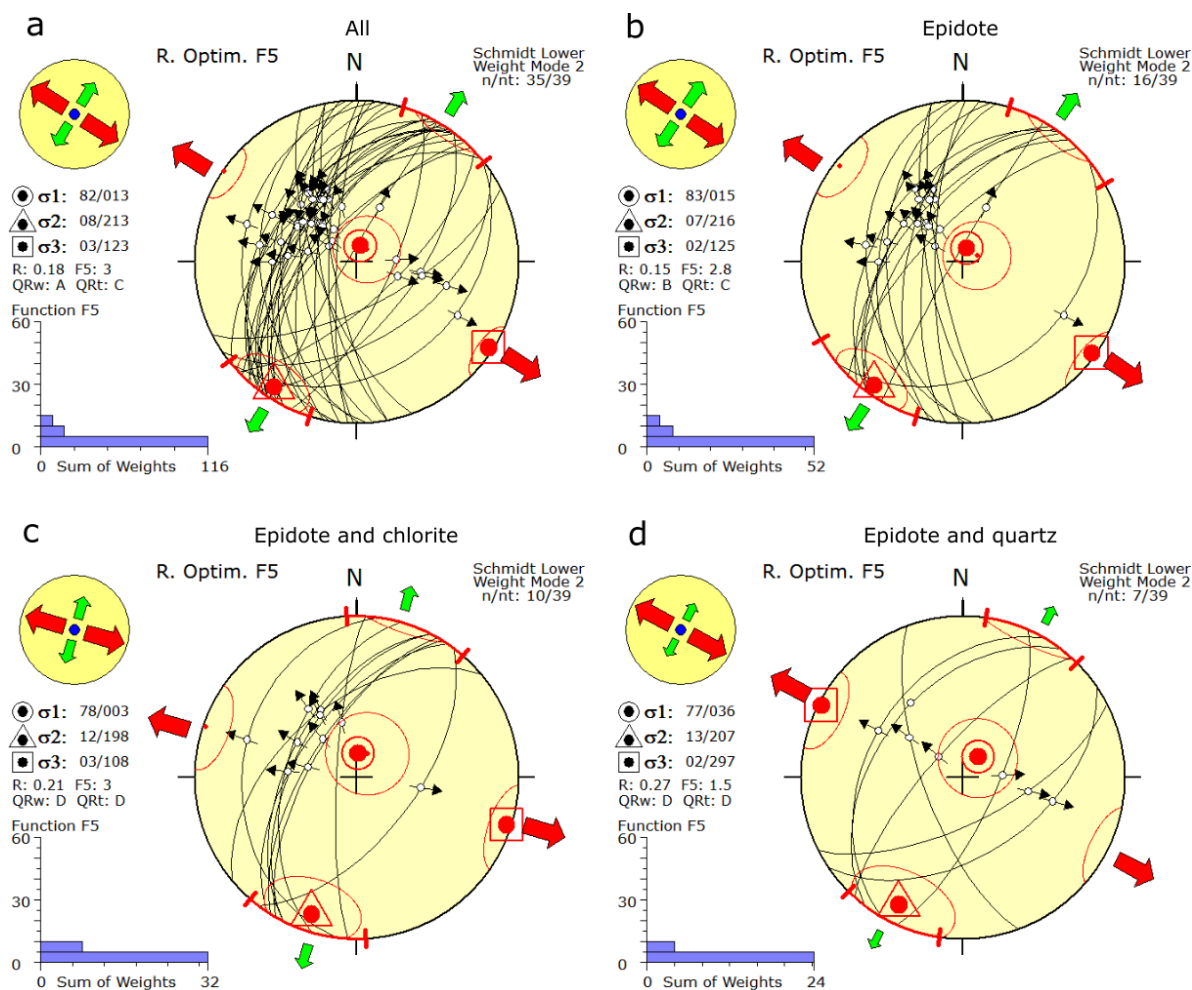


Figure 7.13: a) Stress inversion of all the measured fault planes with related slickenside lineations and sense of shear from the quarry in Rørvika unit. The inversion resulted in a northwest-southeast extension. b) Stress inversion for the fault planes with just mineralization of epidote revealing the same northwest-southeast extension. c) Fault planes with epidote and chlorite mineralizations indicating the same extension. c) Fault planes with epidote and quartz.

σ_1 not being completely vertical inducing an oblique component to the dip-slip system. This discrepancy of σ_1 from vertical was suggested to be a result of block rotation of the rock post-dating the faulting. However, it is not believed that this is the main reason to the extensional orientation observed in the area considering the distance to the Høybakken detachment and that the observations for the original theory by Bunkholt (2006) only were done above the detachment. Also Hull and Adamy (1989) documented normal faults with a dip towards the southeast in the same area as this study. The reasoning given for the direction of these normal faults was as part of an antithetic system to the overall foreland directed thrusting of the Nappes. This theory does not take into account the later extensional structures of the Caledonian orogeny and is not believed to be a valid explanation for the extensional faults in this study.

Fault plane mineralizations: a clue for deciphering relative timing of faulting?

There are several different mineralizations observed on the fault planes implying the presence of circulation of fluids. A variety of epidote, chlorite, quartz and calcite is found, with epidote and chlorite being the most abundant ones. On surfaces where epidote and chlorite was present, the chlorite seemed to be younger than the epidote. This is also supported from the microscopic study of the fault rock from the Rørvika unit, where it seems like the epidote is older, affecting the matrix of the host rock to a further extent than the chlorite, which was only present in the thin core of the fault zone (Fig. 6.13). Bekkedal (2015) observed the same main mineral coating of epidote and chlorite on fault surfaces of the northwest-southeast extensional system. From the literature it is interpreted that quartz and epidote veins predate the quartz, chlorite, and calcite veins and were activated at a time when the rock had denudated into the brittle regime in Late Devonian to Early Carboniferous (Osmundsen *et al.*, 2006; Olsen *et al.*, 2007). The chlorite coating can be a result of later reactivation of the faults under conditions closer to the surface.

The observed faults in the Rødberget unit contain quartz and calcite mineral coating on the fault zone, indicating a younger age than the epidote and quartz mineralized fault planes from the Rørvika unit (Olsen *et al.*, 2007), still showing the same northeast-southwest direction. From microscopic studies of the fault zone of the Rødberget unit, where mineralizations of both quartz and calcite were present, it could seem like the quartz crystallized at a later stage. The calcite had grown in to large crystals, whereas the quartz was only present as a very fine grained matrix. Where voids were present, the quartz had the possibility to grow larger crystals into the empty space. How much of the quartz that is crushed host rock and how much is a secondary crystallized mineral can be discussed.

It is possible that the extensional structures observed in the area are part of a larger system striking sub-parallel to Trondheimsfjorden, which is striking in a northeast-southwest direction (Fig. 2.2). This is supported by the fact that the tectonic units on the northwestern and the southeastern side of the fjord are hard to correlate. Due to the lower metamorphic grade in the Støren Nappes on the south side of the fjord and a higher tectonostratigraphic level compared to the north side of the fjord, including the study area, it is likely to think that a normal down-to-SE dip slip movement has occurred. Several places along the coastline there are observed normal faults with down to northwest and down to southeast (Fig. 4.40 and 4.43), which could be interpreted as antithetic and synthetic faults of this larger normal fault below Trondheimsfjorden. Roberts and Myrvang (2004) and Redfield *et al.* (2004) identified a

Bæverdalen fault/lineament striking northeast-southwest, parallel to Trondheimsfjorden. This regional fault was interpreted to be tectonically active during Cretaceous and Tertiary (Fig. 7.3).

From this it can be deduced that the brittle faults in the study area are the result of the denudation of the rocks into a brittle to brittle-ductile regime most likely related to a Permian or Jurassic-Early Cretaceous extension, or even as late as Cretaceous to Tertiary time (Redfield *et al.*, 2004; Redfield *et al.*, 2005a; Redfield *et al.*, 2005b). There is not found any evidences of the earlier regional sinistral strike-slip movement from the MTFC in the study area. It is very possible that brittle structures from this event could have had a direct impact on the area but later reactivation can have overprinted this information.

Conclusion

The tectonostratigraphic study of the Rødberget-Rørvika-Varpneset transect resulted in a division into four units; Rødberget, Trongen, Rørvika and Varpneset. The Rødberget unit consists of Precambrian basement gneiss called Ingdal granitic gneiss, dated to 1652.9 ± 1.8 Ma (Tucker, 1986) and later intruded by mafic dykes. The mica schists and amphibolites of the Trongen, Rørvika and Varpneset units are correlated with rocks of the Seve Nappe Complex due to the following reasons: 1) the similarity to lithologies in the same nappe in Central Norway and Sweden, 2) metamorphic grade and character, 3) U-Pb zircon age of 435.4 ± 3.3 Ma related to decompressional melting, and 4) geochemistry of aplites and amphibolites comparable with rocks from the Seve Nappe Complex. The metasedimentary rocks preserved in the Seve Nappe Complex are generally interpreted to represent Neoproterozoic rocks deposited on the outer Baltoscandian margin with zircon provenance ages from Late Archean to Late Mesoproterozoic and Early Neoproterozoic (Bingen and Solli, 2009; Ladenberger *et al.*, 2013). The rocks were later intruded by a mafic dyke swarm at about 608 Ma (Svenningsen, 2001) as a source for the amphibolites during the break-up of the Iapetus Ocean (Hollocher *et al.*, 2007). Later, the closing of the Iapetus Ocean and a collision-related event caused subduction of the sedimentary and amphibolitic sequences of the Seve Nappe Complex, up to UHP conditions in Sweden and up to 600-700 °C and 10-16 kbar in the study area (Weigand *et al.*, 2016). Partial melting of amphibolites during exhumation and decompression in high amphibolite facies occurred at ca 435.4 ± 3.3 Ma. When the Seve Nappe Complex was thrust on top of the Baltican margin, this resulted in partial melting and the intrusion of granitic dykes around 430 Ma (Tucker *et al.*, 2004). Two models are proposed for the later structural development of the area; 1) the “obstacle and buckling”-model where MTFC caused an exhumation of basement antiforms, or 2) the “rotation”-model, where the MTFC caused the rotation of an already existing basement window and surrounding rocks. Both models result in a compression of the study area and the formation of a pop-up wedge shape symmetry with

Conclusion

local shear folds and thus the vergence reflects the deformation of the Seve Nappe Complex lithologies. Exhumation of the rocks continued and a northwest-southeast extensional regime in Late Paleozoic to Late Mesozoic or Early Cenozoic caused the formation of normal dip slip brittle fault structures.

References

- ARNBOM, J. O. 1980. Metamorphism of the Seve Nappes at Åreskutan, Swedish Caledonides. *Geologiska Föreningens i Stockholm Förhandlingar*, 102, 359-371.
- BARBARIN, B. 1999. A review of the relationships between granitoid types, their origins and their geodynamic environment. *Lithos*, 46, 605-626.
- BEKKEDAL, E. M. 2015. *High-resolution Meso- and Microstructural Study of polyphase Deformation in the Orkanger Region, Sør-Trøndelag, Central Norway*. Master thesis, Norwegian University of Science and Technology.
- BINGEN, B. & SOLLI, A. 2009. Geochronology of magmatism in the Caledonian and Sveconorwegian belts of Baltica: synopsis for detrital zircon provenance studies. *Norwegian Journal of Geology*, 89, 269-290.
- BRAATHEN, A., OSMUNDSEN, P. T., NORDGULEN, Ø., ROBERTS, D. & MEYER, G. B. 2002. Orogen-parallel extension of the Caledonides in northern Central Norway: an overview. *Norwegian Journal of Geology*, 82, 225-241.
- BRUECKNER, H. K. & VAN ROERMUND, H. 2004. Dunk tectonics: A multiple subduction/education model for the evolution of the Scandinavian Caledonides. *Tectonics*, 23.
- BRUECKNER, H. K. & VAN ROERMUND, H. L. M. 2007. Concurrent HP metamorphism on both margins of Iapetus: Ordovician ages for eclogites and garnet pyroxenites from the Seve Nappe Complex, Swedish Caledonides. *Journal of the Geological Society, London*, 164, 117-128.
- BUNKHOLT, H. S. S. 2006. *Fault-slip inversion and palaeostress analysis above and below a post-Caledonian Extensional Detachment*. Master thesis, Norwegian University of Science and Technology.
- COBBOLD, P. R. & QUINQUIS, H. 1980. Development of shear folds in shear regimes. *Journal of Structural Geology*, 2, 119-126.
- CORFU, F., ANDERSEN, T. B. & GASSER, D. 2014. The Scandinavian Caledonides: main features, conceptual advances and critical questions. *Geological Society, London, Special Publications*, 390, 9-43.
- CORFU, F., GERBER, M., ANDERSEN, T. B., TORSVIK, T. H. & ASHWAL, L. D. 2011. Age and significance of Grenvillian and Silurian orogenic events in the Finnmarkian Caledonides, northern Norway. *Canadian Journal of Earth Sciences*, 48, 419-440.
- CORFU, F., TORSVIK, T. H., ANDERSEN, T. B., ASHWAL, L. D., RAMSAY, D. M. & ROBERTS, R. J. 2006. Early Silurian mafic-ultramafic and granitic plutonism in contemporaneous flysch, Magerøy, northern Norway: U-Pb ages and regional significance. *Journal of the Geological Society*, 163, 291-301.
- DONATH, F. A. & PARKER, R. B. 1964. Folds and folding. *Geological Society of America Bulletin*, 75, 45-62.
- DUNNING, G. & GRENE, T. 2000. U-Pb age dating and paleotectonic significance of trondhjemite from the type locality in the Central Norwegian Caledonides. *Norges Geologiske Undersøkelse Bulletin*, 437.

References

- GEE, D. G. 1975. A tectonic model for the central part of the Scandinavian Caledonides. *American Journal of Science*, 275-A, 468-515.
- GEE, D. G. 1980. Basement-cover relationships in the central Scandinavian Caledonides. *Geologiska Föreningens i Stockholm Förhandlingar*, 102, 455-474.
- GEE, D. G. 1981. The Dictyonema-bearing phyllites at Nordaunevoll, eastern Trøndelag, Norway. *Norsk Geologisk Tidsskrift*, 61, 93-95.
- GEE, D. G. 1985. The central-southern part of the Scandinavian Caledonides. *Gee, D.G. & Stuart B. A. (eds) The Caledonide orogen - Scandinavia and related areas*, 109-133.
- GEE, D. G., JUHLIN, C., PASCAL, C. & ROBINSON, P. 2010. Collisional Orogeny in the Scandinavian Caledonides. *Geologiska Föreningens i Stockholm Förhandlingar*.
- GEE, D. G., LADENBERGER, A., DAHLQVIST, P., MAJKA, J., BE'ERI-SHLEVIN, Y., FREI, D. & THOMSEN, T. 2014. The Baltoscandian margin detrital zircon signatures of the central Scandes. *Corfu, F., Gasser, D. & Chew, D. M. (eds) New Perspectives on the Caledonides of Scandinavian and Related Areas. Geological Society, London, Special Publications*, 390, 131-155.
- GRENE, T., IHLEN, P. M. & VOKES, F. M. 1999. Scandinavian Caledonide Metallogeny in a plate tectonic perspective. *Mineralium Deposita*, 34, 422-471.
- GRIFFIN, W. P., AUSTREIM, H., BRASTAD, K., BRYHNI, I., KRILL, A., KROGH, E. J., MØRK, M. B. E., QVALE, H. & B., T. 1985. High-pressure metamorphism in the Scandinavian Caledonides. In *Gee, D. G. & Stuart B. A. (eds.), The caledonide Orogen - Scandinavia and Related Areas: Chichester, John Wiley and Sons*, 783-801.
- GRØNLIE, A., NILSEN, B. & ROBERTS, D. 1991. Brittle deformation history of fault rocks on the Fosen Peninsula, Trøndelag, Central Norway. *Norges Geologiske Undersøkelse Bulletin*, 421, 39-57.
- GRØNLIE, A. & ROBERST, D. 1989. Resurgent strike-slip duplex development along the Hitra-Snåsa and Verran Faults, Møre-Trøndelag Fault Zone, Central Norway. *Journal of Structural Geology*, 11, 295-305.
- GRUJIC, D. & MANCKTELOW, N. S. 1995. Fold with axes parallel to the extension direction: an experimental study. *Journal of Structural Geology*, 17, 279-291.
- HACKER, B. R. & GANS, P. B. 2005. Continental collisions and the creation of ultrahigh-pressure terranes: Petrology and thermochronology of nappes in the central Scandinavian Caledonides. *Geological Society of America Bulletin*, 117, 117.
- HANDKE, M. J., TUCKER, R. D. & ROBINSON, P. 1995. Constraining U-Pb Ages for the Risberget Augen Gneiss in the Norwegian Caledonides: Getting to the root of the problem. *Geological Society of America Abstracts with Programs*, 27, A-226.
- HANSEN, J., SKJERLIE, K. P., PEDERSEN, R. B. & DE LA ROSA, J. 2002. Crustal melting in the lower parts of island arcs: an example from the Bremanger Granitoid Complex, west Norwegian Caledonides. *Contributions to Mineralogy and Petrology*, 143, 316-335.
- HARTEL, T. H. D. & PATTISON, D. R. M. 1996. Genesis of the Kapuskasing (Ontario) migmatitic mafic granulites by dehydration melting of amphibolites: the importance of quartz to reaction progress. *Journal of Metamorphic Geology*, 14, 591-611.
- HEDIN, P., MALEHMIR, A., GEE, D. G., JUHLIN, C. & DYRELIUS, D. 2014. 3D interpretation by integrating seismic and potential field data in the vicinity of the proposed COSC-1 drill-site, central Swedish Caledonides. *Corfu, F., Gasser, D. & Chew, D. M. (eds) New Perspectives on the Caledonides of Scandinavian and Related Areas. Geological Society, London, Special Publications*, 390, 301-319.
- HEIM, M. 1993. Hovedtrekk av berggrunnen i deler av kartblad Leksvik 1622-3. *Norges Geologiske Undersøkelse Rapport*.
- HOFFMAN, P. F. 1999. The break-up of Rodinia, birth of Gondwana, true polar wander and the snowball Earth. *Journal of African Earth Sciences*, 28, 17-33.
- HOLLOCHER, K., ROBINSON, P., WALSH, E. & ROBERST, D. 2012. Geochemistry of amphibolite-facies volcanics and gabbros of the Støren nappe in extensions west and southwest of Trondheim, Western Gneiss Region, Norway: a key to correlations and paleotectonic settings *American Journal of Science*, 312, 357-416.

- HOLLOCHER, K., ROBINSON, P., WALSH, E. & TERRY, M. P. 2007. The neoproterozoic Ottefjället dike swarm of the Middle Allochthon, traced geochemically into the Scandian hinterland, Western Gneiss Region, Norway. *American Journal of Science*, 307, 901-953.
- HULL, J. & ADAMY, J. 1989. Basement-cover relationships on Fosen Peninsula along Trondheimsfjorden, Trøndelag, Norway. *Geologiska Föreningens i Stockholm Förhandlingar*, 111, 390-394.
- HURICH, C. A., PALM, H., DYRELIUS, D. & KRISTOFFERSEN, Y. 1989. Deformation of the Baltic continental crust during Caledonide intracontinental subduction: Views from seismic reflection data. *Geology*, 17, 423-425.
- HURICH, C. A., PALM, P., DYRELIUS, D., KRISTOFFERSEN, Y., WOLFF, F. C. & ROBERTS, D. 1988. Activation of Precambrian basement in the Scandinavian Caledonides: View from seismic reflection data. *Norges geologiske undersøkelse Special Publication*, 3, 66-69.
- IRVINE, T. N. & BARAGER, W. R. A. 1971. A guide to the classification of the common volcanic rocks. *Canadian Journal of Earth Sciences*, 8, 523-548.
- JACKSON, S. E., PEARSON, N. J., GRIFFIN, W. L. & BELOUSOVA, E. A. 2004. The application of laser ablation-inductively coupled plasma-mass spectrometry to in situ U–Pb zircon geochronology. *Chemical Geology*, 211, 47-69.
- JOHNSEN, S. O. 1979. Geology of the Area West and Northwest of Orkdalsfjorden, Sør-Trøndelag. *Norges Geologiske Undersøkelse*, 348, 33-46.
- JUHOJUNTII, N., JUHLIN, C. & DYRELIUS, D. 2001. Crustal reflectivity underneath the Central Scandinavian Caledonides. *Tectonophysics*, 334, 191-210.
- KIRKLAND, C. L., DALY, J. S. & WHITEHOUSE, M. J. 2005. Early Silurian magmatism and the Scandian evolution of the Kalak Nappe Complex, Finnmark, Arctic Norway. *Journal of the Geological Society*, 162, 985-1003.
- KLONOWSKA, I., MAJKA, J., JANAK, M., GEE, D. G. & LADENBERGER, A. 2014. Pressure-temperature evolution of a kyanite-garnet pelitic gneiss from Åreskutan: evidence of ultra-high-pressure metamorphism of the Seve Nappe Complex, west-central Jämtland, Swedish Caledonides. *Corfu, F., Gasser, D. & Chew, D. M. (eds) New Perspectives on the Caledonides of Scandinavian and Related Areas. Geological Society, London, Special Publications*, 390, 321-336.
- KOLLUNG, S. 1990. The Surna, Rinna and Orkla Nappes of the Surnadal-Orkdal district, southwestern Trondheim Region. *Norges Geologiske Undersøkelse*, 418, 9-17.
- KRABBENDAM, M. & DEWEY, J. F. 1998. Exhumation of UHP rocks by transtension in the Western Gneiss Region, Scandinavian Caledonides. *Geological Society, London, Special Publications*, 135, 159-181.
- KRILL, A. G. 1985. Relationship between the western gneiss region and the Trondheim region; Stockwer-tectonics reconsidered. *in Gee, D. G. & Stuart B. A. (eds.), The Caledonide Orogen - Scandinavia and Related Areas: Chichester, John Wiley and Sons*, 475-483.
- LADENBERGER, A., BE'ERI-SHLEVIN, Y., CLAEISSON, S., GEE, D. G., MAJKA, J. & ROMANOVA, I. V. 2013. Tectonometamorphic evolution of the Åreskutan Nappe - Caledonian history revealed by SIMS U-Pb zircon geochronology. *In Corfu, F., Gasser, D. & Chew, D. M. (eds) New Perspectives on the Caledonides of Scandinavia and Related Areas. Geological Society, London, Special Publications*, 390.
- LE BAS, M. J., LE MAITRE, R. W., STRECKEISEN, A. & ZANETTIN, B. 1986. A Chemical Classification of Volcanic Rocks Based on the Total Alkali-Silica Diagram. *Journal of Petrology*, 27, 745-750.
- LUDWIG, K. R. 2001. User's manual for Isoplot/Ex v. 2.49, a geochronological toolkit for Microsoft Excel. *Berkeley Geochronology Center Spec. Publ.*, 1a, 59 pp.
- MAJKA, J., BE'ERI-SHLEVIN, Y., GEE, D. G., LADENBERGER, A., CLAEISSON, S., KONECNY, P. & KLONOWSKA, I. 2012. Multiple monazite growth in the Åreskutan migmatite, evidence for a polymetamorphic Late Ordovician to Late Silurian evolution in the Seve Nappe Complex of west-central Jämtland, Sweden. *Journal of Geosciences*, 57, 3-23.
- MANIAR, P. D. & PICCOLI, P. M. 1989. Tectonic discrimination of granitoids. *Geological Society of America Bulletin*, 101, 635-643.

References

- MIDDLEMOST, E. A. K. 1994. Naming minerals in the magma/igneous rock system. *Earth Science Review*, 37, 215-224.
- NILSEN, O. 1978. Caledonian Sulphide Deposits and Minor Iron-formations from the Southern Trondheim Region, Norway. *Norges Geologiske Undersøkelse*, 340, 35-85.
- NILSEN, O., CORFU, F. & ROBERTS, D. 2007. Silurian gabbro-diorite-trondhjemite plutons in the Trondheim Nappe Complex, Caledonides, Norway: petrology and U-Pb geochronology. *Norwegian Journal of Geology*, 87, 329-342.
- NILSEN, O. & WOLFF, F. C. 1989. *Geologisk kart over Norge, berggrunnskart RØROS og SVEG - 1:250 000*. Norges Geologiske Undersøkelse.
- NORDGULEN, Ø., BICKFORD, M. E., NISSEN, A. L. & WORTMAN, G. L. 1993. U-Pb zircon ages from the Bindal Batholite, and the tectonic history of the Helgeland Nappe Complex, Scandinavian Caledonides. *Journal of the Geological Society*, 150, 771-783.
- NORDGULEN, Ø., BRAATHEN, A., CORFU, F., OSMUNDSEN, P. T. & HUSMO, T. 2002. Polyphase kinematics and geochronology of the late-Caledonian Kollstraumen detachment, north-central Norway. *Norwegian Journal of Geology*, 82.
- NORGESKART.NO. 2015. <http://www.norgeskart.no/>.
- NYSTUEN, J. P., ANDRESEN, A., KUMPULAINEN, R. & SIEDLECKA, A. 2008. Neoproterozoic basin evolution in Fennoscandia, East Greenland and Svalbard. *Episodes*, 31, 35-43.
- OLSEN, E., GABRIELSEN, R. H., BRAATHEN, A. & REDFIELD, T. F. 2007. Fault systems marginal to the Møre-Trøndelag Fault Complex, Osen - Vikna area, Central Norway. *Norwegian Journal of Geology*, 87, 59-73.
- OSMUNDSEN, P. T., EIDE, E. A., HAABESLAND, N. E., ROBERTS, D., ANDERSEN, T. B., KENDRICK, M., BINGEN, B., BRAATHEN, A. & REDFIELD, T. F. 2006. Kinematics of the Hoybakken detachment zone and the More-Trøndelag Fault Complex, central Norway. *Journal of the Geological Society*, 163, 303-318.
- PALM, P., GEE, D. G., DYRELIUS, D. & BJÖRKLUND, L. 1991. A reflection seismic image of Caledonian structure in Central Sweden. *Sveriges Geologiska Undersökning*, 75, 36.
- PAULSSON, O. & ANDRÉASSON, P.-G. 2002. Attempted break-up of Rodinia at 850 Ma; geochronological evidence from the Seve-Kalak Superterrane, Scandinavian Caledonides. *Journal of the Geological Society, London*, 163, 303-318.
- PEACEY, J. S. 1963. Deformation in the Gangåsvann Area. *Norges Geologiske Undersøkelse*, 223, 275-293.
- PEARCE, J. A. 1982. Trace element characteristics of lavas from destructive plate boundaries *Andesites*, 8, 525-548.
- PEARCE, J. A. 1983. Role of the sub-continental lithosphere in magma genesis at active continental margins. *Hawkesworth, C. J. and Norry, M. J. eds. Continental basalts and mantle xenoliths, Nantwich, Cheshire: Shiva Publications*, 230-249.
- PEARCE, J. A. & CANN, J. R. 1973. Tectonic setting of basic volcanic rocks determined using trace element analyses. *Earth and Planetary Science Letters*, 19, 290-300.
- PEARCE, J. A. & NORRY, M. J. 1979. Petrogenetic implications of Ti, Zr, Y, and Nb variations on volcanic rocks. *Contributions to Mineralogy and Petrology*, 69, 33-47.
- PEDERSEN, R. B., BRUTON, D. L. & FURNES, H. 1992. Ordovician faunas, island arcs and ophiolites in the Scandinavian Caledonides. *Terra Nova*, 4, 217-222.
- PIASECKI, M. A. J. & CLIFF, R. A. 1988. Rb-Sr dating of strain induced mineral growth in two ductile shear-zones in the Western Gneiss Region of Nord-Trøndelag, Central Norway. *Norges Geologiske Undersøkelse Bulletin*, 413, 33-50.
- POWELL, C., LI, Z. X., MCELHINNY, M. W., MEERT, J. G. & PARK, J. K. 1993. Paeomagnetic constraints on timing of the Neoproterozoic breakup of Rodinia and the Cambrian formation of Gondwana. *Geology*, 21, 889-892.
- RAMBERG, H. 1973. Beskrivelse til berggrunnsgeologisk kart over strøket Agdenes-Hemnefjord, Sør-Trøndelag. *Norges Geologiske Undersøkelse*, 299, 1-11.

- RAMBERG, I. B., BRYHNI, I., NØTTVEDT, A. & RANGNES, K. 2008. *The Making of a Land - Geology of Norway*, Trondheim, Norsk Geologisk Forening.
- RANALLI 2000. Rheology of the crust and its role in tectonic reactivation. *Journal of Geodynamics*, 30, 3-15.
- REDFIELD, T. F., BRAATHEN, A., GABRIESEN, R. H., OSMUNDSEN, P. T., TORSVIK, T. H. & ANDRIESEN, P. A. M. 2005a. Late Mesozoic to Early Cenozoic components of vertical separation across the Møre-Trøndelag Fault complex, Norway. *Tectonophysics*, 395, 233-249.
- REDFIELD, T. F., OSMUNDSEN, P. T. & HENDRIKS, W. E. 2005b. The role of fault reactivation and growth in the uplift of western Fennoscandia. *Journal of the Geological Society*, 162, 1013-1030.
- REDFIELD, T. F., TORSVIK, T. H., ANDRIESEN, P. A. M. & GABRIESEN, R. H. 2004. Mesozoic and Cenozoic tectonics of the Møre-Trøndelag Fault Complex, central Norway: constraints from new apatite fission track data. *Physics and Chemistry of the Earth*, 29, 673-682.
- RICKARD, M. J. 1985. The Surnadal synform and basement gneisses in the Surnadal-Sunndal district of Norway. *Gee, D. G. and Stuart, B. A., eds The Caledonide Orogen - Scandinavia and Related Areas: Chichester, John Wiley and Sons*, 485-497.
- ROBERTS, D. 2003. The Scandinavian Caledonides: event chronology, palaeogeographic settings and likely modern analogues. *Tectonophysics*, 365, 283-299.
- ROBERTS, D. & MYRVANG, A. 2004. Contemporary stress orientation features in bedrock, Trøndelag, Central Norway, and some regional implications. *Norges Geologiske Undersøkelse Bulletin*, 442, 53-63.
- ROBERTS, D., NORDGULEN, Ø. & MELEZHNIK, V. M. 2007. The Uppermost Allochthon in the Scandinavian Caledonides: From a Laurentian ancestry through Taconian orogeny to Scandian crustal growth on Baltica. *The Geological Society of America Memoir* 200, 357-377.
- ROBERTS, D. & STEPHENS, M. 2000. Caledonian Orogenic Belt. *Lundqvist, T., and Autio, S. (eds.), Description of the Bedrock Map of Central Fennoscandia (Mid-Norden): Geological Survey of Finland, Special Paper*, 28, 79-104.
- ROBERTS, D. & STURT, B. A. 1980. Caledonian deformation in Norway. *Journal of the Geological Society*, 137, 241-250.
- ROBERTS, D., WALKER, N., SLAGSTAD, T., SOLLI, A. & KRILL, A. 2002. U-Pb zircon ages from the Bymarka ophiolite, near Trondheim, Central Norwegian Caledonides, and regional implications. *Norsk Geologisk Tidsskrift*, 82, 19-30.
- ROBINSON, P. 1995. Extension of Trollheimen tectono-stratigraphic sequence in deep synclines near Molde and Brattvåg, Western Gneiss Region. *Norsk Geologisk Tidsskrift*, 75, 181-198.
- ROBINSON, P. 1997. Quartzites of Reksdalshesten, Moldefjorden, Western Gneiss Region: Another parallel with the tectonostratigraphy of Trollheimen (extended abstract). *Norges Geologiske Undersøkelse Bulletin*, 433, 15-16.
- ROBINSON, P. & ROBERTS, D. 2008. A tectonostratigraphic transect across the central Scandinavian Caledonides, Storlien-Trondheim-Lepsøy. Part II: Excursion guide in Norway. *NGU report nr 2008.064*.
- ROFFEIS, C. & CORFU, F. 2013. Caledonian nappes of southern Norway and their correlation with Sveconorwegian basement domains. *Geological Society, London, Special Publications*, 390, 193-221.
- ROOT, D. & CORFU, F. 2012. U-Pb geochronology of two discrete Ordovician high-pressure metamorphic events in the Seve Nappe Complex, Scandinavian Caledonides. *Contributions to Mineralogy and Petrology*, 163, 769-788.
- SERANNE, M. 1992. Late Palaeozoic kinematics of the Møre-Trøndelag Fault Zone and adjacent areas, central Norway. *Norsk Geologisk Tidsskrift*, 72, 141-158.
- SIEDLECKA, A., ROBERTS, D., NYSTUEN, J. P. & OLOVYANISHNIKOV, V. G. 2004. Northeastern and northwestern margins of Baltica in Neoproterozoic time: evidence from the Timanian and Caledonian Orogens. *Gee, D. G. & Pease, V. (eds). The Neoproterozoic Timanide Orogen of Eastern Baltica. Geological Society, London, Memoirs*, 30, 169-190.

References

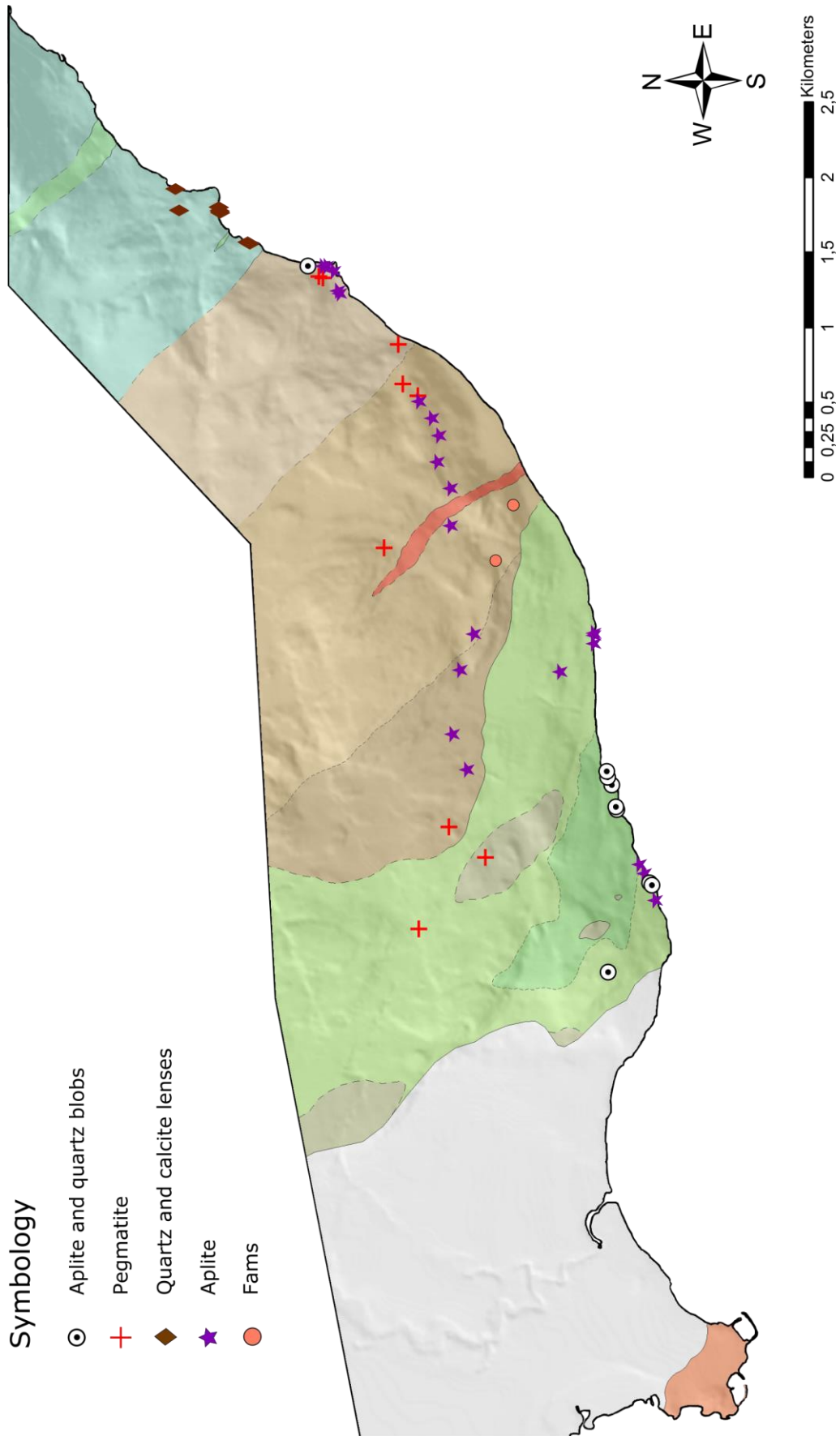
- SKÅR, Ø. 2002. U-Pb geochronology and geochemistry of early Proterozoic rocks of the tectonic basement windows in central Nordland, Caledonides of north-central Norway. *Precambrian Research*, 116, 265-283.
- SKJERNAA, L. 1980. Rotation and deformation of randomly oriented planar and linear structures in progressive simple shear. *Journal of Structural Geology*, 2, 101-109.
- SLAGSTAD, T. 2003. Geochemistry of trondhjemites and mafic rocks in the Bymarka ophiolite fragment, Trondheim, Norway: Petrogenesis and tectonic implications. *Norwegian Journal of Geology*, 83, 167-185.
- SLAGSTAD, T., PIN, C., ROBERTS, D., KIRKLAND, C. L., GRENNE, T., DUNNING, G., SAUER, S. & ANDRESEN, T. 2014. Tectonomagmatic evolution of the Early Ordovician suprasubduction-zone ophiolites of the Trondheim Region, Mid-Norwegian Caledonides. *Corfu, F., Gasser, D. & Chew, D. M. (eds) New Perspectives on the Caledonides of Scandinavian and Related Areas. Geological Society, London, Special Publications*, 390, 541-561.
- SOLYOM, Z., ANDRÉASSON, P.-G. & JOHANSSON, I. 1979. Geochemistry of amphibolites from Mt. Sylarna, Central Scandinavian Caledonides. *Geologiska Föreningens i Stockholm Förhandlingar*, 101, 17-25.
- STEEL, R. J., SIEDLECKA, A. & ROBERTS, D. 1985. The Old Red Sandstone basins of Norway and their deformation: a review. *The Caledonide Orogen - Scandinavia and Related Areas: Chichester, John Wiley and Sons*, 293-315.
- STEIGER, R. H. & JÄGER, E. 1977. Subcommission on geochronology: Convention on the use of decay constants in geo- and cosmochronology. *Earth and Planetary Science Letters*, 36, 359-362.
- STEPHENS, M. B. & GEE, D. G. 1985. A tectonic model for the evolution of the eugeoclinal terranes in the central Scandinavian Caledonides. *In Gee, D. G. & Stuart B. A. (eds.), The Caledonide Orogen - Scandinavia and Related Areas: Chichester, John Wiley and Sons*, 953-978.
- SVENNINGSEN, O. M. 2001. Onset of seafloor spreading in the Iapetus Ocean at 608 Ma: precise age of the Sarek Dyke Swarm, northern Swedish Caledonides. *Precambrian Research*, 110, 241-254.
- THOMPSON, R. N., DICKIN, A. P., GIBSON, I. L. & MORRISON, M. A. 1982. Elemental Fingerprints of Isotopic Contamination of Hebridean Palaeocene Mantle-Derived Magmas by Archaean Sial. *Contributions to Mineralogy and Petrology*, 79, 159-168.
- TORSVIK, T. H., SMETHURST, M. A., MEERT, J. G., VAN DER VOO, R., MCKERROW, W. S., BRASIER, M. D., STURT, B. A. & WALDERHAUG, H. J. 1996. Continental break-up and collision in the Neoproterozoic and Palaeozoic - A tale of Baltica and Laurentia. *Earth-Science Reviews*, 40, 229-258.
- TORSVIK, T. H., STURT, B. A., RAMSAY, D. M., GRØNLIE, A., ROBERTS, D., SMETHURST, M. A., ATAKAN, K., BØE, R. & WALDERHAUG, H. J. 1989. Palaeomagnetic Constraints on the Early History of the Møre-Trøndelag Fault Zone, Central Norway. *Paleomagnetic Rotations and Continental Deformation*, 254, 431-457.
- TORSVIK, T. H., VAN DER VOO, R., PREEDEN, U., MAC NIOCAILL, C., STEINBERGER, B., DOUBROVINE, P. V., VAN HINSBERGEN, D. J. J., DOMEIER, M., GAINA, C., TOHVER, E., MEERT, J. G., MCCAUSLAND, P. J. A., ROBIN, L. & COCKS, L. R. M. 2012. Phanerozoic polar wander, palaeogeography and dynamics. *Earth-Science Reviews*, 114, 325-368.
- TUCKER, R. D. 1986. Geology of the Hemnefjord-Orkanger Area, Southern-Central Norway. *Norges Geologiske Undersøkelse*, 404, 1-21.
- TUCKER, R. D., BRADLEY, D. C., VER STRAETEN, C., HARRIS, A. G., EBERT, J. & MCCUTCHEON, S. R. 1998. New U-Pb zircon ages and the duration and division of Devonian time. *Earth and Planetary Science Letters*, 158, 175-186.
- TUCKER, R. D., KROGH, T. E. & RÅHEIM, A. 1990. Proterozoic evolution and age -province boundaries in the central part of the Western Gneiss Region, south-central Norway: Results of U-Pb dating of accessory minerals from Trondheimsfjorden to Geiranger. *Middle Proterozoic Geology of the Southern Margin of Proto Laurentia-Baltica: Geological Association of Canada Special Paper*, 38, 149-173.

- TUCKER, R. D. & KROGH, T. E. 1988. Geochronological investigation of the Ingdal Granite Gneiss and discordant pegmatites from the Western Gneiss Region, Norway. *Norsk Geologisk Tidsskrift*, 68, 201-210.
- TUCKER, R. D., RÅHEIM, A., KROGH, E. J. & CORFU, F. 1986. Uranium-lead zircon and titanite ages from the northern part of the Western Gneiss Region, south-central Norway. *Earth and Planetary Science Letters*, 81, 203-211.
- TUCKER, R. D., ROBINSON, P., SOLLI, A., GEE, D. G., THORSNES, T., KROGH, T., E., NORDGULEN, Ø. & BICKFORD, M. E. 2004. Thrusting and extension on the Scandian hinterland, Norway: New U-Pb ages and tectonostratigraphic evidence. *American Journal of Science*, 304, 477-532.
- VAN ACHTERBERG, E., RYAN, C. G., JACKSON, S. E. & GRIFFIN, W. L. 2001. Data reduction software for LA-ICP-MS. In: SYLVESTER, P. J. (ed.) *Laser ablation-ICP-mass spectrometry in the Earth sciences: Principles and applications*. Ottawa, Ontario, Canada: Mineralog. Assoc. Canada (MAC) Short Course Series.
- VAN ROERMUND, H. L. M. 1985. Eclogites of the Seve nappe, central Scandinavian Caledonides. In Gee, D. G. & Stuart B. A. (eds.), *The Caledonide Orogen - Scandinavia and Related Areas*, 873-886.
- WEIGAND, S., HAUZENBERGER, C. & GASSER, D. 2016. A petrological and geochemical study of the Surna Nappe (Seve Nappe Complex?) in the Central Scandinavian Caledonides, Norway. *EGU*.
- WIEDENBECK, M., ALLÉ, P., CORFU, F., GRIFFIN, W. L., MEIER, M., OBERLI, F., QUADT, A. V., RODDICK, J. C. & SPIEGEL, W. 1995. Three natural zircon standards for U-Th-Pb, Lu-Hf, trace element and REE analyses. *Geostandards Newsletter*, 19, 1-23.
- WINTER, J. D. 2010. *An Introduction to Igneous and Metamorphic Petrology*, Pearson Education, Inc.
- WOLFF, F. C. 1976. *Geologisk kart over Norge, berggrunnskart TRONDHEIM 1:250 000*. Norges Geologiske Undersøkelse.
- WOLFF, F. C. 1978. *RISSA, berggrunnsgeologisk kart 1522 II - M. 1:50 000*. Norges Geologiske Undersøkelse.
- ZIEGLER, P. A. 1987. Evolution of the Arctic-North Atlantic borderlands. Brooks, J & Glennie, K. : *Petroleum Geology of North West Europe*. Graham & Trotman, London.
- ZWART, H. J. 1974. Structure and metamorphism in the Seve-Køli nappe complex (Scandinavian Caledonides) and its implications concerning the formation of metamorphic nappes. *Centenaire de la société géologique de Belgique, Géologie des domaines cristallines, Liège*, 129-144.

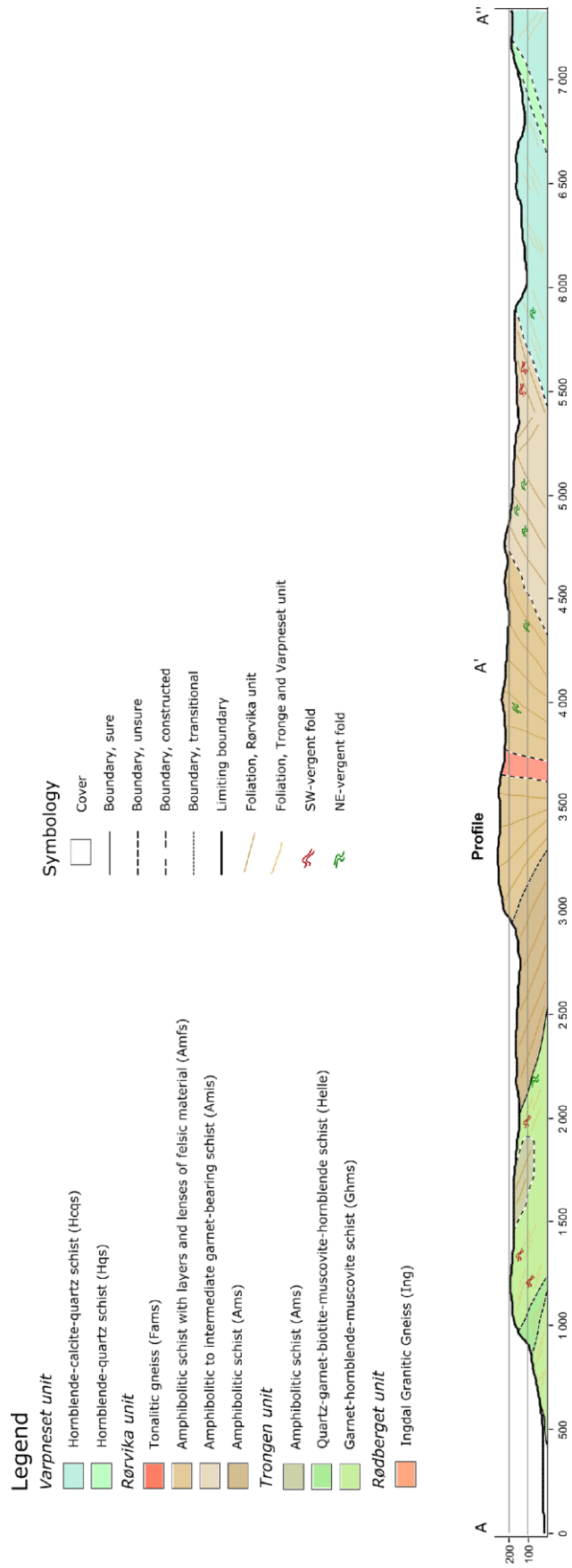
Appendix

- A. Geological map
- B. Map of felsic material
- C. Map of foliations and lineations
- D. Map of axial planes and fold axes
- E. Map of brittle structures
- F. Profile
- G. Localities for thin section samples and samples for geochronology
- H. Thin sections
- I. Sample analysis, XRF
- J. U-Pb zircon analysis
- K. Localities

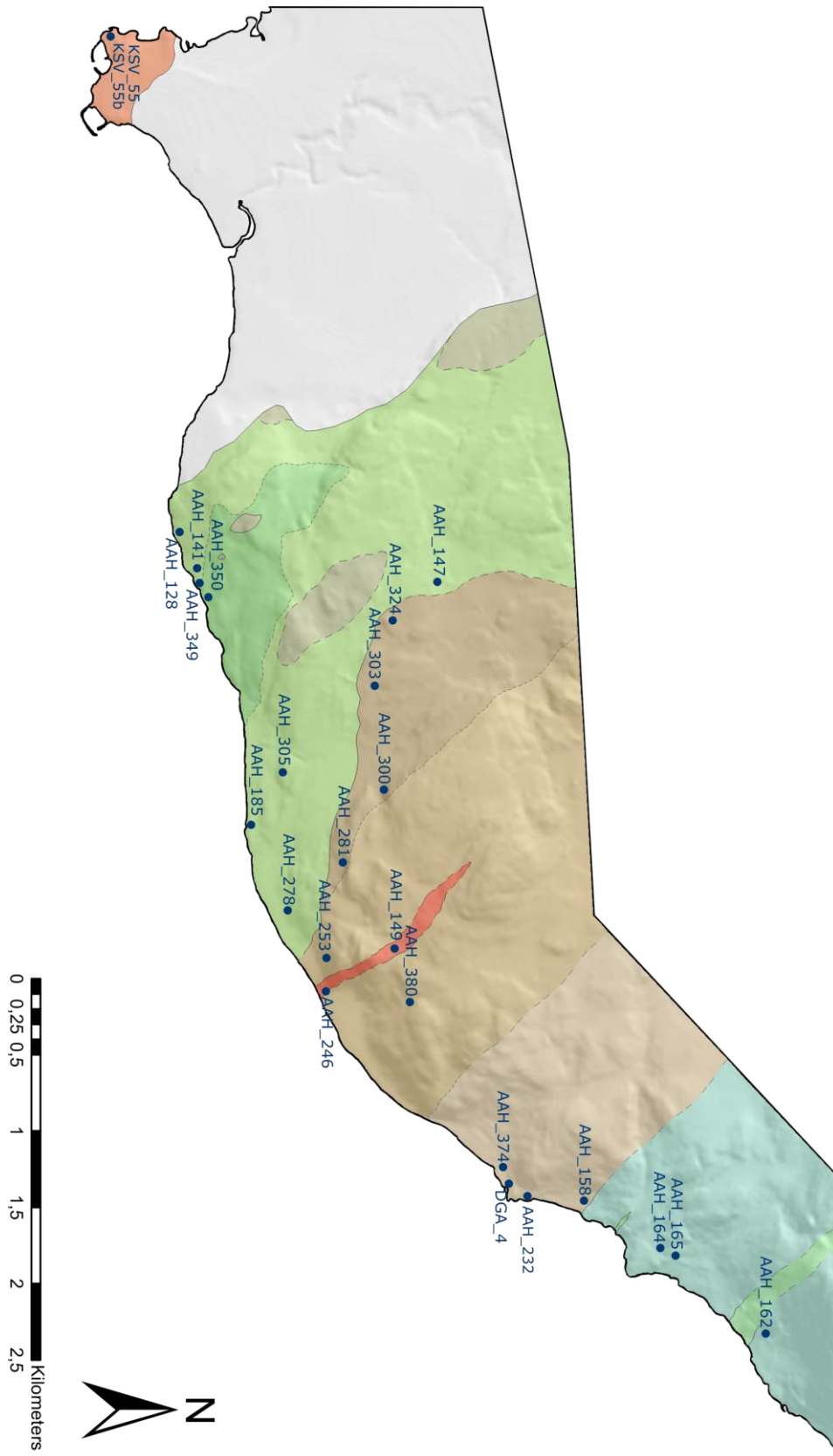
Appendix B – Map of felsic material



Appendix F – Profile



Appendix G – Localities for thin section samples and samples for geochronology



Appendix H – Thin sections



Rock name	Ingdal granitic gneiss	Location	KSV_55b	Unit	Rødberget
------------------	------------------------	-----------------	---------	-------------	-----------

Macroscopic description

Fine grained pink granitic gneiss. Foliated with pink and darker layers. The darker material is very fine grained.

Microscopic description

Granoblastic texture, foliated, platy quartz.

Mineral content	Essentials	Modal %	Accessory
	Quartz	30	Opaques
	Microcline	55	Epidote
	Plagioclase	12	Rutile
	Biotite	2	
	Muscovite	1	

Texture

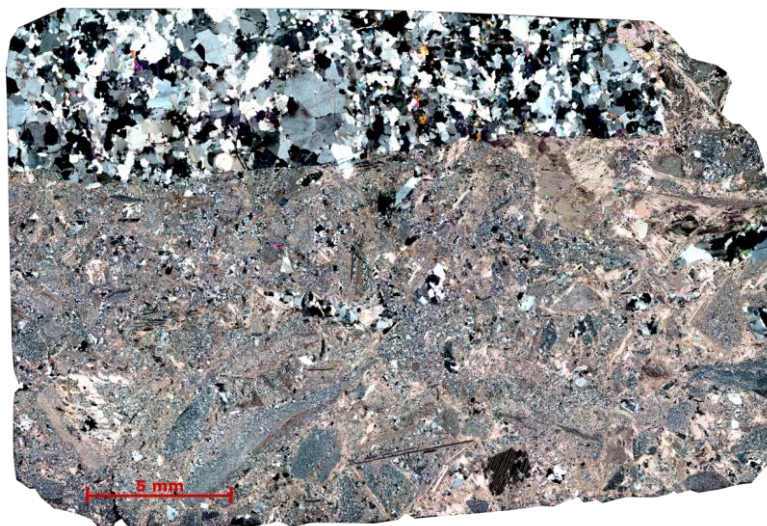
Seriate interlobate

Mineral description

Anhedral quartz, some with subgrains and undulose extinction. Quartz in lenticular quartz aggregates.

Plagioclase with polysynthetic twinning. Orthoclase with exsolution lamellae and a few show microcline twinning. Some feldspars show sericitization into muscovite. Main recrystallization mechanism is by subgrain rotation (SGR).

Biotite and muscovite with cleavage, acicular. Biotite has low interference colour.



Rock name	Ingdal granitic gneiss	Location	KSV_55	Unit	Rødberget
------------------	------------------------	-----------------	--------	-------------	-----------

Macroscopic description

Fault rock. The porphyroclasts of granitic gneiss are pink. Minerals are quartz, feldspars and calcite. The faulted rock is very fine grained with a white colour. Within the white fault rock larger clasts of granitic gneiss and quartz.

Microscopic description

Thin section showing fault rock and a slice of the host rock. The host rock is a K-feldspar and quartz-rich rock. In the fault zone larger fragments of host rock and calcite crystals can be seen. The matrix around consists of very fine grained calcite, quartz and K-feldspar.

Mineral content	Essentials	Modal %	Accessory
	Calcite	40	Opaques
	Microcline	25	Chlorite
	Quartz	20	Biotite
	Muscovite	10	
	Plagioclase	5	

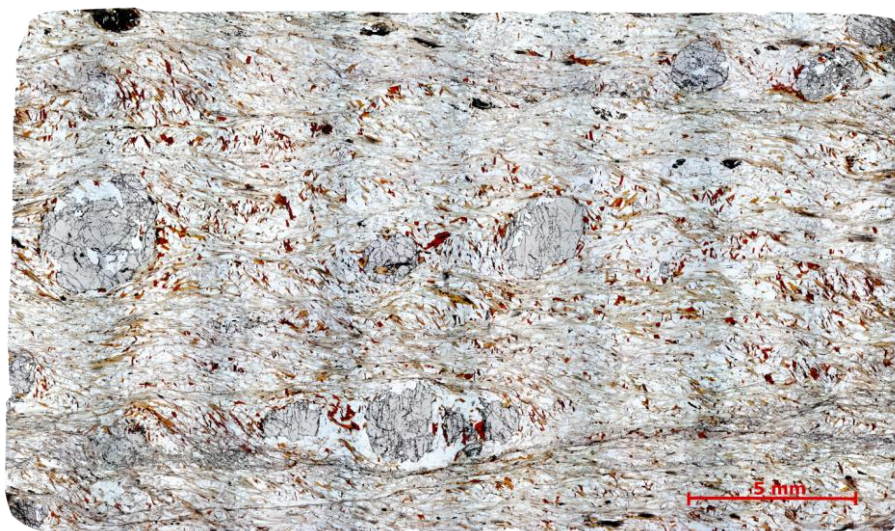
Texture

Seriate interlobate

Mineral description

The calcite occurs as very fine grains in the matrix, and as larger anhedral to subhedral grains in the fault zone, 0.5-1.5mm, with twinning.

The quartz and feldspar in the matrix are very fine grained and appear both as randomly distributed grains and as concentrated aggregates.



Rock name	Ghms	Location	AAH_278	Unit	Trongen
------------------	------	-----------------	---------	-------------	---------

Macroscopic description

Dark grey to grey and fine grained hand specimen. Foliated with lighter grey quartz rich layers, 0.1-1cm thick. Red to pink garnets 0.5-3 mm big, not found in the quartz-rich layers. Silver luster on surface from mica.

Microscopic description

Garnet, 1-4mm, and biotite-rich thin section. Foliated through orientation of micas. Biotite is bent around the garnets. Fractures/shear zones running parallel to the foliation.

Mineral content	Essentials	Modal %	Accessory
	Quartz	20	Calcite
	Feldspar	35	Rutile
	Garnet	5	
	Biotite	29	
	Chlorite	6	
	Hornblende	4	
	Muscovite	1	

Texture

Porphyroblastic garnets and matrix is equigranular polygonal.

Mineral description

Syn-deformed, fractured, poikiloblastic and anhedral garnets, some indicating two stages of growth. Inclusions of quartz, feldspar, biotite and rutile. One garnet *also* has a void with calcite.

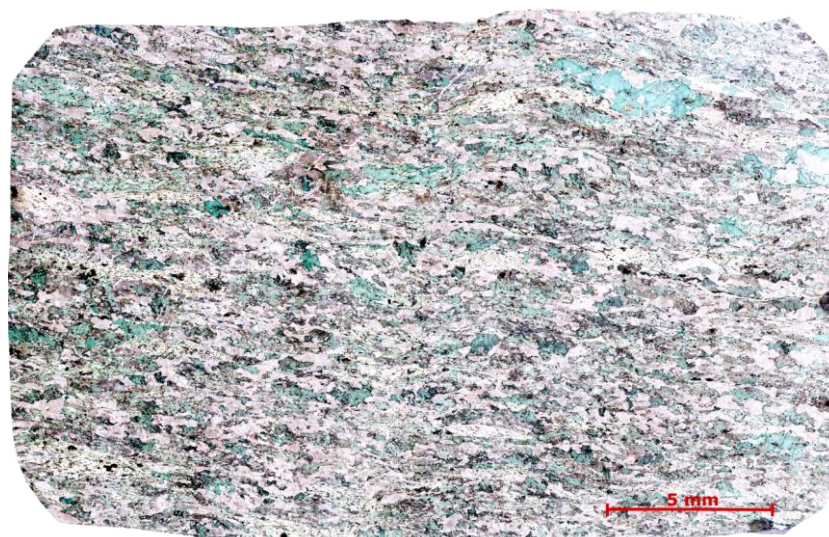
The plagioclase shows sericite and polysynthetic twinning.

The hornblende is dissolved, deformed and fractured.

Biotite is acicular and oriented. Orientation of biotite indicates two generations of foliation oblique to each other, the younger being dominant.

Recrystallisation of feldspar and quartz through SGR and grain boundary migration (GBM).

Facies	Amphibolite
Shear	Sinistral (note that thin section is not oriented)



Rock name	Ghms	Location	AAH_128	Unit	Trongen
------------------	------	-----------------	---------	-------------	---------

Macroscopic description

Fine grained, dark grey to green and foliated rock with a 1.5 mm thick quartz vein cutting the hand specimen. Pink and fine grained garnets are spread throughout.

Microscopic description

Foliated rock with anhedral grains of chlorite and plagioclase. Fine grain size.

Mineral content	Essentials	Modal %	Accessory
	Chlorite	33	Rutile
	Plagioclase	30	Calcite
	Epidote	2	
	Clinozoisite	13	
	Amphibole	12	
	Titanite	5	
	Quartz	5	

Texture

Granoblastic (equigranular) polygonal.

Mineral description

Amphibole shows reaction into chlorite.

The chlorite is foliated, sericitized and poikiloblastic with inclusions of epidote, Clinozoisite and rutile. It shows interference colours from grey to strong purple.

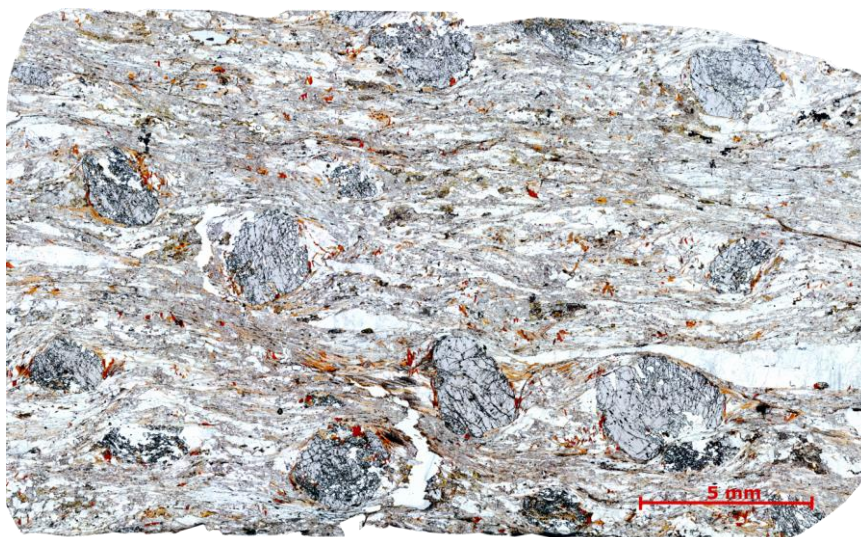
Anhedral titanite grains with rutile enclosed.

Small and elongated grains of calcite cutting the foliation.

Quartz appears as single grains and as elongated aggregates with deformation bands.

Strong seritization of the equigranular polygonal plagioclase. Recrystallization mechanism dominated by SGR.

Facies Amphibolite. Shows evidence of retrograde metamorphism.



Rock name	Ghmbs	Location	AAH_147	Unit	Trongen
------------------	-------	-----------------	---------	-------------	---------

Macroscopic description

The hand specimen is grey, foliated and has a medium grain size. Red garnets, 2-3 mm in diameter throughout. Silver luster from specific angles from the muscovite and biotite. Lenticular quartz veins, up to 4 cm long and 3 mm thick.

Microscopic description

Foliated thin section with 2-4 mm big garnets spread throughout the thin section. The thin section has a brown to orange to green colour. 0.2-1 mm thick lenticular quartz aggregates parallel to the foliation.

Mineral content	Essentials	Modal %	Accessory
	Plagioclase	40	Rutile
	Biotite	18	Mg-chlorite
	Quartz	15	
	Muscovite	10	
	Garnet	10	
	Calcite	5	

Texture

Porphyroblastic garnets and equigranular to inequigranular polygonal matrix.

Mineral description

Poikiloblastic garnets that are pre- to synkinematic. Within the garnets, rutile, calcite and quartz are present in voids and cracks.

Quartz appears as both lenticular aggregates with a granoblastic texture, and as a very fine grained matrix together with calcite.

Both muscovite and biotite are acicular and parallel to the foliation, but bend around the porphyroblasts.

Sericitisation of the plagioclase.

Calcite present as very fine grained accumulates in the matrix.

Bladed Mg-chlorite with grey interference colour.

Facies Amphibolite



Rock name	Ghms	Location	AAH_141	Unit	Trongen
------------------	------	-----------------	---------	-------------	---------

Macroscopic description

Foliated and fine to medium grain size. Weak layering with dark grey and dark grey to greenish layers. Silver to green luster.

Microscopic description

Foliated rock with a shear zone crossing through. Phenocrysts of garnets are spread randomly around, varying in size from 0.1-1mm. Green to brown colour in plane polarized light.

Mineral content	Essentials	Modal %	Accessory
	Feldspar	45	Calcite
	Chlorite	25	
	Quartz	15	
	Muscovite	10	
	Garnet	5	

Texture

Granoblastic garnets and equigranular (granoblastic) polygonal matrix.

Mineral description

Chlorite purple interference colour and green pleochroism.

Lenticular, 0.5-1 mm long quartz aggregates parallel to the foliation.

Garnets are subhedral to euhedral, synkinematic and poikiloblastic. The foliation bends around the garnets with muscovite indicating a sense of shear.

Some sericitization of the plagioclase.

Facies Amphibolite. Shows evidence of retrograde metamorphism.

Shear Dekstral (note that thin section is not oriented)



Rock name	Helle	Location	AAH_350	Unit	Trongen
------------------	-------	-----------------	---------	-------------	---------

Macroscopic description

Homogeneous and dark grey hand specimen. Dark grey silver luster and fine grained. Abundant 0.5-1.5 mm dark red garnets throughout.

Microscopic description

Foliated sample with 0.5-1.5 mm garnet phenocrysts spread throughout the thin section. The garnets are fractured and poikiloblastic. Brown to orange to green in colour from the biotite, which also gives the foliation a crenulated look. Semi-brittle and parallel fractures cutting the thin section and the foliation.

Mineral content	Essentials	Modal %	Accessory
	Plagioclase	35	Opagues
	Biotite	33	Rutile
	Quartz	15	Zircon
	Garnet	10	Titanite
	Muscovite	5	
	Chlorite	2	

Texture

Porphyroblast of garnets with an equigranular polygonal matrix.

Mineral description

Foliation bends around the garnets. The garnets are fractured and poikiloblastic.

Radiating Mg-chlorite.

Acicular biotite and muscovite. The biotite shows pleochroic halos.

The quartz and plagioclase is granular excluding a few lenticular quartz aggregates showing subgrains. Main recrystallization mechanism is SGR.

Facies Amphibolite



Rock name	Ams	Location	AAH_305	Unit	Trongen
------------------	-----	-----------------	---------	-------------	---------

Macroscopic description

Layered and foliated dark grey to light grey hand specimen. Some of the darker layers show small isoclinal folds. Fine grained and with weak black luster.

Microscopic description

Green and foliated thin section rich in hornblende. Two zones with less quartz and coarser hornblende crystals show isoclinal folds.

Mineral content	Essentials	Modal %	Accessory
	Hornblende	50	
	Plagioclase	40	
	Quartz	5	
	Opaques	2	
	Titanite	3	

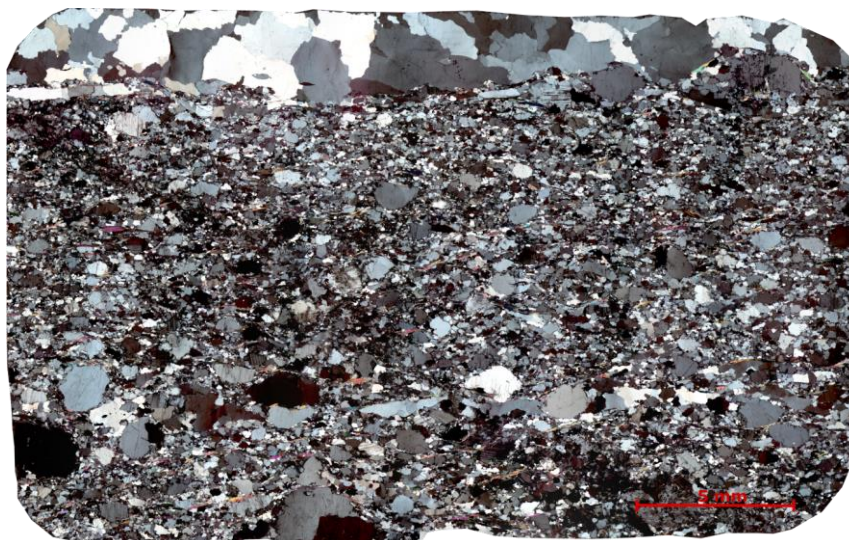
Texture

Inequigranular interlobatte matrix with equigranular polygonal zones of hornblende.

Mineral description

Zones with porphyroblastic anhedral hornblende grains that show some poikiloblastic texture. The matrix consists of fine grained, anhedral to subhedral columnar hornblende, and granular plagioclase and quartz. Both grain sizes of hornblende are foliated. Some of the plagioclase grains show polysynthetic twinning. Main recrystallization mechanism is SGR. Very fine grained subhedral titanite oriented parallel to the foliation throughout the thin section.

Facies Amphibolite



Rock name	Aplite	Location	AAH_349	Unit	Trongen
------------------	--------	-----------------	---------	-------------	---------

Macroscopic description

White to light grey hand specimen. Shows a weak foliation and fine grain size. Contains a 4 mm thick quartz vein. Very fine grained dark minerals give the rock the greyish colour.

Microscopic description

The thin section is rich in feldspar and quartz of varying grain size, 0.05-1 mm, with fine grained micas running parallel to the foliation. A granular and coarse grained vein of quartz parallel to the foliation. Fracture running through the thin section.

Mineral content	Essentials	Modal %	Accessory
	Quartz	40	Opagues
	Plagioclase	52	Chlorite
	Muscovite	7	Biotite

Texture

Seriate interlobate (core and mantle texture). The quartz vein is equigranular interlobate.

Mineral description

Plagioclase showing sericite, some grains with polysynthetic twins.

Micas are acicular and are oriented parallel to the foliation.

Coarsened grained band of quartz represents quartz vein.

Main recrystallization mechanism is SGR



Rock name	Aplite	Location	AAH_185	Unit	Trongen
------------------	--------	-----------------	---------	-------------	---------

Macroscopic description

White and fine grained with weak foliation. Fine grained muscovite grains are parallel to the foliation and show a silver luster.

Microscopic description

Foliated and granoblastic. Biotite and muscovite are acicular and parallel to foliation. Fractures through the rock.

Mineral content	Essentials	Modal %	Accessory
	Plagioclase	56	Chlorite
	Quartz	28	
	Muscovite	8	
	Orthoclase	4	
	Biotite	2	
	Garnet	2	

Texture

Seriate interlobate.

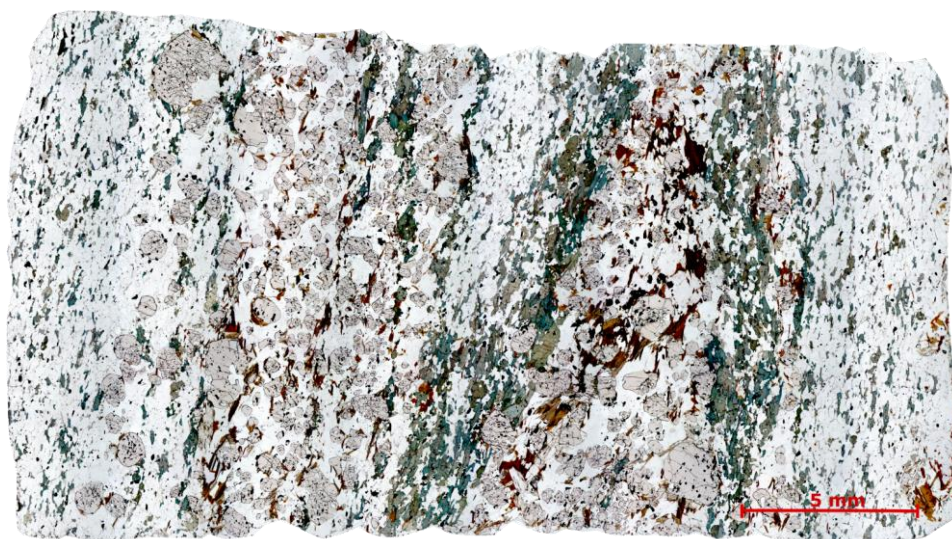
Mineral description

Plagioclase showing sericite, some with twins, both polysynthetic twinning and microcline twinning.

Acicular micas are oriented parallel to the foliation.

Two garnets (upper right corner of thin section) that are fractured, subhedral and poikiloblastic with chlorite in the fractures.

Main recrystallization mechanism is through SGR.



Rock name	Ams	Location	AAH_303	Unit	Rørvika
-----------	-----	----------	---------	------	---------

Macroscopic description

Black and foliated hand specimen. 0.5-1 cm thick layers where garnets, 0.1-5 mm in diameter, are concentrated. Fine grained.

Microscopic description

Layered and foliated thin section. Two zones rich in anhedral to subhedral garnets, 0.1-2 mm, and two thinner zones with oriented amphibole grains. The garnet-rich zones also contain more biotite. Granular and oriented quartz and feldspar.

Mineral content	Essentials	Modal %	Accessory
	Feldspar	40	Apatite
	Garnet	20	Titanite
	Amphibole	15	
	Quartz	10	
	Biotite	10	
	Opaques	5	

Texture

Porphyroblastic with equigranular polygonal to interlobate matrix.

Mineral description

The garnets vary in size from 0.2-2 mm in diameter; they are poikiloblastic, fractured, and anhedral to subhedral.

The biotite has a brown colour in plane polarized light, are acicular, and are found in the zone rich in garnet.

A few of the plagioclases shows polysynthetic twins and are recrystallized primarily through SGR.

Opaques are anhedral with a higher concentration in the garnet zones.

Facies Amphibolite



Rock name	Ams	Location	AAH_281	Unit	Rørvika
------------------	-----	-----------------	---------	-------------	---------

Macroscopic description

Medium to fine grained foliated rock. Homogeneous and dark grey in colour. 0.1-0.5 mm thick lenses of felsic material throughout.

Microscopic description

Green and foliated thin section with anhedral and oriented hornblende. Fracture cutting the thin section. Some zones contain more quartz, which are fine grained and granular.

Mineral content	Essentials	Modal %	Accessory
	Hornblende	60	Rutile
	Plagioclase	25	Biotite
	Titanite	7	
	Quartz	5	
	Epidote (Czo?)	3	

Texture

Porphyroblastic hornblende with equigranular polygonal matrix.

Mineral description

Hornblendes are porphyroblastic, poikiloblastic, anhedral to subhedral, columnar and foliated. Subhedral and oriented titanite grains parallel to hornblende foliation, concentrated in layers. Polysynthetic twinning in a very few plagioclase grains. The plagioclase and quartz are granular and recrystallized chiefly through SGR.

Facies Amphibolite



Rock name	Ams	Location	AAH_324	Unit	Rørvika
------------------	-----	-----------------	---------	-------------	---------

Macroscopic description

Foliated and layered with pink and dark grey alternating layers. Fine grained and faulted with several parallel faults showing an offset of the layers. The faults zones are white, about 1 mm thick or less, and abundant through the hand specimen.

Microscopic description

Foliated and cataclastic thin section. Green to brown in colour and very fine grained. Green zones (plane polarized light) are rich in hornblende and the white areas are feldspar- and quartz-rich. Epidote concentrated along fault in near proximity. Clasts of host rock within the fault zone.

Mineral content	Essentials	Modal %	Accessory
	Feldspar	55	Rutile
	Epidote	20	
	Hornblende	10	
	Quartz	5	
	Clinozoisite	5	
	Epidote	5	

Texture

Equigranular polygonal to interlobate.

Mineral description

Strong sericitation of plagioclase.

Chlorite and Clinozoisite is found in and close to the fault zones.

Fault zones show very fine grained and crushed grains with smaller clasts of host rock.

Facies Amphibolite



Rock name	Amis	Location	AAH_232	Unit	Rørvika
------------------	------	-----------------	---------	-------------	---------

Macroscopic description

Layered and foliated dark grey to light grey specimen. 2-5 mm big pink garnets found mainly in the light grey layers and with <1 mm thick white halos around the garnets. Fine grained.

Microscopic description

Foliated green thin section segregated into layers rich in hornblende and rich in quartz. Fine grained free of garnets.

Mineral content	Essentials	Modal %	Accessory
	Feldspar	45	Zircon
	Hornblende	40	Titanite
	Quartz	13	
	Opaques	2	

Texture

Equigranular polygonal with porphyroblastic hornblende.

Mineral description

Quartz and feldspar show granoblastic polygonal texture and some of the larger grains show subgrains, indicating recrystallization through SGR

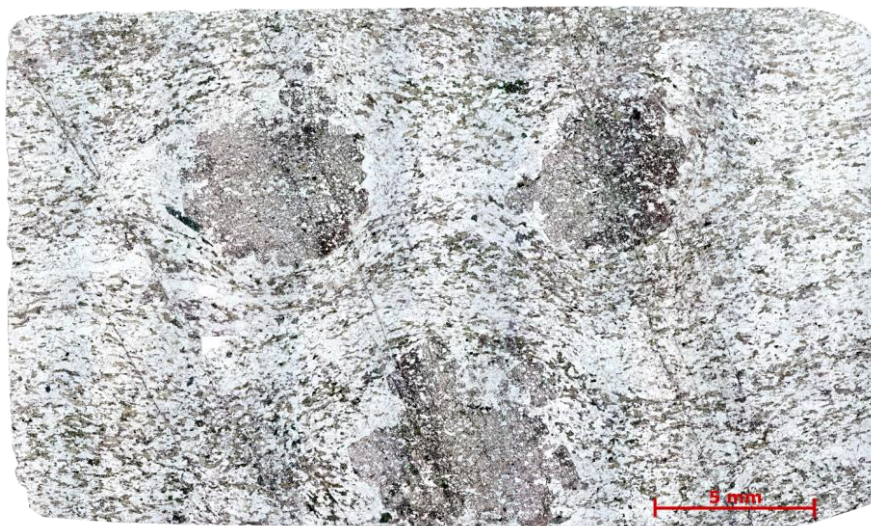
Hornblende grains are anhedral and bladed, some show cleavage and in plane polarized light have a green colour.

The hornblende grains vary in size from 0.1-1mm while the quartz and feldspar have a grain size of about 0.05-0.2mm.

Rounded zircons.

Rhombic and subhedral titanite parallel to the foliation.

Facies Amphibolite



Rock name	Amis	Location	AAH_374	Unit	Rørvika
------------------	------	-----------------	---------	-------------	---------

Macroscopic description

Light grey hand specimen with abundant 0.5-1.5 cm big redish garnets. 0.1-1 mm thick halos around the garnets. Homogeneous matrix with matt luster.

Microscopic description

Green and foliated thin section with three 5-6 mm big garnets. The hornblende is bent around the garnets, which are poikiloblastic and fractured. Fractures running through the thin section also cut the garnets.

Mineral content	Essentials	Modal %	Accessory
	Feldspar	40	Fe-chlorite
	Hornblende	25	Apatite
	Quartz	20	Zircon
	Garnet	13	
	Titanite	2	

Texture

Porphyroblastic garnets with inequigranular interlobate matrix.

Mineral description

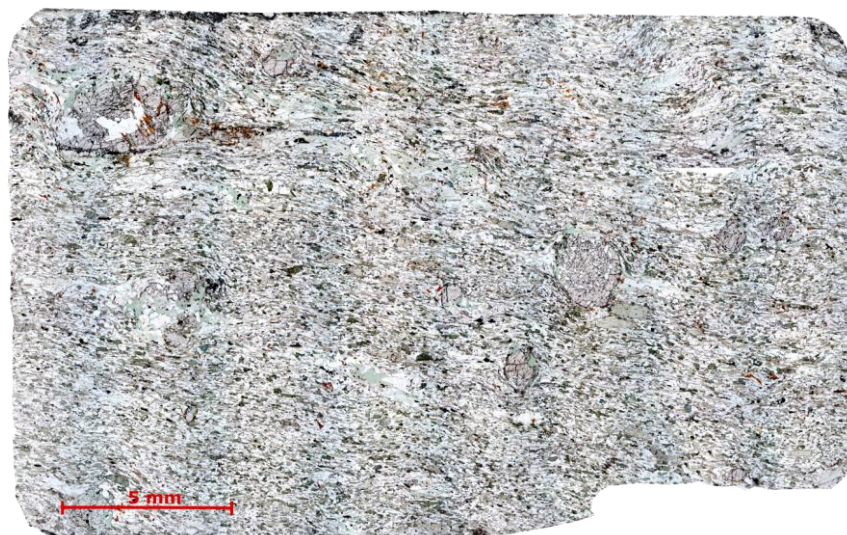
Large porphyroblasts of garnets (skeletal garnet). The garnets are poikiloblastic with inclusions of feldspar, quartz, chlorite, hornblende, and titanite.

The hornblende is foliated and some show alterations to Fe-chlorite.

The foliation is bent around the garnets.

Halos around garnets vary in thickness, being 0.1 mm thick on the upper and lower part of the garnet, and up to 3 mm in lateral extend. The halos consist of equigranular feldspar and quartz grains

Facies	Amphibolite
---------------	-------------



Rock name	Amis	Location	AAH_158	Unit	Rørvika
------------------	------	-----------------	---------	-------------	---------

Macroscopic description

Homogeneous, fine to very fine grained and dark grey in colour. A few 1-2 mm big garnets are spread randomly around. Weakly foliated.

Microscopic description

Foliated thin section with green and oriented hornblende crystals. Fractured and poikiloblastic garnets are found throughout the thin section and vary in size from 0,5-3 mm. Green hornblende concentrated around the garnets.

Mineral content	Essentials	Modal %	Accessory
	Plagioclase	40	Rutile
	Hornblende	30	Spinel?
	Biotite	10	
	Quartz	5	
	Mg-chlorite	5	
	Garnet	5	
	Opaques	3	
	Calcite	2	

Texture

Porphyroblasts of garnets in an equigranular polygonal matrix.

Mineral description

Granular plagioclase and quartz recrystallized primarily through SGR.

Chlorite both as larger and fibrous grains and as fine grained matrix.

Biotite is oriented and acicular.

Hornblende is found as both as subhedral and columnar porphyroblasts, and as fine grained anhedral columnar grains in the matrix.

The garnets are poikiloblastic and fractured. Mg-chlorite with grey interference colour and some calcite in fractures and voids, together with rutile and opaques. Garnets are synkinematic.

Facies	Amphibolite
---------------	-------------



Rock name	Amfs	Location	AAH_253	Unit	Rørvika
------------------	------	-----------------	---------	-------------	---------

Macroscopic description

Coarse grained black and white speckled hand specimen. Matt luster. Some grains seem to show an orientation.

Microscopic description

Coarsed grained quartz- and hornblende-rich thin section. The porphyroblasts are 1-15mm big, while the matrix, consisting of mainly quartz is fined grained. Foliated.

Mineral content	Essentials	Modal %	Accessory
	Plagioclase	47	Rutile
	Hornblende	38	Clinozoisite
	Quartz	10	
	Epidote	3	
	Opaques	2	

Texture

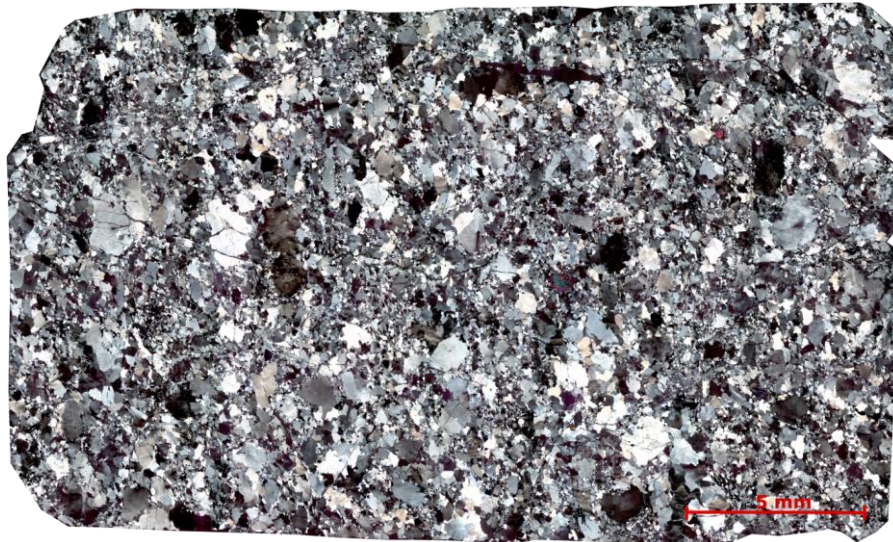
Porphyroblasts of plagioclase and hornblende in an inequigranular polygonal to interlobate matrix.

Mineral description

Porphyroblasts of hornblende and plagioclase, 1-10 mm. Matrix of mainly plagioclase, hornblende, and quartz. The quartz and plagioclase show granoblastic polygonal texture, and the hornblende is anhedral and oriented.

Some plagioclase grains are affected by sericite and some show polysynthetic twinning.

Facies Amphibolite



Rock name	Fams	Location	AAH_149	Unit	Rørvika
------------------	------	-----------------	---------	-------------	---------

Macroscopic description

Light grey to white and fine grained. Zones richer in darker minerals but too fine grained to determine the mineralogical composition.

Microscopic description

White thin section in plane polarized light consisting of quartz and feldspars. Some of the larger feldspar grains are fractured.

Mineral content	Essentials	Modal %	Accessory
	Plagioclase	65	Epidote
	Quartz	32	Muscovite
	Fe-chlorite	3	

Texture

Seriate interlobate (core and mantle texture).

Mineral description

Quartz showing subgrains. Granular and equant.

A very few plagioclase grains show polysynthetic twinning.

Chlorite with blue interference colour indicating high Fe-content.

Main recrystallization mechanism through SGR



Rock name	Fams	Location	AAH_246	Unit	Rørvika
------------------	------	-----------------	---------	-------------	---------

Macroscopic description

Grey to white weakly foliated hand specimen. Very fine grained micas give the rock some luster.

Microscopic description

Granular thin section of quartz and feldspar. In plane polarized light it is white, with a few brown and oriented biotite grains.

Mineral content	Essentials	Modal %	Accessory
	Feldspar	65	Muscovite
	Quartz	30	
	Biotite	4	
	Clinozoisite	1	

Texture

Seriate interlobate (core and mantle texture).

Mineral description

Foliated and acicular biotite.

A few feldspar grains show polysynthetic twinning

Quartz with subgrains.

Chiefly recrystallization mechanism through SGR.



Rock name	Tonalite	Location	AAH_300	Unit	Rørvika
------------------	----------	-----------------	---------	-------------	---------

Macroscopic description

Felsic layer, 11 cm thick and white. Foliated and fine grained. Dark minerals are parallel to the foliation.

Microscopic description

Thin section rich in feldspars and quartz. The thin section is divided in two with one zone showing abundant sericite of the plagioclase and the other does not.

Mineral content	Essentials	Modal %	Accessory
	Feldspar	65	Muscovite
	Quartz	33	Calcite
	Biotite	2	

Texture

Seriate interlobate (core and mantle texture).

Mineral description

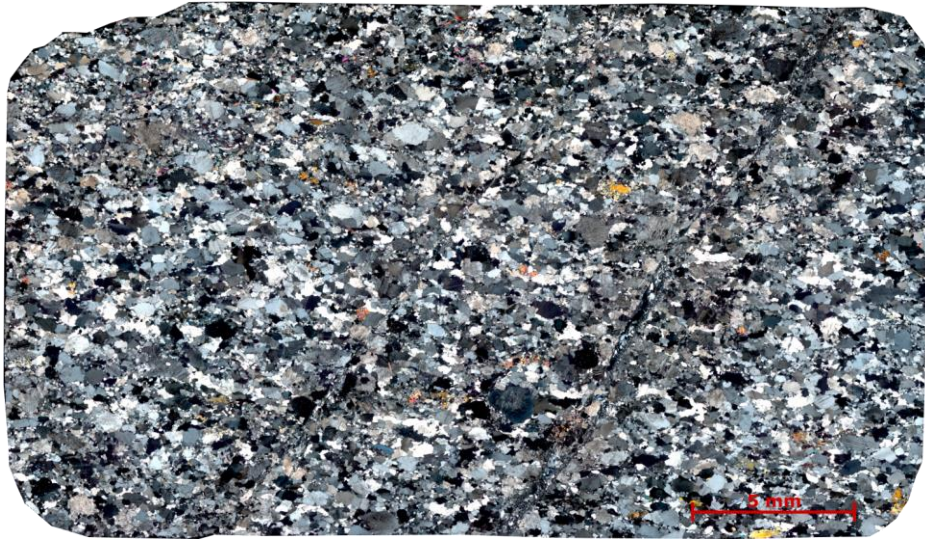
Feldspars show sericite and a few grains show polysynthetic twinning. Some are fractured.

Porphyroblasts of plagioclase and a more fine grained matrix of quartz and plagioclase.

Muscovite found as sericite.

Biotite show green pleochroism and high second order interference colour

Recrystallization has occurred mainly through SGR.



Rock name	Tonalite	Location	AAH_380	Unit	Rørvika
------------------	----------	-----------------	---------	-------------	---------

Macroscopic description

White and medium to fine grained hand specimen. Some very fine grained black minerals. Homogeneous.

Microscopic description

Thin section rich in feldspars and quartz. Subgrains and newly formed grains of quartz. Fractures cutting the sample.

Mineral content	Essentials	Modal %	Accessory
	Feldspar	65	Opagues
	Quartz	33	Epidote
	Hornblende	2	Biotite
	Muscovite	1	Chlorite
			Clinozoisite

Texture

Seriate interlobate.

Mineral description

The quartz and plagioclase show granoblastic texture with quartz showing subgrain domains and fine grained newer quartz grains.

Some of the feldspar grains display polysynthetic twinning.

The epidote and amphibole are poikiloblastic.

Biotite and muscovite are fine grained, acicular, and oriented parallel to sub parallel to the foliation.

Fracture zones consisting of crushed host rock and some chlorite.

Recrystallization through SGR.



Rock name	Hcqs	Location	AAH_164	Unit	Varpneset
------------------	------	-----------------	---------	-------------	-----------

Macroscopic description

Coarse grained and grey rock with larger amphibole crystals showing random orientation. Red garnets spread throughout. Silver luster and strong orange weathering colour.

Microscopic description

Coarse grained thin section with 2-4mm big garnets, 1-8mm big bladed and dissolved anhedral actinolite and hornblende grains. Orientation of minerals show foliation, most clear in the mica-rich zones.

Mineral content	Essentials	Modal %	Accessory
	Plagioclase	25	Rutile
	Amphibole	20	Zircon
	Calcite	15	
	Biotite	13	
	Quartz	10	
	Garnet	5	
	Chlorite	2	

Texture

Porphyroblastic garnets, actinolites and hornblende with an equigranular interlobate matrix.

Mineral description

Secondary calcite as grains and as very fine grained aggregates.

Plagioclase with sericite. Quartz is granular. Chlorite is fibrous.

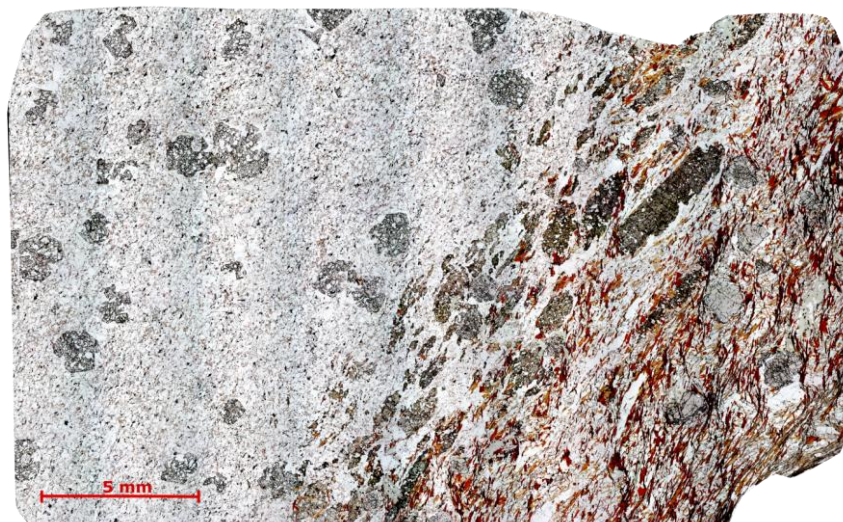
Large amphibole crystals are poikiloblastic and anhedral, with inclusions of quartz and muscovite, grey. 1 order interference colour, and with abundant pleochroic halos. Not parallel to the foliation. Smaller amphibole crystals are subhedral, parallel to foliation, have higher interference colours and with fewer inclusions.

Garnets are anhedral to subhedral and poikiloblastic.

Coarse grained muscovites are deformed and show a crenulated appearance.

The micas are acicular and the biotite contains pleochroic halos.

Facies Amphibolite



Rock name	Hcqs	Location	AAH_165	Unit	Varpneset
------------------	------	-----------------	---------	-------------	-----------

Macroscopic description

Foliated and layered medium grained rock. White layers rich in quartz and darker layers containing micas and hornblende. 0.2-1 mm big pink to reddish garnets throughout. Orange weathering colour.

Microscopic description

Thin section divided into two parts, one quartz- and feldspar-rich part and one part with bladed hornblende and biotite. Subhedral porphyroblasts of garnets throughout. Foliated.

Mineral content	Essentials	Modal %	Accessory
	Feldspar	35	Muscovite
	Calcite	25	Rutile
	Biotite	15	
	Quartz	10	
	Garnet	8	
	Amphibole	6	
	Mg-chlorite	1	

Texture

Porphyroblasts of garnets and amphibole in a granular polygonal matrix.

Mineral description

The amphiboles form oriented prismatic sub- to anhedral grains.

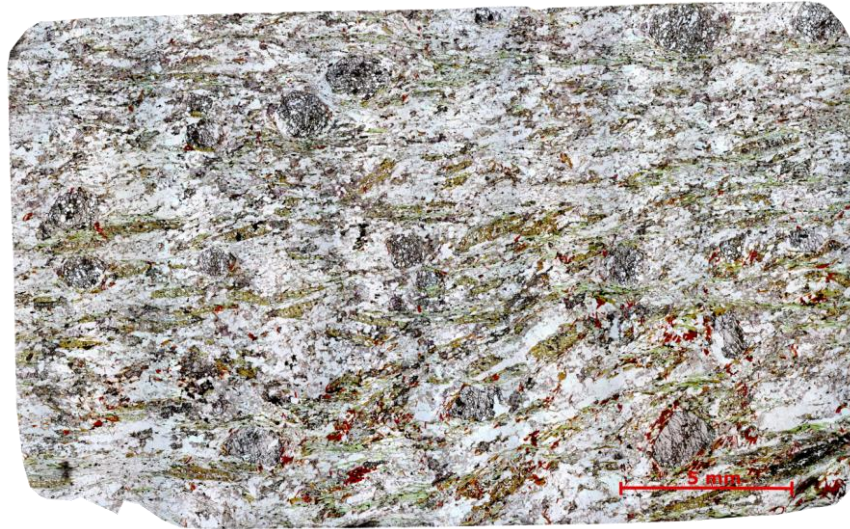
Bladed biotite parallel to sub parallel of the direction of amphiboles.

Garnets are poikiloblastic with mostly quartz and feldspars inclusions. Garnets in the quartz-rich zone are more poikiloblastic than the garnets within the biotite- and amphibole-zone.

Matrix contains quartz, feldspars and calcite with a granular texture. Higher concentration of calcite in the zone lacking biotite and amphibole.

Mg-chlorite with grey interference colours.

Facies	Amphibolite
---------------	-------------



Rock name	Hcqs	Location	AAH_162	Unit	Varpneset
------------------	------	-----------------	---------	-------------	-----------

Macroscopic description

Dark grey to greenish sample with dark grey silver luster. Fine to medium grain size. Foliated and rich in quartz.

Microscopic description

Foliated sample with 1.5-3 mm big anhedral to subhedral garnets. With green amphiboles and brown biotite. The oriented amphiboles are bladed and poikiloblastic.

Mineral content	Essentials	Modal %	Accessory
	Plagioclase	30	Rutile
	Calcite	20	
	Quartz	15	
	Biotite	15	
	Amphibole	6	
	Mg-chlorite	6	
	Muscovite	5	
	Garnet	3	

Texture

Porphyroblastic with equigranular polygonal matrix.

Mineral description

Biotite is acicular and brown, parallel to foliation. Porphyroblasts of garnet and hornblende. Garnets are fractured and poikiloblastic (skeletal garnets). Within the garnets inclusions of quartz and calcite are found. The amphiboles show anhedral to subhedral prismatic grains, also these are poikiloblastic, with chlorite in voids. Granular quartz and calcite. There are replacements with chlorite in the garnets. Plagioclase shows some sericite. Main recrystallization mechanism is SGR.

Facies	Amphibolite
---------------	-------------

Appendix I – Sample analysis XRF

Results from sample analysis with XRF

Main elements

Sample Unit Type	AAH_349 Trongen Aplite %	AAH_185 Trongen Aplite %	AAH_149 Rørvika Fams %	AAH_246 Rørvika Fams %	AAH_300 Rørvika Aplite %	AAH_380 Rørvika Aplite %	AAH_281 Rørvika Ams %
SiO ₂	74.1	72.5	71.1	71.3	69.6	71.7	50.8
Al ₂ O ₃	15.4	15.7	16.8	16.5	17.9	17.0	14.5
Fe ₂ O ₃	0.746	0.528	0.992	1.10	0.608	0.547	9.76
TiO ₂	0.076	0.085	0.144	0.145	0.144	0.062	2.26
MgO	0.255	0.291	0.319	0.314	0.257	0.198	6.45
CaO	1.83	1.85	2.32	2.51	1.88	2.71	10.3
Na ₂ O	5.91	5.91	7.10	6.68	8.64	6.95	3.35
K ₂ O	0.962	1.09	0.352	0.546	0.331	0.409	0.111
MnO	0.014	0.011	0.010	0.013	<0.01	<0.01	0.146
P ₂ O ₅	0.041	0.048	0.040	0.045	0.048	0.049	0.198
LOI	0.560	0.848	0.469	0.255	0.255	0.325	0.834
SUM	99.9	98.9	99.7	99.4	99.6	99.9	98.8
BaO	0.028	0.049	b.d	b.d	b.d	b.d	b.d
Cr ₂ O ₃	b.d	b.d	b.d	b.d	b.d	b.d	b.d
CuO	b.d	b.d	b.d	0.014	b.d	b.d	b.d
NiO	b.d	b.d	b.d	b.d	b.d	b.d	b.d
PbO	b.d	b.d	b.d	b.d	b.d	b.d	b.d
SrO	0.100	0.095	0.099	0.101	0.075	0.068	b.d
ZnO	b.d	b.d	b.d	b.d	b.d	b.d	b.d
V ₂ O ₅	b.d	b.d	b.d	b.d	b.d	b.d	0.069
ZrO ₂	b.d	b.d	b.d	b.d	b.d	b.d	0.024
SO ₃	b.d	b.d	b.d	b.d	b.d	b.d	b.d

b.d = below detection limit

Trace elements

Sample	AAH_349	AAH_185	AAH_149	AAH_246	AAH_300	AAH_380	AAH_281
Unit	Trongen	Trongen	Rørvika	Rørvika	Rørvika	Rørvika	Rørvika
Type	Aplite	Aplite	Fams	Fams	Aplite	Aplite	Ams
	Mg/kg	Mg/kg	Mg/kg	Mg/kg	Mg/kg	Mg/kg	Mg/kg
As	b.d	b.d	b.d	b.d	b.d	b.d	b.d
Ba	252	387	133	162	67	181	27
Cd	b.d	b.d	b.d	b.d	b.d	b.d	b.d
Ce	b.d	b.d	b.d	b.d	b.d	b.d	26
Co	b.d	b.d	b.d	b.d	b.d	b.d	27.3
Cr	15.1	b.d	b.d	b.d	8.8	9.7	124
Cu	21.1	b.d	b.d	b.d	b.d	b.d	7.6
Ga	13.9	14.6	16.7	15.9	14.5	13.9	17.4
La	b.d	b.d	b.d	b.d	b.d	b.d	b.d
Mo	b.d	b.d	b.d	b.d	b.d	b.d	b.d
Nb	3.0	2.8	2.8	2.6	2.6	2.6	7.3
Nd	b.d	b.d	b.d	b.d	b.d	b.d	14
Ni	b.d	b.d	b.d	b.d	b.d	b.d	45.9
Pb	18.9	11.4	b.d	b.d	b.d	5.3	<5
Rb	26.6	29.6	b.d	13.2	b.d	7.8	<5
Sb	b.d	b.d	b.d	b.d	b.d	b.d	b.d
Sc	b.d	b.d	b.d	b.d	b.d	b.d	28.7
Sn	b.d	b.d	b.d	b.d	b.d	b.d	8.1
Sr	863	848	862	885	650	587	191
Th	b.d	b.d	b.d	b.d	b.d	b.d	b.d
U	b.d	b.d	b.d	b.d	b.d	b.d	b.d
V	11.2	7.8	14.3	12.8	20.9	6.7	348
W	b.d	b.d	b.d	b.d	b.d	b.d	b.d
Y	b.d	b.d	b.d	b.d	b.d	b.d	46.0
Yb	b.d	b.d	b.d	b.d	b.d	b.d	b.d
Zn	8.0	11.1	5.7	20.7	b.d	b.d	25.3
Zr	45.1	66.3	87.5	89.8	74.1	56.5	151
Cl	b.d	b.d	b.d	b.d	b.d	b.d	b.d
F	b.d	b.d	b.d	b.d	b.d	b.d	b.d
S	b.d	b.d	b.d	b.d	b.d	b.d	b.d
Cs	b.d	b.d	b.d	b.d	b.d	b.d	b.d
Hf	b.d	b.d	b.d	b.d	b.d	b.d	b.d
Sm	b.d	b.d	b.d	b.d	b.d	b.d	b.d
Ta	b.d	b.d	b.d	b.d	b.d	b.d	b.d

b.d = below detection limit

Appendix J – U-Pb zircon analysis (DU = Detector unreliable)

Analysis number	Concordia output				Terra-Wasserburg output				Age estimates (ma)						Concentrations				Pb com.	Comment		
	$\frac{Pb207}{U235}$	1s%	$\frac{Pb206}{U238}$	1s%	roh	$\frac{U238}{Pb206}$	1s%	$\frac{Pb207}{Pb206}$	1s%	$\frac{Pb207}{U235}$	1s	$\frac{Pb206}{U238}$	1s	conc	Th/U	U	Th	Phtot				
1SDGA4_026	0.5423	1.34	0.0695	0.75	0.56	14.380	0.75	0.0565	1.11	474	25	440	5	433	3	91	0.41	701	285	60	2	DU
1SDGA4_025	0.5084	1.54	0.0664	0.77	0.5	15.048	0.77	0.0555	1.33	432	29	417	5	415	3	96	0.26	477	126	37	2.6	DU
1SDGA4_024	0.5109	1.41	0.0624	0.75	0.53	16.020	0.75	0.0593	1.2	581	26	419	5	390	3	67	0.35	398	138	30	3	
1SDGA4_023	0.5297	1.39	0.0692	0.75	0.54	14.432	0.75	0.0554	1.17	430	26	432	5	432	3	100	0.29	321	92	26	-	
1SDGA4_022	0.5209	1.33	0.0662	0.74	0.56	15.103	0.74	0.0570	1.1	494	25	426	5	413	3	84	0.46	859	391	70	1	DU
1SDGA4_021	0.5865	1.34	0.0752	0.74	0.56	13.290	0.74	0.0565	1.11	473	25	469	5	468	3	99	0.52	760	399	71	1	DU
1SDGA4_020	0.5642	1.71	0.0737	0.79	0.46	13.553	0.79	0.0554	1.51	431	33	454	6	459	4	106	0.32	192	62	17	6	
1SDGA4_019	0.5478	1.38	0.0702	0.75	0.55	14.226	0.75	0.0565	1.15	473	25	444	5	438	3	93	0.43	601	256	52	2	DU
1SDGA4_018	0.5543	1.52	0.0701	0.77	0.51	14.253	0.77	0.0573	1.31	503	29	448	6	437	3	87	1.14	121	1382	106	1	DU
1SDGA4_017	0.5564	1.85	0.0704	0.81	0.44	14.194	0.81	0.0572	1.66	502	36	449	7	439	3	87	0.96	147	141	13	-	
1SDGA4_016	0.5411	1.56	0.0696	0.77	0.5	14.351	0.77	0.0563	1.35	464	30	439	6	434	3	94	1.25	690	861	61	-	
1SDGA4_015	0.5855	1.53	0.0727	0.77	0.5	13.753	0.77	0.0584	1.32	545	29	468	6	453	3	83	1.31	761	999	72	1	DU
1SDGA4_014	0.5472	1.5	0.0698	0.77	0.52	14.310	0.77	0.0567	1.29	483	28	443	5	436	3	90	0.95	503	478	43	3	DU
1SDGA4_013	0.5249	1.49	0.0678	0.78	0.53	14.734	0.78	0.0560	1.27	456	28	428	5	423	3	93	0.19	975	181	72	-	DU
1SDGA4_012	0.5425	1.49	0.0705	0.78	0.52	14.180	0.78	0.0557	1.27	444	28	440	5	439	3	99	0.42	405	171	32	5	
1SDGA4_011	0.5325	1.55	0.0700	0.79	0.51	14.281	0.79	0.0551	1.34	419	29	434	6	436	3	104	0.69	253	174	21	-	
1SDGA4_010	0.5285	1.46	0.0700	0.77	0.53	14.269	0.77	0.0546	1.24	400	27	431	5	437	3	109	1.31	131	1728	117	1	DU
1SDGA4_009	0.5422	1.46	0.0677	0.77	0.53	14.758	0.77	0.0580	1.24	531	27	440	5	423	3	80	0.99	922	913	77	1.4	DU
1SDGA4_008	0.5446	1.84	0.0708	0.82	0.44	14.122	0.82	0.0557	1.65	443	36	441	7	441	4	99	1.34	127	170	12	-	DU
1SDGA4_007	0.5612	2.05	0.0740	0.84	0.41	13.504	0.84	0.0549	1.87	411	41	452	8	461	4	112	1.29	67	86	6	-	DU
1SDGA4_006	0.6029	1.46	0.0780	0.78	0.54	12.809	0.78	0.0560	1.23	452	27	479	6	485	4	107	2.24	603	1351	66	-	
1SDGA4_005	0.5965	1.57	0.0786	0.79	0.5	12.722	0.79	0.0550	1.36	414	30	475	6	488	4	118	1.12	986	1107	95	1	DU
1SDGA4_004	0.5954	1.4	0.0761	0.77	0.55	13.133	0.77	0.0567	1.16	480	26	474	5	473	4	99	1.34	143	1921	139	-	DU
1SDGA4_003	0.5843	1.38	0.0759	0.76	0.55	13.163	0.76	0.0557	1.15	444	25	467	5	472	4	106	1.2	122	1468	116	1	DU
1SDGA4_002	0.5574	1.5	0.0717	0.78	0.52	13.929	0.78	0.0563	1.28	464	28	450	5	447	3	96	1.13	447	504	40	5	
1SDGA4_001	0.5539	1.35	0.0727	0.77	0.57	13.751	0.77	0.0552	1.1	422	25	448	5	453	3	107	1.59	376	5978	356	0	DU

Appendix K - Localities

Locality number	Longitude	Latitude	Lithology	Unit
KSV_102	551618.8433	7041375.626	Ams	Trongen
KSV_103	551672.0585	7041380.267	Ams	Trongen
KSV_104	552264.7056	7041158.024	Hbs	Trongen
KSV_105	552340.7886	7041192.062	Hbs	Trongen
KSV_106	552408.863	7041178.046	Am	Trongen
KSV_107	552601.0728	7041376.263	Helle	Trongen
KSV_108	552801.2914	7041370.256	Helle	Trongen
KSV_109	552827.5656	7041365.764	Helle	Trongen
KSV_110	552870.9111	7041356.328	Helle	Trongen
KSV_111	552909.1135	7041355.333	Helle	Trongen
KSV_112	552970.9032	7041365.145	Helle	Trongen
KSV_113	552757.9132	7041523.234	Ghms	Trongen
KSV_114	552865.7311	7041461.718	Helle	Trongen
KSV_115	552978.7657	7041453.668	Ams	Trongen
KSV_116	552982.3476	7041465.608	Ams	Trongen
KSV_117	553000.854	7041487.696	Ams	Trongen
KSV_118	553107.0199	7041532.5	no outcrop	Trongen
KSV_54	549240.4949	7040205.898	Ing	Rødberget
KSV_55	549164.0793	7040239.748	Ing	Rødberget
KSV_56	549201.6645	7040354.828	Ing	Rødberget
KSV_57	549246.9084	7040461.985	Ing	Rødberget
KSV_58	549209.6021	7040454.047	Ing	Rødberget
KSV_59	549212.626	7040523.218	Ing	Rødberget
KSV_60	549198.3384	7040604.181	Ing	Rødberget
KSV_61	549191.1947	7040626.406	Ing	Rødberget
KSV_62	549171.3509	7040701.812	Ing	Rødberget
KSV_63	549262.6323	7040291.443	Ing	Rødberget
KSV_83	553396.3043	7041081.243	Helle	Trongen
KSV_84	553433.7124	7041085.4	Ghms	Trongen
KSV_85	553394.2261	7041079.165	Ghms	Trongen
KSV_86	553344.3487	7041052.148	Helle	Trongen
KSV_87	553306.9406	7041060.461	Helle	Trongen
KSV_88	553279.9237	7041085.4	Helle	Trongen
KSV_89	553291.2235	7041086.736	Helle	Trongen
KSV_90	552184.9177	7041516.843	Helle	Trongen
KSV_91	552892.0334	7041157.473	Helle	Trongen
KSV_92	552948.7678	7041200.407	Helle	Trongen
KSV_93	552649.403	7041205.165	Helle	Trongen
KSV_94	552551.7167	7041074.917	Helle	Trongen
KSV_95	552577.0428	7041013.41	Ams	Trongen
KSV_96	552597.8628	7041010.713	Ams	Trongen
KSV_97	552606.1513	7041015.548	Ams	Trongen
KSV_98	552610.0436	7041013.257	Ghms	Trongen
KSV_99	552623.5648	7041021.578	Helle	Trongen

table continued on following page

table continued from previous page				
AAH_111	554978.6577	7041451.334	Ghms	Trongen
AAH_112	554953.054	7041441.965	Ghms	Trongen
AAH_113	554924.9019	7041432.744	Ghms	Trongen
AAH_114	554817.1361	7041413.902	Ghms	Trongen
AAH_115	554709.9796	7041417.21	Ghms	Trongen
AAH_116	554653.7555	7041437.053	Ghms	Trongen
AAH_117	554427.8009	7041487.457	Ghms	Trongen
AAH_118	554249.6037	7041417.342	Ghms	Trongen
AAH_119	554221.1609	7041410.727	Ghms	Trongen
AAH_120	553142.9817	7041003.268	Hbs	Trongen
AAH_121	553164.2882	7041012.559	Hbs	Trongen
AAH_122	553181.1729	7041013.382	Hbs	Trongen
AAH_123	553194.4021	7041016.028	Hbs	Trongen
AAH_124	553213.9152	7041018.343	Hbs	Trongen
AAH_125	552524.871	7040745.02	Ghms	Trongen
AAH_126	552524.871	7040745.02	Ghms	Trongen
AAH_127	552552.2041	7040759.24	Ghms	Trongen
AAH_128	552575.6615	7040764.312	Ghms	Trongen
AAH_129	552590.2432	7040765.58	Ghms	Trongen
AAH_130	552597.217	7040783.332	Hbs	Trongen
AAH_131	552620.0405	7040766.214	Ghms	Trongen
AAH_132	552642.23	7040764.312	Ghms	Trongen
AAH_133	552675.8312	7040786.502	Ghms	Trongen
AAH_134	552692.9488	7040802.351	Ghms	Trongen
AAH_135	552692.9488	7040802.351	Ghms	Trongen
AAH_136	552700.5566	7040800.449	Ghms	Trongen
AAH_137	552704.9945	7040805.521	Ghms	Trongen
AAH_138	552704.9945	7040805.521	Ghms	Trongen
AAH_139	552731.5516	7040826.088	Ghms	Trongen
AAH_140	552757.9518	7040834.069	Ghms	Trongen
AAH_141	552768.3891	7040843.892	Ghmbs	Trongen
AAH_142	552976.6196	7042027.28	Ghms	Trongen
AAH_143	551319.2398	7042734.549	Ams	Trongen
AAH_144	551283.0658	7042745.631	Ams	Trongen
AAH_145	551205.6406	7042788.98	Ams	Trongen
AAH_146	550953.5056	7042911.815	Ams	Trongen
AAH_147	552712.5035	7042455.676	Ghmbs	Trongen
AAH_148	555319.5658	7042126.449	Amfs	Rørvika
AAH_149	555179.0481	7042096.84	Fams	Rørvika
AAH_150	555130.167	7042039.434	Amfs	Rørvika
AAH_151	556977.9878	7043661.233	Hcqs	Varpneset
AAH_152	556977.9878	7043661.233	Hcqs	Varpneset
AAH_153	556944.2243	7043648.036	Hqs	Varpneset
AAH_154	556860.7551	7043548.171	Hqs	Varpneset
AAH_155	556847.3403	7043528.794	Hcqs	Varpneset
AAH_156	556829.4541	7043527.304	Hcqs	Varpneset

table continued on following page

Appendices

table continued from previous page				
AAH_157	556829.4541	7043498.984	Hcqs	Varpneset
AAH_158	556775.0089	7043400.331	Amis	Rørvika
AAH_159	556752.9609	7043313.189	Amis	Rørvika
AAH_160	558032.6616	7044760.303	Hcqs	Varpneset
AAH_161	557759.5974	7044648.747	Hcqs	Varpneset
AAH_162	557689.7005	7044557.881	Hqs	Varpneset
AAH_163	557563.8859	7044439.056	Hqs	Varpneset
AAH_164	557169.0443	7043955.913	Hcqs	Varpneset
AAH_165	557169.0443	7043927.038	Hcqs	Varpneset
AAH_166	557108.6704	7043840.415	Hcqs	Varpneset
AAH_167	557011.5472	7043722.292	Hcqs	Varpneset
AAH_168	557537.5573	7044246.149	Hcqs	Varpneset
AAH_169	557514.438	7044221.895	Hcqs	Varpneset
AAH_170	557496.1539	7044214.581	Hcqs	Varpneset
AAH_171	557439.4735	7044146.93	Hcqs	Varpneset
AAH_172	557419.3611	7044108.534	Hcqs	Varpneset
AAH_173	557401.0771	7044066.48	Hcqs	Varpneset
AAH_174	557401.0771	7044066.48	Hcqs	Varpneset
AAH_175	557357.1954	7044006.143	Hcqs	Varpneset
AAH_176	557313.3138	7043953.119	Hcqs	Varpneset
AAH_177	554424.4046	7041166.984	Hbs	Trongen
AAH_178	554544.6251	7041197.516	Ghms	Trongen
AAH_179	554477.3954	7041180.03	Ghms	Trongen
AAH_180	554401.3194	7041166.016	Hbs	Trongen
AAH_181	554378.0997	7041171.672	Ghms	Trongen
AAH_182	554355.7998	7041171.933	Hbs	Trongen
AAH_183	554343.0997	7041170.874	Ghms	Trongen
AAH_184	554288.0663	7041176.166	Ghms	Trongen
AAH_185	554253.1412	7041179.341	Ghms	Trongen
AAH_186	552378.504	7041586.416	Helle	Trongen
AAH_187	552310.7537	7041560.284	Helle	Trongen
AAH_188	552327.2074	7041505.116	Helle	Trongen
AAH_189	552322.3681	7041465.434	Helle	Trongen
AAH_190	552254.6178	7041564.93	Hbs	Trongen
AAH_191	552059.11	7041441.044	Helle	Trongen
AAH_192	552017.492	7041409.104	Ghmbs	Trongen
AAH_193	552012.6527	7041356.84	Helle	Trongen
AAH_194	552150.0889	7041215.532	Ghms	Trongen
AAH_195	552087.9218	7041035.788	Ghmbs	Trongen
AAH_196	552012.9836	7041042.506	Ghms	Trongen
AAH_197	552064.5775	7040948.05	Ghms	Trongen
AAH_198	552097.6504	7040919.21	Ghmbs	Trongen
AAH_199	552251.6383	7040981.123	Helle	Trongen
AAH_200	552392.926	7041028.748	Helle	Trongen
AAH_201	552354.826	7041135.111	Ams	Trongen
AAH_202	552318.3134	7041119.236	Helle	Trongen

table continued on following page

table continued from previous page				
AAH_203	557288.5563	7043831.03	Hcqs	Varpneset
AAH_204	557236.2941	7043671.493	Hcqs	Varpneset
AAH_205	557192.2838	7043663.241	Hcqs	Varpneset
AAH_206	557175.6117	7043650.599	Hcqs	Varpneset
AAH_207	557165.2173	7043655.252	Hcqs	Varpneset
AAH_208	557155.4795	7043654.919	Hcqs	Varpneset
AAH_209	557128.5878	7043664.194	Hcqs	Varpneset
AAH_210	557085.6723	7043646.877	Hcqs	Varpneset
AAH_211	557055.9066	7043632.987	Hcqs	Varpneset
AAH_212	557030.7711	7043601.898	Hqs	Varpneset
AAH_213	557019.5263	7043593.299	Hqs	Varpneset
AAH_214	556993.0679	7043571.471	Hcqs	Varpneset
AAH_215	556984.4689	7043531.783	Hcqs	Varpneset
AAH_216	556959.4346	7043496.821	Hcqs	Varpneset
AAH_217	556955.7604	7043471.715	Hcqs	Varpneset
AAH_218	556946.5751	7043453.956	Hcqs	Varpneset
AAH_219	556938.6145	7043441.097	Hcqs	Varpneset
AAH_220	556944.738	7043434.973	Hcqs	Varpneset
AAH_221	556931.2662	7043392.108	Hcqs	Varpneset
AAH_228	556755.36	7042978.102	Amis	Rørvika
AAH_229	556787.3917	7043114.117	Amis	Rørvika
AAH_230	556804.3251	7043091.892	Amis	Rørvika
AAH_231	556801.15	7043069.667	Amis	Rørvika
AAH_232	556803.2667	7042973.358	Amis	Rørvika
AAH_233	556395.4924	7042759.368	Amis	Rørvika
AAH_234	556339.2127	7042696.296	Amis	Rørvika
AAH_235	556314.3087	7042612.605	Amis	Rørvika
AAH_236	556277.951	7042469.868	Amis	Rørvika
AAH_237	556236.8248	7042295.285	Amfs	Rørvika
AAH_238	556017.9305	7042441.658	Amfs	Rørvika
AAH_239	555936.4958	7042338.923	Amfs	Rørvika
AAH_240	555916.4152	7042334.224	Amfs	Rørvika
AAH_241	555900.2282	7042334.609	Amfs	Rørvika
AAH_242	555786.3468	7042250.588	Amfs	Rørvika
AAH_243	555746.9564	7042231.683	Amfs	Rørvika
AAH_244	555672.8035	7042201.014	Amfs	Rørvika
AAH_245	555388.4129	7041645.626	Amfs	Rørvika
AAH_246	555441.1241	7041686.998	Fams	Rørvika
AAH_247	555434.2234	7041734.465	Amfs	Rørvika
AAH_248	555407.0114	7041724.408	Fams	Rørvika
AAH_249	555356.5987	7041699.793	Fams	Rørvika
AAH_250	555330.9836	7041718.183	Amfs	Rørvika
AAH_251	555300.2734	7041717.427	Amfs	Rørvika
AAH_252	555293.2729	7041721.986	Amfs	Rørvika
AAH_253	555279.7603	7041723.158	Amfs	Rørvika
AAH_254	555262.8711	7041720.679	Amfs	Rørvika

table continued on following page

Appendices

table continued from previous page				
AAH_255	555213.4588	7041721.606	Fams	Rørvika
AAH_256	555206.487	7041713.015	Amfs	Rørvika
AAH_257	555201.2409	7041699.662	Amfs	Rørvika
AAH_258	555168.4453	7041701.434	Amfs	Rørvika
AAH_259	555139.3484	7041705.277	Amfs	Rørvika
AAH_260	555120.8666	7041705.738	Amfs	Rørvika
AAH_261	555099.3075	7041711.383	Amfs	Rørvika
AAH_262	555080.9927	7041707.946	Amfs	Rørvika
AAH_263	555047.6341	7041690.43	Amfs	Rørvika
AAH_264	555014.9966	7041677.273	Amfs	Rørvika
AAH_265	555002.0072	7041659.552	Ghms	Trongen
AAH_266	555049.2523	7041642.87	Amfs	Rørvika
AAH_267	555058.3236	7041625.084	Amfs	Rørvika
AAH_268	555055.6624	7041623.478	Ghms	Trongen
AAH_269	555079.5425	7041598.815	Ghms	Trongen
AAH_270	555079.935	7041599.156	Ghms	Trongen
AAH_271	555088.6223	7041594.96	Ghms	Trongen
AAH_272	555101.6757	7041603.21	Ghms	Trongen
AAH_273	555101.4892	7041611.119	Amfs	Rørvika
AAH_274	555121.1081	7041582.371	Ghms	Trongen
AAH_275	555116.9367	7041575.947	Ghms	Trongen
AAH_276	555072.9172	7041544.204	Ghms	Trongen
AAH_277	555001.7391	7041447.131	Ghms	Trongen
AAH_278	554935.6615	7041429.498	Ghms	Trongen
AAH_279	554512.6623	7041674.547	Ams	Trongen
AAH_280	554594.285	7041752.507	Ams	Rørvika
AAH_281	554559.5814	7041813.431	Ams	Rørvika
AAH_282	554590.9248	7041681.236	Ghms	Trongen
AAH_283	554757.5582	7041746.727	Ams	Rørvika
AAH_284	554821.7475	7041792.744	Fams	Rørvika
AAH_285	554958.1614	7041949.78	Amfs	Rørvika
AAH_286	555057.8505	7042018.48	Amfs	Rørvika
AAH_287	555073.2664	7042123.282	Amfs	Rørvika
AAH_288	555114.9131	7042257.18	Fams	Rørvika
AAH_289	555108.9166	7042675.778	Amfs	Rørvika
AAH_290	554923.0751	7042564.021	Ghms	Rørvika
AAH_291	554880.2949	7042567.964	Amfs	Rørvika
AAH_292	554936.5304	7042664.22	Amfs	Rørvika
AAH_293	554895.7717	7042426.695	Fams	Rørvika
AAH_294	554841.5102	7042380.29	Fams	Rørvika
AAH_295	554805.5813	7042246.272	Amfs	Rørvika
AAH_296	554691.8272	7042039.926	Amfs	Rørvika
AAH_297	554640.656	7042010.184	Amfs	Rørvika
AAH_298	554433.0995	7041965.508	Amfs	Rørvika
AAH_299	554352.757	7041973.164	Amfs	Rørvika
AAH_300	554111.2594	7042065.008	Ams	Rørvika

table continued on following page

table continued from previous page				
AAH_301	553687.3606	7042112.334	Ams	Rørvika
AAH_302	553683.0014	7042335.596	Ams	Rørvika
AAH_303	553447.7728	7042015.027	Ams	Rørvika
AAH_304	554209.2894	7041406.585	Hbs	Trongen
AAH_305	554097.9645	7041399.233	Hbs	Trongen
AAH_306	553590.6694	7041721.765	Ghms	Trongen
AAH_307	553462.6514	7041727.638	Ghms	Trongen
AAH_308	553722.5061	7041356.44	Ghms	Trongen
AAH_309	553517.0559	7041251.346	Helle	Trongen
AAH_310	553478.5438	7041198.878	Helle	Trongen
AAH_311	553457.9974	7041218.37	Helle	Trongen
AAH_312	553443.2882	7041234.283	Helle	Trongen
AAH_313	553449.6716	7041177.331	Helle	Trongen
AAH_314	553401.3603	7041150.777	Helle	Trongen
AAH_315	553316.5263	7041140.107	Helle	Trongen
AAH_316	553263.2591	7041132.864	Helle	Trongen
AAH_317	553220.6909	7041149.985	Helle	Trongen
AAH_318	553107.2834	7041120.566	Helle	Trongen
AAH_319	553076.1034	7041075.915	Helle	Trongen
AAH_320	553109.6894	7041074.803	Helle	Trongen
AAH_321	553133.3975	7041035.858	Hbs	Trongen
AAH_322	553139.3654	7041000.518	Hbs	Trongen
AAH_323	553112.0333	7040972.982	Ghms	Trongen
AAH_324	553067.2119	7042133.15	Ams	Rørvika
AAH_325	553167.4913	7041870.03	Ghms	Trongen
AAH_326	552743.3879	7042230.079	Ghms	Trongen
AAH_327	552388.5268	7042335.668	Ghms	Trongen
AAH_328	552857.3643	7041928.84	Ams	Trongen
AAH_329	552863.0547	7041900.962	Ams	Trongen
AAH_330	552697.6581	7041728.939	Ams	Trongen
AAH_331	552457.1956	7041590.57	Ghms	Trongen
AAH_332	552479.9472	7041563.641	Ghms	Trongen
AAH_333	552612.165	7041412.14	Ghms	Trongen
AAH_334	552455.6691	7041429.174	Ghms	Trongen
AAH_335	552515.3908	7041346.687	Ams	Trongen
AAH_336	552382.2823	7041207.086	Ams	Trongen
AAH_337	552356.279	7041195.403	Ams	Trongen
AAH_338	552244.2111	7041184.203	Ghms	Trongen
AAH_339	552258.3086	7041056.385	Ghms	Trongen
AAH_340	552306.6433	7041121.593	Ghms	Trongen
AAH_341	552100.2238	7041078.315	Ghms	Trongen
AAH_342	549735.2201	7040274.042	Ing	Rødberget
AAH_343	549752.9002	7040334.942	Ing	Rødberget
AAH_344	549756.2106	7040355.833	Ing	Rødberget
AAH_345	549767.1563	7040426.881	Ing	Rødberget
AAH_346	549682.2188	7040273.996	Ing	Rødberget

table continued on following page

Appendices

table continued from previous page				
AAH_347	549361.0688	7040647.24	Ing	Rødberget
AAH_348	552169.0805	7040714.353	Ghmbs	Trongen
AAH_349	552817.7287	7040868.238	Hbs	Trongen
AAH_350	552887.0962	7040899.032	Helle	Trongen
AAH_351	556810.1759	7043000.573	Amis	Rørvika
AAH_352	556794.3692	7042964.965	Amis	Rørvika
AAH_353	556800.5037	7042948.402	Amis	Rørvika
AAH_354	556803.571	7042932.452	Amis	Rørvika
AAH_355	556801.7306	7042919.57	Amis	Rørvika
AAH_356	556799.8903	7042913.435	Amis	Rørvika
AAH_357	556737.5445	7043160.2	Amis	Rørvika
AAH_358	556743.0465	7043130.64	Amis	Rørvika
AAH_359	556744.5216	7043101.138	Amis	Rørvika
AAH_360	556744.5216	7043101.138	Ams	Rørvika
AAH_361	556743.0465	7043074.587	Amis	Rørvika
AAH_362	556760.7475	7043058.361	Amis	Rørvika
AAH_363	556735.8205	7043021.666	Amis	Rørvika
AAH_364	556729.2544	7042997.371	Amis	Rørvika
AAH_365	556721.3751	7042970.45	Amis	Rørvika
AAH_366	556682.3568	7042932.613	Amis	Rørvika
AAH_367	556741.9304	7042941.778	Amis	Rørvika
AAH_368	556564.3554	7042884.496	Amis	Rørvika
AAH_369	556445.2083	7042763.057	Amis	Rørvika
AAH_370	556465.8299	7042790.553	Amis	Rørvika
AAH_371	556515.0926	7042811.174	Amis	Rørvika
AAH_372	556564.3554	7042835.233	Amis	Rørvika
AAH_373	556596.4334	7042848.981	Amis	Rørvika
AAH_374	556618.2007	7042860.437	Amis	Rørvika
AAH_375	556637.7075	7042874.827	Amis	Rørvika
AAH_376	556669.1262	7042886.29	Amis	Rørvika
AAH_377	556704.7906	7042894.782	Amis	Rørvika
AAH_378	556742.1534	7042899.027	Amis	Rørvika
AAH_379	556765.9297	7042901.15	Amis	Rørvika
AAH_380	555498.8684	7042212.559	Amfs	Rørvika
AAH_381	552159.9543	7040778.186	Hbs	Trongen
AAH_382	552236.0281	7040759.168	Hbs	Trongen
AAH_383	552291.725	7040722.489	Ghmbs	Trongen
AAH_384	552220.4058	7040683.094	Ghmbs	Trongen
AAH_385	552302.5927	7040727.244	Ghms	Trongen
AAH_386	552367.1195	7040772.753	Hbs	Trongen
AAH_387	552398.3641	7040701.433	Ghms	Trongen
AAH_388	552451.3441	7040721.131	Ghms	Trongen
AAH_389	556910.0358	7043615.579	Hcqs	Varpneset
AAH_390	557279.5272	7044202.955	Hcqs	Varpneset
AAH_391	557375.1742	7044343.856	Hcqs	Varpneset
AAH_392	557754.1906	7044638.328	Hcqs	Varpneset

table continued on following page

table continued from previous page				
AAH_393	558004.6192	7044753.025	Hcqs	Varpneset
AAH_394	558267.7479	7045020.519	Hcqs	Varpneset
AAH_395	558218.0061	7044804.619	Hcqs	Varpneset
AAH_396	558208.4811	7044746.939	Hcqs	Varpneset
AAH_397	558080.4225	7044632.1099	Hcqs	Varpneset
AAH_398	557963.4765	7044562.789	Hcqs	Varpneset
AAH_399	557740.6968	7044446.372	Hqs	Varpneset
AAH_400	557488.4161	7044208.511	Hcqs	Varpneset
AAH_401	557432.3244	7044137.338	Hcqs	Varpneset
AAH_402	557368.5596	7044018.805	Hcqs	Varpneset
AAH_403	557288.1261	7043769.302	Hcqs	Varpneset
AAH_404	557299.2387	7043697.335	Hcqs	Varpneset